Universidad
Carlos III de Madrid

TESIS DOCTORAL

Hybrid walking therapy with fatigue management for spinal cord injured individuals

Autor:

Antonio José del Ama Espinosa

Directores:

Juan Camilo Moreno Sastoque

Ángel Gil Agudo

Luis Moreno Lorente

Department of Systems Engineering and Automation

Leganés, Octubre 2013

TESIS DOCTORAL

Hybrid walking therapy with fatigue management for spinal cord injured individuals

Autor: Antonio José del Ama Espinosa

Directores: Juan Camilo Moreno Sastoque, Ángel Gil Agudo
y Luis Moreno Lorente

Firma del Tribunal Calificador:

Presidente:	Carlos Balaguer Bernaldo de Quirós	_____
Vocal:	Thierry Keller	_____
Secretario:	Jaime Prat Pastor	_____

Calificación:

Leganés, 25 de Octubre de 2013

A mis padres, por su ejemplo.
A Ángela, por absolutamente todo.
Una vez más, sólo queda el camino...

Acknowledgements

I would like to start by thanking all people with spinal cord injury who participated in the experiments performed in the framework of this dissertation. Without their friendly and patient collaboration, none of the results and findings here reported would have been possible.

Next, I would like to acknowledge my supervisors for guiding, challenging, and encouraging me during these years. Dr. Juan Moreno, for its patience, wise guiding and friendship. I know sometimes was tough! Thanks joven!. Dr. Ángel Gil, whose confidence allowed me to grow, both personally and professionally. By transmitting his enthusiasm he has made me to finish this thesis. I am also very grateful for considering and respecting my opinions. Both provided an excellent atmosphere for doing research. And last, but not least, Prof. Luís Moreno, whose advices and encouragement words have always helped me. His comments have contributed to improve this dissertation.

A very important role has also been played by my friends at the Biomechanics and Technical Aids Unit and also at the Bioengineering Group. I appreciate the support and help they give me at any time. Everyone have contribute here, by providing encouragement, advise or just a short talk. Thanks for being here; it made surviving these years easier. I would also thank to Prof. José Pons and Prof. Ramón Ceres for providing me the opportunity of collaborating with the BioEngineering Group.

I would like to thank to the clinical staff of the National Hospital for Spinal Cord Injury for its collaboration throughout my research.

To my friends and family. I have stolen you too much time. This cannot be repaired, but I will try to compensate. I have missed you a lot. I do not forget the wholehearted support of my family. In everything I have done; in everything I will do. My parents are still the best mirror to look yourself. And I am proud of it.

Finally, I would like to thank my wife, Ángela. She was always there cheering me up and stood by me through the good times and bad. This dissertation would not have be possible without her encouragement, staunch work and fond. *Once again, still harder...*

Abstract

In paraplegic individuals with upper motor neuron lesions the descending path for signals from central nervous system to the muscles are lost or diminished. Motor neuroprosthesis based on electrical stimulation can be applied to induce restoration of motor function in paraplegic patients. Furthermore, electrical stimulation of such motor neuroprosthesis can be more efficiently managed and delivered if combined with powered exoskeletons that compensate the limited force in the stimulated muscles and bring additional support to the human body. Such hybrid overground gait therapy is likely to be more efficient to retrain the spinal cord in incomplete injuries than conventional, robotic or neuroprosthetic approaches. However, the control of bilateral joints is difficult due to the complexity, non-linearity and time-variance of the system involved. Also, the effects of muscle fatigue and spasticity in the stimulated muscles complicate the control task. Furthermore, a compliant joint actuation is required to allow for a cooperative control approach that is compatible with the assist-as-needed rehabilitation paradigm.

These were direct motivations for this research. The overall aim was to generate the necessary knowledge to design a novel hybrid walking therapy with fatigue management for incomplete spinal cord injured subjects. Research activities were conducted towards the establishment of the required methods and (hardware and software) systems that required to proof the concept with a pilot clinical evaluation. Specifically, a compressive analysis of the state of the art on hybrid exoskeletons revealed several challenges which were tackled by this dissertation.

Firstly, assist-as-needed was implemented over the basis of a compliant control of the robotic exoskeleton and a closed-loop control of the neuroprosthesis. Both controllers are integrated within a hybrid-cooperative strategy that is able to balance the assistance of the robotic exoskeleton regarding muscle performance. This approach is supported on the monitoring of the leg-exoskeleton physical interaction. Thus the fatigue caused by neuromuscular stimulation was also subject of specific research. Experimental studies were conducted with paraplegic patients towards the establishment of an objective criteria for muscle fatigue estimation and management. The results of these studies were integrated in the hybrid-cooperative controller in order to detect and manage muscle fatigue while providing walking therapy.

Secondly, closed-loop control of the neuroprosthesis was addressed in this dissertation. The proposed control approach allowed to tailor the stimulation pattern regarding the specific residual motor function of the lower limb of the patient. In order to uncouple the closed-loop control from muscle performance monitoring, the hybrid-cooperative control approach implemented a sequential switch between closed-loop and open-loop control of the neuroprosthesis.

Lastly, a comprehensive clinical evaluation protocol allowed to assess the impact of the hybrid walking therapy on the gait function of a sample of paraplegic patients. Results demonstrate that: 1) the hybrid controller adapts to patient residual function during walking, 2) the therapy is tolerated by patients, and 3) the walking function of patients was improved after participating in the study. In conclusion, the hybrid walking therapy holds potential for rehabilitate walking in motor incomplete paraplegic patients, guaranteeing further research on this topic.

This dissertation is framed within two research projects: *REHABOT* (Ministerio de Ciencia e Innovación, grant DPI2008-06772-C03-02) and *HYPER* (Hybrid Neuroprosthetic and Neurorobotic Devices for Functional Compensation and Rehabilitation of Motor Disorders, grant CSD2009-00067 CONSOLIDER INGENIO 2010). Within these research projects, cutting-edge research is conducted in the field of hybrid actuation and control for rehabilitation of motor disorders. This dissertation constitutes proof-of-concept of the hybrid walking therapy for paraplegic individuals for these projects.

Resumen

En individuos parapléjicos con lesiones de la motoneurona superior, la conexión descendente para la transmisión de las señales del sistema nervioso central a los músculos se ve perdida o disminuida. Las neuroprótesis motoras basadas en la estimulación eléctrica pueden ser aplicadas para inducir la restauración de la función motora en pacientes con paraplejia. Además, la estimulación eléctrica de tales neuroprótesis motoras se puede gestionar y aplicar de manera más eficiente mediante la combinación con exoesqueletos robóticos que compensen la generación limitada de fuerza de los músculos estimulados, y proporcionen soporte adicional para el cuerpo. Dicha terapia de marcha ambulatoria puede ser probablemente más eficaz para la recuperación de las funciones de la médula espinal en lesiones incompletas que las terapias convencionales, robóticas o neuroprotésicas. Sin embargo, el control bilateral de las articulaciones es difícil debido a la complejidad, no-linealidad y la variación con el tiempo de las características del sistema en cuestión. Además, la fatiga muscular y la espasticidad de los músculos estimulados complican la tarea de control. Por otra parte, se requiere una actuación robótica modulable para permitir un enfoque de control cooperativo compatible con el paradigma de rehabilitación de asistencia bajo demanda.

Todo lo anterior constituyó las motivaciones directas para esta investigación. El objetivo general fue generar el conocimiento necesario para diseñar un nuevo tratamiento híbrido de rehabilitación marcha con gestión de la fatiga para lesionados medulares incompletos. Se llevaron a cabo actividades de investigación para el establecimiento de los métodos necesarios y los sistemas (hardware y software) requeridos para probar el concepto mediante una evaluación clínica piloto. Específicamente, un análisis del estado de la técnica sobre exoesqueletos híbridos reveló varios retos que fueron abordados en esta tesis.

En primer lugar, el paradigma de asistencia bajo demanda se implementó sobre la base de un control adaptable del exoesqueleto robótico y un control en lazo cerrado de la neuroprótesis. Ambos controladores están integrados dentro de una estrategia híbrida-cooperativa que es capaz de equilibrar la asistencia del exoesqueleto robótico en relación con el rendimiento muscular. Este enfoque se soporta sobre la monitorización de la interacción física entre la pierna y el exoesqueleto. Por tanto, la fatiga causada por la estimulación neuromuscular también fue objeto de una investigación específica. Se

realizaron estudios experimentales con pacientes parapléjicos para el establecimiento de un criterio objetivo para la detección y la gestión de la fatiga muscular. Los resultados de estos estudios fueron integrados en el controlador híbrido-cooperativo con el fin de detectar y gestionar la fatiga muscular mientras se realiza la terapia híbrida de rehabilitación de la marcha.

En segundo lugar, el control en lazo cerrado de la neuroprótesis fue abordado en esta tesis. El método de control propuesto permite adaptar el patrón de estimulación en relación con la funcionalidad residual específica de la extremidad inferior del paciente. Sin embargo, con el fin de desacoplar el control en lazo cerrado de la monitorización del rendimiento muscular, el enfoque de control híbrido-cooperativo incorpora una conmutación secuencial entre el control en lazo cerrado y en lazo abierto de la neuroprótesis.

Por último, un protocolo de evaluación clínica global permitió evaluar el impacto de la terapia híbrida de la marcha en la función de la marcha de una muestra de pacientes parapléjicos. Los resultados demuestran que: 1) el controlador híbrido se adapta a la función residual del paciente durante la marcha, 2) la terapia es tolerada por los pacientes, y 3) la función de marcha del paciente mejora después de participar en el estudio. En conclusión, la terapia de híbrida de la marcha alberga un potencial para la rehabilitación de la marcha en pacientes parapléjicos incompletos motor, garantizando realizar investigación más profunda sobre este tema.

Esta tesis se enmarca dentro de los dos proyectos de investigación: *REHABOT* (Ministerio de Ciencia e Innovación, referencia DPI2008-06772-C03-02) y *HYPER* (Hybrid Neuroprosthetic and Neurorobotic Devices for Functional Compensation and Rehabilitation of Motor Disorders, referencia CSD2009-00067 CONSOLIDER INGENIO 2010). Dentro de estos proyectos se lleva a cabo investigación de vanguardia en el campo de la actuación y el control híbrido de la combinación robot-neuroprótesis para la rehabilitación de trastornos motores. Esta tesis constituye la prueba de concepto de la terapia de híbrida de la marcha para individuos parapléjicos en estos proyectos.

Contents

List of Figures

List of Tables

Nomenclature

10mWT	10 meters walking test
6mWT	6 minutes walking test
α_d	Actual (patterned) kinematics for knee joint
ϵ	Unitary strain
σ	Stress
τ_a	Actual interaction torque
τ_d	Torque reference for admittance controller
τ_e	Torque error for admittance controller
ω_a	Actual motor velocity
ω_d	Velocity reference for velocity controller
ω_e	Velocity error
A/D	Analog to digital
AAN	Assist-as-needed
AFO	Ankle foot orthosis
AIS	ASIA impairment scale
AM	Amplitude modulation
AMC	American motion control
ASIA	American Spinal Injury Association
AT	Assistive technology
BP	Blood pressure
C	Cervical
CFA	Constant frequency and amplitude
c-FSM	Cycle-domain finite state machine
CFT	Constant frequency trains
C_k	Torque field damping
CO	Cooperative-only controller configuration
CPG	Central pattern generator
CSIC	Consejo Superior de Investigaciones Científicas
DC	Direct current
DFT	Doublet (or n) frequency trains
E	Elastic Young's constant
eEMG	Evoked electromyography

EMG	Electromyography/electromyogram
FEM	Finite element analysis
FES	Functional electrical stimulation
FM	Frequency modulation
FSM	Finite state machine
FSR	Force sensing resistor
FTI	Force-time integral
GUI	Graphical user interface
HC	Hybrid-stiff controller configuration
HD	Harmonic drive
HGO	Hip guidance orthosis
HKAFO	Hip knee ankle foot orthosis
HNP	Hospital Nacional de Parapléjicos
HP	Hybrid-cooperative controller configuration
HR	Heart rate
ILC	Iterative learning control/controller
IPI	Inter-pulse interval
IRGO	Isocentric reciprocating gait orhtosis
ISA	Industry standard architecture
KAFO	Knee ankle foot orthosis
K_D	Derivative constant for admittance controller
K_d	Derivative constant for neuroprosthesis controller
K_I	Integral constant for admittance controller
K_i	integral constant for neuroprosthesis controller
K_k	Torque field stiffness
K_P	Proportional constant for admittance controller
K_p	Proportional constant for neuroprosthesis controller
K_w	Velocity feedforward conversion constant
L	Lumbar
MES	Muscular electrical stimulation
MFE	Muscle fatigue estimator
MMT	Manual muscle test
MNP	Motor neuroprosthesis
NFTI	Normalized force-time integral
NILC	Normalized stimulation intensity
NP	Neuroprosthesis/neuroprosthetic
NTTI	Normalized torque-time integral
PA	Pulse amplitude
PD	Pulse duration
PID	Proportional integral derivative
PWM	Pulse width modulate

QUEST	Quebec user evaluation of satisfaction with assistive technology
RCT	Randomized controlled trial
RGO	Reciprocating gait orthosis
RMS	Root mean square
S	Sacral
SCI	Spinal cord injury
SEA	Series-elastic actuator
SMA	Shape memory alloy
SoA	State of the art
SW	Switch
T	Thoracic
t-FSM	Time-domain finite state machine
TTI	Torque-time integral
VAS	Visual-analog scale
VFT	Variable frequency trains
WISCI II	Walking Index for Spinal Cord Injury Version 2

Chapter 1

Introduction to spinal cord injury and walking rehabilitation

This introductory chapter gives an overview about the main consequences of a spinal cord injury, including physiological, functional, social and economical impacts. Within a rehabilitation framework, this chapter highlights the importance of walking function for improving quality of life of the person with spinal cord injury. Trends for walking rehabilitation currently available in clinical settings are reviewed, with emphasis on robotic approaches. Recent evidences shows that novel approaches are needed to increase the potential of robotic interventions for rehabilitation of walking ability of spinal cord injured persons. This motivates the work presented in this dissertation. Objectives and organization of the work are presented in the last section of this chapter.

1.1 The spinal cord

The spinal cord is a long, thin, tubular bundle of nervous tissue and support cells that extends from the brain, down to the space between the first and second lumbar vertebrae, terminating in a fibrous extension known as the *filum terminale* [1] (figure 1.1). It has three major functions: to conduit motor information down the spinal cord, to conduit sensory information in the reverse direction, and as center for coordinating certain reflexes. It is contained in a spinal canal inside the vertebral column, which consists of 24 articulating vertebrae, separated by intervertebral discs, and 9 fused vertebrae in the sacrum and the coccyx. The vertebral column is divided into four different regions: the cervical, comprised by 7 vertebrae, thoracic, comprised by 12 vertebrae, lumbar, comprised by 5 vertebrae, and sacral, comprised by 5 vertebrae. All regions are visually distinguishable from one another, as shown in figure 1.1.

The spinal cord is organized in similar way to the vertebrae in 31 segments. Each spinal segment, except the first, has nerve dorsal roots entering and nerve ventral roots exiting the cord below their corresponding vertebrae. As in the case of the vertebral column, the spinal cord and its nerves are divided into 8 cervical (C), 12 thoracic (T), 5 lumbar (L), 5 sacral (S), and 1 coccygeal nerve. The point at which the spinal cord ends is not anatomically well defined, and occurs near

lumbar nerves L1 and L2, called the *conus medullaris*. After the spinal cord terminates, the spinal nerves continue as a bundle of nerves called the *cauda equina*.

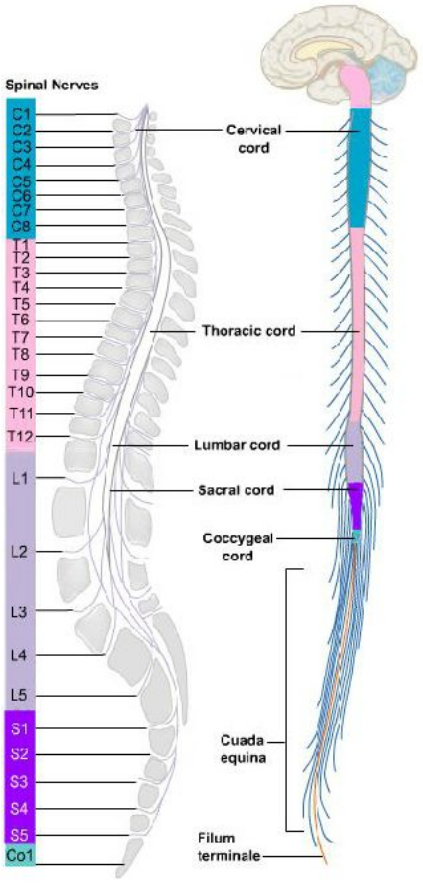

FIGURE 1.1: Spinal cord.

A cross-section through the spinal cord shows a butterfly-shaped core of gray matter surrounded by white matter (figure 1.2) [1]. Grey matter is made up of neuronal cell bodies, whereas the white matter is composed of bundles of axons, which connect various gray matter areas and carry nerve impulses between neurons. The gray matter is shaped like the letter "H" or a "butterfly". The shape and size of the gray matter varies according to spinal cord level: at the lower levels, the ratio between gray matter and white matter is greater than in higher levels, mainly because lower levels contain less ascending and descending nerve fibers.

The butterfly shape of the gray matter allows to distinguish four main columns: dorsal horn, intermediate column, lateral horn and ventral horn column (figure 1.2). The dorsal horn is found at all spinal cord levels and is comprised of sensory nuclei that receive and process incoming sensory information. From there, ascending projections emerge to transmit the sensory information to the midbrain and diencephalon. The intermediate column and the lateral horn comprise autonomic neurons innervating visceral and pelvic organs and the ventral horn comprises motor neurons that innervate skeletal muscle.

Each spinal nerve is composed of nerve fibers that are related to the region of the muscles and skin that develops from one body *dermatome*, which is an area of skin supplied by peripheral nerve fibers originating from a single dorsal root ganglion [2]. Because each segment of the cord

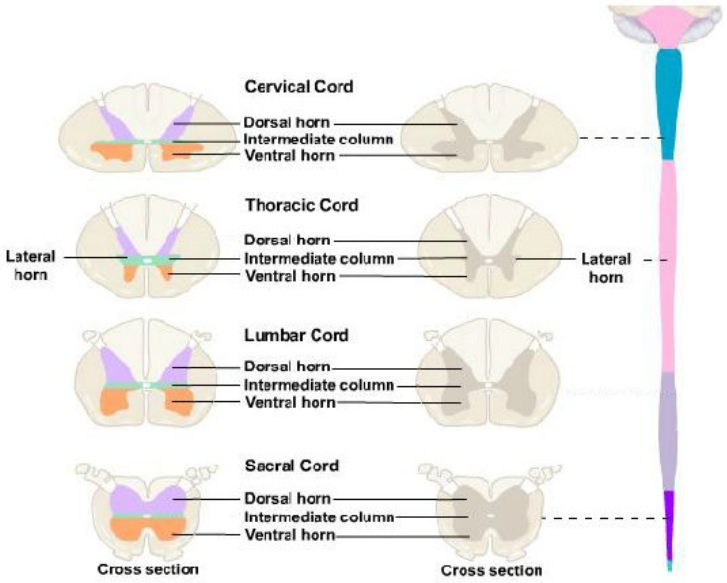

FIGURE 1.2: Spinal cord cross-section.

innervates a different region of the body, dermatomes can be precisely mapped on the body surface, although there is some overlap between neighboring dermatomes (figure 1.3). Loss of sensation in a dermatome can indicate the level of spinal cord damage in clinical assessment of injury.

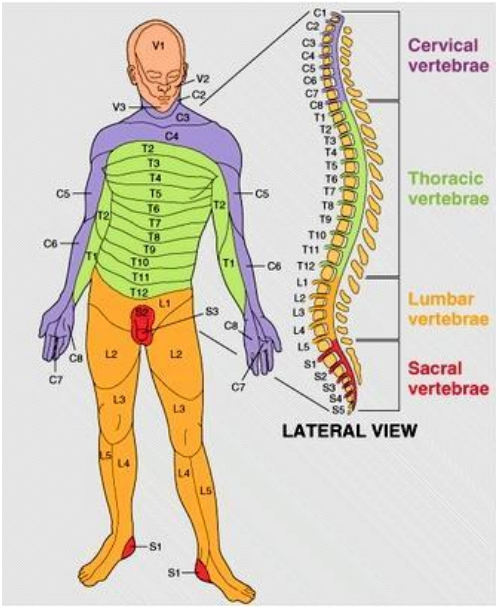

FIGURE 1.3: Spinal cord dermatomes.

1.2 Spinal cord injury

Spinal cord injury (SCI) can be defined as any alteration of the spinal cord that interrupts nervous impulse from the brain to periphery and vice versa, causing alterations in the sensory-motor and autonomous systems under the level at which the lesion is located [3]. It should be noted that bony column injuries not always correlate with spinal cord injures. It is one of the most devastating clinical circumstances, due to the functional loss resulting, which causes loss of independence of the person. This absence of functionality coupled with the limited possibilities of spontaneous recovery and the lack of a cure makes the SCI a serious social, economic and physical problem.

1.2.1 Spinal cord injury classification

Depending on where the spinal cord and nerve roots are damaged, the symptoms can vary widely, from pain to paralysis and to incontinence. One of the most used classifications are the terms *paraplegia* and *tetraplegia* [2]. While paraplegia refers to a loss of lower limb function, which results from damage to the thoracic, lumbar and, to a lesser extent, sacral cord segments, tetraplegia stands for the loss of function in all four limbs, which results from damage to cervical segments. In both conditions there is impairment of autonomic function, including bladder and bowel.

In addition, for a injury location SCIs are described at various levels of *incomplete* to a *complete* [2]. A complete SCI means that all neurological functions are lost below the level of the lesion. In an incomplete SCI there is partial preservation of neurological function. Any combination of motor, sensory and autonomic function may be spared, but these incomplete lesions usually fit into a number of recognizable syndromes.

Despite former definitions, the American Spinal Injury Association (ASIA) published a classification of spinal cord injury, called the International Standards for Neurological and Functional Classification of Spinal Cord Injury, which is worldwide used to document sensory and motor impairments following SCI (figure 1.4) [2,4]. This classification is based on neurological responses: touch and pinprick sensations tested in each dermatome, and strength of ten key muscles on each side of the body, including hip flexion (L2), shoulder shrug (C4), elbow flexion (C5), wrist extension (C6), and elbow extension (C7). Following these standards, after identifying the level of lesion, a SCI is classified into five categories on the ASIA Impairment Scale (AIS):

- Category A indicates a *complete* spinal cord injury where no motor or sensory function is preserved in the sacral segments S4-S5.
- Category B indicates an *incomplete* spinal cord injury where sensory but not motor function is preserved below the neurological level and includes the sacral segments S4-S5. This is typically a transient phase and if the person recovers any motor function below the neurological level, that person essentially becomes a motor incomplete, i.e. ASIA C or D.
- Category C indicates an *incomplete* spinal cord injury where motor function is preserved below the neurological level and more than half of key muscles below the neurological level

have a muscle score lower than 3, measured by the Manual Muscle Test (MMT[1]). This score indicates active movement with full range of motion against gravity.

- Category D indicates an *incomplete* spinal cord injury where motor function is preserved below the neurological level and at least half of the key muscles below the neurological level have a muscle grade of 3 or more.
- Category E indicates *normal* where motor and sensory scores are normal. Note that it is possible to have spinal cord injury and neurological deficits with completely normal motor and sensory scores.

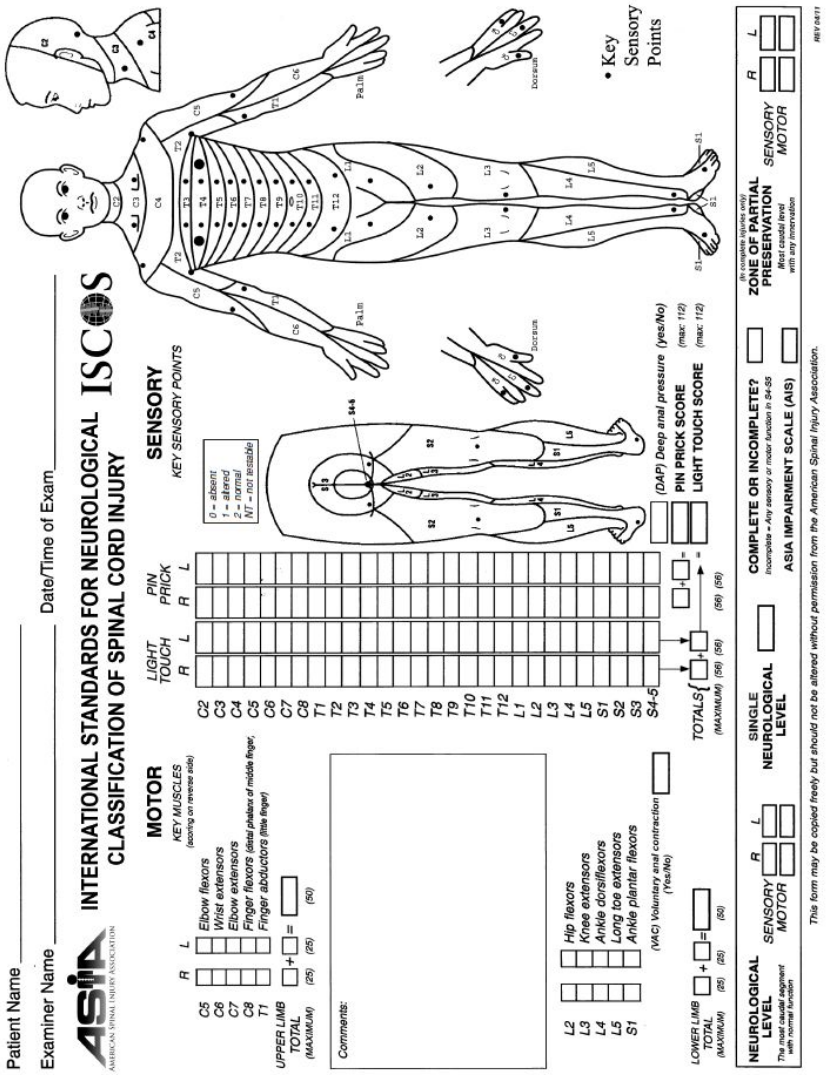

FIGURE 1.4: ASIA standards for injury classification [4]

[1]The MMT is a manual test that measures the force-production ability of a muscle [5]. It ranges from 0 (no contraction) to 5 (muscle force enough to move the joint against gravity and external resistance)

1.2.2 Socioeconomic impact of spinal cord injury

SCI has a strong impact on the individual and society. It is a chronic situation for the person, thus the impact on the healthcare system is not limited to acute phase of the lesion. Besides, the person with a SCI must face during his/her lifetime chronic diseases derived from the SCI, as the appearance of pressure ulcers, spasticity, urinary disorders, psychological disorders and many others. Furthermore, the person with a SCI has to deal with social and labor integration issues, lack of productivity, the need of use of assistive technology, and even the need of in home caregivers.

Advances in medicine, technology and social policy have lead to an increase of life expectancy of people with SCI. The current median survival of people aged between 25 and 34 years old who suffer a SCI is at least 40 years after injury, with the exception of high levels of SCI [6]. SCI incidence varies among countries. In the United States and Japan, the incidence is estimated in 40 new cases per million of inhabitants [7,8], 10,4 in Holland [9]. With respect to Spain, incidence varies among 12.1 [10] and 13.1 [11], with a mean age at the time of injury of 41.8 years, and a male/female ratio of 2,6. The most common cause of SCI in Spain is traffic accidents (52,23 %), followed by falls (27,39 %) [11]. Prevalence of SCI is estimated in 350-380 cases per million of inhabitants [10], with a 38% of the tetraplegic injuries and 38% of complete injuries.

The mean cost of medical care and adaptation due to a SCI depends on the time since of injury and the level of injury. Estimates corresponding to Spain give a mean hospitalization cost in the range of EUR 60.000 to 100.000 during the first year of injury [12]. It has been estimated that the economic cost associated with the SCI ranges between EUR 92 millions and 212 millions, depending on the injury mechanism. This estimate includes medical, adaptation, material, administrative, policy, firefighters and roadside assistance costs, productivity losses and sick leave, as well as an estimate of productivity losses of carers, and productivity losses due to death [12].

1.3 Spinal cord injury rehabilitation

The American Board of Physical Medicine and Rehabilitation defines Rehabilitation, also Physiatry, as *a medical specialty concerned with diagnosis, evaluation, and management of persons of all ages with physical and/or cognitive impairment and disability, which involves diagnosis and treatment of patients with painful or functionally limiting conditions, the management of comorbidities and coimpairments, diagnostic and therapeutic injection procedures, electrodiagnostic medicine, and emphasis on prevention of complications of disability from secondary conditions* [13]. Physiatrists provide leadership to multidisciplinary teams concerned with maximal restoration or development of physical, psychological, social, occupational and vocational functions in persons whose abilities have been limited by disease, trauma, congenital disorders or pain to enable people to achieve their maximum functional abilities [13].

SCI rehabilitation practices were influenced greatly by the pioneering efforts of Sir Ludwig Guttman who was instrumental in the creation of specialized spinal units to care for injured soldiers returning to England during and after World War II [14]. Eventual adoption of this more specialized and integrated approach followed in many additional centers [15, 16] was bolstered by reports of reduced mortality and enhanced long-term survival, which was attributed

in part to more effective management of secondary conditions associated with SCI, as pressure sores or respiratory conditions [17–19].

At present, the ideal scenario for modern SCI care is purported to be treatment in specialized and integrated centers, with an interdisciplinary team of health care professionals providing care as early as possible following injury, and throughout a rehabilitation process with appropriate discharge to the community, characterized by ongoing outpatient care and follow-up [20,21]. Within this framework, rehabilitation should begin as soon as possible, conveyed by a multidisciplinary team responsible for developing a treatment program to achieve the maximum independence in a timely manner [22]. However, there is little consensus among rehabilitation specialists for what constitutes the essential elements of SCI rehabilitation. As with most forms of rehabilitation, rehabilitation programming directed towards persons with SCI has been likened to a "black box", with research endeavors focused on the entire "rehabilitation package" but little emphasis on investigating the effectiveness of specific therapeutic practices [23]. A definition have been proposed by the the Spinal Cord Injury Rehabilitation Evidence project [24], originated after reviewing several service offerings among 16 SCI rehabilitation programs of the United States, the World Health Organization definition of rehabilitation, and the International Classification of Functioning Disability and Health [25]:

> *A specialized SCI rehabilitation program provides comprehensive, and patient-focused rehabilitation services, for inpatient, transitional living, outpatient and follow-up care, to empower people with SCI and their families to achieve optimal quality of life continuing into the community, focusing on increasing self-reliance and gaining independence. Through organized regional referrals, care is delivered through a multidisciplinary team provided by board certified physician specialists and accredited allied health professionals (i.e. physical/occupational/speech recreational therapists, nurse specialists, psychologists, dietitians, engineers, social workers, etc.). As a rehabilitation program specialized in the care of people with SCI, experienced through trauma or disease, active participation in research is facilitated through university affiliated teaching institutions.*

This definition points out the functional approach for rehabilitation of SCI, given that the final main objective is to maximize user independence. Getting into more detail, SCI rehabilitation during inpatient traditionally consists of three main phases prior to discharge: acute phase, sitting phase and the sub-acute rehabilitation phase [26]. In the *acute phase*, kinesitherapy activities are conducted, including active mobilization of the joints above the level of injury to prevent disuse atrophy, and passive joints below the level of injury to keep and maintain muscle trophism and unrestricted joint movement. After this phase, the *sitting phase* consist of a progressive transition from bed to sitting, preventing neurovegetative reactions secondary to spinal cord injury. Once the sitting has been achieved, rehabilitative treatment in the *sub-acute phase* can be initiated, with different specific therapeutic activities depending on several factors, such as level of injury, secondary lesion-related aspects (fractures, head injuries, cognitive dysfunction, prior chronic disease and many others) and person-related aspects as age, weight, cardiorespiratory state, psychological state and motivation. The rehabilitation program is focused on maximizing functional independence of the patient: bladder/bowel function, sexual function, limb function, daily living activities, ambulation and walking among others.

Although all functions are of the most importance, relative importance among them is perceived by clinicians and patients. Identification of such relative importance for both groups

may allow optimizing rehabilitation resources: personnel, therapy intensity and research and development investment. Actually consumer[2] preference and satisfaction are indeed important and essential components of the rehabilitation paradigm defined in the United States [27] and the United Kingdom [28]. Documenting consumer satisfaction gives an outcome measure that allows to ensure that rehabilitation services addresses the needs of patients, and allowing also to tailor rehabilitation program to specific individual needs. This procedure has been found to be effective in rehabilitation program planning with positive correlations between goals set and those achieved and, in the other hand, active patient involvement in the rehabilitation process enhances compliance and is a good predictor of a positive outcome [29].

Despite the efforts being made to enhance the quality of life of SCI population, people with SCI tended to report a lower quality of life than non-disabled individuals [30]. Factors such as access to the community, marriage, social support, and community integration have a profound impact on quality of life. In this sense, several studies have attempted to identify the most important functions in the SCI population by asking people with SCI what would improve their quality of life, with a view to enhancing quality of life [31–35]. Although different methods were used, mobility was identified as one of the main objectives for the injured individuals.

1.3.1 Rehabilitation of walking ability after SCI

Human motion control for walking is hierarchically distributed within the nervous system. The main component of such organization are interneuronal circuits (interneurons and possibly motoneurons) at the spinal cord, whose combined operation produces the fundamental spatio-temporal muscle activation patterns. Such circuits have been defined as Central Pattern Generators (CPG) [36], which are an intrinsic capability of the spinal cord and are present at birth. CPG activity is modulated by afferent inputs from a variety of sources within the visual, vestibular and proprioceptive systems. The role of this afferent activity is to shape the locomotor pattern, to control phase-transitions and to reinforce ongoing activity [37].

Brain plays a fundamental role on the activation and modulation of CPG's [38]. Brain centers can initiate CPG activity, which then becomes modulated by sensory input from the periphery. However, these actions do not control the fundamental CPG rhythmicity. Especially in humans, supraspinal input is required for walking: both the CPG and the reflex mechanisms that mediate afferent input to the spinal cord are under the control of the brainstem [38], as specific centers in the brainstem triggers locomotion [37]. For safe locomotion, cortical input might play a more prominent role when adjustments of the locomotor pattern are required to meet certain environmental demands. For example, when stepping over an obstacle, the cortical control of the swing trajectory becomes enlarged as compared to normal stepping [39]. Thus, the generation of an appropriate locomotor pattern depends on a combination of central programming and afferent inputs as well as the instruction for a respective motor condition. Any damage within the central or peripheral nervous system due to SCI can affect to one or more of those interneuronal circuits, followed by an impairment of pattern generation that leads to a movement disorder. Furthermore, a movement disorder is the consequence not only of the primary motor lesion but also of secondary processes that can be supported during rehabilitation [40].

[2]Here consumer refers to both clinicians and patients

Several mechanisms are responsible for the improvement in function observed during and after rehabilitation [40–42]. One of the most important mechanism is the *neural plasticity*, a rather broad range of changes in neural connections that can occur either spontaneously and/or be induced after an incomplete SCI. Neural plasticity occurs not only at cortical sites but also at the brainstem and spinal cord sites [43], and is assumed to play a role in the recovery of locomotion [44]. An improvement in locomotor function, without a corresponding improvement in neurological deficit, might be caused by task-specific training of the CPG within the spinal cord [43]. It must be noted here that neural plasticity does not lead to regeneration and neural repair of the central cord system, which is unlikely to spontaneously occur [41].

Another mechanism that contributes to improve locomotion is *muscle strength training*, resulting in muscle hypertrophy and an improved coordination between leg muscle groups [45]. However, an improvement in leg muscle strength does not necessarily result in improved locomotion and vice versa [46]. Finally subjects with SCI exhibit *compensation*, which refers to a change in function without an accompanying change in the neurological deficit, for example by adapting existing movement strategies or by adopting new strategies, as the use of assistive technologies.

Walking rehabilitation in SCI is thus directed towards the re-learning of motor skills. Neuronal centers below the level of lesion exhibit plasticity that can be exploited by specific training paradigms [37]. In individuals with SCI, human spinal locomotor centers can be activated by appropriate afferent input, providing sensory cues consistent with normal walking. This mechanism is predominant in the case of incomplete SCI, whereas compensation-driven functional recovery is more predominant in complete SCI [41], where recovery depend on the presence of spinal circuitry capable of generating activation of muscle groups [47].

1.4 Technology for functional compensation and rehabilitation of walking of SCI

This section brings an overview about the current technologies available for rehabilitation and functional compensation of walking. Differences among those two categories is determined by the objective of the device. As reviewed, walking rehabilitation aims to impact on the walking abilities of the patient. On the contrary, functional compensation aims to restore the affected walking function, usually driven by an external device, regardless the rehabilitative effects on the walking ability of the patient.

1.4.1 Assistive technology for functional compensation of walking

Assistive technology (AT) is used by individuals with disabilities in order to perform functions that might otherwise be difficult or impossible. Under this term it is included any assistive, adaptive, and rehabilitative device for people with disabilities, to promote independence by enabling people to perform tasks that they were formerly unable to accomplish, or had great difficulty accomplishing, by providing enhancements to, or changing methods of interacting with, the technology needed to accomplish such tasks [48].

There are several assistive devices to improve walking. The simplest are canes and crutches, which increase the base of support of the user. This way balance and stability are improved,

load to one of the lower limbs is reduced, and sensory cues through the hand are transmitted. Canes and crutches are usually prescribed when the person with a disability have a good lower and upper limb strength and only balance is somehow compromised [49]. In those cases where the person is affected by weak lower limb function, an orthosis can support and sometimes enhance lower limb function, by providing joint support as shown in next section. Furthermore, active orthoses, also named robotic exoskeletons, provides external controlled power to the impaired joints to compensate walking function, as reviewed in section 1.4.1.2.

1.4.1.1 Passive gait orthoses

The first orthosis introduced clinically for compensating lower limb weakness was the knee-ankle-foot orthosis (KAFO, figure 1.5(a)), a mechanical structure whose main objective is to lock or limit joint movement during the stance phase of gait. It was developed in the 1950s to assist ambulatory management after poliomyelitis epidemics [50] (figure 1.5(a)). KAFOs allow swing-through mobility, with the use of walkers or crutches. The addition of a mechanical joint for the hip (figure 1.5(b)) allowed to provide lower limb support to SCI persons. The mobility achieved with this device is aesthetically poor and requires higher metabolic energy expenditure. Indeed, the energetic cost associated with this kind of ambulation is up to 43% higher than that of wheelchairs [51], which partially explains the low rate of use of such orthoses compared to wheelchairs.

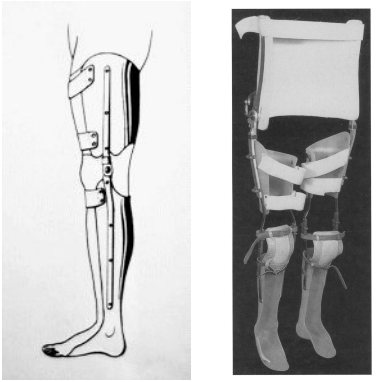

(a) KAFO (b) HKAFO

FIGURE 1.5: Passive gait orthoses.

Some years later, in an effort to develop a less demanding ambulation, dynamic orthoses that allowed passive hip joint movement were developed. These dynamic orthoses can be classified into two main groups. The first group is composed of cross-linked hip joint orthoses, such as the *Reciprocating Gait Orthosis* (RGO, figure 1.6(a)) [52], the *Advanced Reciprocating Gait Orthosis* (ARGO, figure 1.6(b)) [53] and the *Isocentric Reciprocating Gait Ortosis* (IRGO, figure 1.6(c)) [54]. Those orthoses have a mechanical linkage between hip joints, hip flexion provides coupled contralateral hip extension while keeping the knee and ankle fixed, allowing to move the leg in a fixed reciprocal pattern [55]. This reciprocating mechanism results in an improvement in the mechanical efficiency of paraplegic gait and a reduction in the energy cost of ambulation [56]. The differences between RGO and ARGO is that ARGO utilizes a single push-pull cable to link the mechanical hip joints instead of two that RGO uses. The IRGO, on the other hand, replaces the two bowden cables with a centrally placed pivoting bar and tie rod arrangement.

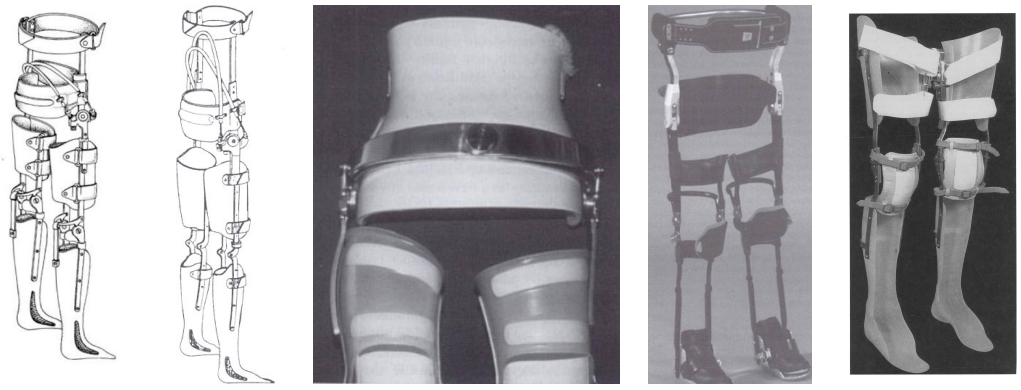

(a) RGO [52] (b) ARGO [53] (c) IRGO [54] (d) HGO [57,58] (e) WalkAbout [59]

FIGURE 1.6: Reciprocating gait orthoses.

The second group is composed of freely hinged hip joint orthoses, including the *Hip Guidance Orthosis* (HGO, figure 1.6(d)) [57, 58] and the *Walkabout* (figure 1.6(e)) [59]. This orthoses are focused on the ease of donning and doffing, by removing the corset, and of the clearance of the swing-leg for reciprocal walking. The gait achieved with cross-linked hip joint orthotic systems is improved with respect to the first group rigid HKAFO's [60], although it still does not enable subjects to be fully independent in the key skills necessary for functional ambulation [61]. Furthermore, regardless of the device used, some general problematic aspects associated with ambulation with this kind of devices arise, such as susceptibility to diseases of shoulder, elbow and wrist when using canes or walkers, the high energy cost, and low travel speed reached when compared to wheelchair mobility, which have been identified as reasons for discontinuing the use of these orthoses [62–64].

1.4.1.2 Robotic exoskeletons for functional compensation of walking

Robotic exoskeletons intends to overcome limitations related to energy cost of ambulation with orthoses by adding actuators at the joints of the orthosis, providing an external mean of adding or dissipating power at the user's joints. This way, if properly designed, the robotic exoskeleton substitutes the motor function of the lower limbs for walking by driving the user's joints through a functional walking pattern. The first examples of active exoskeletons appeared almost forty years ago, when an active orthosis was developed comprised of actuators on the hip, knee and ankle joints to assist movement in the sagittal plane [65,66]. Since then, many active exoskeletons have been developed for functional compensation of walking, with much variation in the actuator and sensing technologies, and in the control strategies. A search of the literature reveals exoskeletons driven by electric motors [67–70], pneumatic actuators [65,71] and hydraulic actuators [72]. The number of joints controlled also varies between exoskeletons. Most actively control hip and knee joints, with the ankle joint controlled by an elastic actuator [67–70, 72].

Nowadays there are a few devices that are being commercially available for functional compensation of walking of SCI persons. The first is the *ReWalk* (Argo Medical Technologies, figure 1.7(b)) [73,74]. ReWalk features electric motors for the hips and knees joints, which drives user's legs providing erect ambulation with the help of forearm crutches. The user operates Rewalk by

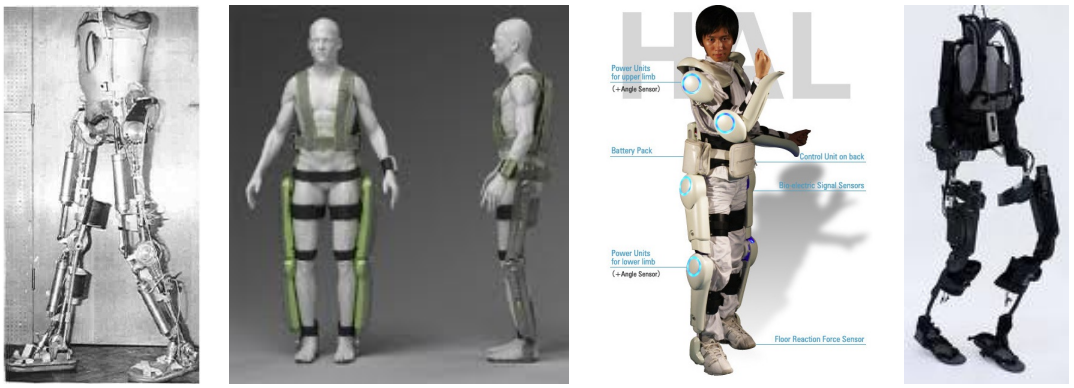

(a) Assistive suit [66] (b) ReWalk [73, 74] (c) Hybrid Assistive Limb [75, 76] (d) eLegs [77]

FIGURE 1.7: robotic exoskeletons for functional compensation of walking.

a button interface placed at the wrist for selecting among several movement procedures: walking, sitting up and down, or stairs climbing. An accelerometer placed at the user's torso allows the user to control initiation and stop of automatic walking. A similar device that was recently introduced is the *eLegs* (Berkeley Bionics, figure 1.7(d)) [77]. Similar to ReWalk, eLegs also features electric motors for providing movement to the user's joints, while measures users arm motion for initiating/stop a step. A further device that has significant operational experience with able-bodied users is the *Hybrid Assistive Limb* (Cyberdyne, figure 1.7(c)) [75, 76]. HAL is able to augment the users capabilities by measuring the volitional effort through the electromyographic (EMG) signals of the lower limb muscles, providing torque to the user's joints proportional to the muscle activation.

Few exoskeletons have been subject to evaluation with impaired population regarding safety, tolerance, and ease of use of these systems for walking compensation. For example, HAL has been tested preliminary with stroke subjects, and has not shown any significant improvement in terms of stride length, walking speed or energy cost [78]. Preliminary experiments targeting SCI persons are undergoing [79]. In a recent study, ReWalk was evaluated with six SCI subjects, using a comprehensive set of functional variables. There were no adverse effects during the course of the study, but there were needed an average of fourteen training sessions for the patients to be able to walk 100 meters[3] [80,81]. These results suggests that functional compensation of walking with robotic exoskeletons is still far from constituting an alternative to wheeled mobility. Despite the advances made in recent years, many limitations remain to be resolved. The most commonly highlighted improvement directions found in literature are the following [82–85]:

- Specific weight of both actuators and energy supplies needs to be improved.
- Truly bio-inspired actuators are needed, compatible with the forces provided by the user.
- The kinematic compatibility of the human body and exoskeletons needs to be improved to increase comfort and safety.
- The interfaces that determine the interaction forces must be optimized for efficient support of human joints.

[3]These studies and the implications for this dissertation are further discussed in chapter 7

- The exchange of both physical and cognitive information between user and exoskeleton must be improved in order to design more transparent and user-friendly systems.
- Further work focusing on user safety and usability is required.
- Further work on user evaluation of these systems, including technological and clinical aspects, is required.

1.4.2 Assistive technology for walking rehabilitation

During the last decades there is a trend in rehabilitation procedures among practitioners that focus on the functional movements to recover walking ability [40,86]. These include task-specific physiotherapy (standing on parallel bars, training of equilibrium), bracing, manual supported over ground gait training and manual bodyweight supported treadmill training among others. Furthermore, intensive training strategies were showed to stimulate CPG's and provide adequate modulation of reflexes during walking, which supports the fact that manual bodyweight supported treadmill training improved gait and lower limb motor function in patients with SCI [87–92].

FIGURE 1.8: Manual body weight supported treadmill training [93]

These interventions has several major limitations. Hands-on traditional techniques, such as active-assist exercise, are advocated in practice guidelines and standard texts and is labor-intensive [93]. Therefore, training duration is usually limited by personnel shortages and therapist fatigue, rather than patient fatigue. Furthermore, therapists often experience back pain because the training is performed in an ergonomically unfavorable seating or even standing posture [94–98]. Consequently training sessions are shorter than may be required for an optimal therapeutic outcome. Finally, manually training lacks repeatability and objective measures of patient performance and progress [99].

1.4.2.1 Robotic gait training

In this framework, robotic technology for walking rehabilitation has emerged as response to therapist's and therapeutic needs. Robotic technology can partially automate movement training following a lesion of the brain and nervous system. Because of their programmable force-producing ability, robots can replicate some features of a therapist's manual assistance, allowing

patients to semi-autonomously practice their movement training. Besides, robotic devices can also implement novel forms of physical manipulation impossible for therapists to emulate because of limited speed, sensing, strength, and repeatability of the therapist's manual labor. The progression of therapy with electromechanical devices is possible by, for example, varying the force, decreasing assistance, increasing resistance and expanding the movement amplitude.

The assist-as-needed (AAN) control concept has emerged to encourage the active motion of the patient. In this approach, the goal of the robotic device is to either assist or correct the motions of the user. Patients attempt to move along a trajectory while the robot provides only as much assistance as necessary. The amount of assistance depends on the magnitude of deviation of the given trajectory, which is generated for each patient and gait scenario separately. The AAN approach is intended to manage simultaneous activation of efferent motor pathways and afferent sensory pathways during training [100]. It has been demonstrated in animal models that a fundamental strategy of the neural control of a given motor task is to incorporate a degree of variability in the sensorimotor pathways. Therefore, imposing a "fixed" stepping pattern produces a continuous incongruity between the input and the output signals, which hinders the ability of the spinal cord to learn [101, 102].

There are several robotic treadmill training devices described in the literature. The *Lokomat* (Hocoma, figure 1.9(a)) is undoubtedly the most introduced device in clinical settings worldwide. It consists of a robotic gait orthosis and an advanced body weight support system, combined with a treadmill [103, 104]. The Lokomat has four degrees of freedom actuated by linear drives: left and right hip and knee joints. The legs of a patient are attached to the Lokomat by one upper-leg and two lower-leg braces. The drives are precisely synchronized with the speed of the treadmill to assure a precise match between the speed of the gait orthosis and the treadmill. The AAN approach was implemented in the Lokomat, allowing the patients to move actively along a spatial path of a defined walking pattern, which is referred to as *path control* [105]. This strategy was reported to result in larger temporal variability more active EMG recruitments in tests performed with a group of incomplete spinal cord injury subjects than traditional position controlled training.

Besides to Lokomat, there are several others treadmill training robotic devices. The Lower Extremity Powered Exoskeleton (LOPES, University of Twente, figure 1.9(b)), has a more compliant actuation than Lokomat. Its actuators are build on the basis of series-elastic actuators and bowden cables [106, 107]. This design pursues the idea of built a light weight and compliant exoskeleton, allocating the actuator inertia out of the exoskeletal structure, to maximize the AAN capabilities. Besides, LOPES increases the number of actuated degrees of freedom with respect to Lokomat, with two actuated degrees of for pelvis rotations, hip sagittal and frontal plane rotations and knee sagittal plane rotations. There is a preliminary evaluation of LOPES therapy with chronic stroke patients showing little but positive improvements on gait velocity, stride length and cadence on the paretic leg [107].

Another existing approach for automated treadmill training of walking is to design robots with an end-effector approach, in which the robot drives the user's foot following a stepping movement. Those devices are able to simulate trajectories like walking on an even floor and up/down staircases. One representative example is the *LokoHelp* [108, 109] (LokoHelp Group, (figure 1.9(c)), that can be placed in the middle of the treadmill surface parallel to the walking direction and fixed to the front of the treadmill with a simple clamp. Lokohelp also incorporates a body weight

support system. A variety of devices with similar approach can be found in the literature and also available in the market. A comprehensive review about treadmill training robotic devices can be found at [85, 110].

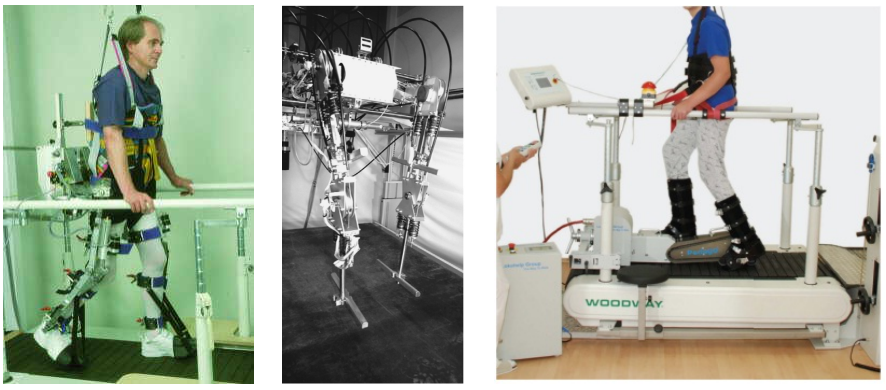

(a) Lokomat [104] (b) LOPES [106] (c) LokoHelp [108]

FIGURE 1.9: Robots for automated treadmill training.

The efficacy of these robotic systems for walking rehabilitation in SCI is still controversial. Randomized Controlled Trials (RCT) are showing that robotic treadmill training provides similar improvements in walking ability and performance in SCI as conventional therapy [40, 86, 111] regardless of the approach [112]. The efficacy of conventional physiotherapy should therefore not be underestimated and studies on how robotic and conventional interventions could optimally combined to result in the most effective gait rehabilitation program should be evaluated. These results from RCT and systematic revisions, make to call into question the basic principles behind the interventions based on mass practice, treadmill walking and its robotic counterpart, robotic treadmill training training. Several authors have recently proposed several recommendations to further design new rehabilitation interventions [113–115]:

- Results extrapolated from animals models have limitations, mainly in behavioral interventions, that make difficult to extrapolate results to human response.
- There is a need to improve design of proof-of-concept pilot studies. This pilot studies shall lead to a size effect estimate that allows to adequately design a RTC. This strategy may also lead to clinically important improvements in the design of the robotic device.
- The environmental context of training may matter. Interventions may put patients outside of the usual context of real-world demands, where environmental challenges can be overcome and problem solving is highly motivated.
- Combinational therapies ought to be promoted, even in RCT of a novel intervention.
- The metrics to evaluate walking function should not be limited to clinical test made in controlled environment. Massive remote monitoring can be applied to track the daily number of bouts of walking and exercise, as well as the speeds and distances walked in the home and community. This will also provide RCT with clinically meaningful, ratio scale outcome measurements drawn from real-world settings.

In conclusion, design of the interventions should be reconsidered, to increase the ability for providing richer walking experiences, more interactive with the environment, and with continuous

and massive monitoring of patient walking activity. In this context, robotic technology still holds its potential, stated at the beginning of this section, to provide this massive, controlled and continuously monitored walking training and support. New therapies that combine robotic with pharmacological and/or electric stimulation of impaired muscles are showing potential for improve rehabilitation outcomes [116–118].

In this dissertation, a combinational approach, where robotic technology is combined with artificial stimulation of impaired muscles, is investigated and clinically evaluated. Nevertheless, prior to describe the objectives and organization, an overview on stimulation technology and its applications is given in next section.

1.4.3 Neuroprosthetic functional compensation and rehabilitation of walking

Another technological approach for rehabilitation and/or functional compensation of walking in SCI is the electrical stimulation of neuromuscular tissue of the lower limbs. By adequate configuration of the stimulation, paralyzed muscles of the person with SCI can generate walking movement with a rehabilitative or compensating aim.

Electrical stimulation of muscular tissue has been known since the first observations of Luigi Galvani in 1790, who first observed motion after applying electrical wires to leg muscles severed from frogs. Later in 1831, Michael Faraday showed that electrical currents applied to nerves could create active movement [119]. Since the earliest application of superficial electrical stimulation at the peroneal nerve for correction of drop foot in persons with hemiplegia [120], it has been widely investigated as a means for rehabilitation and compensation of motor disorders [121, 122]. Alternate forms of stimulation can be found in the literature for different applications from muscular stimulation [122], but are out of the scope of this dissertation, which focus on the application of stimulation of paralyzed muscles through superficial electrodes.

Muscle Electrical Stimulation (MES) has been widely explored as a means of walking compensation in SCI subjects, whereby the muscles of the user are stimulated by previously configured electrical impulses to generate joint movement [123, 124] (figure 1.10). Here, the *Functional Electrical Stimulation* (FES) refers to the process of *pairing the stimulation simultaneously or intermittently with a functional task* [125], constituting a *motor neuroprosthesis* (NP).

FIGURE 1.10: Parastep system [126]

The first applications of a NP in paraplegia used superficial FES to stimulate the quadriceps and gluteus to induce gait patterns [127], and to study the correction of drop-foot [120]. The NP developed by Krajl in 1983 [128] was the first that achieved walking in a paraplegic patient by closed-loop stimulation of the quadriceps muscle group and the peroneal nerves. The last two decades have since seen the development of several NP systems based on pioneering designs [129–137]. The use of NP-assisted walking enhances walking ability and distance in complete and incomplete SCI, even when the NP is not in use [86].

Several effects due to use of NP in SCI persons are described in literature: strengthening muscles, enhancing circulation and blood flow, reducing pain, healing tissue, retarding muscle atrophy, and reducing spasticity [86, 138–140]. These benefits are dependent on the nature of the injury [86, 139]. Besides, the artificial activation of the person's paralyzed muscles provides further physiological benefits to the impaired user [137, 139]. However, electrical stimulation has shown to induce muscle damage, revealed as histological changes of muscle fibers and connective tissue, increases in circulating creatine, changes in muscle strength and development of delayed onset muscle soreness [141–144]. Results in the literature are contradictory, showing that stimulated muscle damage are of similar magnitude than voluntary-induced isometric contractions [141], or higher [142]. Related to SCI persons, the myofiber damage due to FES-training was shown to be of similar magnitude than the denervation process [145].

NP technology features several unresolved limitations for widespread use for rehabilitation or functional compensation of walking. The specific nature of muscle force developed by electrical stimulation challenges the control task of a NP. Stimulated muscle response is non-linear and time-varying, changing as the muscle fatigues, and also dependent on the training effects over different sessions, strengthening the muscle and increasing its fatigue resistance [146–148]. Furthermore there is a significant time delay between the stimulation onset and the force production [149]. Muscle fatigue is one of the main difficulties for controlling muscle force generated by the NP, as the muscle performance dramatically changes with it [150–152].

The neuromuscular system is highly multidimensional, with several muscles acting over the same movement direction of a joint [153]. Recent advances in NP technology offer the possibility of achieving more complex and efficient stimulation [154]. The control of NP systems has been improved by using multichannel stimulators that can be combined with percutaneous and implanted electrodes, leading to improved muscle selectivity, as each muscle uses a different electrode [124, 155]. Closed-loop control of NP improves functional output by automatically adjusting the stimulation in the presence of perturbations or fatigue. Most of the commercial systems are operated in an open-loop fashion [121], since small, implantable sensors for force or position feedback are not available yet.

1.5 Conclusion

Consequences of a damage on the spinal cord varies widely. While there is not a complete cure developed yet, multidisciplinary approaches of rehabilitation programs are focused to increase functional independence of the person with a SCI. Among the several functions addressed, literature suggest that at the end of the rehabilitation process, mobility should be fully addressed, being restoration of walking ability a highly important objective for persons with SCI.

Therapies for rehabilitation of walking relies on the assumption that task-oriented practice promotes mechanisms of neural plasticity, muscle strength and learning of compensation strategies that increase walking ability of the person with SCI. Robotic technology holds a considerable potential to drive such interventions, but nowadays functional outcomes are similar to traditional therapy. A more challenging and rich walking therapy under the AAN approach, along with combinational therapies have been recently proposed to increase rehabilitation outcomes. The combination of robotic and NP technologies holds potential for it, due to the benefits that the NP technology provides to SCI patients along with the possibility of minimize its main disadvantages through adequate use of robotic technology.

1.6 Framework, objectives and organization of the dissertation

1.6.1 Framework

The topic of this dissertation is the combination of robotic and neuroprosthetic technology as a novel approach to provide hybrid rehabilitation therapies of walking after a SCI. Limitations of current robotic rehabilitation therapies motivate the combination of a robotic exoskeleton with a NP in an attempt to maximize the advantages of each approach and mutually overcome their respective limitations. Early muscle fatigue generated by stimulation is a major limitation that prevents its widespread use for rehabilitation or compensation of walking. This is an essential feature that must be targeted within the hybrid approach, taking advantage of robotic technology to actively manage fatigue. Furthermore, the combination of both technologies posses its own challenges due to the lack of hybrid NP-robot control proposals in the literature.

The work presented in this dissertation towards the development and clinical evaluation of a innovative hybrid walking therapy is framed within two research projects: *REHABOT* (Ministerio de Ciencia e Innovación, grant DPI2008-06772-C03-02) and *HYPER* (Hybrid Neuroprosthetic and Neurorobotic Devices for Functional Compensation and Rehabilitation of Motor Disorders, grant CSD2009-00067 CONSOLIDER INGENIO 2010). Within these research projects, cutting-edge research is conducted in the field of hybrid robot-NP actuation and control for rehabilitation of motor disorders. This dissertation constitutes the proof-of-concept of hybrid walking therapy for SCI patients for these projects.

1.6.2 Objectives

The objective of this dissertation is **to design and validate a hybrid walking therapy with fatigue management for spinal cord injured individuals**. Around this main objective, several open issues are stated, with a set of key scientific and technical questions that need to be addressed in this dissertation. Those questions constitute the partial objectives that contributes to the main objective.

PROBLEM 1: *To propose a conceptual design for combining stimulation and robotic actuation in a single ambulatory device.* The proposed hybrid walking therapy is a novel approach

where few devices can be extensively analyzed to extract good design criteria to address SCI walking rehabilitation. Therefore a precise and comprehensive analysis of the devices must be performed. This analysis must answer following questions:

Q1: What specifications are better suited for designing a hybrid exoskeleton for implementing a hybrid control of walking in SCI?

Q2: What is the most suitable way of assessing the impact of the hybrid walking therapy on SCI patients?

Q3: Which SCI patients can benefit from hybrid walking therapy?

A detailed state-of-the-art (SoA) will provide information and criteria to answer these questions. Besides technical aspects, the SoA analysis must also provide criteria for investigating the effects of this therapy on SCI patients, which ought to be implemented when designing a validation protocol.

PROBLEM 2: *Muscle fatigue prevents the use of neuroprosthesis.* This problem has being extensively addressed in the literature pertaining MES but specific open issues prevent the application of an effective fatigue management strategy in an ambulatory hybrid device. Among them, quantification of muscle fatigue still remains unsolved. Thus the following questions are answered:

Q4: Which type of criteria would be useful for estimating muscle fatigue?

Q5: How can this criteria be integrated in the robotic controller to manage muscle fatigue during walking therapy?

Q6: What muscle fatigue management strategy can be implemented with early detection of muscle fatigue?

Monitoring muscle fatigue is of the most importance for implementing walking therapy with NP. A suitable criteria would allow to monitor this phenomena, adapting the therapy to the specific muscle response. Furthermore, novel strategies for muscle fatigue management based on the personalized fatigue response can be investigated. Integrating this criteria within the hybrid controller would allow to modulate the balance between the NP and robotic controllers regarding the specific muscle response.

PROBLEM 3: *Control of a hybrid system, comprised by a neuroprosthesis and a robotic exoskeleton, needs specific control developments that effectively manages these systems in combination with the remaining functional ability of the SCI patient.* There are no proposals for hybrid control of exoskeletal robots in which the controller balances both technologies. Most hybrid walking exoskeleton in the literature features a parallel actuation of the NP and the robot. The non-linear characteristic of muscular force generation due to stimulation posses challenges to the hybrid control task. To address these problems, the following questions are answered:

Q7: How to control the robotic exoskeleton in order to cooperate with the NP control?

Q8: How to implement a NP controller that can be modulated within the hybrid controller?

Q9: How to design the hybrid controller to balance NP and exoskeleton actuation?

Q10: What is the impact of hybrid walking therapy on SCI patients?

Precise control of joint movement generated by stimulation is a difficult task that depends on complex control strategies and muscle dynamics. Besides, the robotic exoskeleton must implement a compliant behavior that can allow for improved performance of the power generated by the muscles under the AAN approach.

1.6.3 Organization

This dissertation is organized in seven chapters. Chapters 2 to 7 addresses specific topics that are related to the development and validation of the hybrid approach, providing answer to the questions stated, while chapter 8 resumes the main conclusions of the work and provides future research and development activities, proposed to improve the work presented in this dissertation.

Chapter 2 presents the SoA on hybrid ambulatory exoskeletal robots. From this analysis, hardware and controller design criteria, as well as evaluation criteria, are derived to guide the developments and studies presented in this dissertation. In this chapter answers to Q1 and Q2 are provided.

Chapter 3 presents the design and development of the robotic platform that implements the hybrid therapy of walking for SCI. Experiments with healthy subjects are conducted to characterize the joint controller. In this chapter the target SCI population, that also determine the design of the robotic exoskeleton and the control approach, is defined. Criteria for selection of this target population is given. In this chapter, answers to Q3, Q5 and Q7 are provided.

Chapter 4 presents two experimental studies related to fatigue of artificially stimulated muscles, conducted with SCI patients. These studies address specific topics related to muscle fatigue estimation and management strategies, compatible with the hybrid approach developed in this dissertation. This chapter addresses Q4 and Q6.

Chapter 5 presents the development of the NP controller and a novel approach for hybrid control of walking. Experiments with healthy subjects are conducted to characterize the NP controller. Answer to Q8 is provided in this chapter.

In chapter 6, experimental results of a validation study conducted with a group of healthy subjects are presented. The experiment aims to validate the hybrid-cooperative approach prior to the clinical evaluation with a group of patients. Answer to Q9 is provided in this chapter.

Chapter 7 investigates the effects of the hybrid walking therapy in a population of SCI patients. This study represents the proof-of-concept of the hybrid walking therapy with fatigue management for SCI, therefore addressing Q10.

Chapter 8 concludes the dissertation, gathering the main conclusions attained from this dissertation. Publications and dissemination activities originated from this dissertation are summarized. Finally, future research and development activities originated in this dissertation are proposed.

Chapter 2

State of the Art on Hybrid Exoskeletons[1]

As proposed in chapter 1, the combination of NP and robotic technologies has emerged as a promising approach for both gait compensation and rehabilitation, bringing together technologies, methods, and rehabilitation principles that can overcome the drawbacks of each individual approach. This chapter reviews the literature pertaining lower limb hybrid robotic exoskeletons. The main challenges in designing and developing hybrid lower limb hybrid robotic exoskeletons are identified, along with the most relevant features that must be considered for the functional assessment of individuals with SCI. Two approaches for designing were identified in the literature, which was assumed for sorting the hybrid robotic exoskeletons. The literature shows the feasibility of the hybrid approach, although several challenges are not adequately targeted. Effective closed-loop control of the NP along with AAN control approaches should be implemented for effective management of muscle fatigue and implementing control criteria for balance NP and robotic actuation. Besides, clinical evaluation must comprise clinically relevant evaluation procedures and metrics.

2.1 Introduction

There have been many attempts to improve gait performance and decrease energy expenditure by combining a NP with different types of passive or reciprocating orthoses. However, such approaches provided little improvement in terms of energy cost and gait velocity. Specifically, a recent review has concluded that there is limited evidence to support the use of both bracing and NP for additional functional ambulation benefit in paraplegic patients with complete SCI [86].

[1]This chapter is partially based on the following articles:
A. del-Ama, A. Koutsou, and J. Moreno, **Review of hybrid exoskeletons to restore gait following spinal cord injury,** Journal of Rehabilitation Research and Development, vol. 49, no. 4, pp. 497514, 2012.
A. J. del-Ama, J. C. Moreno, A. Gil-Agudo, A. de-los-Reyes, and J. L. Pons, **Online assessment of human-robot interaction for hybrid control of walking,** Sensors, vol. 12, no. 1, pp. 21525, Jan. 2012.

Thus, the high energy cost associated with these hybrid bracing systems appears to be the main drawback [156–159].

The addition of a NP to a robotic exoskeleton has been proposed to take advantage of the muscle power generated to reduce the energy demand of the robotic exoskeleton, which would result in a lighter system. Moreover, such hybrid robotic exoskeletons should promote more effective neural plasticity than other standard practices like treadmill training, due to the intensive, community-based, gait practice involved. This gait practice takes place during daily training and thus, increased user participation is promoted during walking training. While FES-induced gait has several benefits, mainly related to muscle strength and cardio-respiratory fitness [86,139,140,160], it is perhaps not so effective in gait restoration [86, 161] and is an approach that is limited to a therapeutic environment [137]. Furthermore, muscle fatigue induced by MES leads to interruptions in training. Improved management of muscle stimulation is therefore crucial to the development of successful hybrid robotic exoskeletons that can be used for longer periods of time.

For the purpose of this chapter, it is defined "hybrid exoskeletons" as *those systems that aim to compensate or rehabilitate gait in activities of daily living by means of delivering and controlling power to the lower limb joints, in which the net joint power results from the combination of muscle activation with NP and electromechanical actuation at the joint level.* This concept was first introduced in 1978 [162], though actual physical construction and preliminary results were not reported until 1989 [67]. Different systems have since been proposed, with diverse actuation and control principles. However, two main categories can be distinguished in relation to the actuation principle of the robotic joint: a) power dissipation at joint (braking or clutching), and b) active joint actuators. This criteria was adopted in for the review of hybrid exoskeletons.

2.2 Semi-active hybrid exoskeletons

Attaching controllable brakes to a passive gait orthosis allows the use of NP as a power source to generate gait, controlling joint movements by closed-loop control of joint trajectory. This poses a solution to the problem of joint trajectory control generated by NP [163]. In addition, placing joint brakes on the orthosis obviates the need for stimulation of muscles during stance phases of gait, which is very exhausting for the muscles under stimulation.

2.2.1 Variable Hip Constraint Mechanism (VHCM)

Several modifications have been introduced in the HKAFO design in order ti improve walking performance. Among these, unlocking the knee joint during swing to improve foot clearance [133], and increasing the hip coupling ratio to 2:1 to increase step length and reduce energy cost [164] have been tested. Accordingly, a hybrid exoskeleton was developed in which the hip and knee joints are driven by spring clutches that either release or block the joints [165]. While more flexible step length and improved walking speeds were achieved, the posture and stability of the user was compromised due to the hip actuation principle (spring clutch), and the onset of muscle fatigue in hip extensor muscles.

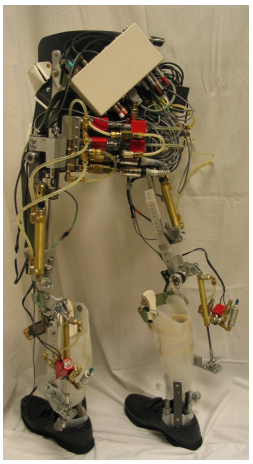

FIGURE 2.1: Variable Hip Constraint Mechanism (VHCM).

To overcome the limitations related to the hip mechanism, newer designs include a variable hip coupling mechanism, in which the coupling ratio between the hip joints could be modified by means of a controllable hydraulic system (figure 2.1) [166–168]. In this apparatus, hydraulic cylinders fixed by rack-and-pinion transmission produce hip actuation. The losses due to friction in the mechanism were quantified as 7% of the hip flexor muscle power required to overcome the passive resistance of the actuator [167, 168]. However, the amount of torque required to move the hip mechanism was later reported to be 10% of the hip torque generated during NP-driven gait [166]. The control of the hydraulic circuit avoids bilateral hip flexion, while providing trunk and hip stability, and free or coupled hip movement during the swing phase of gait. This allows the user to modify their step length without the intervention of the system.

This hybrid exoskeleton also features a solenoid-activated spring clutch mechanism for the knee joint, blocking flexion of the knee during stance while allowing some degree of knee flexion during swing. The ankle is driven by a purely elastic element. The NP includes 16 channels of intramuscular stimulation, which collectively control the hip, knee and ankle extensor and flexor muscles, including the hip abductors and trunk extensors. The FES system is preprogrammed with a set of stimulation parameters to generate gait. Control of hybrid walking, hereinafter hybrid control[2], is achieved by means of a finite-state machine that detects gait events and sends those events to both the NP and the exoskeleton controller. NP-driven gait works in an open-loop and the robotic exoskeleton can block or release the knee joints and couple or uncouple the hip joints.

The effects of the hybrid exoskeleton on kinematics were studied in five non-disabled subjects and compared to a reciprocating orthosis and FES-driven gait. Knee and hip kinematics when walking with the hybrid exoskeleton resembled a normal pattern. Hip kinetics was also improved when the finite-state machine of the hydraulic hip mechanism was enabled [169]. This represented a remarkable improvement over the RGO with a fixed hip-coupling ratio. However, the total weight of the system (22 kg.) reduced gait speed (25% lower) increased muscle activation.

[2]In the field of automatic control, hybrid control refers to the control of systems comprised by continuous and sequential states. In this dissertation, hybrid control (or hybrid controller) refers to the control of a hybrid exoskeleton to provide walking.

The effect of the hybrid exoskeleton system on knee kinematics was also studied in a subject with paraplegia resulting from complete SCI (T7, ASIA A) [166], but no details on gait performance or energy expenditure were reported. As in non disabled subjects, this hybrid system may result in energy exhaustive gait. More research is pending to extend the benefits of the variable hip coupling mechanisms to rehabilitation outcomes.

2.2.2 Controlled-Brake Orthosis (CBO)

The concept of controlling the joint movement generated by FES with joint brakes was first studied by Durfee and Hausdorff [163]. Following this concept, the Controlled Brake Orthosis (CBO) with eight degrees of freedom and four FES-channels have been developed (figure 2.2) [170,171]. In this system, FES is applied to the quadriceps and peroneal nerve to generate knee extension and a flexion reflex respectively, while the orthosis controls the knee and hip flexion-extension using magnetic brakes. The ankle is driven by an elastic actuator that controls the dorsal flexion to avoid foot drop; free hip adduction-abduction is provided with a limited range of movement [171]. This configuration results in a light orthosis (6 kg.) with highly backdrivable joint actuators (magnetic brakes).

(a) Lateral view of CBO. (b) Walking experiment with CBO.

FIGURE 2.2: Controlled Brake Orthosis (CBO) [170].

The control strategy (figure 2.3) relies on the use of joint brakes to control the limb position and velocity generated by the NP. The joint position error and brake torque are used to detect excessively low and high levels of stimulation, respectively. Both parameters are integrated on the basis of one step and combined in a weighted difference. The amplitude of muscle stimulation is controlled as a function of trajectory and torque error, averaged on a step-by-step basis to stimulate the muscles with the amplitude necessary to achieve joint movement (figure 2.3). As a result, this combined metric acts as a NP regulator on the next step [170]. With this control strategy, the CBO system is the only system that attempts to actively control muscle fatigue by closing the NP control loop.

This hybrid approach was first evaluated in a subject with paraplegia resulting from complete SCI (T6). The results with the CBO revealed a reduction in the duty cycle of muscle stimulation from 85% during NP gait to 10% with the hybrid system and an improvement in knee trajectory with

respect to NP-only gait [170]. However, the flexion reflex was found to change considerably with time, leading to poor performance at the hip joint. A further evaluation was later performed in a study on four subjects with complete and incomplete paraplegia resulting from SCI (ranging from T7 complete to T8 incomplete). This study evaluated the performance of the CBO in terms of muscle fatigue, metabolic cost and gait performance when compared to NP-only gait [172]. One subject increased its walking speed, while distance increased in two subjects. Muscle fatigue was also assessed by measuring the quadriceps isometric recruitment curve as the relative decrease in peak torque. This parameter revealed a lower torque decrease when using the CBO. This study also investigated the relative effects on metabolic cost when using the CBO rather than NP alone, in terms of heart rate, blood pressure and oxygen consumption. No differences were observed between the two systems.

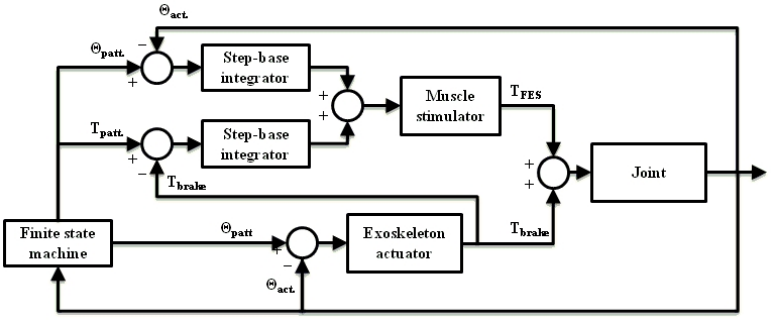

FIGURE 2.3: Hybrid control strategy of CBO [170].

As previously mentioned, the CBO actively manages muscle fatigue controlling stimulation amplitude based on the effect of the stimulation on the joint trajectory. Another approach followed by other groups to manage muscle fatigue depends on the optimization of the stimulation strategy and the use of energy storage. By the combined use of an elastic element and a joint brake, it is possible to store energy from the quadriceps stimulation during swing, which is the less demanding condition for the muscle, and release the energy in other phase of gait or joint. Therefore the need for muscle stimulation is reduced by the combined use of joint brakes for the stance phases of gait and the use of energy storage. Also stored spring energy could be used to replace stimulation of the hip flexors or withdrawal reflex, which has shown low effectiveness for eliciting hip flexion [67, 172].

2.2.3 Spring Brake Orthosis (SBO)

One of the hybrid orthosis with energy storage was developed by Gharooni et al., the Spring Brake Orthosis (SBO) (figure 2.4) [173,174]. In this system, knee flexion after toe-off is generated by the energy released by a spring, which also causes the hip to flex due to gravity action, therefore driving the hip and knee joints to a flexed equilibrium position [173]. At mid-swing, knee extension is achieved by quadriceps stimulation, at the maximum intensity which is safe and can be tolerated by the subject, to accelerate the shank until the knee reaches full extension. Extension of the knee during this phase stores energy in the spring placed at the knee actuator [174]. A fuzzy inference system determines burst duration to control knee joint kinematics on the basis of knee joint position and velocity error [173]. Recently a Proportional-Integral-Derivative (PID) controller has been introduced [175]. The NP control system is intended to achieve the

limb's maximum acceleration in the shortest period of time to minimize muscle fatigue, whereas hip and knee joint brakes are used to give support during stance phase [173]. A preliminary test on a non-disabled subject was reported as a proof-of-concept in which the knee and hip kinematics were addressed as a result of the combined NP, joint brake and energy storage at the knee actuator [173, 174].

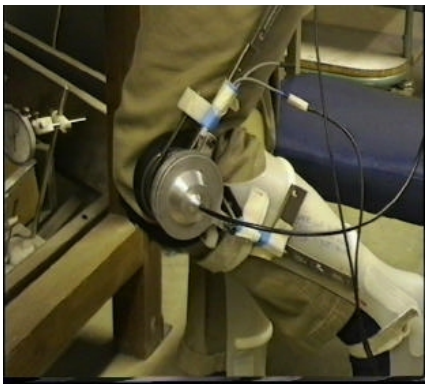

FIGURE 2.4: Spring Brake Orthosis (SBO) [173].

2.2.4 Joint Coupled Orthosis (JCO)

The Joint Coupled Orthosis (JCO) was developed based on the elastic-energy storage concept, but in this case, the elastic element acts across both hip and knee joints (figure 2.5) [176]. A unidirectional mechanical coupling allows a spring to bias the knee and hip joints towards an equilibrium position in which both joints are flexed; therefore, flexion of the knee generate hip flexion. The exoskeleton also have hip and knee friction brakes that provide control of hip and knee joints during the stance phase and release after toe-off. As in the former hybrid exoskeleton, two NP channels are used to stimulate quadriceps muscles of both legs at the peak of hip flexion, which fully extended the knee during the swing phase and also stores energy on the spring [176, 177]. In this case, FES pulse parameters are fixed and the stimulation timing is not controlled. A preliminary evaluation of walking performance was performed on 10 non-disabled subjects wearing the exoskeleton on one leg. The experiments consisted of three cycles of 5 minutes walking and 1 minute relaxation while measuring the range of knee movement. While the range of knee movement was reduced during the first three cycles, it then stabilized at 85% of the range of movement measured at the beginning of the experiment [176]. These results indicate that this energy storage approach may delay the onset of muscle fatigue, although to our knowledge, the performance of this system has not been evaluated with SCI subjects.

2.2.5 Energy Storing Orthosis (ESO)

A hybrid exoskeleton that stores energy from the stimulation of the quadriceps muscles has also been developed (figure 2.6) [178]. A peculiarity of this system is that the Energy Storing Orthosis (ESO) uses the energy-storing concept to decouple hip extension and flexion; pneumatic circuitry is used to extract, store, transfer and release energy from the quadriceps to the hip [178, 179]. Also elastic actuators are included to keep the hip and knee joints in a flexed equilibrium position [178,180]. At mid-swing, the quadriceps is stimulated and the knee extends, storing energy in the

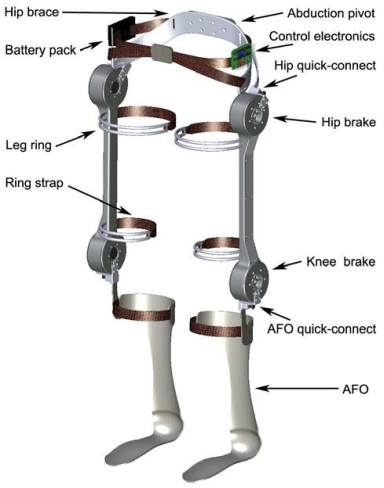

FIGURE 2.5: Joint Coupled Orthosis (JCO) [176].

pneumatic accumulator. Simultaneously, energy is also stored in the elastic storage element at the knee joint. After full extension, the knee is locked and energy is released into the hip actuator and hip extends, enabling forward progression and storing energy in the hip elastic storage element. Therefore, this pneumatic system allows to decouple control of hip and knee joints. A wrap spring brake controls joint trajectory and gives joint support during stance [178, 179]. An optimized version of this design with rubber bands as the elastic elements was tested on a subject with paraplegia resulting from SCI injury (T12) [180]. However, the results of this preliminary evaluation were restricted to safety and fitting functions of the orthosis, and thus, no conclusions can be made with respect to gait parameters.

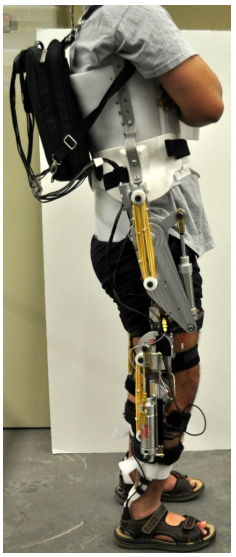

FIGURE 2.6: Energy Storing Orthosis (ESO) [180].

2.3 Active hybrid exoskeletons

The main drawback of the hybrid exoskeletons controlled by joint brakes is the inability to provide full control of the joint, since joint brakes are not capable of delivering torque. Therefore, movement is generated only by the muscular action induced by the neuroprothesis; since movement quality is low in terms of joint trajectory and velocity, and muscle fatigue is likely to hinder the muscle power for driving the limbs, an external source of controlled power is deemed necessary. This requirement is more important if the neuroprosthesis features an open-loop control, where variations in muscle power are controlled only by the robotic exoskeleton.

Therefore, in contrast to joint brake hybrid exoskeletons, active actuator hybrid exoskeletons have been investigated. These allow control of the power delivered at the joint, which potentially allows to perform effective closed-loop control of joint movement.

2.3.1 Hybrid Assistive System (HAS)

One of the first hybrid systems developed and tested [67] was based on an existing concept, the Self Fitting Modular Orthosis (SFMO) [162]. To develop the Hybrid Assistive System (HAS), the SFMO was configured with a lightweight knee-ankle brace equipped with a direct current (DC) servomotor and a motor-driven drum brake coupled to the knee joint with a ball screw. The actuator delivers provides controlled power for assisting extension and flexion joint movement. The ankle joint is actuated by a spring mechanism to control dorsal flexion. The NP system consists of six channels acting on the gluteus medius for balance; the quadriceps for hip flexion and knee extension; and the peroneal nerve to generate the flexion reflex, allowing knee, hip, and ankle dorsal flexion. The stimulation parameters for each channel are fixed following prior calibration of the subject. Potentiometers are used to measure joint rotation. Force transducers and switches on walkers or crutches are used to detect external loading.

Initial results with the HAS focused on testing finite-state control algorithms to combine brake, motor and muscle stimulation. Further evaluation with a patient who suffered an incomplete cervical (C) C5/C6 lesion with no voluntary control of the lower extremities compared walking performance in three scenarios: SFMO-only, NP-only and HAS. The results with HAS revealed a small improvement in gait velocity and physiological cost (measured by oxygen consumption) with respect to the other systems. However, the knee flexion reflex generated by the HAS can be problematic, with flexion deteriorating after 10 minutes of walking, limiting gait duration [67].

2.3.2 Hybrid Power Assist Orthosis (HyPo)

The active control of hip and knee joints by means of actuators was also explored with the Hybrid Powered Orthosis (HyPo, figure 2.7) [181, 182]. The HyPo is designed with the motors and gearboxes located in the front part of the orthosis, allowing the user to wear it while sitting. DC motors (70 Watts, 0.14 Nm) and gearboxes (156:1) are included to control the hip and knee joints of both legs, allowing the gait to be generated without NP. Open-loop NP control is used for the quadriceps of both legs, while the DC motors are used for compensation of joint trajectories with proportional control of position and velocity. Note that in this case, the actuators are dimensioned to allow the generation of gait without NP, therefore taking into account that

muscle fatigue can make useless the use of NP while walking. Stimulation pattern and joint control are synchronized throughout an entire gait cycle because no information is provided to discriminate between stance and swing. The optimization of the stimulation patterns for knee joint movement were reported as a proof-of-concept, although no quantitative data was included in this study.

FIGURE 2.7: Hybrid Powered Orthosis (HyPo) [181].

2.3.3 WalkTrainer

The WalkTrainer was developed as a hybrid exoskeleton with closed-loop control of NP that relies on an estimate of the interaction forces between the user and the robotic exoskeleton (figure 2.8) [183]. The WalkTrainer robotic exoskeleton controls hip, knee and ankle joints, as well as pelvis movement, with six degrees of freedom, and it is attached to a moving frame which supports the robotic exoskeleton and the user via a weight bearing system similar to treadmill training systems (figure 2.8). Motorized wheels assist walking with the robotic exoskeleton. The NP closed-loop controller combines the feed-forward model of the torque-intensity characteristics of the muscle involved in the movement and a classic PID controller to compensate for torque error, while the DC motors control joint trajectories [184]. The joint torque exerted by the user is estimated based on structural forces that result from the interaction of the body segments and the robotic exoskeleton. The system is intended to minimize such interaction forces by modulating muscle stimulation during walking.

FIGURE 2.8: WalkTrainer [183].

A preliminary clinical evaluation of the WalkTrainer was performed on six subjects with paraplegia due to SCI lesions. Two of the subjects suffered complete paraplegia (ASIA A) and four had incomplete paraplegia (1 ASIA C and 3 ASIA D), although no information on the level of the lesion was provided [183]. The experiments consisted of trials of 1 hour per week for 12 weeks, resulting in a reduction in the Ashworth Spasticity Scale[3]. This NP closed-loop control scheme formed the basis to develop several other systems: MotionMaker [184, 186, 187], a stationary programmable test and training system for the lower limbs, and The lambda [188], a training system for the lower limbs based on an end effector controller. Although the MotionMaker and Lambda systems are regarded as hybrid exoskeletons, they are beyond the scope of this review as it is focused on hybrid exoskeletons intended to compensate gait.

2.3.4 Vanderbilt exoskeleton

This is one of the most recent robotic exoskeleton that have been proposed. The Vanderbilt robotic exoskeleton (figure 2.9) was designed for providing walking function compensation to paraplegic patients [189, 190]. This robotic exoskeleton features DC motors for hip and ankle joints, in addition to normally-locked knee electro-mechanical brakes [189, 190]. Hip ab/adduction is accommodated by compliance of the hip segment. The robotic exoskeleton includes potentiometers for measuring joint rotation and accelerometers in each thigh segment. This set of sensors gives the robotic exoskeleton the ability of estimate the location of the center of pressure over the floor, which is used for implementing user commands. This device features a distributed control architecture, in which a high level controller, in the form of a finite-state-machine, triggers the kinematic patters to the low-level joint controllers. Joint controllers consist of variable-gain proportional-derivative feedback control scheme. The authors state that with this design, the impedance of the tracking task can be modulated. Lastly, the robotic exoskeleton features a custom-made stimulator module that plugs into the main control board.

FIGURE 2.9: Vanderbilt exoskeleton [189, 190].

A preliminary evaluation with a T10 complete paraplegic (ASIA A) was conducted regarding ability of the robotic exoskeleton for providing robotic compensation of walking and transferring from a wheelchair [189, 190]. In further studies, two hybrid controllers were proposed, each for controlling knee extensor and flexor muscles. Regarding knee extensor muscles, a gradient-based adaptative controller was proposed [191]. This controller aims to iteratively find a simplified model of the muscle dynamics, comprised by a proportional gain and a time-delay. The control

[3] Asworth scale measures the severity of the spasticity in a range from 0 to 4 [185]

approach was evaluated with the aforementioned patient during lifting tasks, in which the patient remained sitting while extending the knee lifting a dead weight. Among the results provided, the stimulation controller needed 16 repetitions for convergence. The stimulation affected to the trajectories developed during the task, which were closer to the reference than without using the stimulation. The energy reduction due to the contribution of the stimulation was reported as 56% [191].

Hybrid control of the knee flexor muscles was proposed in a further study [192]. There, an on/off controller for stimulating the muscles during stance phase was proposed. The controller modulates the stimulation timing regarding the extension torque provided by the motors during stance phases of gait, which was modulated in a cycle-to-cycle adaptative controller. The results showed that the stimulation decreased the power delivered by the motors 34%. Muscle fatigue was observed by the authors, although it was claimed that not affectting to the overall system performance.

2.4 Discussion

2.4.1 Main achievements

The hybrid exoskeletons reviewed here demonstrate the feasibility of combining a neuroprosthesis with a robotic exoskeleton to provide joint control and reduced energy demand. Various approaches have been used to combine NP with a robotic exoskeleton, and the NP systems reviewed range from implanted systems with up to 16 channels [166] to single channel stimulation [173, 177, 179]. The robotic exoskeletons are designed to provide joint support during stance and trajectory control by means of brakes or clutches [171, 173, 177, 179]. Other robotic exoskeletons have active actuators that can either dissipate or add power to the joints, thereby providing a means of control while allowing complete joint movement to improve system performance [67, 182–184, 190].

Among the systems reviewed, the simplest means of implementing a hybrid control strategy is to use open-loop electrical stimulation and closed-loop joint movement or torque by means of an actuator (e.g., brakes [166, 177, 179] or motors [67, 193]) (figure 2.10).

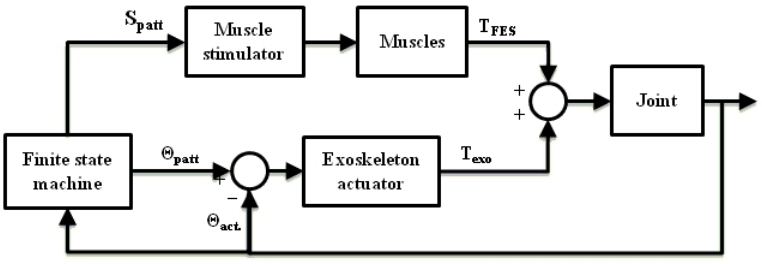

FIGURE 2.10: Scheme for open-loop NP control. Implemented in hybrid exoskeletons [67, 166, 177, 179, 193].

This control strategy has the disadvantage that no information about joint movement or the torque produced by the NP is fed into the controller, and therefore, there is no direct muscle control. Closed-loop muscle stimulation in a hybrid configuration is a complex task that depends

on the availability of robust parameters directly related to muscle performance. Some indirect measurements have been proposed in order to estimate the performance of the stimulated muscle for closed-loop control. These include monitoring the induced joint movement to estimate the timing of stimulation in order to minimize muscle fatigue [173,174], or monitoring of interaction forces between the robotic exoskeleton and the legs [183,186,187,194] to generate a specific joint torque pattern (figure 2.11). Combining these two approaches, the CBO scheme controls the amplitude of the stimulation on the basis of both position and the torque error produced by the electrical stimulation, aiming at a reference joint movement during the swing phase [170] (figure 2.3). In a recent proposal for a hybrid controller, the motor control signal is minimized within a gradient-based adaptative controller for obtaining a simplified muscle model for control of stimulation [191].

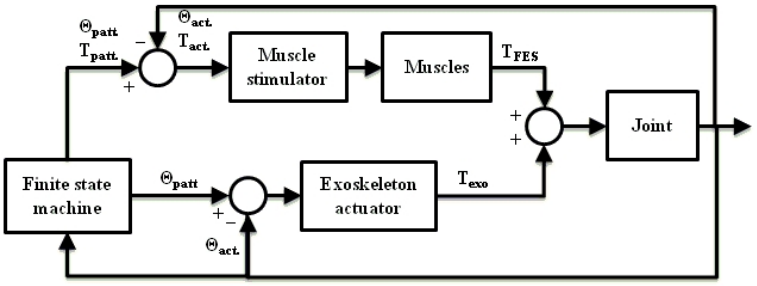

FIGURE 2.11: scheme for closed-loop NP control. Implemented in hybrid exoskeletons [173,174,183,186,187,194].

Managing muscle fatigue is a critical factor in the design of a hybrid exoskeleton, because the unnatural aspect of muscle recruitment with current NP systems, which leads to early muscle fatigue. This effect is critical in cases of muscle atrophy, which are typically found in the SCI population. Various approaches have been used to address the issue of muscle fatigue. One approach is to minimize the muscle stimulation duty cycle. This has been tested using joint brakes that block the joints during the stance phase, eliminating the need for stimulation in this demanding phase [166, 171, 173, 176, 178]. Extending this concept, other approaches store energy from the quadriceps muscle during swing, taking advantage of the power of the quadriceps muscle and its accessibility to surface electrodes. The stored energy can then be released and transferred to generate hip flexion [173, 176] or extension [178]. In an experiment performed with nondisabled subjects [177], muscle fatigue was addressed by measuring the range of knee movement during a walking trial with the robotic exoskeleton. This range of movement stabilized at 85% of the initial steps, indicating that this approach maintains the level of muscle fatigue in nondisabled subjects [176,177]. While this is an energy-efficient strategy, it cannot be regarded as a rehabilitation approach because it is restricted to a single leg muscle and the stimulation pattern does not resemble normal muscle activation during nondisabled gait.

A second approach involves the management of the stimulation parameters based on indirect evaluation of muscle fatigue. Using this approach, the CBO controls the stimulation amplitude as function of the position and torque error resulting from stimulation. The position error is used to detect when muscle performance is insufficient to achieve the trajectory, while the brake torque is used to detect excessive stimulation intensity. Combining the two measures, control of the stimulation is regulated for the next step [170]. However, this approach lacks the ability to compensate joint trajectory when the muscle does not generate enough joint torque to achieve

movement. As a result, this strategy is not effective when muscle fatigue or habituation occur [172]. An effective muscle fatigue strategy within the framework of rehabilitation involves the implementation of active actuators on the robotic exoskeleton, allowing muscle relaxation while performing functional movement by changing the stimulating parameters, primarily the intensity. A similar approach was considered in the development of the WalkTrainer by monitoring the current delivered by the FES and the joint power generated by the muscles through force sensors on the robotic exoskeleton. It is hypothesized that as long as muscle fatigue appears, more stimulation must be delivered to the muscles to maintain the power generated at the joints. However, no detailed information on the control strategy when muscle fatigue appears has been reported [186].

Because hybrid systems are intended for subjects with SCI, a preliminary evaluation in such patients is critical. Some systems have been tested with nondisabled subjects to verify the capacity of the orthosis to provide safe single- and double-stance support and to detect gait transitions [166,169,176,180]. In other studies, the nondisabled tests served to assess the control strategy more than the safety issues [173, 193]. Safety and comfort are issues that must be considered in the design process and must be verified prior to SCI testing. Functional evaluation with end-users is an area in which we have detected little consensus in the methods and measures used to evaluate such systems. User evaluation is crucial to generate useful information about the functional performance of hybrid exoskeletons. While testing in both nondisabled subjects [173, 174, 176, 177, 182] and SCI subjects has been reported for some systems, the number of subjects is generally limited and heterogeneous. For example, the CBO was tested on 4 patients with SCI [170,172] and the VHCM was tested on only one T7 complete paraplegic [166]. The HAS was only studied on one case with a C5/6 incomplete tetraplegic [67] and similarly, the ESO was tested on one subject with T12 complete paraplegia [180]. Preliminary results from the evaluation of the WalkTrainer were published from a study of six subjects with SCI without information on the neurological level of the SCI [183]. Moreover, in some cases, the subject characteristics are not homogeneous and combine complete and incomplete SCI subjects in the same test protocol [172, 183]. Because of the complexity and heterogeneity of SCI, even when the same levels of lesion are considered, the data obtained frequently lack reliability and are insufficient to produce valid conclusions, even though marked tendencies may be apparent. Thus, performing these evaluations in larger populations of SCI subjects and in groups more homogeneous with respect to lesion level and degree of severity (complete or incomplete) appears to be necessary.

The systems reviewed in this chapter assessed performance in SCI patients [67, 166, 170, 172, 180, 183] by evaluating walking with the hybrid system while certain variables were recorded. A wide range of variables are reported, which can be classified as gait kinematics variables, temporal-spatial gait variables, physiological cost variables, and other variables related to gait function. Gait kinematics are easy to obtain and provide valuable information about the joint control offered by the hybrid system [166, 172, 183], although they are not reported in some studies [67, 180]. Temporal-spatial variables such as speed, walking distance, step distance and gait cadence are reported in most of the studies reviewed [67, 166, 169, 172]. The physiological cost variables are a set of variables intended to assess the metabolic cost associated with the use of a hybrid system. The physiological cost was not evaluated for all the systems reviewed here, and where it was, different variables were used: oxygen consumption normalized as an indirect measure of the physiological cost [67]; heart rate and blood pressure [170, 172]. Muscle fatigue has also been related to the physiological cost [170, 172, 183], assuming that a decrease in the

stimulation cycle leads to a decrease in muscle fatigue [173, 174, 176, 177, 182]. Other variables analyzed are related to spasticity, coordination [183] and system comfort [180].

2.4.2 Challenges

While the different approaches described in this chapter demonstrate the feasibility of the hybrid exoskeleton concept, management of muscle performance during walking has proved to be challenging when a hybrid exoskeleton is used to rehabilitate gait. To extend the benefits of NP-aided gait to functional rehabilitation, the control strategy must modulate stimulation to delay the appearance of muscle fatigue and thereby increase the usage time and walking distance. This modulation must be based on information on muscle performance, which can be estimated from the interaction between the legs and the robotic exoskeleton [181, 183], although this approach also posses inherent limitations from the coupling between voluntary and stimulated sources of muscle power. Precise neuromuscular models which consider the nonlinearity and time-dependent characteristics of the musculoskeletal system, along with novel methods of monitoring muscle activation, would allow to uncouple the voluntary and artificially sources of muscle power, and therefore refine the control of the neuroprosthesis.

All the hybrid exoskeletons reviewed in this chapter features some sort of position control of the joint trajectory, independently of the actuator design. Since quality of the joint movement generated by the stimulated muscles is low in terms of trajectory and velocity, constant control actions over the lower limb are applied by the robotic exoskeleton to track joint trajectory. A compliant control of the robotic exoskeleton allows unhindered joint movement developed by the stimulated muscles, similarly to compliant control approaches developed for gait treadmill robots [195–197]. This way, the contribution of the neuroprosthesis to mobilize the limb can be optimized.

Along with robotic exoskeleton compliance, closed-loop control of the neuroprosthesis within the hybrid strategy can provide the flexibility required to implement strategies under the AAN approach, which along with user-involvement is thought to be essential to promote rehabilitation [38,198]. The latter is the main area where hybrid exoskeletons offer advantages over robotic treadmill trainers, in which user involvement is difficult to obtain [195]. The AAN paradigm can provide user assistance regarding residual function; hybrid exoskeletons must be able to assess residual physical abilities (voluntary muscle force, joint range of motion, bioelectrical residual activity) as well as sensory-motor function in order to adapt their performance and mode of operation according to the specific residual function. This can be realized through different modes of NP implementations as well as novel hybrid NP-robot control paradigms. To our knowledge, the AAN paradigm has not yet been implemented in the field of hybrid exoskeletons, probably because most of the designs are intended to develop energy-efficient systems to restore gait function. Although reducing energy demand allows for the development of more portable robotic exoskeletons, it cannot be expected to provide any long-term improvement in the functional ability of the user. However, a control approach combining the AAN paradigm with a maximization of user involvement may lead to a long-term improvement in the users functional abilities.

All the hybrid exoskeletons reviewed in this chapter have undergone some form of preliminary evaluation focused on aspects of the exoskeletons safety and energy performance. However, the effects of the external (robotic exoskeleton) and internal (muscles) sources of joint torque on

pathological joints have yet to be investigated. While these systems are functional (i.e., they stabilize the joints during stance), no criteria exist regarding the optimum balance between the robotic exoskeleton and muscle joint torque, based on objective knowledge of the influence of the hybrid system on the joints.

The peculiarities of subjects with SCI hamper the extrapolation of performance testing results. For example, the location of the muscles affected, muscular atrophy in the chronic phase of the injury, impaired sensation and decreased physical capacity are clearly differentiating factors that require specific clinical evaluation in patients with SCI. The systems included in this review either lack data relating to testing in SCI subjects [169,176,177], or the number of subjects is insufficient to confidently link the findings to the hybrid systems [67, 165, 166, 171, 172, 183]. Furthermore, the metrics used to evaluate hybrid robotic exoskeletons vary considerably across studies. Other parameters frequently used in a clinical setting to quantify gait function may be more suitable to evaluate the performance of these systems within the scope of the pathology. Walking speed (10 m walking test, 10mWT [199]), walking distance (6-minute walking test, 6mWT [200]) and the Walking Index for Spinal Cord Injury Version 2 (WISCI II [201]) are three scales used to quantify muscle weakness due to paralysis, and they have been evaluated for their utility, validity and reliability in clinical practice and as research tools [202, 203]. Moreover, the combination of 10mWT, WISCI II and 6mWT could represent the most valid measure of improvements in gait and ambulation [204], providing an objective tool to measure gait improvement when comparing the hybrid exoskeleton with other approaches. A comprehensive evaluation of the performance of a hybrid system should include a combination of variables, such as joint kinematics and kinetics, clinically relevant gait functional scales (10mWT, 6mWT, WISCI-II), parameters related to the physiological cost, such as oxygen consumption and muscle fatigue during use, and usability measures.

2.5 Conclusion

Hybrid exoskeletons have emerged as a promising approach that blends complementary robotic and NP technologies. Two main types of hybrid exoskeletons exist based on the exoskeletons driving principle: braking or active. The state of the art demonstrates that hybrid exoskeletons are feasible systems in which the stimulation is provided with adequate control of joint movement, reducing the energy requirements of the robotic exoskeleton. Management of muscle fatigue is addressed by development of optimized systems that minimize the need for muscular stimulation or by active control of stimulation by closing the NP control loop.

Nevertheless, many challenges remain. Effective closed-loop control of the robotic exoskeleton and the NP will enable implementation of real-time strategies to manage muscle performance. AAN control strategies must also be implemented, taking advantage of NP and robotic systems that work in parallel with the human system. These systems should be used to promote user involvement by performing gait in a challenging real environment. Clinical evaluation must be comprehensive, addressing gait performance, user-perception, and physiological cost through clinically validated functional scales and protocols. This dissertation tackles these challenges. The theoretical and experimental research activities conducted towards the development of a hybrid walking therapy system are presented in the following chapters, bringing new proposals for overcoming these challenges.

2.5.1 Answer to research questions

This chapter provides provides the following answers to research questions Q1 and Q2 stated in section 1.6.2 as follows:

Q1: **What specifications are better suited for designing a hybrid exoskeleton for implementing a hybrid control of walking in SCI?** The analysis of the state of the art identified three challenges. First, muscle fatigue must be addressed, by integrating effective closed-loop control of the NP that allows active management of muscle performance. Second, the exoskeleton must provide compliant joint control, allowing to optimize the NP contribution. Third, assist-as-needed control strategies are needed that maximizes user contribution and adapts to patient residual abilities.

Q2: **What is the most suitable way of assessing the impact of the hybrid walking therapy on SCI patients?** A comprehensive clinical evaluation must address gait performance, user-perception, and physiological cost through clinically validated functional scales and protocols, including the 6mWT and 10mWT walking test and the WISCI II scale.

Chapter 3

Lower limb robotic exoskeleton for hybrid walking therapy[1]

This chapter presents the design of the robotic platform and the low level joint controller that supports the hybrid-cooperative walking therapy (named Kinesis). The chapter begins with the definition of the target population, whose functional needs are translated into design requirements in the second section. As result, the robotic exoskeleton is comprised by active actuators for the knee joints and elastic actuation for the ankle joints. The actuators were selected and dimensioned regarding joint biomechanics during healthy walking. Sensory system of Kinesis includes a force sensor for monitoring leg-exoskeleton physical interaction. An adaptative, hybrid position-velocity admittance controller was developed for compliant control of walking, through a first order torque field imposed around knee trajectory. Experiments performed with healthy subjects confirmed the controller ability for providing compliant assistance during swing and stance phases of walking.

3.1 Target population characteristics

Definition of the target population was undertaken based on the conclusions of an expert panel discussion. The expert panel was comprised by clinicians from the National Hospital for Spinal Cord Injury (HNP) and researchers from the Bioengineering Group of the National Council for Scientific Research (CSIC). The expert panel reached a consensus on defining a target population whose lesion characteristics had preserved hip function. There were several rationales for this decision. Firstly, it initially limited the joints to compensate to knee and ankle, simplifying the problem of control all six joints with hybrid actuation, which allowed to focus on the hybrid control strategy development. Secondly, SCI patients that preserved hip function typically have

[1]This chapter is partially based on the following:
A. J. del-Ama, J. C. Moreno, A. Gil-Agudo, A. de-los-Reyes, and J. L. Pons, **Online assessment of human-robot interaction for hybrid control of walking,** Sensors, vol. 12, no. 1, pp. 215-25, Jan. 2012.
A. J. del-Ama, **Plataforma robótica cooperativa para la compensación de la marcha en lesionados medulares,** Master Thesis, Universidad Carlos III de Madrid, 2011.

preserved abdominal musculature, allowing good trunk control and therefore good balance function. Finally, this group of patients usually features incomplete lesions, preserving innervation at lower limbs muscles, which assures muscular response to the electrical stimulation. Note that in case of complete lesions, denervation develops within the first weeks after lesion, which prevents the muscles from responding to stimulation.

As a result of the above mentioned process, the target population was comprised by patients whose lesion was categorized as *Conus Medularis* [205]. This name is given to injuries that affect the spinal levels among L1 and L2. These lesions are incomplete syndromes, affecting mainly to the nerve branch at the end of the cord. Key muscles for walking that are likely preserved in this kind of lesion are hip flexors and partial innervation of quadriceps muscles. The prognosis of functional recovery of walking is that the patient can walk short distances but depending on the wheelchair for community ambulation [26]. Therefore, a successful overground hybrid walking therapy can provide benefits to this population. The functional characteristics of this lesion that determines the walking function of the patient are the following:

- Preserved hip flexion ability.
- Partial ability to generate voluntary knee extension.
- Paralysis of ankle joint.
- Presence of mild to severe spasticity.

Spasticity is one of the biggest and common secondary symptoms due to SCI. Its main characteristic is an increased muscle tone due to the hyperexcitability of the stretch reflex, elicited by a tonic stretch reflex speed-dependent [206]. The result is an increased muscular tone during external mobilization of the leg that could cause dangerous situations, e.g. the exoskeleton could harm the patient or compromise the balance, and thus can hamper the delivery of robotic walking therapy. Therefore and additional criteria for the target population was to include patients whose spasticity index is lower than 3 as measured by the Asworth scale [185].

These functional characteristics correspond to the ideal Conus Medularis lesion. Nevertheless, other incomplete lesion can meet these functional characteristics and can be also targets of the therapy proposed in this dissertation. In summary, the target population was comprised by SCI subjects with:

- Muscular balance score for hip flexion between 2 and 3, measured by the MMT [5].
- Knee flexor and extensor muscles response to electrical stimulation. As exposed above, there is a need of partial innervation of the muscles to meet this criteria.
- Spasticity index of hip, knee and ankle joints must be lower than 3 in the Asworth scale [185].
- Preserved upper limbs strength.
- Ability to maintain balance between parallel bars.

3.2 Conceptual design

The conceptual design refers to the main concepts derived from the application requirements that drive the design process. The main requirement is hybrid actuation, which affects to actuator selection and design (section 3.3), the control strategies of the robotic exoskeleton (section 3.4), and the stimulation and the high level cooperative control strategy (developed in chapter 5).

Regarding the design of the robotic exoskeleton, the target population features preserved hip flexion ability. Hip extension is ensured by contralateral leg flexion combined with trunk forward lean, resulting from walking with crutches or walker. As result, there is no functional rationale for implementing hip actuation. Therefore the robotic exoskeleton is comprised by knee and ankle actuators. Monitoring and control of trunk orientation was not considered necessary. As exposed in the previous section, the patients features trunk control, which allows to maintain balance during walking using crutches or walker.

The prototype of lower limb robotic exoskeleton developed in this chapter, showed in figure 3.12, was given the name of ***Kinesis***, a Greek word to denote movement. This name aims to highlight the rehabilitative approach of "moving" the legs of the patient by its own muscles during hybrid walking therapy. Hereinafter Kinesis refers to the robotic exoskeleton implementing the hybrid walking approach with muscle fatigue management.

3.2.1 Support structure

Critical exoskeleton characteristics are portability, low-weight, versatility, usability and easy to don and doff. These can be fulfilled with a KAFO-type, without pelvic corset as the hip is not actuated. To increase the donning and fitting capabilities, the orthotic structure is comprised by a single lateral bar, adaptable to different anthropometries.

With respect to the orthotic joints, knee and ankle kinematics during walking features a three dimensional motion where the joint axes are neither coincident nor stationary. This provides adaptability features for walking in uneven terrains and performing other task apart from walking. However, knee and ankle joints move essentially in the sagittal plane during walking in straight line in a level surface, so movement in the other two anatomical planes can be disregarded [207, 208]. Most of the walking orthoses for SCI have been designed with one sagital degree of freedom for knee and ankle joints [50, 64, 84, 85, 103, 209, 210]. This decision simplifies the mechanical design of the orthotic structure and the actuator.

3.2.2 Leg muscles for NP-induced knee and ankle motion

The knee joint torque exerted in sagital plane by leg muscles is a consequence of the agonist-antagonist contractile play between quadriceps muscle group (extensor muscles), and hamstrings muscle group (flexor muscles), which flex the knee (figure 3.1). Quadriceps muscle group is comprised by four main muscles: the *Crural*, the *Vastus Medialis*, the *Rectus Femoris* and the *Vastus lateralis*. The combined activation of these muscles generates an extensor torque around knee joint which extends the leg thanks to the lever arm formed by the patellar ligament and the patella (figure 3.1(a)).

Hamstrings muscle group is comprised by three main muscles: the *Semitendinosus*, the *Semimembranosus* and the *Biceps Femoris* (figure 3.1(b)). This muscle group is responsible for knee flexion, with the semitendinosus contributing also to the extension of the hip joint.

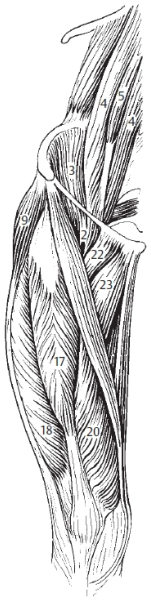

(a) Knee extensor muscle group. *Vastus medialis* (20), *Rectus Femoris* (17), *Vastus Lateralis* (18) and *Crural* (under 17, *Rectus Femoris*)

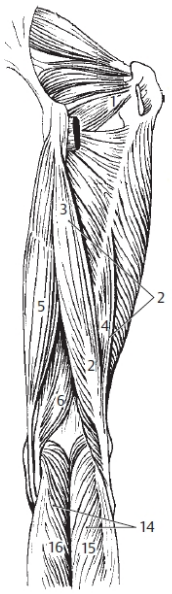

(b) Knee flexor muscle group. *Semitendinosus* (5), *Semimembranosus* (6) and *Biceps femoris* (2).

FIGURE 3.1: Knee joint muscles. Images adapted from [211].

Ankle dorsal flexion is performed by the combined action of *Tibialis Anterior*, *Extensor Digitorum Longus* and *Extensor Hallicus Longus*, whereas ankle plantar flexion is performed by the combined action of *Triceps Surae*, *Peroneus Longus*, *Peroneus Brevis*, *Flexor Digitorum Longus* and *Tibialis Posterior*. Only tibialis anterior for dorsal flexion and triceps surae for plantar flexion are superficial muscles that can be stimulated by surface electrical stimulation. The remaining muscles are under these, which prevents the electric impulse to reach muscle fibers (figure 3.2).

In healthy walking, the role of the tibialis anterior muscle is to keep the foot in neutral position during swing phase to ensure toe-clearance. During stance, from heel strike to ankle rocker, tibialis anterior muscle performs an eccentric control of foot plantar flexion. In contrast, the role of gastrocnemious muscles is to provide step propulsion, by a concentric action from barefoot rocker until toe-off. However, SCI walking with crutches or walker is a non-accelerated, sequential walking where balance plays a prominent role in detriment of leg proposion provided by the gastrocnemius. Besides, plantar flexion during swing can be guaranteed by placing an elastic device to hold the foot, usually by an elastic ankle-foot orthosis (AFO). In conclusion, stimulation of ankle muscles during walking was not deemed necessary.

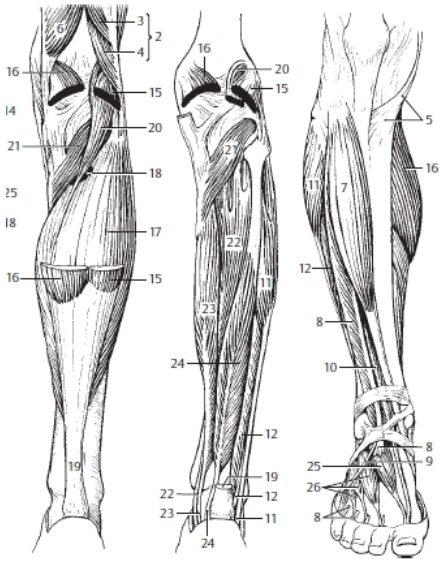

FIGURE 3.2: Ankle joint muscles. Images adapted from [211]. *Tibialis Anterior* (7), *Extensor Digitorum Longus* (8), *Extensor Hallicus Longus* (10), *Triceps Surae* (13), *Peroneus Longus* (11), *Peroneus Brevis* (12), *Flexor Digitorum Longus* (23) and *Tibialis Posterior* (22).

3.2.3 Electromechanical actuation

The analysis of the SoA presented in chapter 2, recommended active actuators for designing a rehabilitation hybrid exoskeleton, in order to implement muscle fatigue management strategies and AAN control. If adequately dimensioned and controlled, an active actuator can provide the power needed to effectively balance the neuroprosthesis regarding muscle fatigue, and maximize the residual abilities of the user.

Going one step further in this concept, the actuators to be implemented must allow compliant actuation in order to optimize the movement generated by the stimulation rather than constraining the total movement to a fixed trajectory. Several research groups are recognizing these limitations of position controlled exoskeletons, implementing control architectures to provide a more flexible robot, adaptable to the functional capabilities of the subject [195]. The technologies that most commonly are implemented in exoskeletal robotics and that were considered for designing the knee and ankle actuators, were the following:

Elastic technologies. These technologies can store and release energy during the phases of gait and have been successfully employed in a KAFO orthosis for compensating lower limb weakness [212]. These technologies are robust and do not require energy sources, however it is not possible to perform precise and fast control of the actuator displayed stiffness.

Direct current motors. DC motors are one of the most employed technologies in the robotic field. Its operational and control characteristics are well documented, have a fast response and can be operated at moderate voltages. However, DC motors needs to be used with gearboxes to adapt torque and velocity to the application, reducing the performance and increasing backlash.

Ultrasound motors. These motors exhibit adequate torque and velocity characteristics that could better match the needs of a lower limb exoskeleton than DC motors. Similar to the combination of DC motor and gearbox, ultrasound motors are non-backdrivable. Besides, ultrasound motors feature low efficiency, increasing system's power requirements.

Shape memory alloys (SMA). SMAs are metals that have the property to revert back to their original shape when heated at certain temperature, by a change in their crystal structure. SMAs enable large forces and movements. Deactivation typically occurs by free convective heat transfer to the ambient environment. Consequently, SMA actuation is typically asymmetric, featuring faster shortenings than lengthening changes.

Pneumatic muscles. Its operation is inspired by biological muscles. When its elastic cylindric chamber is filled with compressed air, the cylinder is shortened. Pneumatic muscles are light and backdrivable, but need for a noisy source of compressed air, which usually features a low efficiency and limited actuation bandwidth.

Hydraulic actuators. Similarly to pneumatic muscles, hydraulic actuators feature a good power/weight ratio, but need for a noisy source of compressed air and actuation bandwidth is lower than DC motors.

Series-elastic actuator (SEA). SEAs are a combination of a DC motor and a spring through a mechanical transmission. SEAs are suitable for precise force control applications, offer good properties against shocks and can store and release energy. However, SEAs are heavier than other actuators, as the SEA is comprised by a DC motor, a set of springs and the mechanical transmission. Furthermore, choice of the stiffness of the springs is a difficult task.

Once exposed the candidate technologies for implementing the knee and ankle actuators, the analysis of the actuation requirements is presented in next sections. The actuation requirements are extracted from biomechanical analysis of healthy walking. It was considered that the patient could not exert volitional control in either joint and the NP is not able to generate muscle contraction. This comprises the scenario in which the actuators are responsible of driving the joints during walking.

3.2.3.1 Knee joint actuation

Knee biomechanics during walking have been analyzed to estimate the power and torque requirements of a knee actuator for the hybrid exoskeleton. Nondisabled gait data at self selected speed collected at the Biomechanics and Technical Aids Unit of the HNP were analyzed. Figure 3.3 shows the mean knee joint kinematics, torque and power for a normalized gait cycle. Joint torque and power are normalized to subject weight. From the biomechanical data of figure 3.3, the parameters that determine the requirements of the actuator were extracted and particularized for a 90 kg user (table 3.1).

Parameters showed in table 3.1 are distributed within two characteristic sub-phases that knee exhibits during walking: load response, between 0% of gait cycle after heel strike and 20 - 25% of gait cycle, and the swing phase, between 40% of gait cycle after toe-off and the 100% of gait cycle just before heel strike. These two sub-phases are significantly different in terms of the mechanical role played by the leg. Load response phase is quasi-static, in which knee collapse

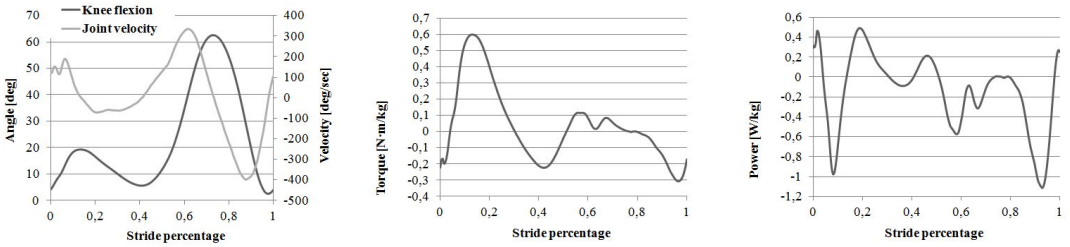

(a) Kinematics. (b) Torque. (c) Power.

FIGURE 3.3: Representative example of knee joint biomechanical data from nondisabled walking (flexion-extension axis).

TABLE 3.1: Parametrization of knee joint biomechanics during walking.

Parameter	Average value	Maximum expected
Range of movement	2.5 to 62 deg	–
Maximum velocity	400 deg/s	–
Torque at maximum velocity	0.09 $N \cdot m/kg$	8.1 $N \cdot m$
Maximum torque	0.60 $N \cdot m/kg$	54 $N \cdot m$
Joint velocity at maximum torque	6.9 deg/s	–
Torque at zero velocity	0.60 $N \cdot m/kg$	54 $N \cdot m$
Maximum delivered power	0.49 W/kg	44.1 W
Maximum dissipated power	-1.1 W/kg	99 W

due to body weight and movement inertia must be controlled. In contrast, swing phase is a dynamic movement in which the leg swings to avoid floor contact.

Maximum joint velocity is achieved during the swing phase, with two similar peaks at both flexion and extension directions. The maximum joint velocity achieved during extension coincides with the maximum power dissipated at the joint during swing phase, by the eccentric action of quadriceps to decelerate the leg and prepare it for heel strike in full extension. A similar value of dissipating power is developed prior to the maximum torque, near the 15% of gait cycle at load response sub-phase, that corresponds to the concentric action of quadriceps muscle to control knee collapse just after heel strike. It is important to notice that the maximum knee torque is achieved in this phase with a near-zero joint velocity.

Observational analysis of biomechanical data shows that designing an actuator that could meet these requirements is a challenging task. Knee joint during non-disabled walking features quasi-static and dissipative features at load response sub-phase, and dynamic characteristics during swing phase. On the other hand, as outlined in section 3.2.2, SCI walking is a non-accelerated, sequential walking where balance plays a prominent role in detriment of leg propulsion and thus, load response phase is diminished and body acceleration that tends to collapse knee joint is also decreased. Therefore, a knee joint actuator must provide good dynamic characteristics for driving the leg during swing, and partial ability to dissipate power at near-zero velocity for stance.

To conclude, electric DC motors were selected to implement the knee joint actuator, taking into consideration the characteristics of the candidate technologies and the operational characteristics of the knee joint discussed in this section. Electric DC motors features good dynamic characteristics and can be controlled to dissipate power when the rotor is stalled, although caution must be paid to the heating of winding. This technology allows a fast response, which can provide high actuation bandwidth. Furthermore, control characteristics are well documented, as this technology is being extensively used for traditional robotics and exoskeletons. This provides the flexibility for controlling the exoskeleton in combination with the neuroprosthesis.

3.2.3.2 Ankle joint actuation

Ankle biomechanics was analyzed to estimate the power and torque requirements for the ankle actuator following the same procedure (figure 3.4 and table 3.2).

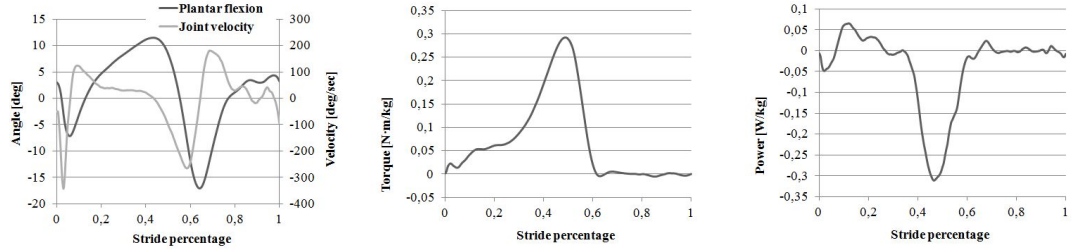

(a) Kinematics. (b) Torque. (c) Power.

FIGURE 3.4: Representative example of ankle joint biomechanical data from nondisabled walking (plantar-dorsal flexion axis).

TABLE 3.2: Parametrization of ankle biomechanics during walking.

Parameter	Average value	Maximum expected
Range of movement	-11.5 to 17 deg	–
Maximum velocity	342 deg/s	–
Torque at maximum velocity	0.13 $N \cdot m/kg$	11.7 $N \cdot m$
Maximum torque	1.33 $N \cdot m/kg$	119.7 $N \cdot m$
Joint velocity at maximum torque	68.7 deg/s	–
Torque at zero velocity	1.22 $N \cdot m/kg$	109.6 $N \cdot m$
Maximum delivered power	3.12 W/kg	280 W
Maximum dissipated power	-0.58 W/kg	52 W

During human gait, ankle joint features the same two phases than for the knee, determined by ground-foot contact. During stance, two main functions of ankle joint can be identified: firstly, damping of the heel rocker after the initial contact, by eccentric action of the dorsal flexor muscles; secondly, controlled delivery of power during last stance by the plantar flexor muscles. The later posses a challenge for designing an active actuator. Just before toe-off (approximately at 50% of gait phase), the maximum power is developed at ankle joint at low velocity, thus coincident with the largest torque generated. The power developed in this interval is responsible for increasing step length and gait velocity [207,208]. Note that the power and torque developed

are the highest of the lower limb joints. This feature of nondisabled gait represents a complex task for designing an ankle actuator, since the ankle is the most distal joint of the leg, thus the mass of the actuator must be minimized to not hinder the dynamics of the proximal joints. This rationale is behind the fact that ankle actuation has been disregarded in the design of most rehabilitation exoskeletons, both stationary [103, 106] and ambulatory [165, 171, 173, 177, 182]. Again, SCI walking with walkers or crutches gives priority to balance, disregarding leg propulsion. Step progression can thus be achieved by hip flexion and knee extension along with contralateral hip extension as a result of trunk forward lean.

During the swing phase, dorsal flexor muscles maintain the ankle in a near-neutral position to avoid stumble with ground. The torque developed by the muscles during this phase is small enough to lift the foot weight (figure 3.4(b)). This function is usually achieved by elastic devices that controls the so called *drop foot*. The most simple and frequent device is the elastic AFO, where a plastic orthosis covers the foot sole and the posterior part of the leg, with a suitable stiffness to avoid the drop foot during swing and to allow for relatively unhindered movement during stance. This concept is followed in section 3.3.2 to implement the ankle joint actuator.

3.3 Mechanical design and actuation sensory system

In section 3.2.1, the preliminary characteristics for the exoskeletal structure were derived from the analysis of the target population: the mechanical structure will be inspired by an orthotic KAFO with a single lateral bar adaptable to different sizes, and a single sagittal degree of freedom for ankle and knee joints.

The mechanical design took as starting point a previous design of a KAFO-type exoskeleton (figure 3.5), intended to compensate leg weakness in patients with post-polio syndrome. The original design comprised two elastic actuators at knee and ankle joints (not shown). Further details about this design is presented in [212, 213].

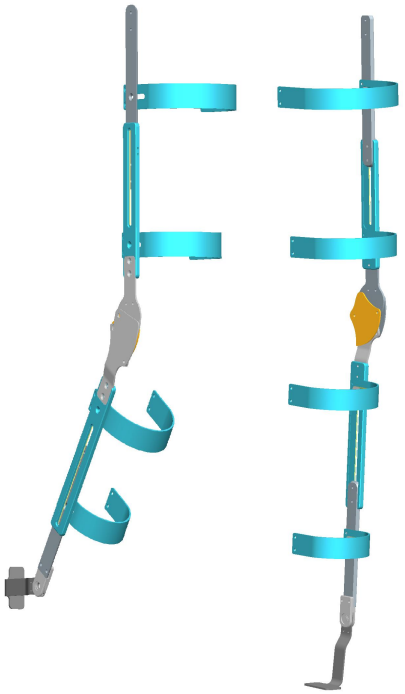

FIGURE 3.5: KAFO-type exoskeletal structure.

The exoskeleton structure was designed to withstand the forces generated during walking. Further characteristics make it suitable to fulfill the requirements stated at the beginning of this section: the structure comprises telescopic bars and rods for continuous adjusting to several sizes, the metallic girth provides high stiffness in the frontal plane, and knee joint features a bio-inspired design that increases the kinematic compatibility between the leg and the exoskeleton, previously developed [214]. The following sections show the design process of the actuators and sensors for the exoskeletal structure of figure 3.5.

3.3.1 Active knee joint

In order to design a lightweight and compact actuator, a brushless flat motor and a Harmonic Drive gearbox were selected. A further search on the catalogs of *Maxon Motors* (Maxon motor ag, Sachseln Switzerland), *Harmonic Drive* (Harmonic Drive LLC Peabody, Massachussetts), and *Advanced Motion Controls (AMC)* (Advanced Motion Controls LLC, Camarillo, California) as intermediate control driver was performed.

As showed in section 3.2.3.1, the extreme operation conditions demanded to the knee actuator challenges the design and selection of the actuator. In this case, the main criteria for selecting the combination of motor, gearbox and driver, was to design an actuator that guaranteed knee joint support during the stance phase. The final components selected were EC90-48V brushless motor, harmonic drive gearbox CSD17-100, and a control driver BE15A8-H.

Table 3.3: Requirement comparison for knee actuator.

Parameter	Required	Achieved
Maximum velocity	400 deg/s at 8.1 $N \cdot m$	125 deg/s at 8.1 $N \cdot m$
Maximum torque	54 $N \cdot m$	53 $N \cdot m$ (nominal)

The principal performance of this combination are shown in table 3.3. It can be noticed that the requirement of maximum torque, achieved during stance phase, are meet with the maximum nominal torque of the actuator. However, the maximum velocity achieved during swing phase is not meet with this actuator. Lower reduction ratios and/or faster motors could not be eligible as the combinations did not achieve the requirements for stance phase. On the other hand, data from table 3.1 were extracted from nondisabled walking at self selected speed, hence overestimated with respect to the real values expected during pathological walking. Furthermore, a velocity of 120 deg/s is the mean velocity for a swing phase of 1 second, similar to values obtained for swing phase of paraplegic walking with crutches [215].

Figure 3.6 shows an exploded view of the knee actuator design. As the exoskeleton, all pieces were designed and manufactured in aluminum (series 7000). The harmonic gearbox and the motor stator are both referenced to the proximal part of the exoskeleton through support pieces, which have cylindrical protrusions that ensure concentricity and increase assembly stiffness. The motor shaft has not machining for attachment with external parts so the harmonic drive input shaft and the motor shaft were mounted by mechanical interference.

The output of the harmonic gearbox drives the distal part of the exoskeleton. Thus, one of the bars of the knee joint was modified to transmit the movement from the actuator to the distal part of the exoskeleton. A finite element analysis (FEM) of the modified bar was conducted to verify structural integrity under maximal actuation demands. Figure 3.7(a) depicts the FEM analysis result, where a small zone inside the connecting bore between bars 1 and 3 is seen to exceed the yield strength. As the zone is relatively small, this would not affect the structural integrity due to the plastic harden that would take place [216]. A further modification on the four bar mechanism was made in order to mechanically limit the range of movement of the joint between 10 degrees beyond full extension (figure 3.7(b)) and 100 degrees of flexion (figure 3.7(c)).

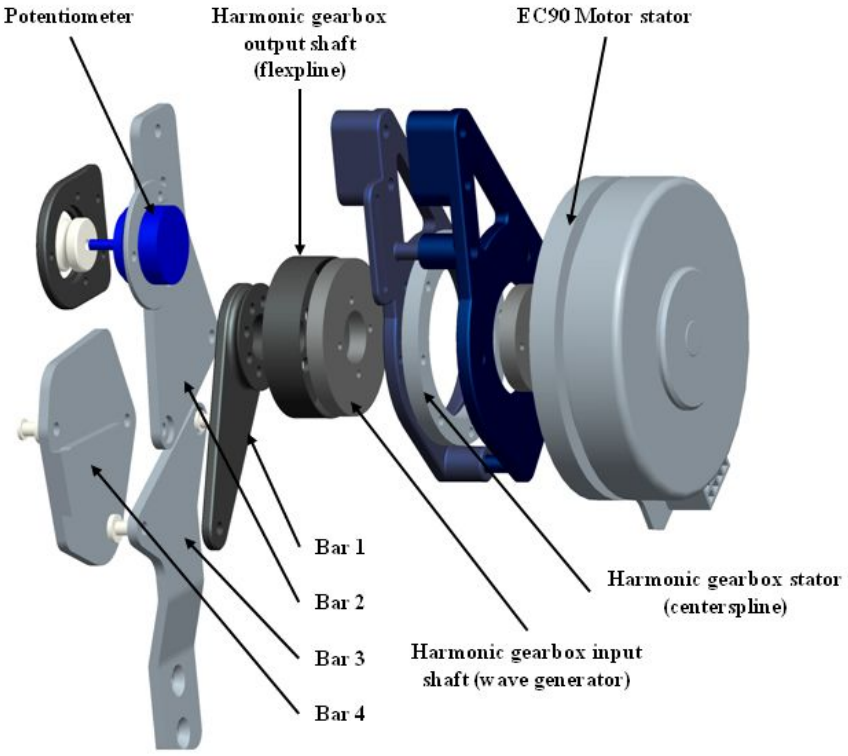

FIGURE 3.6: Exploded view of the knee actuator design.

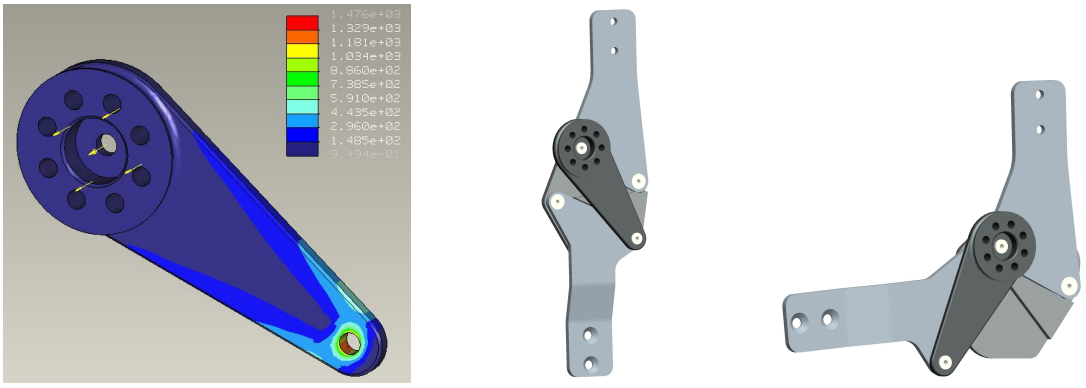

(a) FEM results for bar number 1.

(b) Maximum knee extension.

(c) Maximum knee flexion.

FIGURE 3.7: Knee joint modified mechanism.

3.3.2 Ankle joint

The conceptual design presented in section 3.2.3.2 led to consider only foot control during the swing phase by means of elastic actuation. Plastic AFOs are designed to meet this requirement and are widely used by SCI persons that need to compensate that function. Adapting a traditional AFO to the exoskeleton of figure 3.5 was discarded because several sizes of AFO were needed, due to traditional AFOs are dressed beneath the foot, inside the shoe (see the AFO part of the device showed in figure 1.5(b)). The actuator design presented here is easier to wear, as is comprised by an external insole that fits most of the shoe sizes (figure 3.8(a)). This insole

supports the foot from the heel to the first metacarpophalangeal joint, allowing free movement of the forefoot rocker.

TABLE 3.4: Requirements for ankle actuator.

Variable	Definition	Value for a 90 kg user
Foot length	Lateral malleolus to the second metatarsal head	25 cm
Foot weight	0.0145·$bodyweight$	1.13 kg
Foot center of mass	0.5·$footlength$	12.5 cm

The elastic behavior of the ankle joint was implemented by means of a torsional spring. The spring stiffness constant was calculated considering that the spring must hold the foot in horizontal position, where the plantar flexion torque produced by its weight is maximum. Anthropometric values were particularized for the heaviest user (table 3.4, [217]). This data allowed to solve the equation 3.1.

$$T_{foot} = M \cdot g \cdot L_{CM} = 1,13 \cdot 9,81 \cdot 0,125 = 1,4\ N \cdot m \tag{3.1}$$

In equation 3.1, T_{foot} is the torque needed to hold the foot in neutral position, M is the foot weight, L_{CM} is the distance between the ankle joint and the center of mass, and g is the gravity. The ankle actuator design is shown in figure 3.8(b): a concentric cylindric mechanism articulated by a needle bearing contained the torsional spring. Mechanical stops were included to limit the range of movement of the actuator from 15 degrees of plantar flexion to 25 degrees of dorsal flexion. Several bores were arranged two degrees apart for adjusting the preload of the actuator.

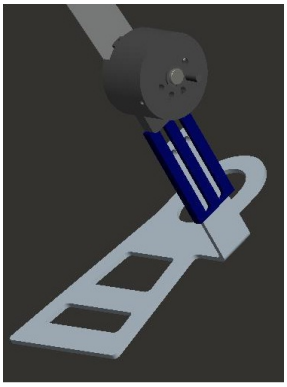

(a) Ankle actuator and foot insole.

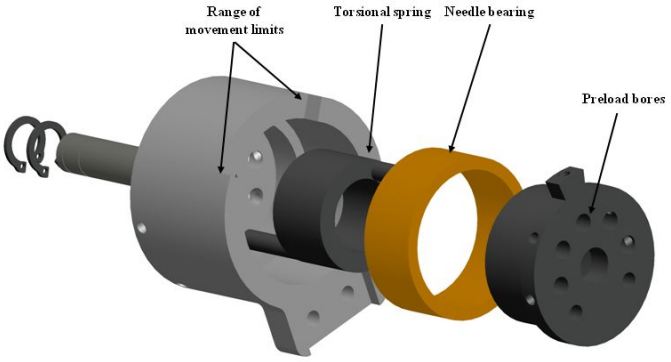

(b) Exploded view of the ankle actuator design.

FIGURE 3.8: Ankle actuator design.

3.3.3 Interaction force sensor

Exoskeletal robots are in close contact with the user, interacting physically among distributed surfaces. Thus, monitoring the forces exerted between the limb and the exoskeleton should

be fed into the control strategy to ensure a safe physical interaction. Furthermore, for the hybrid walking therapy developed in this dissertation, monitoring the interaction forces is of the most importance to estimate the muscular performance due to the stimulation and implement a closed-loop control strategy. Besides, since the knee actuator is non-backdrivable, a force sensor properly designed allows to implement control strategies that permits the user to move the leg freely. Along with the low-level control strategy developed in section 3.4, online monitoring of the leg-exoskeleton physical interaction is highly suitable for implementing both the NP and the hybrid-cooperative controllers, as shown in chapter 5.

A four gauge bridge was implemented over the exoskeleton structure to measure the interaction forces, resulting at the leg-exoskeleton interface during the movement, that is, the girths' inner surface over the leg skin (figure 3.9). This force, depending on the distance at the girths are placed for a specific subject, can be transformed to a torque at the knee joint level. Although there is a broad offer of commercially available force sensors, it was difficult to find an adequate force sensor, with adequate geometry and range of measure, that can be placed at the exoskeleton structure. Moreover, integration of a force sensor will introduce mechanical discontinuities on the structure. Therefore, the distal bar of the exoskeleton was instrumented build a custom force sensor.

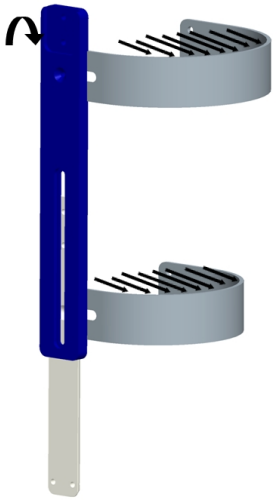

FIGURE 3.9: Loads diagram for the distal part of the exoskeleton.

In order to instrument the structure, we have introduced a full gauge bridge over its distal part, below the knee joint and over the first girth of the distal segment of the exoskeleton. Measurement of forces through strain gauge is based on measuring the deformation of the structure caused by the force [216]. Therefore, the exoskeleton structure must deform adequately in order to measure the interaction torque. Of course, the strain should be enough to provide adequate resolution, but must not be excessive to not overcome the strain limit of the aluminium.

A strain analysis of the exoskeleton structure was performed in an attempt to design the most adequate geometry to achieve a desirable deformation. This analysis had a two-fold objective: first, the geometry should allow to place a full gauge bridge. Second, an adequate measurement range must be achieved, to allow monitoring the forces involved during walking.

The simplified load state of the exoskeleton distal part is shown in figure 3.9: the actuator joint torque results in distributed forces over the girths that drives the leg. These distributed forces can be reduced to a combined force-moment acting over the exoskeleton-girth linkage. However, the moment contribution can be disregarded with respect to the bending moment originated by the distributed forces. Nevertheless, the moment contribution is further considered at the FEM verification.

As design criteria, the maximum deformation caused by the maximum actuator torque should not exceed the 0.2% [216]. Aluminium strain-deformation behavior follows Hooke's law, which

stablished a linear relationship between the elastic deformation (ϵ) and strain (σ) through the Young's elasticity module (E) (Equation 3.2).

$$\sigma = E \cdot \varepsilon \tag{3.2}$$

$$|\sigma_{max}| = \left| \frac{M}{I_z} \cdot x_{max} \right| \tag{3.3}$$

On the other hand, Navier's law (equation 3.3) gives the relationship between the external bending moment (M) and the internal strain of the material (σ_{max}), in this case particularized for the maximum values. Combining Hooke's and Navier's lows, and imposing the deformation limit to 0.2%, results in the equation 3.4. In this equation, the geometry-related variables (the second moment of inertia of the cross section, I_z and the distance of the most external material fiber from the section baricenter x_{max}) are unknown.

$$|\varepsilon| = 0,002 = \left| \frac{M}{I_z \cdot E} \cdot x_{max} \right| \tag{3.4}$$

Figure 3.10 shows a first proposal of the modified bar cross-section, where a full Wheatstone bridge could be implemented. The second moment of inertia (I_z) of a section is defined in equation 3.5, where x, y and z axis are defined in figure 3.10.

$$I_z = \iint_{x,y} (x \cdot y)^2 dx \cdot dy \tag{3.5}$$

Solving the equation 3.5 for the section proposed in figure 3.10, equation 3.6 is obtained, where the second moment of inertia is parametrized by section-related dimensions: a (section height), b (section width) and h (relative distance between the outer material fibers).

$$I_z = \frac{a \cdot b}{6} \left(4 \cdot a^2 - 6 \cdot a \cdot h + 3 \cdot h^2\right) \tag{3.6}$$

Combining equations 3.4 and 3.6, equation 3.7 is obtained, where three section-related variables are still unknown. Two additional conditions that allow to solve equation 3.7 were imposed: first the thickness of the bar (b) is equal as the original cross-section, to maximize the transversal stiffness of the bar (thus $b = 8mm$). Second, as a thumb design rule, the sub-section height should not be inferior to the half of the bar thickness (thus $a \geq 4mm$) to avoid plastic deformations that could compromise the structure integrity. Solving equation 3.7 with these boundary conditions gives the remaining variable $h = 22mm$.

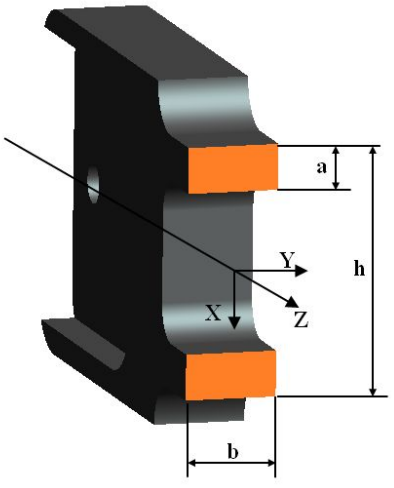

FIGURE 3.10: Resistant area of the bar.

$$0,002 = \left| \frac{M}{E \cdot \left[\frac{a \cdot b}{6}\left(4 \cdot a^2 - 6 \cdot a \cdot h + 3 \cdot h^2\right)\right]} \cdot \frac{h}{2} \right| \quad (3.7)$$

With the obtained cross-sectional geometry for implementing a full Wheatstone bridge, the new design was verified with a FEM analysis. Common radius were made to prevent stress concentration. The load state introduced in the FEM analysis included the force distribution shown in figure 3.9, which induced a more complex tensional state over the bar than the assumed for design.

The FEM analysis was carried out with Ansys. The assembly mesh was lower than 5 mm, whereas in the new designed bar zone, meshing was refine to 1 mm. The load was the maximum moment generated by the actuator over the connecting area (figure 3.9), and the girths were restricted in movement and turn. The analysis results (figure 3.11) showed that the combined load state induced deformations in the designed bar that do not exceed 0.2%. Therefore, the designed bar was considered safe from the structural standpoint and suitable for implementing a full bridge strain gauge.

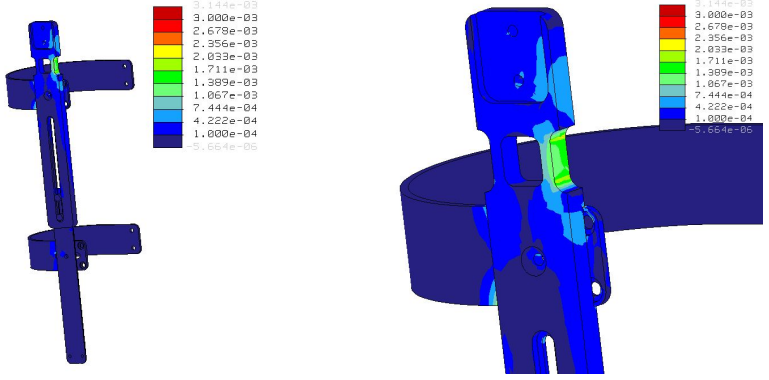

(a) FEM results. (b) Detail of the new bar design.

FIGURE 3.11: FEM verification of the new bar design.

3.3.4 Sensory system and control hardware.

Figure 3.12(a) shows the computerized rendering of the final exoskeleton design. A set of sensors were selected and placed over the exoskeleton to provide means for monitoring walking states and user actions, comprising the sensory system of the exoskeleton. This sensory system provides these data to the joint and hybrid controllers[2].

Walking can be described as a series of states and transitions among them. The main states are stance and swing phases: during stance the foot is contacting the floor, whereas during swing the foot does not contact with the floor. Information regarding foot contact with the floor is provided by two Force Sensing Resistors (FSR) (Interlink Electronics Inc., 38.1 mm × 38.1 mm),

[2]Within this chapter, the joint control strategy is presented, whereas the hybrid control strategy is presented in chapter 5

placed at the heel and tip of the exoskeleton's foot insoles. These FSR provides an on/off signal to the controller to discriminate between swing and stance (figure 3.12(b)).

Each gait state imposes a kinematic reference to the exoskeleton's joint actuator. It is necessary to monitor the actual joint angle. In our design, only knee joint is actively controlled, while ankle joint is passively controlled by a torsional spring. Monitoring of knee angle is implemented through a rotational potentiometer (Vishay Espectrol) (figure 3.12(b)), attached to the actuator output shaft by a belt. The size of the potentiometer pulley was selected to maximize joint positioning resolution. User control of the hybrid system is accomplished by two hand-switches, implemented by a small force-sensing resistor. This implementation allows non-obtrusive use as a hand switch on the user's grip of crutches or walker.

An embedded computer was selected to implement the control software. The computer was a pc104-compatible, which is a standard for embebbed computers in which the architecture is built by adding interconnected modules through the ISA data bus. The modules selected were a motherboard, power source, ethernet communication and the analog to digital (A/D) acquisition card. The later was a Diammond DMM32X-AT (Diammond Systems Corp.), which comprises 32 input channels of 16 bits each, 4 output channels of 12 bits each, and a maximum sampling frequency of 250 kHz. All sensors and the velocity drivers were connected through the A/D card. The control software was developed in *Simulink* using the real time target library. This allowed to rapidly design different control schemes and downloading to the control PC for testing through ehternet communication.

All the control hardware was packed in a backpack, including the stimulator selected, which is described in section 4.2 of chapter 4 (figure 3.12(b)). The prototype of lower limb robotic exoskeleton is shown in figure 3.12.

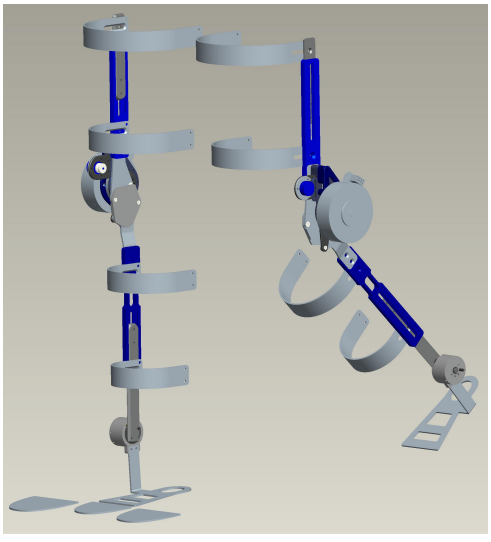

(a) Rendering of the exoskeleton design.

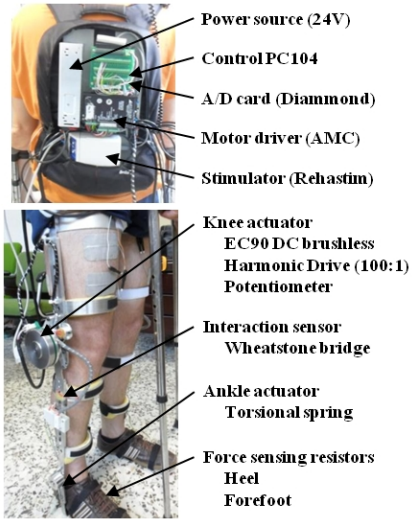

(b) Sensory system.

FIGURE 3.12: Kinesis: lower limb robotic exoskeleton for hybrid walking therapy.

3.4 Design of a control architecture for hybrid walking

From the rehabilitation perspective, one of the main challenges of ambulatory gait exoskeletons is to make robot behavior adaptable to the user residual abilities and furthermore, implement AAN strategies that maximize the user contribution to the movement. This is also a major concern in designing a hybrid-cooperative control approach: how to achieve an effective balance between the NP and robotic controllers in order to exploit their advantages while mitigating its respective disadvantages. In fact, controlling the trajectory of the limb generated by the stimulation through a position-controlled exoskeleton would originate numerous control actions that are energy inefficient.

A complaint exoskeleton controller is therefore needed to further implement a hybrid training approach, in which the exoskeleton allows unhindered joint movement developed by the stimulated muscles, similarly to compliant control approaches developed for gait treadmill robots [195–197]. Most of these control strategies are built on the basis of the impedance control approach, the most habitual control strategy implemented for control of human-robot physical interaction, introduced almost thirty years ago by Neville Hogan [218]. Impedance control is based on the active adjustment of the system's mechanical impedance, this is, the relation between system's force, position and its time-derivate. This relation is given by three components involved in impedance: stiffness, damping and inertia.

Impedance controllers can be actually implemented with different architectures, depending on how measured signals and controlled variables, this is, position, velocity and force magnitudes are used, and how signals and variables are related within the control scheme. The final choice of a control architecture depends on the application characteristics and system's mechanical and mechatronics characteristics [219, 220]. Performance of impedance control is determined by the precision of the position sensor and also the actuator torque precision and bandwidth. A limitation of the impedance control is that the dynamic characteristics of the robot affects to the force displayed to the user in the form of apparent inertia. Compensation of gravitational and inertial forces by torque compensation feed-forwarded to the impedance controller, through the use of a dynamic model of the robot as well as friction compensation, can reduce the apparent inertia of the robot. Besides, impedance controllers become unstable when high stiffness are to be displayed by the robot [195, 221].

One of the variations of the impedance controller is the admittance controller, which represents the inverse of the impedance. Performance of admittance control is determined by the precision of the force sensor and the actuator position precision and bandwidth. Admittance controllers need high position bandwidth actuators, which is achieved by stiff and powerful actuators with low backslash. Contrary to impedance controllers, admittance controllers are stable when displaying high stiffness, but in this case instability arises when low stiffness are needed due to force sensor noise and the high control gains needed. On the other hand, the dynamic characteristics of the robot can be hidden by the actuator if the power and bandwidth are high enough [195, 221].

The joint low lever controller of Kinesis was designed over an admittance control architecture due to several reasons. Firstly, the main concern of the ambulatory hybrid exoskeleton is to achieve a compliant behavior to cooperate with the NP controller, while knee joint support during stance is guaranteed. Secondly, the high and stable stiffness needed to avoid knee collapse during stance is a security concern that impedance controllers can hardly guarantee. Lastly, exoskeleton's

dynamics can be hidden by admittance control scheme. In this case, compensating exoskeleton dynamics would need measuring thigh an leg position and, due to the absence of hip actuator, additional means of monitoring thigh orientation would be needed.

The admittance controller proposed features an outer force control loop implemented over a inner velocity control loop (figure 3.13). Motor controller performs the velocity closed-loop control with information feed from Hall sensors placed at motor structure. Control velocity set point is feed to the motor driver from an external voltage signal and, in combination with velocity sensing, the motor driver generates suitable pulse-width modulate (PWM) pulses to control motor velocity.

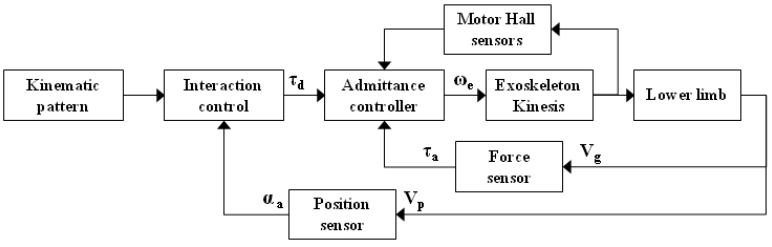

FIGURE 3.13: Low level joint control scheme.

The kinematic pattern that drives the interaction controller and the interaction control strategy are detailed in chapter 5. For the purposes of this section, focused on the low level joint control strategy, the kinematic pattern and the actual limb angle derives a position error signal that is fed into the interaction controller, which generates a first order torque field imposed around knee trajectory. Thus, the torque imposed by the exoskeleton to the joint trajectory depends upon the deviation of the knee trajectory from the reference kinematic pattern, and the stiffness characteristics of the force field (equation 3.8). In this equation, the stiffness K_k of the torque field is modulated depending upon gait events and stimulated muscle performance (as showed in chapter 5) while damping of the torque field (C_k) was included to increase system's stability.

$$\tau_d = K_k \cdot (\alpha_{pattern} - \alpha_{actual}) + C_k \cdot \frac{\Delta (\alpha_{pattern} - \alpha_{actual})}{\Delta t} \tag{3.8}$$

In the control scheme presented in figure 3.13, the velocity set-point (ω_d) feed to the admittance controller is function of the torque given by the interaction controller (τ_d) and the actual leg-exoskeleton interaction torque (τ_a). The admittance controller taken the form of a PID controller follows equation 3.9:

$$\omega_d(t) = K_P \cdot (\tau_d(t) - \tau_a(t)) + K_I \cdot \int ((\tau_d(t) - \tau_a(t)) \cdot dt) + K_D \cdot d(\tau_d(t) - \tau_a(t))/dt \tag{3.9}$$

The admittance control strategy is shown in figure 3.14. In this figure, the torque calculated from the interaction controller τ_d is fed to the PID controller. Here, the torque is compared to the actual torque τ_a, resulting in the torque error τ_e fed to the proportional (K_P), integral (K_I) and derivative (K_D) components of the PID. The output is the velocity set point (ω_d), in the range of -10 to 10 V, that is fed to the motor driver AMC. The velocity set point is compared within the motor driver with the actual motor velocity from the Hall sensors (ω_a) to modulate motor velocity (ω_e). In the following sections, the experiments to adjust and validate the admittance

controller of figure 3.14 for swing (section 3.4.2) and stance (section 3.4.3) phases of walking are presented.

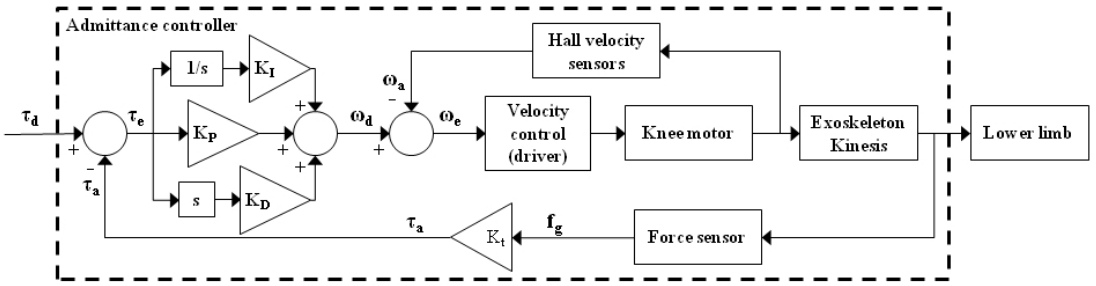

FIGURE 3.14: Admittance control strategy.

3.4.1 Force tracking capability of admittance control.

Tunning controller gains K_P, K_I and K_D was performed following a systematic and empirical procedure, based on the controller's step response of the heuristic procedure developed by Ziegler and Nichols [222], combined with hand-tunning to increase controller performance in terms of stability. The experiments were made with a healthy subject wearing the exoskeleton. The subject was instructed to stiff and not move the leg in response to the torque step and the exoskeleton control actions. This procedure was chosen instead of setting the exoskeleton between two external fixtures in order to best mimic the actual dynamic operation conditions. However, this introduced dynamic uncertainties in the tunning procedure as the subject actions are not guaranteed to be minimum, arising a dynamic interaction between the unconscious user actions and the exoskeleton control actions.

Another limitation arises from the difference in the stiffness and damping characteristics of the frontal and posterior part of the leg, which differ considerably: while the frontal part is characterized by a highly stiff interface to the exoskeleton due to the tibia superficiality, the posterior part confers a more damped interface to the exoskeleton due to the presence of muscular and fat tissues. Both limitations can be noticed in figure 3.15, where the controller step response for leg flexion and extension are showed. For the same controller gains, a higher overshoot can be noticed in figure 3.15(a) (extensor torque) compared to figure 3.15(b) (flexion torque). The stiffer interface of the frontal part of the leg leads to less overshoot and more stable controller response than the more elastic and damped posterior part of the leg.

An experiment for evaluating the controller ability to follow force profiles was performed. A force profiles generator was programmed within Kinesis admittance controller following equation 3.10. The amplitude A was experimentally determined 10 $N \cdot m$ as enough to drive the leg during the swing phase, while the frequency f was increased until 1.5 Hz, similar to the swing phase frequency seen in nondisabled walking.

$$\tau_d = A \sin(2\pi f t) \tag{3.10}$$

Results from this experiment are shown in figure 3.16. Each graph shows the torque reference generated by equation 3.10 (τ_d), the actual torque (τ_a) and the torque error. It can be noted a

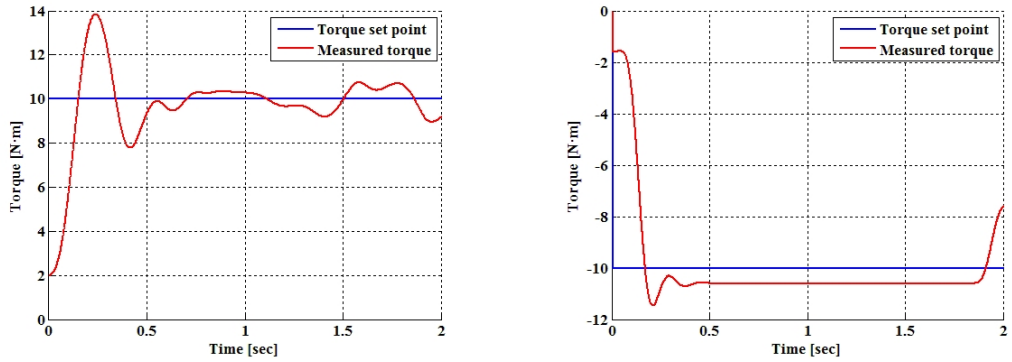

(a) Extensor step response (10 $N \cdot m$)

(b) Flexor step response (10 $N \cdot m$)

FIGURE 3.15: Controller step response.

proportional worsen in the controller response with the increase on the force profile frequency. For 1 Hz the torque root mean square (RMS) error is 1.96% of the torque profile generated and the phase error is 5 degrees. The swing phase of the kinematic pattern stored in the Kinesis high level controller resembles a sinusoid curve with a frequency of 0.25 Hz (see figure 5.12 of chapter 5). This low frequency was chosen in order to provide a slow and stable walking pattern to the patients. Although this frequency correspond to the kinematic patern, this order of magnitude was taken to investigate the force tracking capability of the admittance controller. In conclusion, the controller is deemed adequate for the application, achieving good and stable force tracking for frequencies up to 1 Hz, four times higher than the kinematic frequency, with a RMS error in torque tracking lower than 2 $N \cdot m$.

3.4.2 Modified admittance controller

3.4.2.1 Hybrid velocity-admittance strategy

As discussed at the beginning of section 3.4, a well known limitation of admittance control arise when the admittance displayed by the exoskeleton tends to infinite. This configuration is needed in two circumstances. The first case is when the exoskeleton must not impede the leg movement. In this sense, an experiment performed to quantify the resistant torque showed by the exoskeleton is presented in figure 3.17. In this experiment, the user was asked to induce flexion-extension knee movements while the controller was set to 0 $N \cdot m/deg$. From the experiment, it was concluded that the interaction torque needed to drive the exoskeleton was 1.28 $N \cdot m$ in average (RMS). Compared with the estimation of 10 $N \cdot m$ needed to drive the leg during swing (equation 3.10), the apparent inertia feel by the user is low (13% of the aforementioned estimate), but cannot be disregarded.

The second case when the exoskeleton must display an infinite admittance, is when leg movement is synchronized with the kinematic pattern. In this case, the interaction controller gives a close to zero set point as the angular pattern $\alpha_{pattern}$ and the actual angle α_{actual} are almost equal (equation 3.8 tends to zero) and the interaction force is also close to zero. Thus, thus equation 3.9 tends to zero, depending on the time constant of the integral term. As result, the velocity

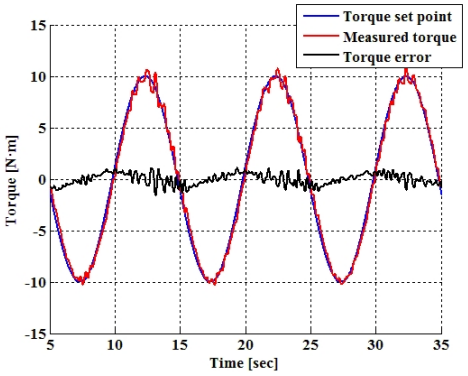

(a) 0.2 Hz. Tracking error: 0.50 $N \cdot m$ (RMS)

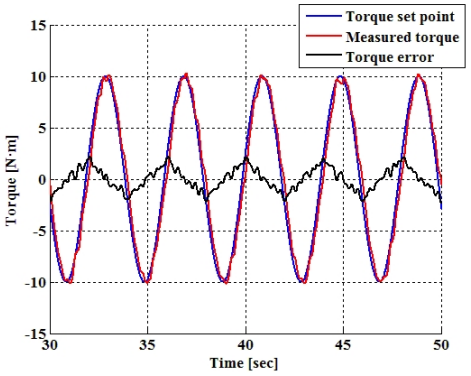

(b) 0.5 Hz. Tracking error: 1.12 $N \cdot m$ (RMS)

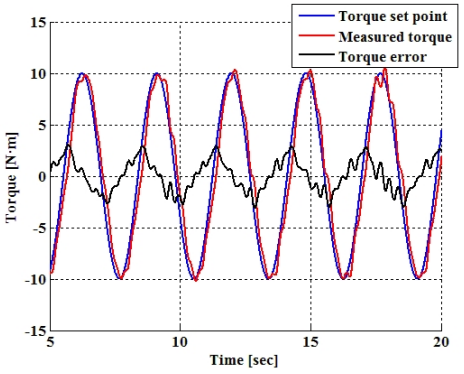

(c) 0.7 Hz. Tracking error: 1.56 $N \cdot m$ (RMS)

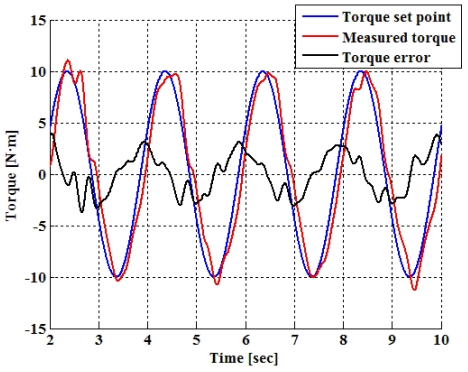

(d) 1 Hz. Tracking error: 1.96 $N \cdot m$ (RMS)

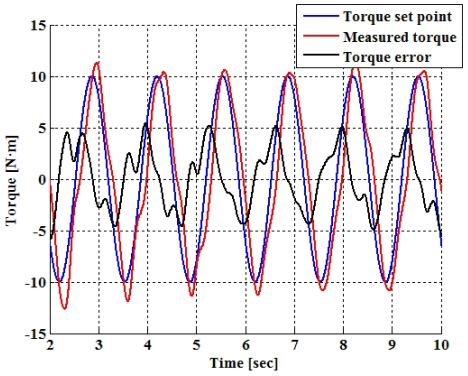

(e) 1.5 Hz. Tracking error: 2.74 $N \cdot m$ (RMS)

FIGURE 3.16: Controller's force tracking response to varying force profiles. Figures show the force profile generated (blue), the actual torque (red) and the torque error (black).

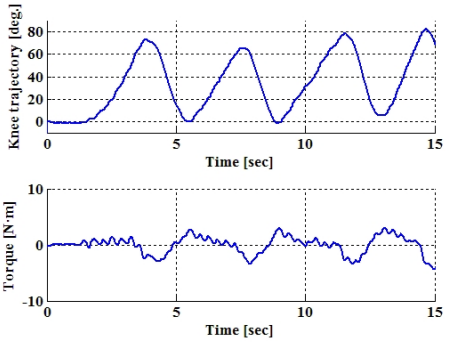

FIGURE 3.17: Resistant torque in zero torque mode.

set point feed to the motor driver further tends to zero, which would result in a braking torque over the leg while it is moving along with the trajectory.

In the second case it is possible to use the kinematic information to improve the controller admittance as follows. In the ideal scenario of a perfect synchronization between the leg and the kinematic pattern, the controller must allow to reproduce the kinematic pattern in absence of interaction torque set point. Given that the motor driver implements a velocity control loop, the time derivate of the kinematic pattern can be feed forwarded to the velocity control loop. This velocity feed forward gives to the motor controller a non-zero set point needed when the interaction forces are close to be zero. The control strategy proposed is showed in figure 3.18, where the kinematic reference α_d is time-derived and scaled to ± 10 Volts by the constant K_w, resulting in the control signal that allows the exoskeleton to reproduce the kinematic pattern whenever equation 3.9 equals to zero.

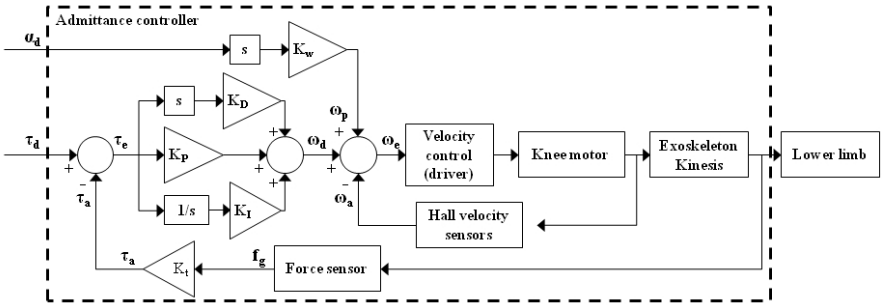

FIGURE 3.18: Admittance control strategy with velocity feed forward.

Experiments were performed to further validate the hybrid velocity-force admittance control approach. In this sense, the validation is comprised by two hypotheses made about the velocity feed forward loop:

1. The controller is able to drive the exoskeleton in the absence of interaction torque.
2. The controller does not interfere with the force tracking task of the admittance controller.

The first hypothesis was immediately verified by the adjustment process of the velocity constant K_w, which gives the constant relation between the velocity set point in deg/sec (the time derivate of the kinematic pattern α_d) and the correspondence in Volts feed to the motor driver, ω_d (figure

3.18). Regarding the second hypothesis, the experiments consisted of inducing high-magnitude disturbances in the system, which allows to investigate the hybrid velocity-admittance system's ability to track the force reference.

For the experimental procedure, a healthy subject dressed one leg of the exoskeleton and stood in a platform, with the leg dressed with the exoskeleton hanging freely. This allowed to replicate consecutive knee flexion-extension cycles comfortable with that leg. Then, the subject was instructed to perform the following actions on the exoskeleton: during the first two flexion-extension cycles, he must worked against exoskeleton flexion trajectory, and the following two cycles against exoskeleton extension trajectory. This experimental procedure ensured to induce greater disturbances than a SCI user would do, in both flexion and extension trajectories. A representative experimental result is shown in figure 3.19. Looking at the top graph (kinematic reference and actual), the two first flexion-extension cycles a deviation in maximum flexion of 10 degrees is seen, resulting from the work performed by the subject against the exoskeleton action whereas in the following cycle an overshoot of 2 degrees is seen, resulting from the work performed by the user in the same direction as the exoskeleton movement. Similar results are seen in the case of the maximum extension movement for the next three cycles. Looking at the bottom graph of figure 3.19 (torque reference and actual), the torque reference generated as response to the user actions over the exoskeleton is actually followed by the controller; overall a good force tracking was obtained in the experiment (2.4 $N \cdot m$ torque RMS error). Thus, it was concluded that the velocity feed forward do not interfere with the control task of the controller.

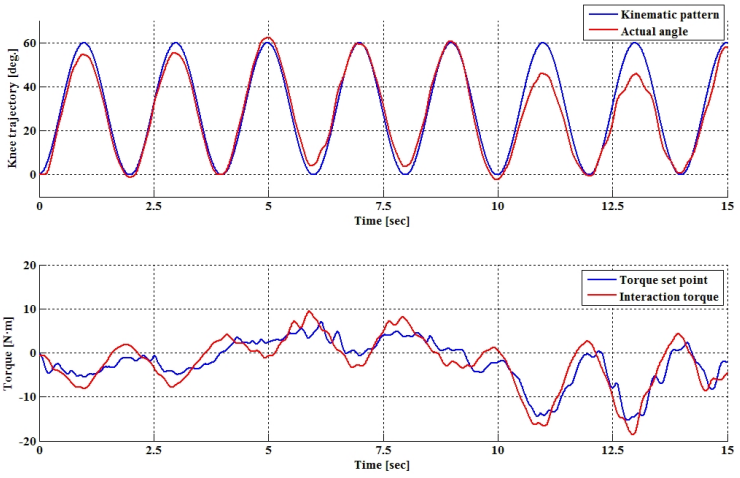

FIGURE 3.19: Hybrid velocity-admittance controller. Results from perturbation experiment. Top figure shows kinematic data: blue curve is the kinematic pattern (α_d), comprised of consecutive knee flexion-extension cycles, and actual knee kinematics (α_a) is depicted in red. Bottom figure shows torque data: blue curve is torque reference generated by equation 3.8 (τ_d), and actual torque is depicted in red (τ_a), 2.5 $N \cdot m$ torque RMS error.

3.4.2.2 Adaptative velocity-admittance controller.

A further characteristic had to be modified in the admittance control strategy of figure 3.18. As explained in detail in chapter 5, the walking control strategy is implemented through an interaction controller that dictates a torque field depending on gait phase and muscle contribution

to knee movement. This concept is further developed and explained in chapter 5, but for the purposes of this section, this strategy implies that the force field stiffness K_k must vary from totally compliant mode ($K_k = 0N \cdot m/deg$), when the muscle contribution is able to drive the leg within the gait pattern, up to a high stiffness needed to guarantee knee stability during stance. The value of K_k depends on the subject weight but in the most demanding scenario, K_k can reach 6 $N \cdot m/deg$ for stance phase.

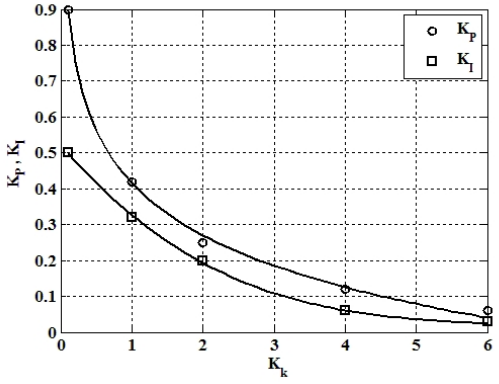

FIGURE 3.20: Controller gains K_P and K_I versus torque field stiffness K_k (equation 3.8)

Similar experiments that those described in section 3.4.2.1 were performed in which K_k was sequentially increased from 0 $N \cdot m/deg$. Those experiments revealed that the controller becomes unstable when the increment on K_k overcome half order of magnitude (i.e. from 0.1 $N \cdot m/deg$ to 0.5 $N \cdot m/deg$). This behavior is due to the fact that varying K_k alters the linear[3] relationship between the torque and the position error of equation 3.8, conferring to the interaction controller of figure 3.13 a non-linear feature to be controlled. Under these conditions, the PID controller of equation 3.9 needs therefore to be tunned again.

In this context, a gain scheduling adaptative control approach was implemented. In this approach, an observable variable, K_k in this case, is used to determine the PID parameters for different operating regions. Experiments were made to obtain the PID gains for several K_k values (table 3.5). In this experiments was revealed that the derivative component K_D remained unchanged between operating regions, due to its low contribution to the total control action. Thus, the relation between K_P and K_I versus K_k was plotted (figure 3.20), and a regression analysis was performed in order to obtain the mathematical formulation that best could explain the relationship between the controller gains and K_k.

In table 3.6, the mathematical functions tested and its coefficient of determination are resumed. The best-fit functions were selected and implemented in the low level joint controller of figure 3.18, resulting in the joint level control strategy showed in figure 3.21.

[3]The force field defined by equation 3.8 includes a first order impedance. Nevertheless, the elastic coefficient of the force field K_k has a predominant effect over the damping coefficient C_k, which confers a elastic behavior to the force field.

TABLE 3.5: Controller gains K_P and K_I versus torque field stiffness K_k (equation 3.8)

K_K	K_P	K_I
0.1	0.9	0.5
1	0.42	0.32
2	0.25	0.20
4	0.12	0.06
6	0.06	0.03

TABLE 3.6: Mathematical functions tested for controller gains K_P and K_I versus torque field stiffness K_k (equation 3.8).

Function tested	R^2 for K_P	R^2 for K_I
Potential	88%	77%
Logarithmic	99%	96%
Polynomial third order	98%	99%
Exponential	97%	98%

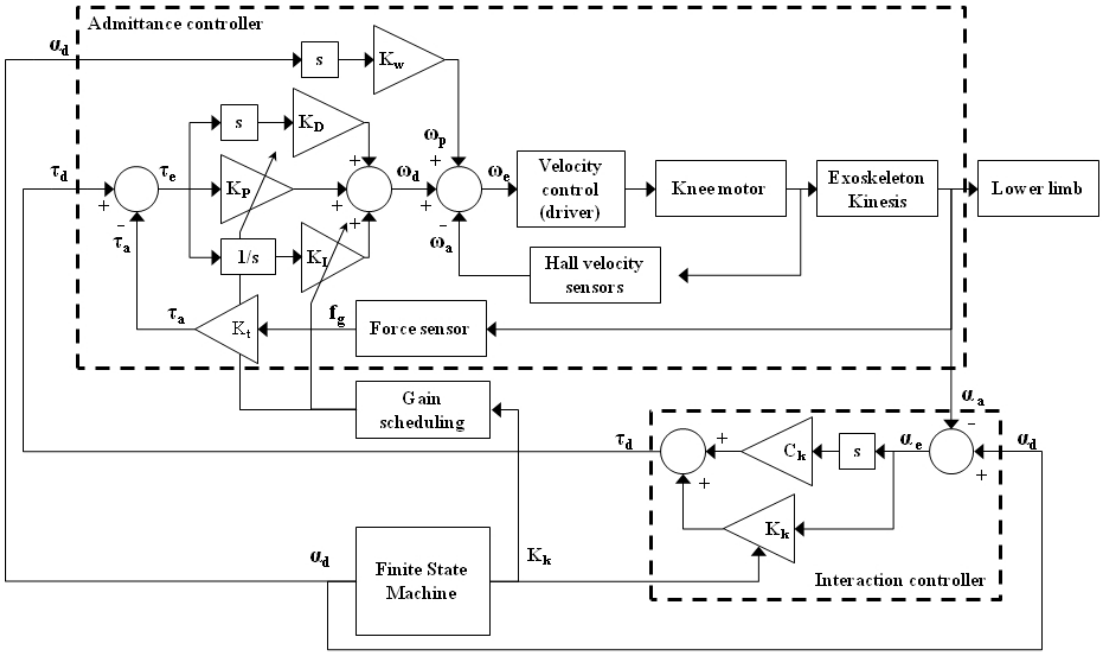

FIGURE 3.21: Adaptative velocity-admittance joint controller.

3.4.3 Stance phase controller experiments.

Experiments were performed to validate the adaptative hybrid low level joint controller ability for providing stable support during the stance phase. To conduct the experiments, a healthy subject dressed one leg of the exoskeleton and stood in a platform between parallel bars. The validation procedure consisted of unloading the user's weight on the exoskeleton, leaving the

knee to flex due to the unloading reference. The kinematic pattern in Kinesis controller was 0 degrees constant, thus the controller task was to keep the knee in full extension. Force field stiffness was set in this case to 6 $N \cdot m/deg$, a value that, as explained in chapter 5, is suitable to control knee collapse during stance.

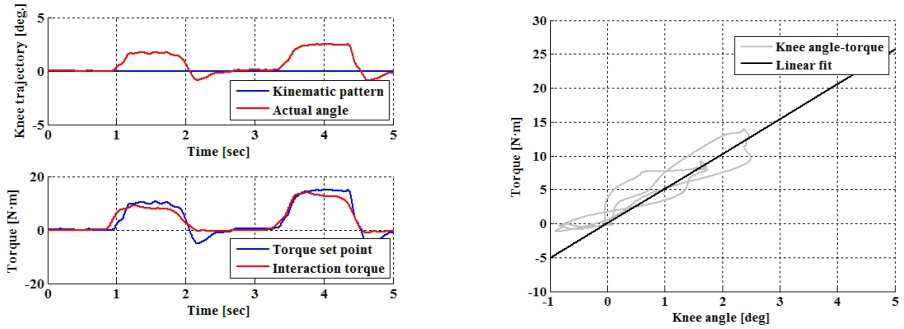

(a) Results from unloading experiment. Top: knee kinematics. Bottom: knee kinetics.

(b) Torque-angle relation during stance.

FIGURE 3.22: Kinesis stance control. Results from unloading experiment.

Figure 3.22(a) shows the kinematic and the kinetics of the knee during the unloading experiment. Force tracking error obtained was 1.8 $N \cdot m$ RMS. Figure 3.22(b) shows the relationship between knee torque and angle during the experiment, in which a linear relationship can be observed. A further linear regression yielded a constant of 5.12 $N \cdot m/deg$ with a coefficient of determination of $R^2 = 93\%$. In ligth of these results, the admittance controller was considered valid for giving support during stance phase of gait.

3.5 Conclusion

In this chapter, the target population of the hybrid walking therapy has been presented. Definition of the target population was derived from the conclusions of an expert panel comprised by clinicians, that considered the pilot development of the hybrid approach developed in this dissertation. The functional characteristics of this population, along with the walking characteristics foreseen during the delivery of the hybrid walking therapy, led to the development of Kinesis, a KAFO-type robotic exoskeleton. Kinesis features robotic actuation over the knee and elastic control of ankle, force sensing capabilities mandatory to implement the low-level control strategy and implement NP and hybrid control strategies. Knee and ankle actuation requirements were difficult to fulfill completely.

The low-level joint control strategy developed allowed to implement a compliant control of the interaction between user and the exoskeleton, as a method to optimize the contribution of the NP to the movement. Admittance control was selected due to its good performance when high interaction forces are needed. Several modifications over the traditional admittance control architecture that increase the force tracking performance of the joint controller for the swing phase. A further adaptative feature was included to solve the non-linearity produced as consequence of varying the knee force field stiffness K_k. Experiments confirmed the controller ability for providing compliant assistance during swing and stance phases of walking under variations of

the stiffness of the force field. These results validate the controller design for implementing the hybrid-cooperative control of walking developed in chapter 5.

3.5.1 Answer to research questions

This chapter provides the following answers to research questions Q3, Q5 and Q7 stated in section 1.6.2 as follows:

Q3: **Which SCI patients can benefit from hybrid walking therapy?** As general guidelines, patients must have preserved upper limb function and strength to provide support and balance during walking. Lower limb muscles must preserve partial innervation, and spasticity should be moderate. The target population defined for the application presented in this dissertation falls within these inclusion criteria.

Q5: **How can muscle fatigue estimation criteria be integrated in the robotic controller to manage muscle fatigue during therapy?** The muscle fatigue estimate is based on monitoring the changes on joint torque developed by the stimulation. Monitoring leg-exoskeleton physical interaction through an interaction force sensor introduced over the exoskeleton structure, allows monitoring changes on joint torque.

Q7: **How to control the exoskeleton in order to cooperate with the NP control?** In order to provide Kinesis the ability to adapt to muscular performance, variable assistance should be provided to joint motion. A stiffness control of joint trajectory was selected and implemented in Kinesis, which provides variable assistance, from free to constrained trajectory control.

Chapter 4

Muscle fatigue management for hybrid walking therapy[1]

Muscle fatigue due to functional electrical stimulation still prevents its widespread use as a gait rehabilitation tool for spinal cord injured subjects. Although there is an active research towards optimization of pulse parameters to delay muscle fatigue, changes in stimulated muscle's performance during repeated contractions due to fatigue have not been yet determined. In this chapter, a muscle fatigue study allowed to develop an objective criteria for detection of fatigue of knee muscles from initial changes is muscle performance. This criteria is further applied in a second study in which a comparison between two fatigue management strategies compatible with the hybrid control of walking is investigated. Results showed that modulation of stimulation frequency delays muscle fatigue.

4.1 Introduction

As introduced in chapter 1, MES has the capacity to produce movement in denervated, paralyzed, or spastic muscles (see section 1.4.3). However, a significant limitation of non-physiologically induced muscle activation is the overall decreased efficiency of contraction and propensity to develop muscular fatigue. FES-driven walking is inherently less efficient than natural human locomotion, requiring more than nine times the energy consumption of healthy walking, due

[1]This chapter is partially based on the following articles:
A. J. del-Ama, E. Bravo-Esteban, J. C. Moreno, J. Gómez-Soriano, A. D. Koutsou, A. Gil-Agudo, and J. L. Pons. **Knee Muscle Fatigue Estimation During Isometric Artificially Elicited Contractions in Incomplete Spinal Cord Injured Subjects,** in 2012 International Conference on Neurorehabilitation (ICNR2012): Converging Clinical and Engineering Research on Neurorehabilitation, 2012, pp. 329-333. **Finalist contribution in the student paper competition.**
A. J. del-Ama, E. Bravo-Esteban, A. D. Koutsou, J. Gómez-Soriano, S. Piazza, A. Gil-Agudo, J. L. Pons and J. C. Moreno. **Customized Strategies to Manage Muscle Fatigue in SCI Patients During Isometric FES-Driven Muscle Contractions,** in 18th Annual Conference of the International Functional Electrical Stimulation Society (IFESS2013), 2013. A. J. del-Ama, A. D. Koutsou, E. Bravo-Esteban, J. Gómez-Soriano, S. Piazza, A. Gil-Agudo, J. L. Pons and J. C. Moreno. **A comparison of customized strategies to manage muscle fatigue in isometric artificially elicited muscle contractions for incomplete SCI subjects,** Journal of Automatic Control. **Invited contribution.** Submitted 30/08/2013.

to the over stimulation of anatomical muscle groups and subsequent unsuitable high torque production [223].

Several causes have influence on muscle fatigue. First, MES alters normal motor unit recruitment order observed in voluntary contractions of healthy muscles [224]. In the human motor system, the smaller and fatigue-resistant motor units are activated first before larger motor units, which helps to delay the onset of fatigue. Motor unit recruitment in electrically evoked contractions is suggested to be random, less systematic or non-selective [225], which compromises the muscle natural rate of fatigue resistance [226].

Second, muscle fibers are simultaneously stimulated, much unlike the normal, unsynchronized, highly-effective recruitment and derecruitment process of motor units seen during voluntary muscle contractions. In these contractions, the human motor system manages fatigue by increasing the firing rate of active motor units and/or recruiting new motor units to replace others that have been derecruited due to fatigue [227]. This simultaneous activation observed during MES can produce sudden, sometimes uncoordinated, inefficient movement patterns rather than the smooth gradation of force typically seen in human movement.

Third, surface-stimulating electrodes direct current precisely beneath the surface area of the electrode, and because the current will travel through various viscosities of subcutaneous tissue that create resistance, its strength will be diminished and the depth of penetration will be limited. Therefore, activation of deeper muscular tissue is usually not possible with standard surface stimulation; however, increasing stimulation parameters can improve penetration of current in an effort to reach muscles distant from the skin surface [119].

In the case of SCI, the muscle fatigue effect is increased by several physiological changes that result from paralysis, including hypertonia, spasticity and disuse atrophy [228]. In the case of hypertonia and spasticity, affected muscles are generally overactive, which can lead to an almost constant fatigue state. Long-term inactivity due to SCI is associated with chronic changes in muscle metabolisms, blood flow and fiber composition [229–232]. The bulk of the transformation in muscle fiber, from slow to fast-type fibers, due to disuse atrophy occurs during the first ten months after injury, with a consequence on muscle fatigue response [233].

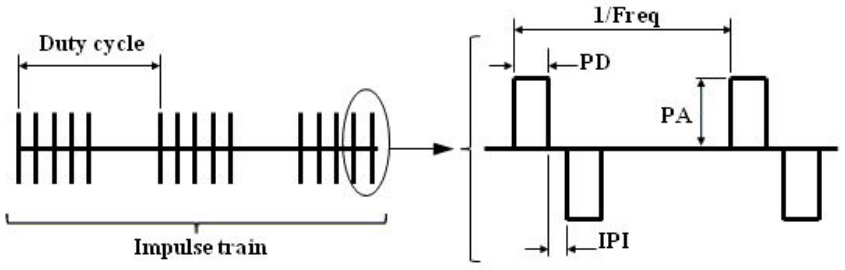

FIGURE 4.1: Definition of electrical stimulation parameters. Example of a biphasic impulse train. Duty cycle: ratio between ON and OFF sections of the stimulation train. PA: pulse amplitude. PD: pulse duration. IPI: inter-pulse interval. Freq: frequency between two consecutive electrical stimulus.

Muscle fatigue management strategies can be implemented towards more efficient surface stimulation of muscles in injured subjects [121,150,234]. Stimulation parameters have an effect on the number of motor units recruited, often referred as *spatial summation of muscle force*, modulating

the charge delivered by each pulse. Furthermore, by modulating the number of stimulus delivered, the recruitment velocity is also modulated, which is often referred as *temporal summation of muscle force*. Stimulation parameters, pulse amplitude (PA), duration (PD), frequency (Freq), and train configuration (figure 4.1) affects to both spatial and temporal summation of force generation and muscle fatigue, although the relationship force versus fatigue is not adequately established yet.

Pulse amplitude and duration are often referred as stimulation intensity as both allow to control the number of recruited motor units. As the pulse amplitude increases, a stronger depolarizing effect is seen in the muscle structures under the electrodes, and more motor units are recruited. The effect of pulse amplitude and duration on muscle fatigue is not as predominant as the effects of pulse duration and frequency [150]. A study that controlled the amount of electrical charge delivered to the muscle demonstrated that, for the same amount of electrical charge, which directly correlates with muscle force, the combination of lower frequencies with longer pulse durations reduces fatigue compared to higher frequencies and shorter pulse durations [150].

Stimulation frequency have thus a predominant effect over muscle fatigue. In general, train frequencies around 100 Hz will produce more muscle fatigue than lower frequencies [151]. Conversely, low frequencies have been reported to induce higher fatigue rate than high frequency stimulation [235], while excessive low frequency,typically under 30 Hz, have shown to induce long-lasting muscle fatigue, known as *low-frequency fatigue*, which effects can last longer than 24 hours [138].

The effect of the stimulation train configuration on muscle fatigue has also been subject of investigation. The stimulation patterns investigated are constant frequency trains (CFT), variable frequency trains (VFT), and doublet or triplet (or n) frequency trains (DFT) [236, 237] (figure 4.2). CFT are stimulation trains in which the frequency remains constant throughout the entire train. Doublet frequency trains (DFT) are stimulation trains in which two closely spaced pulses, with an inter-pulse interval (IPI) typically 5-10 μs apart, are delivered within the stimulation train. In contrast, VFT begin with two closely spaced pulses followed by a CFT at chosen frequency. The use of closely spaced pulses within the stimulation train takes advantage of the *catch-like* property of muscles, which is the tension enhancement seen when a brief, high-frequency, burst is added to the beginning of a subtetanic train of pulses [238, 239].

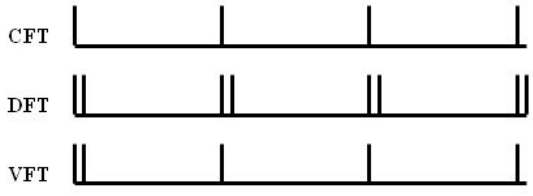

FIGURE 4.2: Stimulation train configurations. CFT: constant frequency trains. VFT: variable frequency trains. DFT: doublet frequency trains.

The catch-like effect induced by DFT has shown to increase muscle force generation after fatiguing the muscle [238]. A further investigation on the use of several closely spaced pulses to reduce fatigue has shown that optimal choice of the number of pulses is subject-dependent [237]. Besides, random modulation of the IPI within stimulation trains decrease fatigue rate compared to stimulation at constant frequency [240], but other experiments have shown that random modulation of frequency did not affect muscle fatigue compared to constant frequency [241]. These

results suggests that there may be several optimal stimulation patterns, dependent on the task, muscle group and population being studied.

As shown, research in the area of MES-related muscle fatigue pursues the optimization of stimulation parameters in an effort to maximize the muscle force generated in each stimulation train. This optimization thus allows the decrease of stimulation intensity to generate an amount of force or joint movement. As result, muscle fatigue is delayed due to a decreased stimulation intensity. However, muscle fatigue would eventually develops as consequence of the artificial contractions made over the muscle.

The use of NP for rehabilitation or functional compensation of walking demands a criteria for monitoring muscular performance to adapt therapy intensity, prevent danger situations due to diminished muscle performance and, in the case of the use within a hybrid exoskeleton, give an objective criteria to adapt robotic actuation to muscle performance. Furthermore, monitor muscle performance allows to tailor muscle fatigue management strategies to the specific fatigue response of the patient.

Few studies have proposed a criteria to customize stimulation strategies to manage human skeletal muscle decline to generate force [241, 242]. However, those criteria were not associated with the actual fatigue response of the muscles. Some research groups have explored the use of the evoked electromyographical signal (eEMG) of the muscle under stimulation as indicator of muscle performance. However, the correlation between eEMG and muscle fatigue of SCI is still controversial [243–245]. Furthermore, the complexity of recording eEMG during stimulation still remains problematic. It requires specific and custom-made equipment for rejecting artifacts from the stimulation [244]. In conclusion, new methods for estimation of muscle fatigue are needed.

This chapter comprises two experimental studies related to muscle fatigue estimation and management conducted in a sample of SCI subjects. The first study is presented in section 4.2. This study aims the establishment of an objective criteria for estimate muscle fatigue from changes in muscle performance. Results of this study are integrated into a online monitor of muscle performance that estimate muscle fatigue, suitable for integration with the hybrid control strategy, presented in section 4.3. This online monitor of muscle performance is employed the second experimental study, presented in section 4.4. This study aims to investigate the effects of stepwise modulation of stimulation frequency and pulse amplitude under a muscle fatigue detection scheme. As discussed later, these strategies were selected regarding compatibility with the hybrid-cooperative control approach.

4.2 Muscle fatigue estimation during isometric FES-elicited contractions in iSCI.

The hypothesis that support this study is that the decrease on muscle performance due to fatigue can be estimated from monitoring the generated force, if muscle stimulation conditions are constant. This study focuses on the fatigue response of the SCI population for which the hybrid walking approach developed in this dissertation is targeted (section 3.1). In order to monitor changes in muscle performance, an isometric muscle contractions experiment was designed. Therefore, the objective of this study was to investigate changes in muscle performance under constant stimulation parameters that can give an estimate of muscle fatigue.

Subject	Age	Gender	Weight	Height	Lesion
1	62	M	70	1.78	C4/5 D
2	49	M	95	1.68	D5 C
3	57	M	90	1.72	D6 C
4	62	M	70	1.75	D8 D
5	56	M	100	1.80	D7 C
6	22	M	70	1.70	D7 C
7	42	F	68	1.59	C6 D
8	45	M	85	1.74	D7 C
9	41	M	74	1.70	C6 D
10	25	M	70	1.90	C4 C
–	47±14	9M, 1F	79±12	1.74±0.08	–

TABLE 4.1: Subject characteristics for fatigue estimation study.

Ten motor incomplete SCI subjects volunteered for this study (table 4.1). Inclusion criteria were knee MMT score between 2 and 3 [5] and spasticity index lower than 3 in the Asworth [185]. All subjects were previously involved in a therapeutical MES training program. The local ethics Review Board approved the study and informed consent was obtained from all subjects.

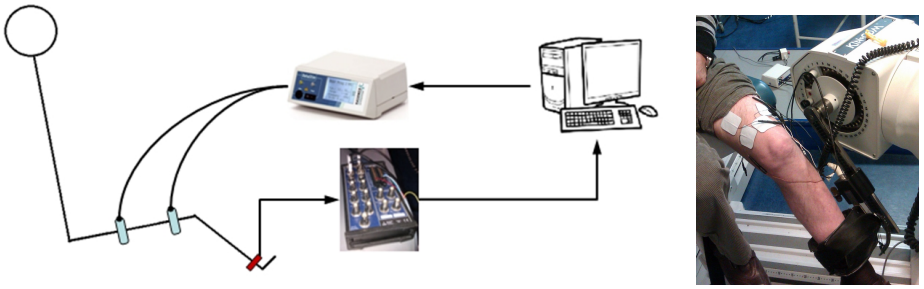

(a) Experimental set up.

(b) Patient positioning on dynamometer.

FIGURE 4.3: Experimental set-up for fatigue study.

Figure 4.4 represents the experimental protocol followed, where boxes represents the protocol steps. Description of each step is provided as follows:

1: Informed consent. Detailed information about the experiment procedure was given to the patient. After confirming that the patient fully understood the information, consent was obtained from the patient.

2: Transfer to dynamometer. Patients were transfered to the dynamometer (KinCom, Chattanooga Group Inc.). The leg being tested was securely attached to the rotating lever arm just above ankle, and trunk, pelvis and tight were stabilized using straps (figure 4.3(b)). Hip joint was flexed 100 degrees and knee joint was flexed 45 degrees with the dynamometer axis aligned with the knee joint. The leg that met inclusion criteria was selected for testing. If both legs met these criteria, the dominant one was selected.

3: Electrode placement. This study involved testing both flexor and extensor muscle groups. Thus, the protocol was repeated twice. The muscle group to be tested first was randomly selected. Electrodes (5 X 5 cm, Alexgaard, Pals-platinum) were placed either over the motor points of *Vastus Lateralis*, *Rectus Femoris* and *Vastus Medialis* knee extension

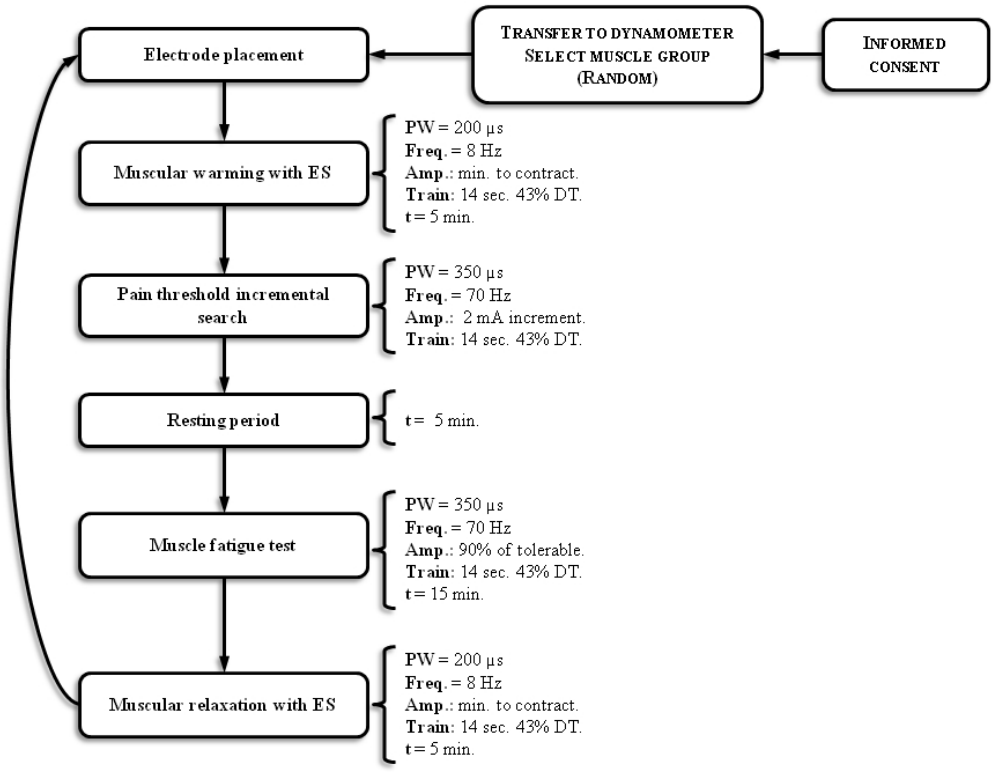

Figure 4.4: Experimental protocol for isometric fatigue study.

muscles, or over the motor points of *Semitendinosus* and *Biceps Femoris* knee flexion muscles.

4: Muscular warming. A muscular warming period was performed during 5 minutes. The patient was instructed to not activate knee muscles and to relax during the whole experimental protocol. Stimulation parameters for this phase were: pulse duration 200 μs, frequency 8 Hz, pulse train duration 14 sec. and duty cycle 43%. Pulse amplitude was set to the minimum value that allowed elicit visible muscle contraction.

5: Pain threshold search. The purpose of this step was to find the maximum stimulation intensity comfortably tolerable by the patient, assuming that this intensity would elicit the maximum muscle force, from which muscle fatigue can be monitored. Stimulation pulse duration was set to 350 μs, train frequency to 70 Hz, pulse train duration 14 sec. and duty cycle 43%. Maximum tolerable pulse amplitude was obtained with an iterative procedure, in which pulse amplitude was sequentially increased (2 mA steps) every stimulation train, until the patient perceived the stimulation as uncomfortable.

6: Resting period. Within this step, no stimulation was delivered during 5 minutes. The purpose of this period was to recover the fatigue that the previous step could induce.

7: Muscle fatigue test. This step corresponds to the actual fatigue test. Stimulation was delivered for 15 minutes while the force generated by the muscles was recorded through the dynamometer force sensor. Stimulation parameters were the same than for step 5, but stimulation amplitude was decreased 10%. This provided the patient enough comfort for tolerating the 15 minutes test.

8: Muscular relaxation. After the fatigue test, a muscular relaxation period was carried out following the same procedure as for warming (step 4). Once completed the relaxation period, the sequence was repeated for the remaining muscle group, comprising steps 3 to 8.

A comment regarding step 5 is made here. There was two rationales for generating the maximum muscle force with the stimulation. Firstly, it was assumed that high muscle demand would provide better observation of changes in muscle performance than sub-maximal muscle activation. Secondly, this study aims to provide a fatigue criteria and a management procedure to be integrated within the hybrid walking therapy. As exposed previously, inefficiency of artificial muscle activation and the impaired muscle condition resulting from SCI hampers generating suitable forces for providing joint support and movement for walking. Therefore, studying the fatigue phenomena under maximal force generation conditions is presented in this study.

A PC-controlled stimulator was used (Rehastim, Hasomed GmbH), which delivers biphasic current-controlled rectangular pulses. Dynamometer force was feed into a data acquisition card (NI PCI-6602, National Instruments) at 1 kHz sampling rate. Stimulator control and data acquisition was implemented on Simulink RealTime Windows Target (figure 4.3(a)).

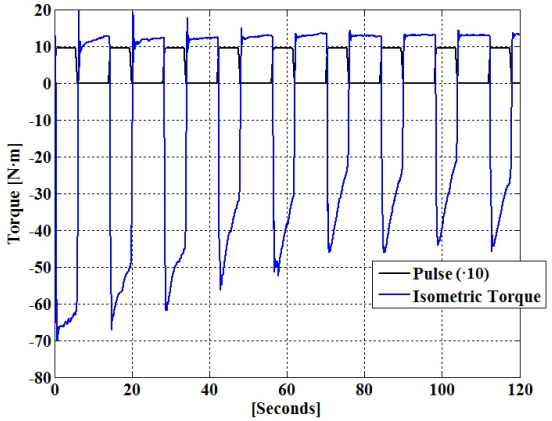

FIGURE 4.5: Force developed in the first pulses of a fatigue experiment (blue curve, negative is extension force). Stimulation duty cycle (ON/OFF) is superimposed in black.

4.2.1 Data analysis

Figure 4.5 depicts an example of the torque values developed by the quadriceps of a patient during the first stimulation trains of an experiment. It can be observed a decrement between consecutive pulses due to muscle fatigue, in both peak value and evolution of the force after reaching the peak. Note that the gravitational torque due to leg weight introduces an offset, which is more noticeable at off periods of the stimulation trains.

After the experiments, gravitational torque was removed and the torque data were normalized by subjects' leg length. Then the force time integral (FTI) was calculated for each stimulation pulse (figure 4.6(a)). FTI data was then normalized to the first pulse FTI for comparison and group average, hereinafter NFTI data (figure 4.6(b)).

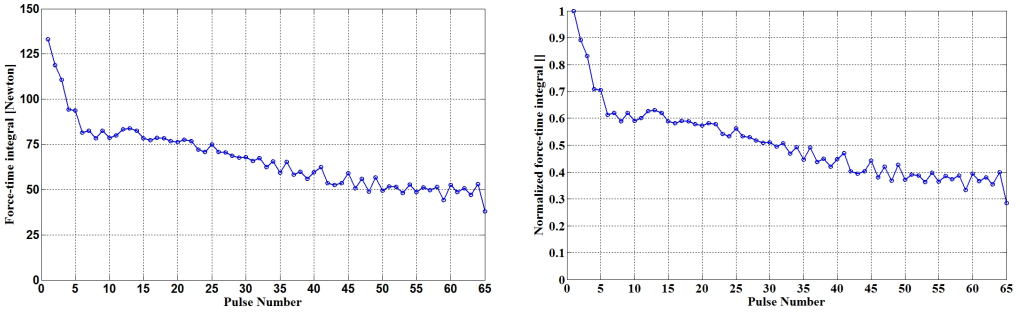

(a) Force-time integral (FTI). (b) Normalized force-time integral (NFTI).

FIGURE 4.6: Post-processed results from fatigue experiment.

For each stimulation train, the NFTI for each muscle group were group-averaged calculating mean and standard deviation of each stimulation train, obtaining a NTFI curve representative for the study group (figure 4.7). Then, the differences between grouped NFTI were statistically tested with Friedman and Wilcoxon post-hoc test with Bonferroni correction.

Initial and last FTI values were group averaged calculating mean and standard deviation for each muscular group (figure 4.8(a)). The number of pulses of NFTI to decay 15, 20 y 50% was also obtained (figure 4.8(b)). Wilcoxon test was applied to test differences between variables. Significance level was $p<0.05$.

4.2.2 Results

Figure 4.7 shows the NFTI for extensor and flexor muscles for the study group. It should be noted that time and pulse number are equivalent since train length and duty cycle are held constant. The regression analysis showed an exponential relationship between FTI VS cycle, which is consistent with previous data [150, 238, 246, 247]. It can be observed that FTI decay for flexor muscles shows a slower decay than extensor muscles. Statistical analysis of differences among NFTI mean values between consecutive pulses showed a significative decay in FTI (11%, $p<0,05$) for extensor muscles at second stimulation train, whereas for flexor the significative decay in FTI occurs in the ninth pulse (19%, $p<0,05$).

Further differences were found in non-normalized FTI (figure 4.8(a)): 79 N for extensor and 41 N for flexor ($p<0,05$), although at the end of the experiments FTI values were similar between muscles ($p=0,80$). FTI at the end of the experiment was significantly lower compared to the beginning of the experiment for both muscle group ($p<0,01$). Figure 4.8(b) right depicts NFTI reduction in relation with number of applied stimulation pulses. Decays of 15, 20 and 50% showed differences within muscle groups. However no differences in pulses to decay were found between muscle groups.

4.2.3 Discussion

The objective of the study presented in this section was to propose an objective criteria to estimate muscle fatigue from changes in muscular performance during electrically elicited isometric

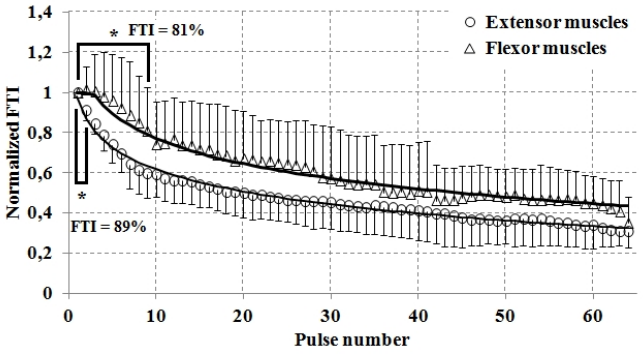

FIGURE 4.7: Fatigue model for flexor and extensor muscles. Mean normalized FTI values for all subjects (N=10). Vertical bars means standard deviation. Coefficient of determination (R^2) for each regression curve: extensor muscles= 0.98, Flexor muscles= 0.95. * denotes p<0,05.

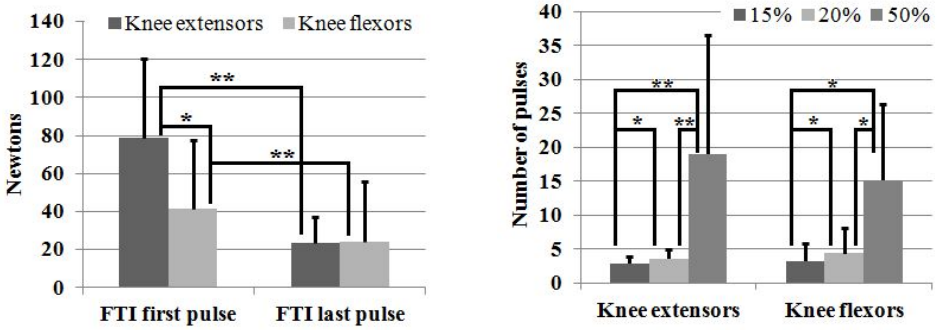

(a) FTI values developed at the beginning and end of the experiment.

(b) Number of pulses to decrease 15%, 20% and 50% of the initial FTI.

FIGURE 4.8: Fatigue study results: absolute force and time to decrease. * denotes p<0,05; ** denotes p<0,01.

muscle contractions in subjects whit incomplete SCI. Monitoring of muscle force was chosen instead of other existing approaches for muscle performance monitoring, as the eEMG of the muscle under stimulation. As shown previously, the controversial existing results on the use of eEMG for monitoring muscle performance does not justify the complexity on the hardware and signal processing needed [245].

Results obtained confirm that through monitoring the muscle force trough FTI, changes in muscle performance are detected. Either FTI and peak force developed during stimulation train have been used without distinction for assessing muscle fatigue, without a consensus on the suitability of each [247–251]. However, peak force can be easily affected by stochastic phenomena related with spasm. FTI on the other hand, represents the mean force value developed by the muscle during the stimulation train, thus is more robust and representative than peak force.

The fatigue models obtained are similar to the models presented in the literature [150, 238, 246, 247], exhibiting an exponential decay. Total FTI decay in the study presented here differs between extensor and flexor muscles, towards a 40% for flexor and 30% for extensor. The variety on stimulation protocols in the literature difficults the comparison and discussion of these results, but are in general in line with the values from literature.

The study presented here is the first that analyzes the fatigue of knee flexor muscles and compares it versus extensor knee muscles. For walking-related functional activities driven by NP, it is of the most importance the studying of fatigue of knee flexor muscles as they play a fundamental role in achieving adequate toe-clearance during the swing phase. Results from figures 4.7 and 4.8(a) show that the relative decay for flexor muscles is slower than for extensor muscles which indicates that flexor muscles develop less fatigue in this protocol. However, this slower decay in muscle performance was not confirmed by the analysis of the time to decay of FTI (figure 4.8(b)). On the other hand, the force developed by the flexor muscles was notably lower than extensor muscle force (figura 4.8(a)). These results suggest that stimulation of flexor muscles is less efficient than for the extensor muscles.

The progress of the NFTI for flexor muscles exhibits a greater variability than flexor muscles, mainly at the beginning of the curve (figure 4.7). This can be attributed to the fact that the potentiation effect[2] was not controlled in the experimental protocol. Whilst there is no a specific criteria for stablishing the number and configuration of the stimulation trains to account for potentiation, it was assumed that potentiation was overcome during the iterative search of the pain threshold (figure 4.4), which took 5 to 10 pulses in average, similar to the number of pulses delivered in the protocols that accounted for muscle potentiation [150,242,250,251,253]. It is noticeable that in the case of quadriceps potentiation was not detected. Nevertheless, performance of extensor muscles seems to be more affected by non-controlled factors than extensor muscles.

Up to the best of the author's knowledge, this is the first study that addressed the establishment of a criteria to discriminate muscle fatigue from changes in muscular performance. The minimum statistically significant change in NFTI was 89% for extensor muscles and 81% for flexor muscles. Given that the stimulation parameters remained fixed, this significative drop in NFTI can be assumed to be due to a decline in muscular performance. In other words, within the population analyzed, a decrease of 11% in extensor muscles NTFI, or 19% for flexor muscles denote the minimum change in this variable that indicates the apearance of muscle fatigue.

Some studies have tested stepwise modulation of stimulation parameters for management of muscle fatigue based on estimates of decreased muscle performance. For example, Chou [242] used a drop of 10% in peak force to estimate muscle fatigue and thus change stimulation parameters. A rationale for this value was however not given. Thrasher [241] stated that a drop of 3 dB (70.8%) in peak force was a criteria for estimate muscle fatigue. The study presented here represents an effort to discriminate muscle performance drop from stochastic effects, assuming this change as a fagitue criteria. It should be noticed here that the fatigue criteria for the extensor muscles, a drop in FTI of 11%, is similar to the 10% drop in peak force proposed by Chou [242]. Nevertheless, the latter was performed in a population of 12 healthy subjects, which limits the comparison between studies.

[2]The *potentiation effect* is the enhacenment of force seen after repetitive activation [252]. This effect is further discussed in section 4.4.3.

4.3 Online monitor for automatic estimation of muscle fatigue due to FES

In previous section, a criteria for muscle fatigue estimation has been extracted from post-processing of the time evolution of the force developed by the stimulated muscles. In this section, the data analysis procedure and the criteria obtained are translated into an algorithm for online monitoring of muscle performance and fatigue estimator (MFE).

Figure 4.9 shows the pseudo-code of the data analysis procedure according to the previous study along with some features needed for automate the process. The algorithm derived from the pseudo-code of figure 4.9 calculates the NTFI curve presented in section 4.2.1 and compares NFTI values of each stimulation train with the fatigue criteria.

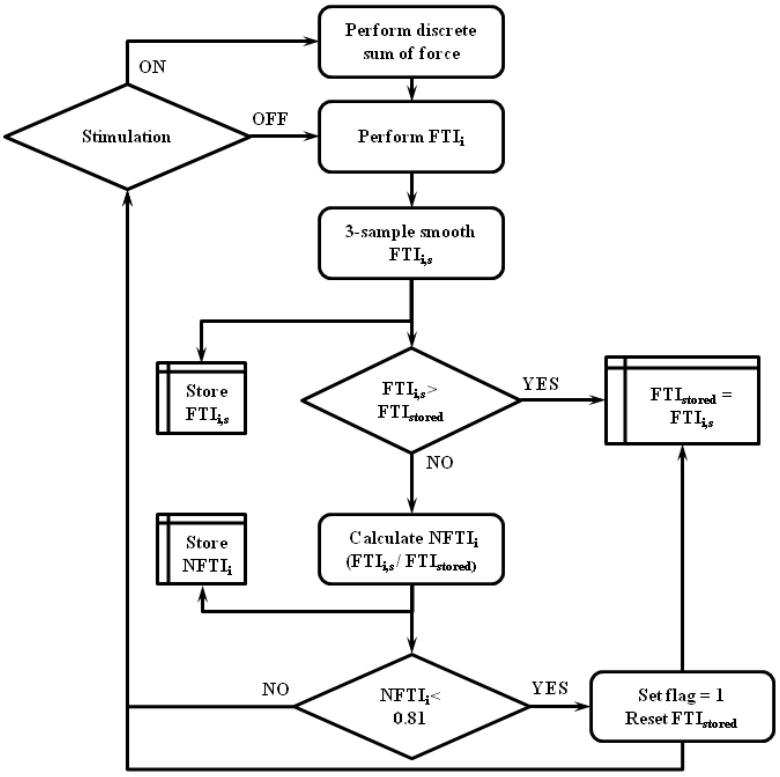

FIGURE 4.9: Pseudo-code for automatic muscle fatigue estimation.

Input to the MFE are actual absolute force measured by the sensor and stimulation duty cycle (ON/OFF). When the stimulation is ON, a discrete sum is performed until the stimulation train changes from ON to OFF. In this time-frame, the discrete sum is divided by the total number of frames during the ON cycle. This gives the FTI for the ON interval, which is stored in memory. FTI data is then 3-sample smoothed, to improve data trend and avoid false fatigue detections (figure 4.10(a)). This value is compared with previous FTI stored in memory and FTI is updated inly if higher than the previous recording. This comparison ensures to store the maximum FTI generated at each stimulation train, which in turn allows to manage the potentiation effect.

After storing the maximum FTI, it is used to calculate the NFTI. Then, NFTI is compared with the fatigue criteria: if NFTI is lower than the fatigue criteria established in section 4.2 (0.89 for extensor muscles, 0.81 for flexor muscles), then muscle fatigue is estimated (figure 4.10(b)). This sets the output of the fatigue estimator block to 1, which can be fed to any control strategy as detection of muscle fatigue. This flag resets the maximum FTI stored in memory and the smooth filter to start again the process with new data.

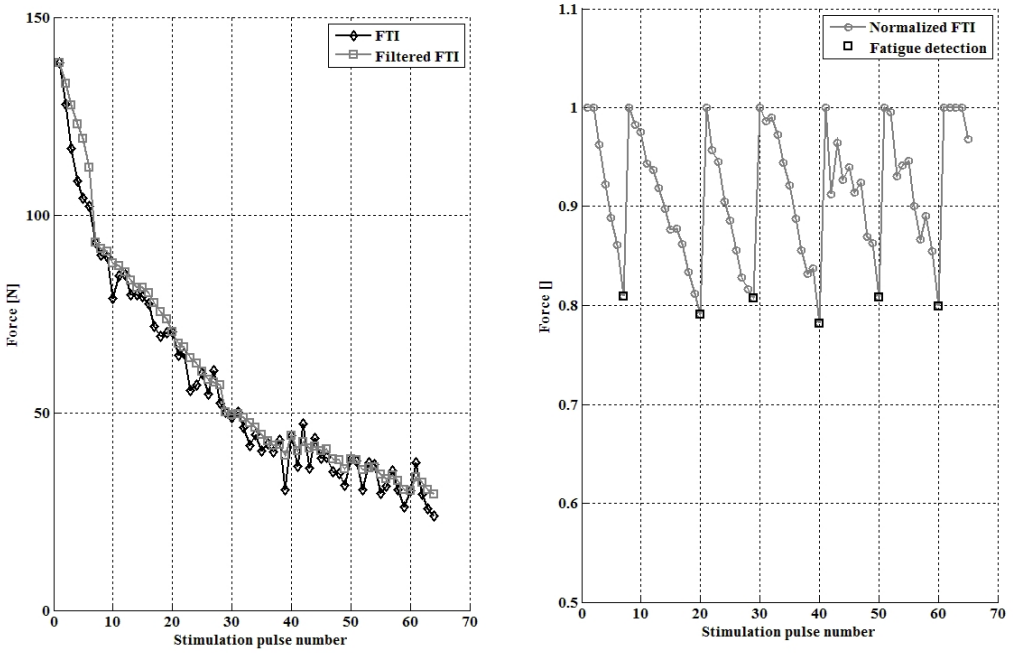

(a) Black diamonds: online FTI for each stimulation train. Grey squares: 3-sample smoothed FTI.

(b) Gray circles: normalized FTI (NFTI). Squares indicates muscle fatigue detection.

FIGURE 4.10: online muscle fatigue estimator operation. Representative example for flexor muscles.

The online MFE was then encapsulated in a single Simulink block, which inputs are the torque generated and the stimulation duty cycle. Figure 4.10 shows the actual application of the Simulink block to a fatigue experiment with a healthy subject.

4.4 Comparative study among frequency and amplitude modulation for muscle fatigue management.

In this section a comparative study of muscle fatigue management strategies based on the proposed MFE is presented. The main approaches described in the literature for muscle fatigue management were discussed previously (section 4.1). Most of those strategies need custom-made stimulators for controlling in real time the stimulation parameters. However, the hybrid-cooperative control of walking approach developed in this dissertation needed for eliciting the maximum muscle force with the NP. Thus, investigating new approaches were needed, compatible with this application. Furthermore, the strategies proposed in this study are easy to implement with commercial stimulators, which can only manipulate the main parameters of the stimulation train in real time, which further simplifies the hybrid control task.

It has been suggested that as the muscle fatigues, motor units decrease their firing rates to match the decreasing contractile speed so that lower frequencies, which are less fatiguing, could still generate relatively higher forces [254]. The study presented in this section hypothesized that decreasing stimulation intensity preserves muscle force generation capability. The objective therefore was to analyze the effects on muscle performance of decreasing stimulation intensity as the muscle fatigues. The strategies proposed for comparison within this study were *frequency modulation* (FM), *pulse amplitude modulation* (AM) and *constant frequency and amplitude* (CFA).

Subject	Age	Gender	Weight	Height	Lesion
1	62	M	70	1.78	C4/5 D
2	49	M	95	1.68	D5 C
3	57	M	90	1.72	D6 C
4	62	M	70	1.75	C5 C
5	56	M	100	1.80	D7 C
6	22	M	70	1.70	D7 C
–	51±15	6M, 0F	83±14	1.74±0.05	–

TABLE 4.2: Subject characteristics for fatigue management strategies study.

As in the study presented in section 4.2, the study presented here focuses on the fatigue response of the SCI population for which the hybrid walking approach developed in this dissertation is targeted (section 3.1). Both studies share the experimental protocol, as showed later. Subjects participating in this study were the same for both studies, although the study presented here was undergone three weeks after the first study. There were four dropouts due to discharge. Therefore, six motor incomplete SCI subjects comprised the sample for this study (table 4.2). As in the previous study, inclusion criteria were knee MMT score between 2 and 3 [5], and spasticity lower than 3 in the Asworth scale [185]. All subjects were previously involved in a therapeutical MES training program. The local ethics Review Board approved the study and informed consent was obtained from all subjects.

Figure 4.11 represents the experimental protocol followed for this study, which is equal to that of section 4.2 but for the muscle fatigue test step. Each muscle fatigue management strategy was evaluated in a day with at least 48 hours between evaluations, thus the experimental protocol was completed in three different days, one for each strategy. The strategies were randomly sorted for each patient participating in the study. Description of each step is provided here:

1: Informed consent. Detailed information about the experiment procedure was given to the patient. After confirming that the patient fully understood the information, consent was obtained from the patient.

2: Transfer to dynamometer and electrode placement. Patients were transfered to the dynamometer (KinCom, Chattanooga Group Inc.). The leg being tested was securely attached to the rotating lever arm just above ankle, and trunk, pelvis and tight were stabilized using straps (figure 4.3(b)). Hip joint was flexed 100 degrees and knee joint was flexed 45 degrees with the dynamometer axis aligned with the knee joint. The leg that met inclusion criteria was selected for testing. If both legs met these criteria, the dominant one was selected.

This study involved testing both flexor and extensor muscle groups for each strategy, so the protocol was repeated twice. The muscle group to be tested first was randomly selected. Electrodes (5 X 5 cm, Alexgaard, Pals-platinum) were placed either over the motor points

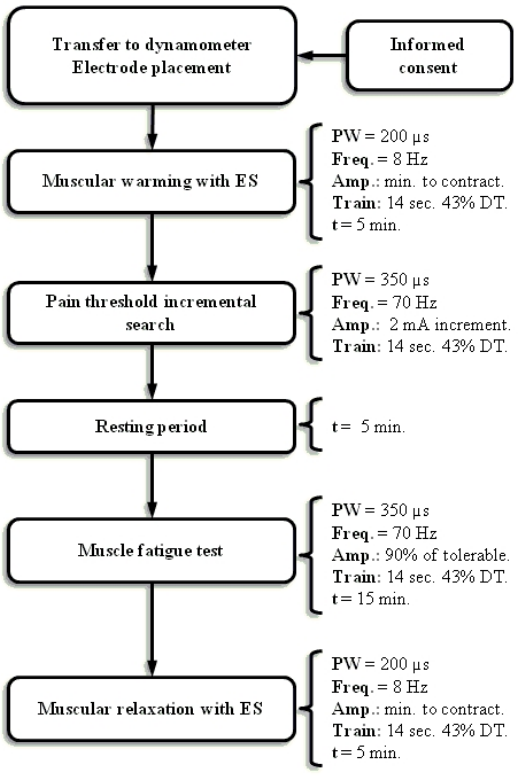

FIGURE 4.11: Experimental protocol for fatigue strategies comparison study.

of *Vastus Lateralis*, *Rectus Femoris* and *Vastus Medialis* knee extension muscles, or over the motor points of *Semitendinosus* and *Biceps Femoris* knee flexion muscles.

3: Muscular warming. A muscular warming period was performed initially during 5 minutes. The patient was instructed to not activate knee muscles and to relax during the whole experimental protocol. Stimulation parameters for this phase were: pulse duration 200 μs, frequency 8 Hz, pulse train duration 14 sec. and duty cycle 43%. Pulse amplitude was set to the minimum value that allowed elicit visible muscle contraction.

4: Pain threshold search. The purpose of this step was to find the maximum stimulation intensity comfortably tolerable by the patient, assuming that this intensity would elicit the maximum muscle force, from which muscle fatigue can be monitored. Stimulation pulse duration was set to 350 μs, train frequency to 70 Hz, pulse train duration 14 sec. and duty cycle 43%. Maximum tolerable pulse amplitude was obtained with an iterative procedure, in which pulse amplitude was sequentially increased (2 mA steps) every stimulation train, until the patient perceived the stimulation as uncomfortable.

5: Resting period. Within this step, no stimulation was delivered during 5 minutes. The purpose of this period was to recover the fatigue that the previous step could induce.

6: Muscle fatigue test. This step corresponds to the actual fatigue test. Stimulation was delivered for 15 minutes while the force generated by the muscles was recorded through the dynamometer force sensor. Stimulation parameters were the same than for step 5, but stimulation amplitude was decreased 10%. This provided the patient enough comfort for tolerating the 15 minutes test. Regarding the strategy tested, stimulation parameters were modulated as follows:

For FM strategy, stimulation frequency was decreased 10 Hz after fatigue detection, remaining the rest of the stimulation parameters (pulse amplitude, pulse duration, train duration and duty cycle) fixed.

For AM strategy, stimulation was decreased in amplitude (2 mA[3]) when fatigue was detected, remaining the rest of the stimulation parameters (frequency, pulse duration, train duration and duty cycle) fixed.

For CFA strategy, none of the stimulation parameters (frequency, pulse amplitude, pulse duration, train duration and duty cycle) remaining fixed during the experiment.

7: Muscular relaxation. After the fatigue test, a muscular relaxation period was carried out following the same procedure as for warming (step 4). Once completed the relaxation period, the sequence was repeated for the remaining muscle group, comprising steps 2 to 7.

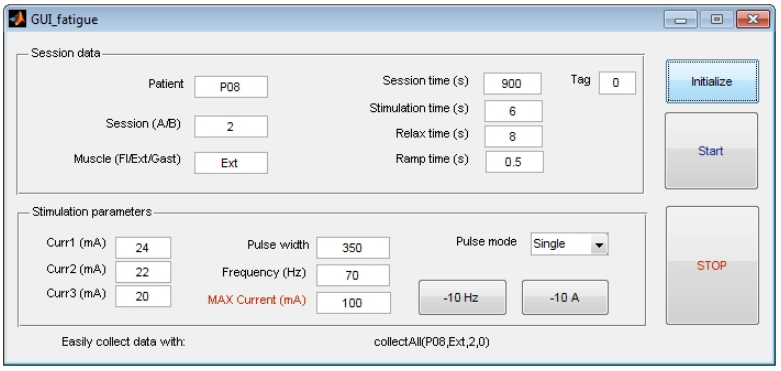

FIGURE 4.12: Graphical User Interface developed for stimulator real-time control.

A customized program was developed in Simulink to implement the online MFE and the stimulation control. A graphical user interface (GUI) was further designed to set and change in real-time stimulator parameters (figure 4.12). During the the experiments, a Simulink scope prompted the main variables controlled during the experiments. Figure 4.13 top shows actual force developed, the FTI and the filtered FTI, and figure 4.13 bottom shows the normalized FTI and the fatigue estimation block output. After muscle fatigue is detected, the pulse amplitude or frequency was changed through the GUI, pressing the button needed (figure 4.12). This change in stimulation parameters was feed in real-time to the stimulator control and had effect on the next stimulation train on which fatigue was estimated.

4.4.1 Data analysis

The analysis performed was equal to that of section 4.2.1 with the addition of a comparison of FTI and NFTI among strategies. Initial and last FTI values were group averaged for each muscular group and strategy. For each stimulation train, the NFTI was group averaged, obtaining a group-NTFI curve for each muscle group and strategy (figures 4.14 and 4.17). The number of pulses of NFTI to decay 15, 20 y 50% for each strategy tested was also obtained (figures 4.16(b) and 4.19(b)). Statistical analysis was performed with Friedman and Wilcoxon post-hoc test with Bonferroni correction. Significance level was $p<0.05$.

[3]This decrement is due to the minimum resolution of the stimulator

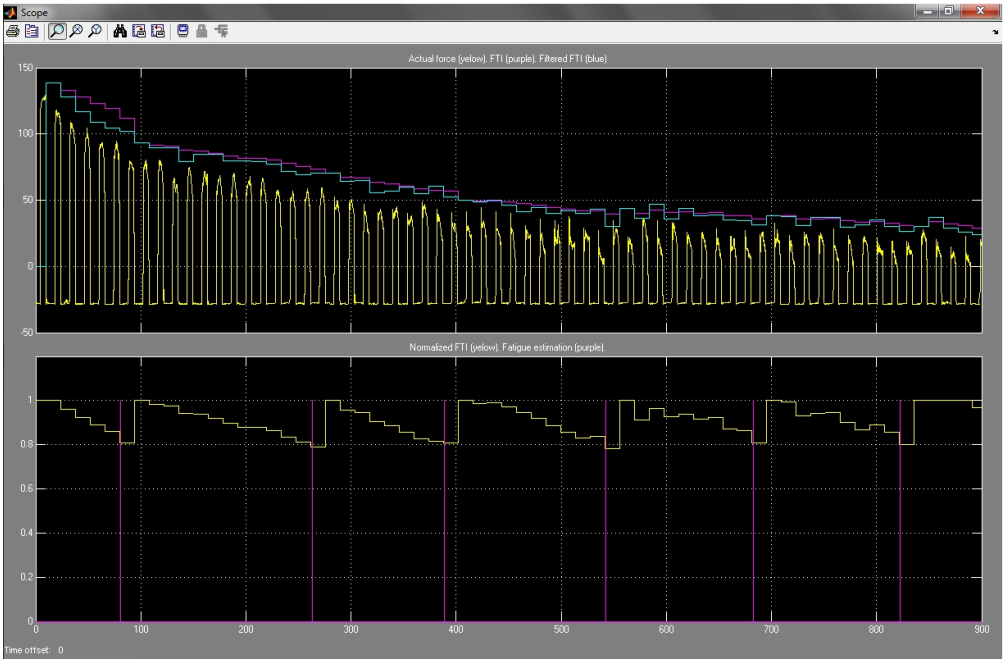

FIGURE 4.13: Information managed within Simulink scope. Top graph: actual force (yelow), FTI (purple) and filtered FTI (blue). Top graph: normalized FTI (yellow) and fatigue estimator blok output (purple).

4.4.2 Results

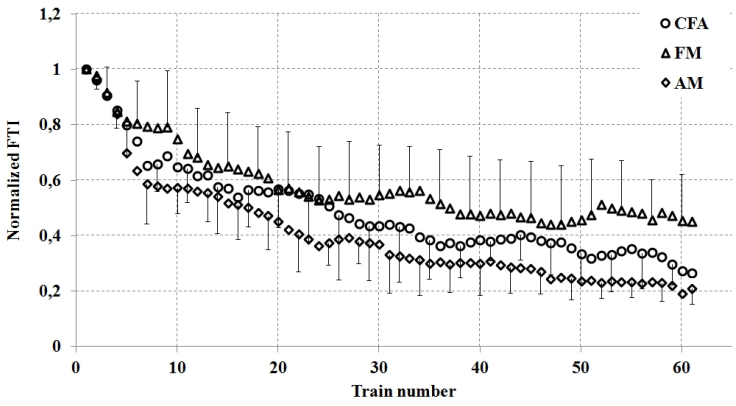

FIGURE 4.14: Comparison of extensor muscles NFTI for the three tested strategies (N=6). Data shows group average for each strategy. Vertical bars means standard deviation.

Figure 4.14 shows the group average results of NFTI for each strategy tested of the knee extensor muscles. Here it can be noticed the different evolution of NFTI for each strategy, which is more noticeable in figure 4.15, where the adjusted data to an exponential decay function for the three tested strategies is showed. It can be noticed a higher NFTI for AM strategy than CFA and AM. Compared with figure 4.7 the CFA strategy shows similar trend as expected.

Figure 4.16(a) shows the absolute values for FTI at the initial and last stimulation trains for extensor muscles. Statistical analysis showed no differences among all three strategies at the

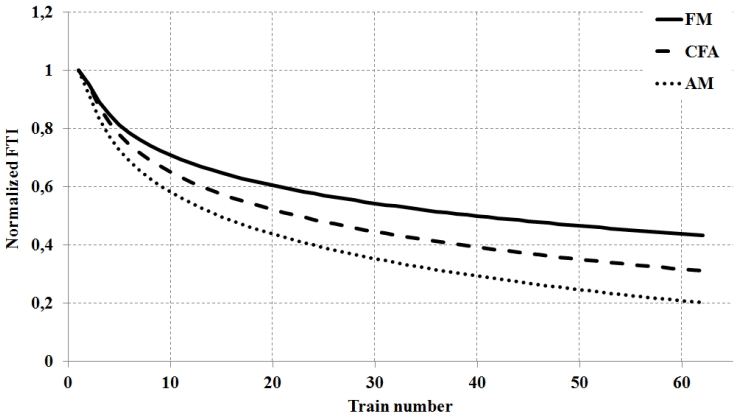

FIGURE 4.15: Extensor muscle fatigue trend data for the three strategies tested. Coefficient of determination (R^2) for each strategy: FM= 0.96, CFA= 0.97, AM= 0.98.

initial FTI. Last values of FTI showed also no differences among strategies, although last FTI value for FM strategy showed a tendency to be higher than AM (p=0,173) and CFA (p=0,075) strategies.

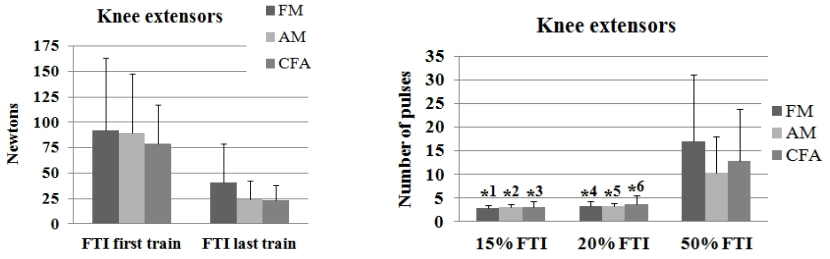

(a) Absolute values for FTI at the initial and last stimulation trains.

(b) Number of pulses to decrease 15%, 20% and 50% of the initial FTI for each strategy, extensor muscles. * denotes p<0,05.

FIGURE 4.16: Effect on FTI and time to decrease NFTI. Extensor muscles.

Figure 4.16(b) shows the number of stimulation trains to the initial NFTI to decay 15%, 20%, and 50% for extensor muscles. Within strategies, the comparison among values showed that there were statistical diferences between 15% to 20% of decay for FM (*1), AM (*2) and CFA (*3) strategies, and between 20% to 50% of decay for FM (*4), AM (*5) and CFA (*6) strategies respectively. No differences were found across strategies for the same decay percentage. In the case of 50% of decay, FM showed a tendency to need a higher number of pulses than AM (p=0,345) and CFA (p=0,500) strategies to decay a 50% of the initial NFTI.

Figure 4.17 shows the group average results of NFTI for each strategy tested of knee flexor muscles. Here it can be noticed the different evolution of NFTI for each strategy, which is more noticeable in figure 4.18, where the adjusted data for the three tested strategies is shown. Comparing between flexor and extensor muscles for each strategy, it can be noticed that extensor muscles have a more pronounced decay than the flexor muscles. This was also observed in figure 4.7.

Figure 4.19(a) shows the absolute values for FTI at the initial and last stimulation trains for flexor muscles. As in the case of extensor muscles, statistical analysis showed no differences

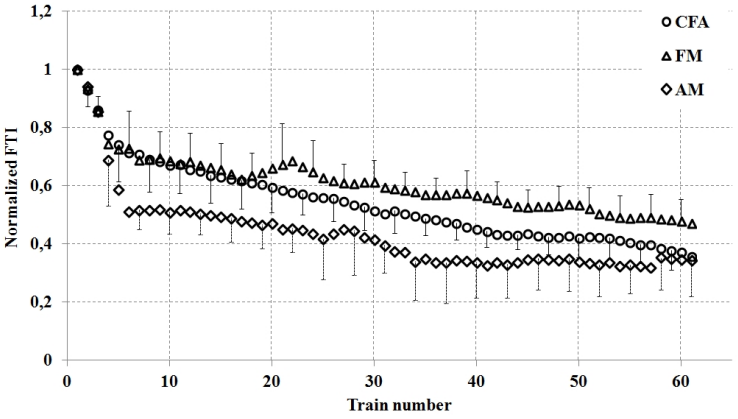

FIGURE 4.17: Comparison of flexor muscles NFTI for the three tested strategies (N=6). Data shows group average for each strategy. Vertical bars means standard deviation.

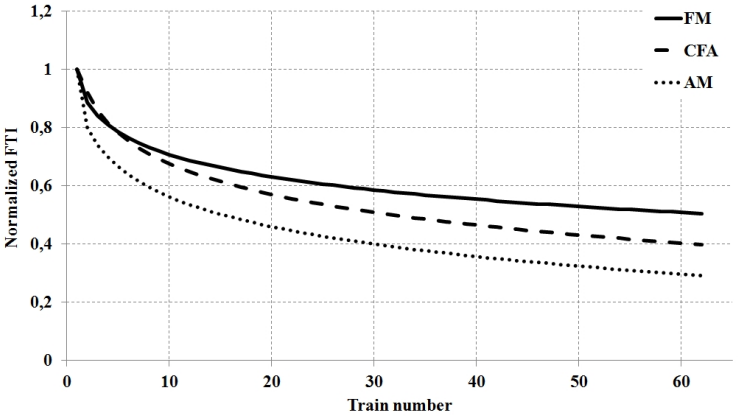

FIGURE 4.18: Flexor muscle fatigue trend data for the three strategies tested. Coefficient of determination (R^2) for each strategy: FM= 0.93, CFA= 0.98, AM= 0.90.

among all three strategies at the initial FTI. Last values of FTI showed significative differences for FM strategy, which was higher than AM and CFA strategies (p<0,05). No differences among all three strategies at the initial FTI were found.

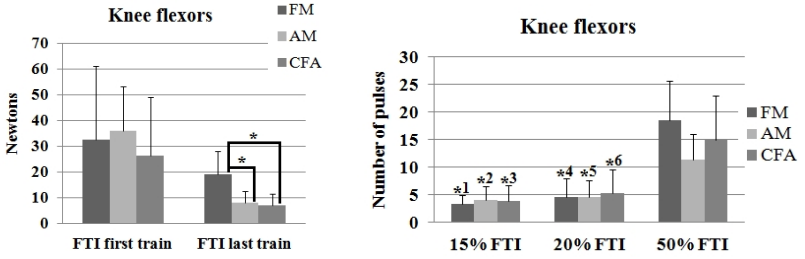

(a) Absolute values for FTI at the initial and last stimulation trains. * denotes p<0,05.

(b) Number of pulses to decrease 15%, 20% and 50% of the initial FTI for each strategy. * denotes p<0,05.

FIGURE 4.19: Effect on FTI and time to decrease NFTI. Flexor muscles.

Figure 4.19(b) shows the number of stimulation trains to decay 15%, 20%, and 50% of the initial NFTI for flexor muscles. Within strategies, the comparison among values showed that there were

statistical diferences between 15% to 20% of decay for FM (*1), AM (*2) and CFA (*3) strategies, and between 20% to 50% of decay for FM (*4), AM (*5) and CFA (*6) strategies respectively. No differences were found across strategies for the same decay percentage, althoug for the case of 50% of decay, FM showed a tendency to higher number of pulses than AM (p=0,075) and CFA (p=0,225) strategies.

4.4.3 Discussion

In the study presented in this section, the MFE developed in section 4.3 has been applied to comparatively analyze the effects on muscle fatigue of two strategies for muscle fatigue management. FM strategy showed that discrete decrements on stimulation frequency of flexor muscles delays muscle fatigue compared to CFA and AM strategies, which was statistically significant for flexor muscles. In the case of extensor muscles, a similar trend was observed, although statistical significance was not obtained. The superior performance showed by FM strategy agrees with general results from other studies, where frequency modulation is shown that delays muscle fatigue [237, 242, 255], and stimulation intensity modulation leads to a decreased muscular performance [242].

In this study, initial stimulation parameters were higher than those reported in literature because the strategies to be tested were based on stepwise decrements on frequency and pulse amplitude. The choice of these stimulation parameters and the decremental stepwise strategies under investigation were selected to tackle the ultimate objective of this dissertation, which is the development of a hybrid robot-NP walking exoskeleton. Therefore, the stimulation parameters were set to obtain the maximum force at the initial steps during the hybrid walking therapy.

The effects of high versus low stimulation frequency in muscle fatigue are still controversial, although recent studies have shown that stepwise increments on stimulation frequency can delay muscle fatigue [242]. A limitation of the study presented here is that the reverse FM strategy (stepwise increments in stimulation frequency) was not considered to compare its effects on fatigue. Furthermore, comparison with other criteria for modulation of stimulation parameters (like the proposed by [242] or others) would shed light into the suitability of the criteria utilized in this work for tailoring fatigue strategies.

The results from thus study are applicable to the generation of force through isometric muscle contractions. Quadriceps muscles work in isometric conditions during the stance phase of walking, thus the results from this study can be directly applied to the actual control of quadriceps muscles during hybrid walking. On the contrary, the swing phase is a dynamic movement, thus the results from this work can differ from the actual flexor muscle fatigue during hybrid walking. An experimental design based on isokinetic muscle contractions matching leg's weight could better resemble the real stimulation conditions and requirements during walking. However, inability of SCI patients to develop enough force for this procedure was foreseen, and was further confirmed with the data obtained in the studies, which complicates setting such isokinetic experiment with this patient sample.

4.5 Conclusion

An objective criterion for early detection of muscle fatigue of electrically stimulated muscles in individuals with incomplete SCI has been presented, using FTI to model muscle performance in time. Force characteristics and fatigue trend differs between flexor and extensor muscles. Flexor muscles develop less force and also less fatigue than extensor muscles.

The developed online MFE allows to implement tailored muscle fatigue strategies between stimulation trains, which has been applied to the comparison of two strategies to delay muscle fatigue in SCI patients. Nevertheless, the fatigue-adapted modulation strategy presented in this work can be combined with other muscle fatigue management strategies.

The results showed that the FM strategy leads to higher NFTI values for both muscle groups thus delaying fatigue, and the worst results were obtained with AM modulation strategy. The implications of these results for the development of the hybrid walking controller are that, although high stimulation parameters are needed to elicit strong muscle contractions to achieve walking, fatigue-specific decreases in stimulation frequency delays muscle fatigue.

Further work is needed to investigate if tailoring muscle fatigue strategies to the specific muscle response of the patient leads to better outcomes than other proposed criteria.

4.5.1 Answer to research questions

This chapter provides provides the following answers to research questions Q4 and Q6 stated in section 1.6.2 as follows:

Q4: **Which type of criteria would be useful for estimating muscle fatigue?** It has been shown that muscle fatigue can be estimated from changes in muscle performance, specifically the average joint torque developed by the muscles during the stimulation train. A quantitative criteria has been proposed for knee extensor and flexor muscle groups.

Q6: **What muscle fatigue management strategy can be implemented with early detection of muscle fatigue?** The stimulation parameters needed to elicit enough muscle force for hybrid walking led to develop a specific strategy for muscle fatigue management. It has been concluded that decreasing stimulation frequency according to the proposed FTI-based criteria is a valid technique for management of muscle fatigue. Further work is needed comparing performance of several strategies and testing in the hybrid control system.

Chapter 5

Cooperative control of hybrid walking[1]

This chapter presents the NP controller and the hybrid-cooperative control approach. Both developments aim to overcome several challenges identified in the SoA (chapter 2). Firstly, the NP features a closed-loop stimulation control strategy, in which a PID and Iterative Learning Controller (ILC) are placed in parallel for control of extensor and flexor knee muscles. Secondly, the cooperative control approach allows to monitor muscle performance and modulating the assistance of the robotic exoskeleton. Experiments conducted with healthy subjects revealed general values for PID control gains. A modified ILC algorithm allows to overcome the electromechanical delay of stimulated muscles. The influence of the parameters that characterize the ILC algorithm (learning, forgetting and time-horizon) is investigated. The best set of parameters, in terms of performance of muscle contribution to the movement, are adopted for the ILC.

5.1 Introduction

Previous chapters have detailed partial aspects of the hybrid walking control approach: the robotic platform Kinesis[2] and its joint controller (chapter 3), and an ad-hoc study for muscle performance monitoring and fatigue estimation (chapter 4). This chapter completes the description of the hybrid walking control approach, presenting the NP controller (section 5.2) and the main controller that coordinates the exoskeleton and NP controllers, aimed to implement a collaborative control of knee trajectory during hybrid walking (section 5.3).

[1]This chapter is partially based on the following articles:
A. J. del-Ama, J. C. Moreno, A. Gil-Agudo, and J. L. Pons. **Hybrid FES-Robot cooperative control of ambulatory gait rehabilitation exoskeleton for spinal cord injured users,** in 2012 International Conference on Neurorehabilitation (ICNR2012): Converging Clinical and Engineering Research on Neurorehabilitation, 2012, pp. 155-159.
A. J. del-Ama, J. C. Moreno, A. Gil-Agudo, and J. L. Pons. **Hybrid FES-Robot cooperative control of ambulatory gait rehabilitation exoskeleton for spinal cord injured users,** Journal of NeuroEngineering and Rehabilitation. **Invited contribution.** Submitted 3/03/2013

[2]It is recalled that Kinesis refers to the robotic exoskeleton that implements the hybrid walking approach with muscle fatigue management. See section 3.2.

For developing the hybrid control of walking, a jerarquized approach was selected (figure 5.1). In this architecture, a main controller orchestrates the NP and exoskeleton controllers, regarding walking phase and the muscle performance. This main controller is a Finite State Machine (FSM), which implements the hybrid-cooperative behavior between the NP and the exoskeleton controllers. The FSM sends discrete commands that represents the identification of the gait events (dashed lines in figure 5.1) and cooperative-related commands (dotted lines in figure 5.1), that allows to balance the contribution of the exoskeleton to the movement regarding muscle performance.

The remaining sub-systems of figure 5.1 have been previously described:

- The muscle fatigue estimator refers to the fatigue criteria, estimator and strategy developed in chapter 4.
- The admittance controller was fully described in section 3.4 (figure 3.21).
- The interaction controller was merely described in section 3.4. In this chapter, the strategy for modulating the force field stiffness K_k is described in section 5.3.1, along with a description of the kinematic database.

This chapter thus develops the remaining components of the hybrid-cooperative controller showed in figure 5.1. The NP controller is developed in section 5.2, prior to the development of the FSM in section 5.3, where the operation of the whole controller is described. Then, chapter 6 presents the results from validation experiments performed with healthy subjects in which the control performances of the hybrid-cooperative approach are investigated.

5.2 Closed-loop control of stimulation

The use of NP to restore standing ability in SCI is known since the early works done by Kantrowitz [127]. Since then, many groups have been developing technology and control strategies to achieve walking ability restoration with the use of FES [128, 130, 132, 160]. In open-loop control of NP, stimulation patterns are handcrafted and sequenced, usually triggered by a hand switch or somewhat automated with a gait sensor, to provide the trigger signals. However, human body is a highly complex musculoskeletal system and, although some systems have a considerable number of electrodes implanted directly in the muscles, the gait patterns generated not resemble typical normal gait of able-bodied individuals.

Closed-loop control of NP has also been proposed in the literature. Among them, adaptative feedback control [146], model based control [147], iterative PID control [256], sliding mode control [257, 258], model predictive control [259], neural networks and fuzzy control [146, 260, 261] iterative error-based learning control [260, 262–267], have been proposed. Despite all these approaches for control of NP, accurate movement control is still difficult to perform due to existing parameter variations, inherent time-variance, time-delay, and strong nonlinearities present in the neuromuscular-skeletal system and in muscle activation relation, muscle dynamics, and skeletal dynamics [149]. Furthermore, most of these proposed control strategies rely on accurate models of the system and are time-consuming for tunning prior its use.

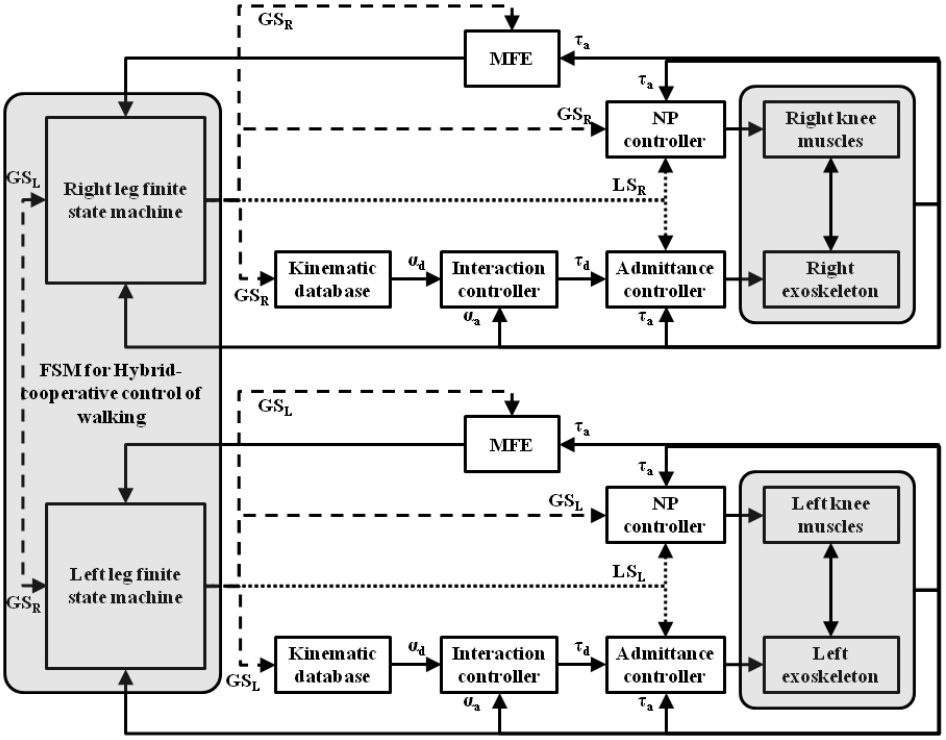

FIGURE 5.1: Hybrid-cooperative controller. Dashed lines means Gait State (GS) data. Dotted lines means Learning State (LS) data. R and L stands for Right and Left leg. Solid lines means continuous variables.

Implementing most of those closed-loop control approaches for application with patients is difficult, due to computational cost and time needed for controller tunning, which make the set-up time unaffordable. However, the specific role played by the lower limbs during stance and swing phase of walking, and the presence of an external exoskeleton that provides joint support and monitoring capabilities, can be exploited in order to select the most suitable controller for the NP. Therefore, the following assumptions can me made:

- During the swing phase, the leg does not interact with the environment. This phase can be regarded as dynamically determined by joint trajectory and time.
- During the stance phase, the leg interacts with the floor. This phase must be determined based on a stability criteria prior to initiate a new step, due to uncertainties that can arise due to limb orientation at floor contact, whole body orientation or balance.

The time- and trajectory- constraints of the swing phase fit exactly within the ILC setting. The ILC approach was proposed for processes which continually repeat the same task over a finite interval with resetting between trials [268, 269]. The idea is to apply a simple algorithm repetitively to an unknown plant, the muscles in this case, until perfect tracking is achieved by iteratively reducing the error. With this approach, high performance can be achieved with low transient tracking error despite large model uncertainty and repeating disturbances. Applications of ILC for NP control have been proposed in [262, 263, 267, 270].

Regarding the stance phase, control of the knee joint can be implemented by PID control of extensor muscles, which is an easy and effective method to control knee joint extension [148].

However, uncertainties and non-linearities that characterizes stimulated muscle performance are not adequately managed by PID controllers. Nevertheless, the presence of the exoskeleton providing knee support reduces the stimulating intensity over the quadriceps muscles during stance. Thus, the non-linear effects are also reduced and the PID controller can be considered for control of quadriceps muscles during stance.

As a result, the NP controller implemented in Kinesis is comprised by two controllers operating in parallel, as showed in figure 5.2, where ILC controller is active only during swing phase, whereas the PID controller can be active during the whole walking cycle. The task of both controllers is to minimize the human-robot interaction forces. These forces arise due to mismatch between leg and exoskeleton trajectories. This way, the NP stimulates the muscles of the leg in order to restore joint trajectory closer to the reference.

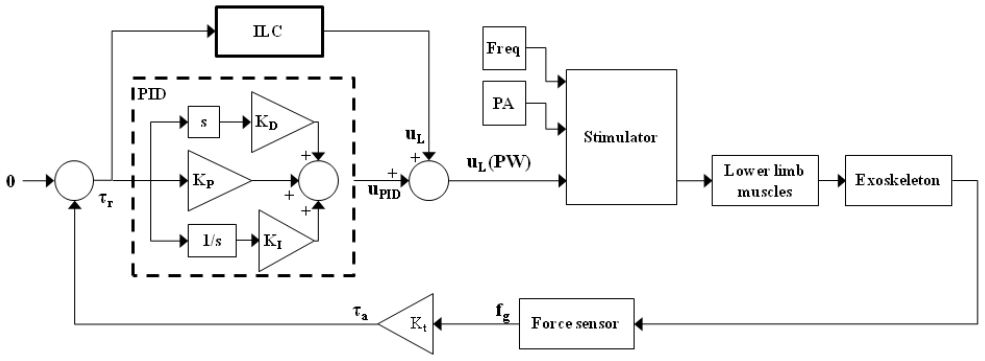

FIGURE 5.2: Kinesis stimulation control strategy.

The stimulator (Rehastim, Hasomed GmbH) delivers biphasic current-controlled rectangular pulses, and allows controlling the main stimulation parameters in real time: PA, PD and frequency. This comprises three degrees of freedom to control muscle force generation. The common approach for control of muscle force generation is fixing stimulation frequency and use stimulation amplitude or pulse duration to modulate force production. In the approach implemented in this dissertation, train frequency is also discretely modulated, according with the conclusions of the muscle fatigue study described in chapter 4. Thus, one of the two remaining train parameters, either PA or PD, had to be selected for controlling muscle force. Several tests conducted with healthy subjects were done comparing pain perception and force generation for PA modulation versus PD modulation, remaining frequency fixed at $70Hz$, and the non-varying parameter (PA when PD was modulated and the contrary) held at moderate level. As a result, PD modulation was perceived more comfortable and produced higher forces than pulse amplitude modulation. Then, the stimulation controller was designed to modulate stimulation PD, with fixed PA tailored to each subject (see next section). Stimulation frequency remains fixed until fatigue is detected which, accordingly to the results of the fatigue study of chapter 4, leads to change stimulation frequency to delay fatigue.

5.2.1 PID control of knee extensor muscles during stance phase of walking: tuning experiments

It was outlined previously that a PID controller can provide quadriceps stimulation during stance, taking advantage from the presence of the support externally provided by the exoskeleton. On

the operating envisioned, bending of the user's knee during stance generates an increase on the interaction force, while the joint support provided by the exoskeleton avoids joint collapse. This interaction force is the controlled signal for the PID NP controller, which stimulates the quadriceps muscles in order to extend the knee, thus minimizing the interaction force. The controller is represented by equation 5.1. The control gains were tunned following the Zielger-Nichols heuristic procedure [222]. It recalled here that this procedure consist of increasing the proportional gain (K_P) until the system response to an impulse oscillated at a sustained period, which is defined as the *ultimate period* (T_u), along with the controller gain (*ultimate gain*, K_u). Those two values are used to calculate K_p, K_i, and K_d constants of the controller, using the relations proposed by Zielger and Nichols (table 5.1).

$$u_{PDI}(t) = K_p \cdot (-\tau_a(t)) + K_i \cdot \int ((-\tau_a(t)) \cdot dt) + K_d \cdot d\left(-\tau_a(t)\right)/dt \tag{5.1}$$

TABLE 5.1: Ziegler-Nichols PID relationships for calculation of PID controller gains K_p, K_i and K_d [222].

Controller type	K_p	K_i	K_d
P	$K_u/2$	–	–
PI	$K_u/2.2$	$T_u/1.2$	–
PID	$K_u/1.7$	$T_u/2$	$T_u/8$

5.2.1.1 Experimental procedure

Performing the tunning procedure proposed by Zielger and Nichols to this specific configuration is challenging. The perturbation introduced have to reflect the operation of the user-exoskeleton system during stance. In this sense, the experimental procedure should induce a perturbation in the leg-exoskeleton system similar to a sudden joint collapse. Due to the impossibility of performing this experiment, the procedure consisted of slowly bending the knee while the exoskeleton remains blocked and the PID controller is disconnected. This results in an increase of the interaction forces. Once a certain value is reached, the PID controller is automatically connected. Given that the control task is to minimize the interaction forces, this procedure generates a step impulse from the reached interaction force to zero. This way, the control task of the PID controller was to quickly extend the knee in order to minimize the interaction force.

The experimental procedure was performed as follows. The testing subject dressed one leg of the exoskeleton and stood in a platform between parallel bars. With the exoskeleton knee joint stalled at 5 degrees of knee flexion, the user was instructed to support its weight through the parallel bars using his/her arms, and then to progressively transfer the weight from the parallel arms to the supporting leg. As the exoskeleton is flexed 5 degrees, this unloading process resulted in a progressive increment on the flexion interaction torque. Once the interaction torque exceeded $10N \cdot m$, the PID controller was activated. This generated a step impulse from $10N \cdot m$ to $0N \cdot m$ (figure 5.3, gray line). To perform the experiments, two stimulation electrodes (Alexgaard, Pals-platinum, 5x9 cm) were placed conveniently to stimulate both *Rectus Femoris* and *Vastus Lateralis* quadriceps muscles.

Prior to start with the procedure, the stimulation parameters were set. At this point, the main stimulation train parameters stablished in chapter 4. To ensure that the stimulation controller output is tolerated by the subject in any operating condition, the maximum stimulation intensity tolerable by the subject was set. This involved determine the maximum PD, PA and frequency that the subject can tolerate. The PID controller modulates PD to control muscle force, remaining PA and frequency unchanged (figure 5.2). Then, the maximum stimulation intensity is a saturated output, in which the stimulation PD is maximum[3], and the stimulation frequency is 70 Hz[4]. Therefore, the remaining stimulation parameter, PA, have to be set to ensure that on the mentioned conditions (450 μs at 70 Hz) the subject tolerates the stimulation.

Similarly to the experimental procedure conducted in chapter 4, an incremental search of the stimulation PA was performed. Stimulation PD was set to 450 μs, train frequency at 70 Hz, pulse train duration 14 sec. and duty cycle 43%. PA was iteratively increased in 2 mA steps every stimulation train, until the subject reported the stimulation as uncomfortable. Then, stimulation PA and frequency were set as constant parameters in the NP controller (figure 5.2), and the tunning experiments begun.

5.2.1.2 Results

Six healthy subjects volunteered for participating in the experiment (age 31.2±2.2 y.o., weight 80.6±9.4 kg., height 1.8±0.2 m.). Table 5.2 shows a) the values obtained for the ultimate gain (K_u) and ultimate period (T_u) for each subject; b) PID controller gains (K_p, K_i and K_d, table 5.1) and c) average values for the experiments. It is noticeable that the obtained ultimate gains and period are similar across subjects, which lead to similar PID gains.This result was assumed for the PID gains to be used with patients, which avoids to conduct the tuning procedure with patients.

TABLE 5.2: PID control gains K_p, K_i and K_d for all subjects.

Subject number	K_u	T_u [sec]	K_p	K_i	K_d
1	32	0.59	19.2	0.29	0.07
2	38	0.78	22.8	0.39	0.10
3	30	0.66	18.0	0.33	0.08
4	45	0.66	27.0	0.23	0.08
5	42	0.63	25.2	0.32	0.08
6	36	0.53	21.6	0.29	0.07
Mean (SD)	37.17±5.74	0.65±0.07	22.3±3.4	0.33±0.04	0.08±0.01

These results were further tested in an experiment performed with a different subject, in which the controller gains were set to the mean values obtained in table 5.2. Figure 5.3 shows the system's output to the same step-like procedure followed to adjust the controller. A damped response of the system can be appreciated, reducing the interaction force with a controlled overshoot of 10% of the step magnitude. This result confirmed the ability of the PID controller to reduce the interaction forces during stance, produced as result of a progressive knee bending while

[3] 450μs, which the maximum achievable by the stimulator.

[4] This frequency was set in chapter 4 for control of stimulation and muscle performance monitoring.

the exoskeleton provides support to the knee. However, these results must be confirmed with further tests during walking. A general limitation of the experimental procedure for adjustment and verifycation of the PID controller arise from the inability of the participants to perform a uniform weight discharge and avoiding voluntary actions during NP-driven knee extension.

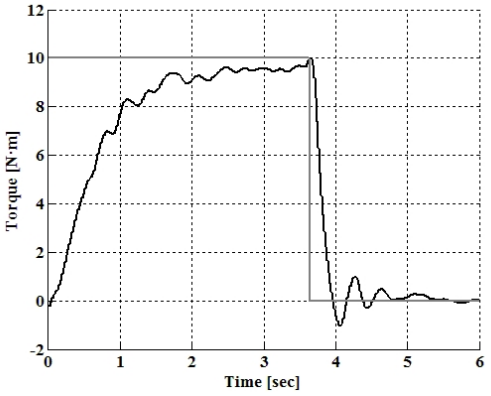

FIGURE 5.3: Stimulation PID control step response. Gray line: step perturbation fed to the system. Black line: actual interaction torque.

5.2.2 Control of knee flexor muscles during swing phase of walking: tuning experiments.

As outlined previously, the ILC is a recursive online control method that relies on less calculation and requires less *a priori* knowledge about the system dynamics, and has the general form given by equation 5.2, which corresponds to a linear ILC algorithm [268, 269]. Although non-linear ILC algorithms could provide better results in controlling non-linear time-varying systems, as the stimulated muscles, linear ILC algorithms have been implemented extensively for NP control [262–264, 266, 267, 270], providing good results and affordable computational cost.

$$\left\{uL_{(n,j+1)}\right\} = [F] \cdot [\{uL_{n,j}\} + [L] \cdot \{e_{n,j}\}] \tag{5.2}$$

The algorithm of equation 5.2 is a recursive, cumulative-proportional controller that generates a control signal proportional to the difference between the current control signal and the output error. Equation 5.2 is expressed in matrix notation, taking advantage of the time-constraint that swing phase can be subject to. Here, the NP controller output in each j cycle would be also time-defined, in the form of a control vector, which number of samples is defined by the sampling frequency and the time length of the swing phase. Thus, sampling of the swing phase defines the number n of elements of the control vector $\{uL_{n,j+1}\}$ and the dimensions of $[L]$ and $[F]$ matrices and the sampled error signal $\{e_{n,j}\}$. Equation 5.3 shows the expanded version of equation 5.2.

$$\begin{Bmatrix} u_1 \\ u_2 \\ \vdots \\ u_n \end{Bmatrix}_{j+1} = F \cdot \begin{bmatrix} 1 & 0 & \cdots & 0 \\ 0 & 1 & \cdots & 0 \\ \cdots & \cdots & \ddots & \cdots \\ 0 & 0 & \cdots & 1 \end{bmatrix} \cdot \left(\begin{Bmatrix} u_1 \\ u_2 \\ \vdots \\ u_n \end{Bmatrix}_j + L \cdot \begin{bmatrix} 1 & 0 & \cdots & 0 \\ 0 & 1 & \cdots & 0 \\ \cdots & \cdots & \ddots & \cdots \\ 0 & 0 & \cdots & 1 \end{bmatrix} \cdot \begin{Bmatrix} e_1 \\ e_2 \\ \vdots \\ e_n \end{Bmatrix}_j \right) \quad (5.3)$$

The control task assigned to the ILC, as in case of the PID controller, is to minimize the interaction torque between the leg and the exoskeleton. During swing, Kinesis drives user's leg following a kinematic reference. As long as the leg does not move along with the trajectory pattern due to insufficient muscle force production, an interaction torque is therefore sensed due to weight and inertia. This interaction is forwarded to the ILC controller ($\{e_{n,j}\}$ in equation 5.2) to generate the control signal for the NP ($\{uL_{n,j+1}\}$ in equation 5.2) to be used in the next step in order to minimize this interaction. Note that within this approach, interaction force has two complementary sources: insufficient power generated by knee muscles, and the desynchronization between actual and exoskeleton's leg movement.

As a recursive algorithm, the control vector $\{uL_{n,j+1}\}$ to be applied in the next step $j+1$ is calculated from the control vector applied within step j, plus the interaction force produced by current j control vector $\{e_{n,j}\}$ multiplied by a learning constant matrix $[L]$. The result of this sum is multiplied by a forgetting constant matrix $[F]$ that accounts for rejecting learned disturbances, but introducing a steady error in the control output. Both matrices are diagonal, n-dimensional square, which non-zero diagonal elements are the learning and forgetting constants respectively. The result of equation 5.2 is a feed forward open loop control in the time domain that becomes closed loop in the iteration domain. Figure 5.4 illustrates the control principle for a 2-dimensional, first order, ICL controller explained above.

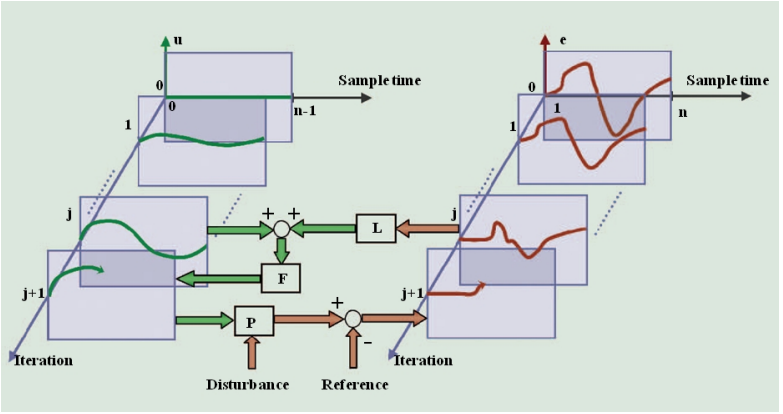

FIGURE 5.4: ILC operation principle. Adapted from [268].

A further characteristic can be added to the ILC algorithm. As it has been described, each $n-th$ component of the output control vector is only affected by the $n-th$ element of equation 5.2, establishing thus a *causal* relationship between the interaction torque (e_n) and the previous control signal (uL_n) through the multiplication of the $n-th$ row of $[L]$ and $[F]$ matrices (equation 5.3). However, a well known characteristic of stimulated muscle force production is the electromehcanical delay between the stimulation onset and the force production [271]. This feature is of the most importance for the application developed in this dissertation given that, as

described previously, the interaction torque is influenced by the synchronism between the kinematic pattern displayed by the robotic exoskeleton and the actual leg movement achieved by the stimulated muscles. To cope with it, the ILC algorithm can be adequately modified, introducing a non-casual learning feature, in order to give to the ILC the ability to take into account errors that the control signal will produce in future samples [268].

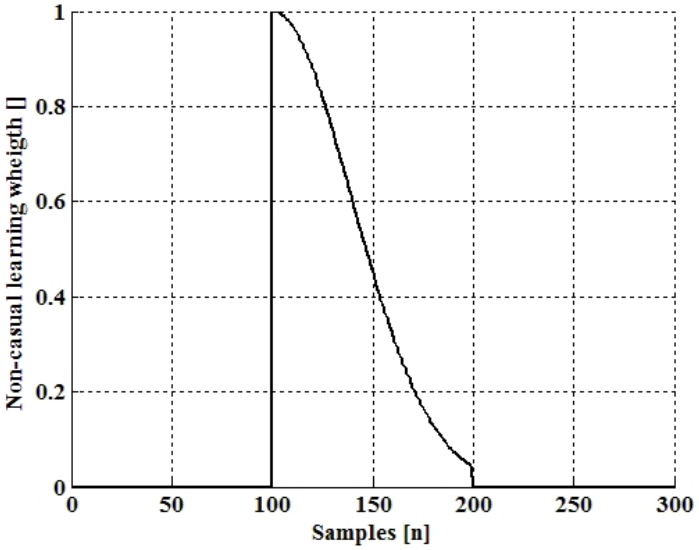

FIGURE 5.5: Semi-Gaussian moving window implementing the non-casual learning feature. Width $m = 100$ samples; centered at sample number 100.

The non-causal learning feature was introduced in the learning matrix $[L]$, taking it the form of a upper-triangular matrix. The length (m in equation 5.4) and module of the $n-th$ row-wise vector of matrix $[L]$ determine the learning rate and number of *future* samples that are taken into account in sample n. Furthermore, the relative weight between future samples can be also manipulated. The approach implemented in this dissertation for non-causal learning was to introduce a semi-Gaussian window centered in the sample n, which module equals to one, multiplied by the learning factor of the ILC (figure 5.5). Equation 5.4 shows the expanded version of the learning matrix $[L]$ with non-causal learning feature.

$$L \cdot \begin{bmatrix} a_1 & a_2 & a_3 & \cdots & a_m & \cdots & 0 & 0 \\ 0 & a_1 & a_2 & \cdots & a_{m-1} & \cdots & 0 & 0 \\ 0 & 0 & a_1 & \cdots & a_{m-2} & \cdots & 0 & 0 \\ \cdots & \cdots & \cdots & \cdots & \cdots & \cdots & \cdots & \cdots \\ \vdots & \vdots & \vdots & \cdots & \vdots & \vdots & \vdots & \vdots \\ \cdots & \cdots & \cdots & \cdots & \cdots & \cdots & a_{m-1} & a_m \\ \cdots & \cdots & \cdots & \cdots & \ddots & \cdots & a_{m-2} & a_{m-1} \\ 0 & 0 & 0 & \cdots & 0 & \ddots & \vdots & \vdots \\ 0 & 0 & 0 & \cdots & 0 & \cdots & a_1 & a_2 \\ 0 & 0 & 0 & \cdots & 0 & \cdots & 0 & a_1 \end{bmatrix} \tag{5.4}$$

where each $n-th$ row of matrix 5.4 holds:

$$\sqrt{\sum_{i=1}^{m} a_i^2} = 1$$

Finally, the ILC algorithm comprises several degrees of freedom that characterize its performance: learning rate constant L, time horizon for non-causal learning m, and forgetting rate constant F. Besides, the presence of a PID controller in parallel also influences its performance. A similar dual configuration have been proposed for NP control [264]. These control architecture are expected to incorporate advantages of both feedforward and the feedback (PID) controllers: the feedforward controllers enable fast movements without delay, whereas the PID controllers are able to compensate for disturbance.

5.2.2.1 Experimental procedure

To investigate the performance of the ILC algorithm upon these values and the contribution of the PID controller, several experiments were undertaken with six healthy subjects, similarly to section 3.4.2.1 for adjusting the admittance controller for the swing phase. However in these experiments the aim was to replicate the operating conditions of the hybrid system during the swing phase in the case of the leg being drove by the NP and the robotic exoskeleton. For the procedure, the subject dressed one leg of the exoskeleton and stood in a platform, with the leg dressed with the exoskeleton hanging freely. The experiments consisted of replicating ten consecutive swing cycles by the exoskeleton one second apart, while the subject kept the leg relaxed. Stiffness of the admittance controller was set to 8 $N \cdot m/deg$, resulting in almost position control of knee trajectory, allowing to drive the user's knee joint close to the kinematic pattern. As result, the interaction force resulting from driving the leg passively was feed to the NP controller to stimulate knee muscles (figure 5.2).

Stimulation electrodes were placed at the knee extensor muscles, similar to the stance control experiment performed in section 5.2.1 to stimulate both *Rectus Femoris* and *Vastus Lateralis* quadriceps muscles, and two channels (four electrodes) over the over the motor points of *Semitendinosus* and *Biceps Femoris* knee hamstring muscles. The subjects were instructed to relax their leg as much as possible prior and during the experiments. To investigate the performance of the dual controller versus a single PID or ILC controller, and the effects of the main parameters of the ILC controller: the learning constant L and the time horizon m, ten configurations were tested for each of the participants in two non-consecutive days, randomly sorted for each subject. The forgetting constant F allows to reject perturbations in successive iterations and was deliberately not introduced as a control parameter in the experiments for simplicity. It was fixed to a moderate value ($F = 0.8$) due to the impossibility at that time to estimate the number and magnitude of the perturbations that could take place during the hybrid walking therapy.

The configurations tested were the following:

Configuration 1: *No stimulation: leg moved passively.* This configuration was included as control condition. It was hypothesized that the subjects were unable to be fully passive. This condition with sham stimulation was included to evaluate this phenomena.

Configuration 2: *on/off stimulation.* The stimulation controller was set to activate the knee flexor and extensor muscles following an intermittent stimulation pattern, synchronized with knee trajectory.

Configuration 3: *PID.* The ILC controller was switched off and only the PID controller stimulated the extensor and flexor knee muscles. PID gains were derived from section 5.2.1.

Configuration 4: *PID-ILC(L=5, m=1*[5]*).* Both PID and ILC controllers were active. The ILC was set with a learning constant $L = 5$ and the number of elements of the semi-Gaussian non-causal learning window was $m = 1$ (causal learning).

Configuration 5: *PID-ILC(L=10, m=1).* Both PID and ILC controllers were active. The ILC was set with a learning constant $L = 10$ and the number of elements of the semi-Gaussian non-causal learning window was $m = 1$ (causal learning).

Configuration 6: *PID-ILC(L=10, m=50).* Both PID and ILC controllers were active. The ILC was set with a learning constant $L = 10$ and the number of elements of the semi-Gaussian non-causal learning window was $m = 50$ (0.5 seconds).

Configuration 7: *PID-ILC(L=8, m=50).* Both PID and ILC controllers were active. The ILC was set with a learning constant $L = 8$ and the number of elements of the semi-Gaussian non-causal learning window was $m = 50$ (0.5 seconds).

Configuration 8: *ILC (L=8, m=50).* The PID controller was switched off and only the ILC controller stimulated the extensor and flexor knee muscles. The ILC was set with a learning constant $L = 8$ and the number of elements of the semi-Gaussian non-causal learning window was $m = 50$ (0.5 seconds).

Configuration 9: *PID-ILC(L=8, m=100).* Both PID and ILC controllers were active. The ILC was set with a learning constant $L = 8$ and the number of elements of the semi-Gaussian non-causal learning window was $m = 100$ (1 second).

Configuration 10: *ILC (L=8, m=100).* The PID controller was switched off and only the ILC controller stimulated the extensor and flexor knee muscles. The ILC was set with a learning constant $L = 8$ and the number of elements of the semi-Gaussian non-causal learning window was $m = 100$ (1 second).

5.2.2.2 Results

Figure 5.6 shows a representative example from a PID-ILC NP controller experiment as described above. In this specific case, the configuration tested was the number 4. Figure 5.6(a) shows the kinematics and interaction torque resulting from the experiment, whereas figure 5.6(b) shows the stimulator output. It can be observed that accurate position tracking is obtained with the admittance controller except for the end of the extension phase, where an overshoot of 3 degrees can be appreciated. Besides, comparing across flexion-extension cycles, decreasing of the interaction torque is appreciated. This leads to a small decrease in the PID output as consequence of the decrease on the interaction torque (figure 5.6(b), red curve), due to muscle

[5]The stimulator controller algorithm worked at $100Hz$, thus the ILC was given a time horizon of 0 ($m = 0$, configurations 4 and 5), 0.5 ($m = 50$, configurations 6, 7, and 8) and 1 seconds ($m = 100$, configurations 9 and 10) for improving the performance and overcome the mechanical delay of stimulated muscles.

contribution from the stimulated muscle. Regarding the ILC controller, it can be appreciated that there was no control output for the first cycle (no previous iteration for the ILC). After the first cycle, the ILC progressively augmented the output until a stationary value was achieved from cycle 7 (figure 5.6(b), blue curve).

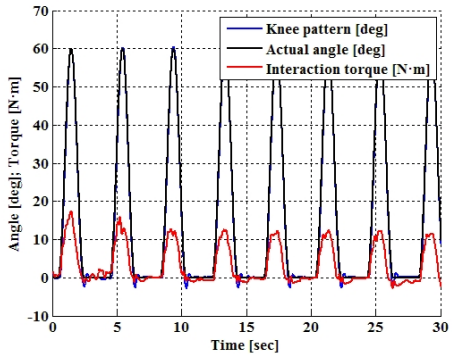

(a) Knee kinematics (blue curve: pattern; black curve: actual) and interaction torque (red curve).

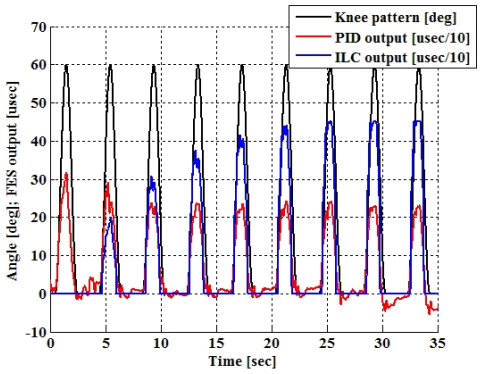

(b) Knee kinematic pattern (black curve) and stimulator output (scaled to fit in the same figure along with the kinematic pattern; red curve: PID; blue curve: ILC).

FIGURE 5.6: Representative example from a PID-ILC NP controller tunning experiment for swing phase.

Interaction torque and stimulation output from the ILC controller were used to calculate a set of metrics that represent the cycle-average performance of the system. Time integral of the interaction torque during the swing phase (TTI) was calculated to obtain the average interaction torque during the swing phase. TTI values were normalized to the TTI of the first cycle (NTTI). The normalized average of the ILC stimulation intensity was also calculated for each tested configuration. This average was calculated integrating the ILC output for the swing phase, and divided by the maximum ILC output theoretically achievable, which corresponds to a $450\mu s$ saturated output for the entire swing phase. This normalized ILC stimulation intensity (NILC) gives a representative value $\in [0, 1]$ where 0 means no stimulation during the swing phase, and 1 means a constant, saturated ILC stimulation output of $450\mu s$ for the whole swing phase. Furthermore, the number of cycles for the ILC to converge across configurations was also obtained. Convergence was assumed when the NILC varied within a $\pm 5\%$ interval between consecutive swing cycles. Table 5.3 shows the results obtained for NTTI, NILC and number of cycles for the ILC to converge.

Figure 5.7 shows the NTTI for the last (10th) swing cycle for each configuration tested. Configuration 1 shows a decrease of 0.90 ± 0.09 in NTTI, confirming that the subjects relaxed their legs during the experiments. Surprisingly, configuration 2 shows an increase on NTTI (1.03 ± 0.08) which as stated earlier, could be attributed to both desynchronization between the stimulated muscles and the kinematic pattern displayed by the exoskeleton, and insufficient muscle contribution to the movement. However, a further feature of the tested stimulation pattern in this configuration influenced the results. The on/off stimulation pattern is sudden, non-modulated, which has the potential to induce the subject to produce reflex actions, that increase their leg's stiffness by co-contracting the muscles. It should be noted that even with no stimulation (configuration 1), non-volitional muscle activations can take place.

TABLE 5.3: Results from NP controller tunning experiments for swing phase. NTTI and stimulation intensity are mean±SD. Cycles to converge are median±inter-quartile range. Data belongs to the 10th, last, swing cycle.

Configuration	NTTI at the last cycle	NILC at the last cycle	Cycles to converge
1	0.90±0.09	N.A.	N.A.
2	1.03±0.08	N.A.	N.A.
3	0.89±0.10	N.A.	N.A.
4	0.88±0.06	0.20±0.07	7±0
5	0.83±0.06	0.34±0.09	6±3
6	0.80±0.09	0.57±0.07	3±2
7	0.70±0.13	0.50±0.16	5±3
8	0.65±0.09	0.50±0.15	3±3
9	0.68±0.15	0.57±0.14	4±2
10	0.58±0.05	0.56±0.15	3±3

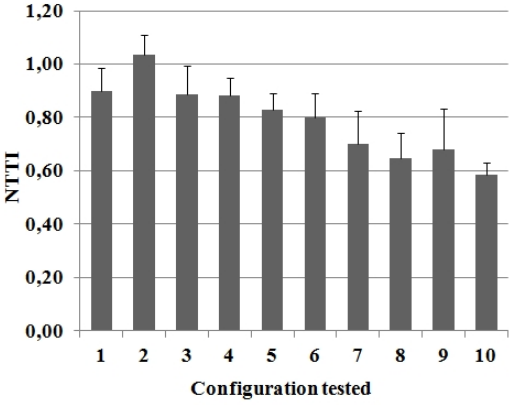

FIGURE 5.7: NTTI at the last (10th) cycle for each configuration tested.

Comparing configurations 3 and 4, similar results on NTTI are observed. Both experiments resulted in similar decrease on NTTI (0.89±0.10 and 0.88±0.06 respectively). Hence in configuration 4 the PID control was predominant and the ILC contribution was negligible. Given that both configurations resulted in a similar decrease on NTTI to configuration 1 (0.90±0.09), the PID stimulation did not contributed significantly in these cases, probably due to the fact that the electromechanical delay of stimulated muscles, estimated in 0.3 s [271], was not compensated. Configurations 5 to 10 show decreased NTTI for the 10th cycle with respect to configuration 1, coincident with increments in the learning constant L and/or the time horizon m, and also depending on the role of the PID controller, as explained below.

The role of the PID can be discussed comparing configurations 7 versus 8, and 9 versus 10. It can be noticed that the dual controller (configurations 7 and 9) leads to higher NTTI at the last cycle (figure 5.7) with similar stimulation intensity (figure 5.8(a)) than the ILC controller alone (configurations 8 and 10). Furthermore, the dual controller needed more cycles to converge than the ILC controller alone (figure 5.8(b)). Thus, in this experimental conditions, the PID controller decreases stimulation performance if placed in parallel with the ILC controller.

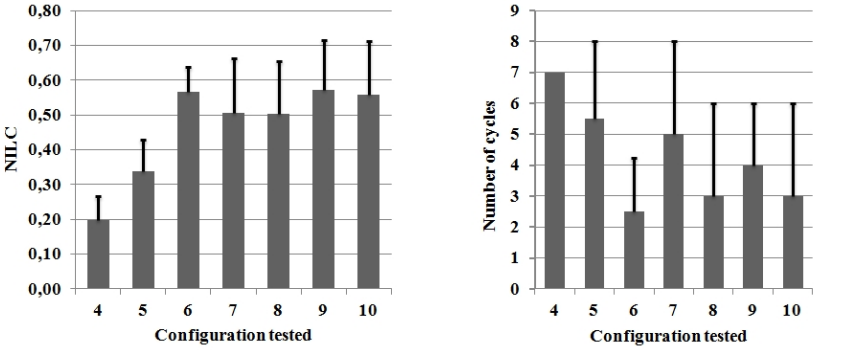

(a) NILC. Data represent mean±SD.

(b) Number of cycles to converge. Data represent median and inter-quartile range.

FIGURE 5.8: NILC and number of cycles to converge.

The impact of increasing the learning rate L can be analyzed comparing configurations 4 versus 5, and 6 versus 7. Increasing L increases also the NILC (figure 5.8(a)) and decreases the number of cycles to converge (figure 5.8(b)). This increase on stimulation intensity leads also to a decreased NTTI (figure 5.7).

Lastly, the influence of the time horizon m can be assessed by comparison between configurations 5 versus 6, and 8 versus 10. Increasing the time-horizon m has a similar effect to increasing L on NTTI (figure 5.7). However, in this case, the stimulation intensity decreases (figure 5.8(a)) and the number of cycles to converge remains almost constant (figure 5.8(b)). Thus, increasing m improves stimulation performance, as more muscle contribution is obtained while decreasing the stimulation intensity, without impact on the convergence velocity. Figure 5.9 shows a representative example of the effects of m on the ILC control output, where the $m = 100$ and $m = 50$ configurations are advanced with respect to $m = 0$ configuration.

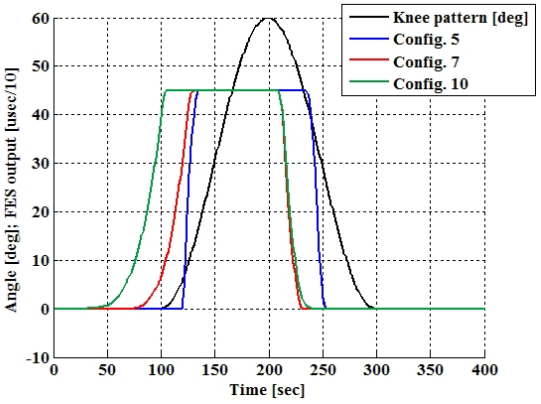

FIGURE 5.9: Representative example of time-horizon parameter m effect on ILC stimulation control output. Knee joint pattern is shown for comparing the advances for each configuration. Stimulation output units are divided by 10 for representation purposes.

Overall, configuration 10 gave the best performance in terms of muscle contribution to the movement, and is adopted for controlling the NP during swing phase. However, it can not be concluded that the best set of parameters ($L = 8$ and $m = 100$) are optimum, but are considered

as a balanced solution regarding the main objective of this dissertation, which is to design and validate a hybrid walking therapy with fatigue management for SCI individuals.

5.3 FSM for hybrid-cooperative control of walking

As shown in previous section, the efficacy of the NP controller to generate the knee movement is limited, due to the low efficiency of the force generated by the stimulated muscles and the electromechanical delay between the stimulus and the onset of joint movement. The goal of the hybrid control strategy is therefore to exploit the joint movement generated by the NP while supporting the movement through the exoskeleton. This was foreseen in chapter 3, where a compliant exoskeleton controller was developed to provide compliant assistance to the knee, depending upon the parameter K_k, the stiffness of the force field applied around the trajectory.

Modulation of K_k is executed depending on the gait phase and the contribution of the NP to knee trajectory, which allows balancing the NP and exoskeleton actuation. These two factors, gait phase and NP contribution, are managed inside a FSM, comprised of two FSM operating in parallel (figure 5.10): one in the time domain (t-FSM), (detailed in section 5.3.1) and other operating in the cycle domain (c-FSM) (detailed in section 5.3.2). While the t-FSM detects the main walking states and the transitions among them (similarly to others FSM for ambulatory exoskeletons [166, 212, 272, 273]), the c-FSM operates with discrete values related to the (stimulated) muscle performance, generated each cycle during the swing phase, similarly to the experiments performed in section 5.2.2.

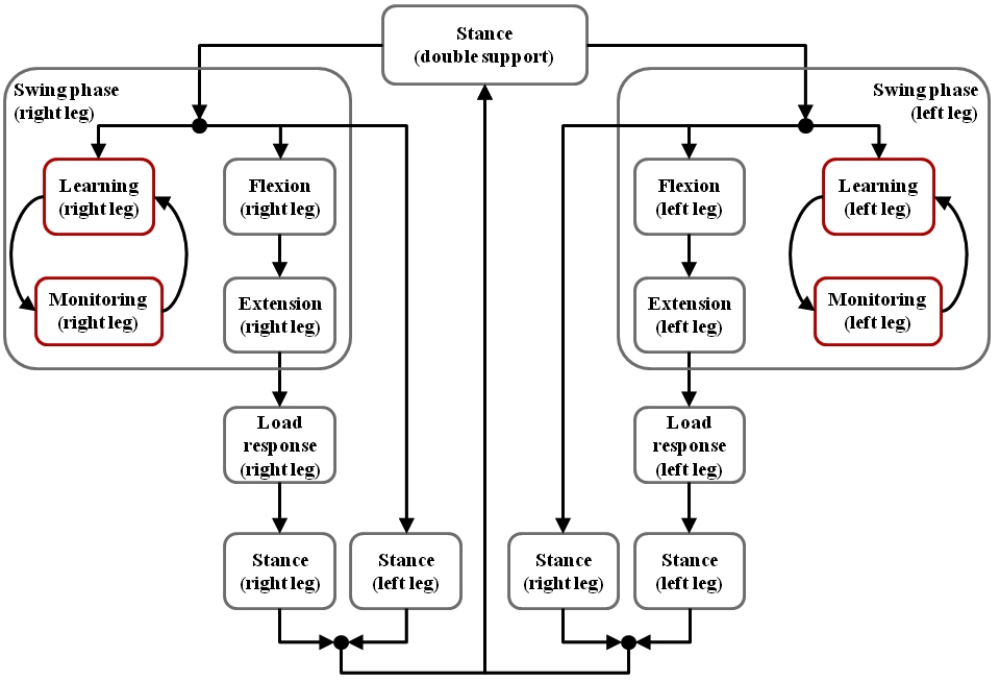

FIGURE 5.10: Dual FSM for hybrid control of walking. Grey boxes represents t-FSM, red boxes represents c-FSM, further extended in figure 5.14.

This design allowed to uncouple the closed-loop control of stimulation from muscle performance monitoring. Muscle fatigue results in a decrease of muscle performance increasing the interaction

torque. This increase is automatically compensated with the closed-loop NP controller, increasing the stimulation and thus reducing the interaction torque. Therefore, to monitor muscle fatigue is mandatory to uncouple closed-loop NP control from muscle fatigue monitoring.

One alternative for estimating muscle fatigue is monitoring the control output. Nevertheless, the non-linear characteristics of the stimulated muscle would hinder the relation between stimulation output and muscle fatigue. This was also a rationale to investigate muscle fatigue through changes in muscle performance, as presented in chapter 4.

The strategy proposed in this dissertation for uncoupling closed-loop NP control from muscle fatigue monitoring is switching between closed-loop and open-loop control of NP for the swing phase. Optimized stimulation patterns are obtained through the closed-loop application of the NP. These patterns are then applied in open-loop configuration while muscle performance is monitored.

5.3.1 Time-domain FSM

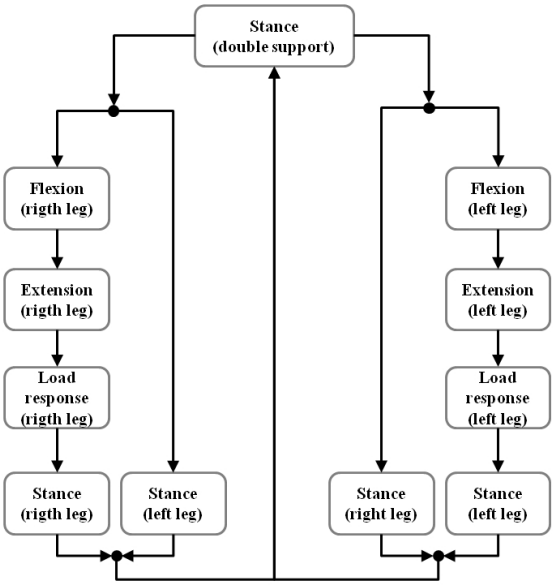

FIGURE 5.11: FSM for control of walking in time domain.

The t-FSM implemented in Kinesis (figure 5.11), was designed to detect the main states of walking (swing and stance) and the transitions among them. Besides, the t-FSM modulates the force field stiffness K_k and sets the kinematic pattern, depending on the walking state. Aside from swing and stance, some states were introduced for adequate modulation of K_k during walking. As introduced in section 3.4, the compliant behavior of the exoskeleton was achieved by controlling knee trajectory through a first order torque field imposed around the trajectory. As a result, the torque imposed by the exoskeleton depends upon the deviation of the knee trajectory from the kinematic reference pattern and the stiffness of the torque field K_k (equation 3.8). The parameter K_k sets the width of a *virtual tunnel* where the knee can actually move as function of the walking phase. During stance, it is paramount to provide joint support to avoid knee collapse, therefore a high stiffness torque field is needed. However, during the swing phase the supportive actions of the exoskeleton must be reduced to allow the contribution of stimulated

muscles and passive dynamics swing the leg. This is achieved by reducing the support of the exoskeleton, through reduction of the force field stiffness K_k. At the end of the swing phase, prior to heel strike, the knee must be close to full extension to ensure adequate support while loading the leg. The exoskeleton gradually increase its support to ensure full knee extension, which is accomplished through a progressive increment in the force field stiffness. Nevertheless, this late stiffness is still low for providing full support during stance, so a fast increment on the stiffness must be performed to achieve the adequate value for stance.

Summarizing, there are four different zones where K_k is modulated within the kinematic pattern as follows:

- Stance: constant high stiffness to provide knee support.
- Flexion: constant low stiffness to avoid interference with the muscle stimulation.
- Extension: linear increase to ensure full knee extension prior to heel strike.
- Load response: fast stiffness increase to achieve the support for the stance phase.

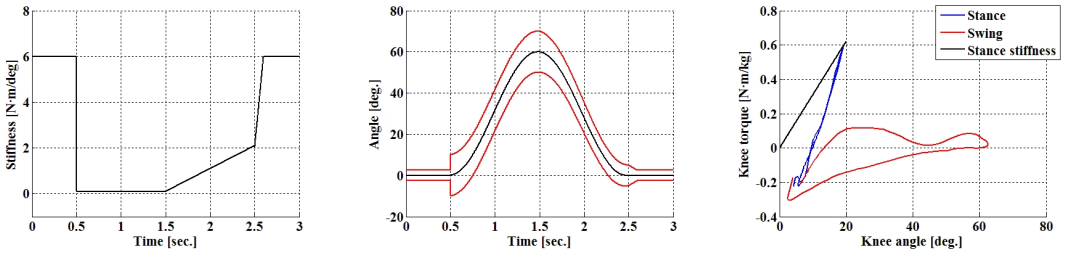

(a) Modulation of K_k with walking cycle.

(b) Kinesis knee torque field approach. Blue curve represent kinematic pattern knee stored in controller memory.

(c) Knee joint phase diagram during normal walking.

FIGURE 5.12: Strategy for modulation of knee torque field stiffness K_k.

To illustrate the proposed concept for modulating K_k, figure 5.12(a) shows the actual modulation, along with figure 5.12(b), where the black curve represents the kinematic pattern and the red curves the boundaries of the torque field. The specific values of K_k for the stance phase were derived following the same approach developed in a previous work [212]. In this work, a linear model for knee stiffness during walking was obtained from the angle-torque knee diagram (figure 5.12(c)). From this model, knee stiffness for stance phase was calculated $6N \cdot m/(kg \cdot deg.)$, related to subject weight. In Kinesis, knee stiffness during swing phase can be reduced to near zero $N \cdot m/deg$. This allows to reduce the support provided by the exoskeleton when knee trajectory is fully developed by the stimulated muscle. Modulation of K_k during swing between these two values is performed by the c-FSM as shown in next section.

The state diagram for the t-FSM is shown in figure 5.11. The initial state corresponds to the double support, where standing is ensured by the high stiffness displayed by the robotic exoskeleton and the action of the NP. Knee kinematic pattern for stance was set to 5 degrees (0 is full extension) to avoid hyperflexion during stance. From this state, the user can start a step by commanding the corresponding switch (SW). In addition to this command, some additional conditions must be satisfied to ensure proper and safe control of the walking states and its

transitions, as shown in table 5.4. In the case of the transition from standing to swing phase, along with the user command, the contralateral leg should be fully supported in the ground, this is, FSR_{heel} and $FSR_{barefoot}$ must be active. Furthermore, for correct step initiation, there must be a transfer of body weight to the contralateral leg so that the leg that begins the step can easily start swing. This weight transfer release the heel while the foot maintaining contact with the floor only in the barefoot. In this case, FSR_{heel} for the stance leg is inactive.

TABLE 5.4: States and transitions for t-FSM, particularized for right leg.

Transition	Condition
Stance - Flexion	SW_{right} = ON AND Left leg = stance AND $FSR_{right\ heel}$ = OFF
Flexion - Extension	Time = 1 sec.
Extension - Load response	$FSR_{left\ heel}$ = ON
Extension - Stance	Time = 0.2 sec.

During flexion and extension states, t-FSM sends the knee kinematic pattern to the admittance controller as well as the correspondent K_k from the values sent by the c-FSM, as shown in following section. Shifting from flexion to extension occurs after completion of the flexion trajectory of the kinematic pattern, whereas shifting from extension to load response is performed when the heel contacts the ground. As mentioned above, load response state was included for a fast increase on K_k to meet the value for stance phase. This was implemented with a linear interpolation over K_k in 0.2 seconds. Once the interpolation is completed, the state is abandoned towards stance. During this process, the contralateral leg is kept in stance state. Stance and double support are equivalent states, but were replicated with different names for ease of implementation. Figure 5.13 illustrate the t-FSM operation for both legs during a walking experiment.

5.3.2 Cycle-domain FSM

As mentioned at the beginning of this section, the FSM comprises two state-machine operating within the cycle domain (c-FSM) for each leg, that allow switching between closed-loop and open-loop stimulation control for monitoring muscle performance (figure 5.10). During swing phases of walking, each c-FSM allows independent stimulation control and fatigue monitoring, which are coordinated by the single t-FSM that manage walking phases for both legs. As shown in figure 5.14, each c-FSM have two states, named *learning* and *monitoring*, corresponding to closed-loop and open-loop stimulation control configuration. The default state is *learning*. Within this state, the ILC iterates among consecutive walking cycles, as described in section 5.2.2. As shown in figure 5.6(b), stimulation output for the first swing cycle is zero, as there is no previous iteration. In this cycle the leg has to be moved passively by the exoskeleton through a force field stiff enough to produce a position control of knee trajectory, in order to drive the knee trough the kinematic pattern. This is achieved by setting the stiffness K_k for the swing phase at the same value than for the stance phase. At second and following swing cycles, the interaction torque decreases (figure 5.6(a)), resulting from the contribution of the stimulated muscles, which is feed as error signal to the ILC for further iterations, as showed in section 5.2.2.

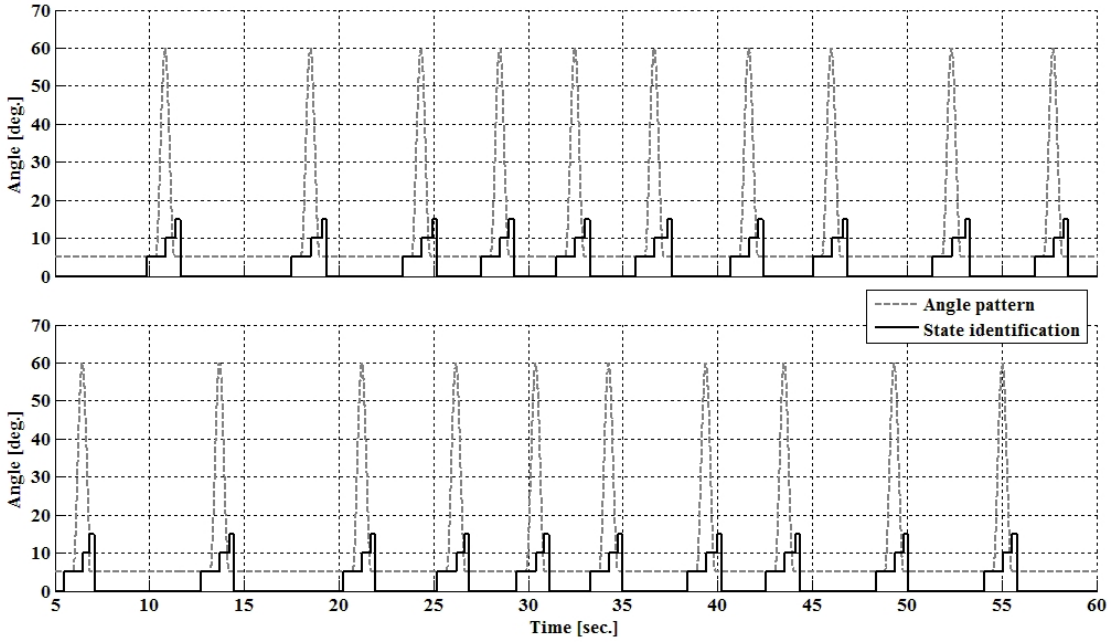

FIGURE 5.13: Operation example of the FSM for control of walking states. Top: right leg. Bottom: left leg. States appears numbered as following: 0 for stance and double support, 5 for flexion, 10 for extension and 15 for load response.

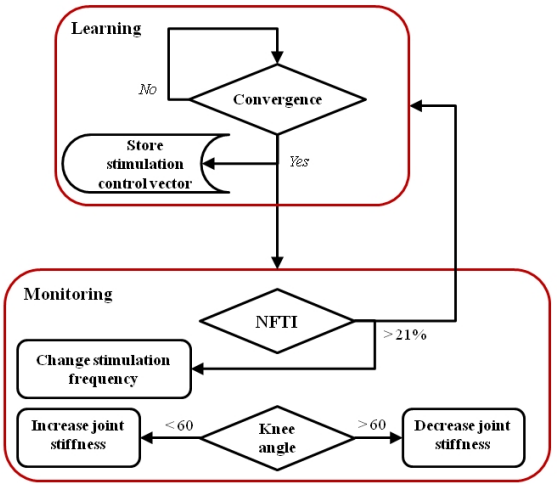

FIGURE 5.14: FSM in cycle domain (c-FSM) to balance NP and robot actuation.

The convergence criteria was outlined in section 5.2.2.2 but for the purposes of the c-FSM operation during walking was modified, adding a second condition. While convergence was assumed when the normalized stimulation intensity varied within a ±5% interval, the added condition was that the observed TTI gradient ought to be non-negative. This criteria synthetize the fact that while iterating, if no decrease on the mean interaction torque is observed, muscle contribution had to be the maximum achievable under these conditions. Besides, the ILC algorithm is near to its convergence state (±5% interval), thus further iterations of the ILC controller would not give further improvements in muscle force generation.

Once the ILC has converged, the *learning* state is leaved, stopping the ILC algorithm and storing the last control vector output into memory, to be used as open-loop stimulation pattern for the

next steps. During *monitoring* state, balance between the NP and the exoskeleton contribution to drive the leg is performed, taking advantage of the compliant control of knee trajectory. Due to the contribution from the stimulated muscles to the movement, the actual knee angle exceeds the patterned angle, which can be better observed at the maximum angle achieved during swing phase (figure 5.15(a)). Consequently, while the maximum flexion angle exceeds 60 degrees (the maximum angle of the kinematic pattern), the force field stiffness K_k can be reduced for the next step, or increased if the flexion angle is lower than 60 degrees. This modulation depends on the amount of deviation from the targeted 60 degrees, implemented as a proportional closed-loop control of the stiffness in the cycle domain, in an approach similar to [256]. The proportional constant was tunned by trial and error to ensure small changes in K_k, this is, an over-damped proportional control of K_k in the cycle domain, to avoid modulations that could result in too low robotic assistance.

While the stiffness is being modulated in *monitoring* state, the TTI for each swing cycle is monitored to estimate muscle fatigue, applying the criteria developed in chapter 4, which leads to detect muscle fatigue when an increase of 19% of TTI is observed. Then, the state is leaved after changing the stimulation frequency to delay muscle fatigue, as concluded in chapter 4. This change on stimulation parameters and muscle characteristics for management of muscle fatigue requires a new iteration period for the ILC in the *learning* state, repeating the operation detailed in this section.

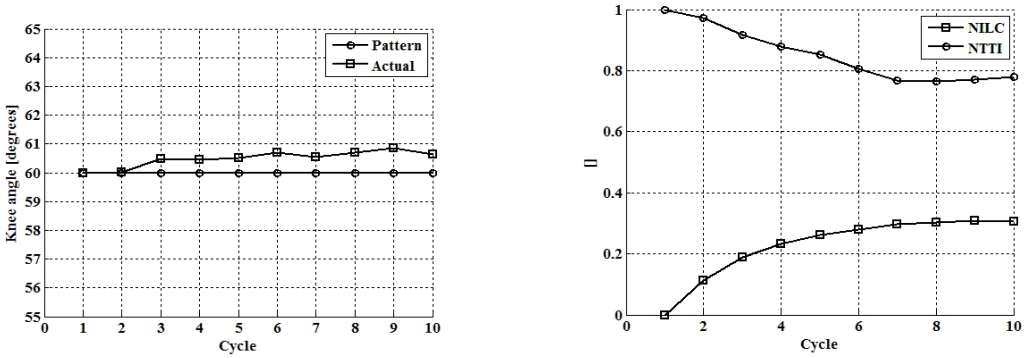

(a) Actual and patterned maximum angle.

(b) Cycle-averaged NILC and NTTI.

FIGURE 5.15: Results from figure 5.6(b) in the cycle domain.

5.4 Conclusion

The biomechanical role of the knee joint during walking and the presence in parallel of the robotic exoskeleton were determinants for implementing a closed-loop NP control. The resulting NP controller is comprised by two architectures operating in parallel: a PID for extensor muscle control, and a ILC. The experiments conducted for PID controller tunning revealed average values for the controller gains. This result further avoids to perform the tunning procedure with patients. The modified ILC algorithm allowed to overcome the electromechanical delay. Experiments performed to investigate the controller configuration for the swing phase concluded that the best configuration correspond to the ILC. The best set of parameters, in terms of performance of muscle contribution to the movement, were adopted for ILC configuration. This

set of parameters are not optimum but a balanced solution that avoids to perform tunning procedures with patients.

The cooperative control approach is implemented on the basis of a FSM. The proposed approach uses cycle-related variables to monitor muscle performance and modulating the assistance of the robotic exoskeleton. This design allowed to uncouple the closed-loop control of stimulation from muscle performance monitoring. Further experiments (presented in chapter 6) have to confirm the performance of this approach prior to testing with SCI patients.

5.4.1 Answer to research questions

This chapter provides the following answer to research question Q8 stated in section 1.6.2 as follows:

Q8: **How to implement a NP controller that can be modulated within the hybrid controller?** The leg-robot physical interaction allowed to implement a closed-loop stimulation approach feeding the user-exoskeleton physical interaction to the stimulation controller. Furthermore, the robotic actuation provided safe support to the joint while reducing the stimulation demand during stance phase.

Chapter 6

Evaluation with healthy users[1]

This chapter presents the experiments conducted with a group of healthy subjects in order to validate the hybrid-cooperative approach prior to the clinical evaluation with a group of patients. The experimental protocol for hybrid walking is designed anticipating the testing procedure with patients. The results show that the cooperative control strategy balances the NP and robotic actuation. Closed-loop control of NP manage changes in muscle performance and walking phase. The proposed control approach overcomes several challenges related to NP control of movement: muscle fatigue is estimated through muscle performance and managed by closed-loop control of NP, and trajectory control through a compliant actuation of the exoskeleton. Besides, a correlation was obtained between the TTI and the actuator power, which shows that the hybrid controller effectively balances the NP and robotic actuation.

6.1 Introduction

The preceding chapters have presented in detail the theoretical and technological developments required to fulfill the objectives set out in this dissertation. This chapter presents the experimental validation of the cooperative control of hybrid walking, comprised by experiments performed with healthy subjects (figure 6.1). These experiments aimed to test the whole system operation in a real walking scenario. The goal is to validate the control approach and also safety and usability issues prior to testing with SCI patients.

[1]This chapter is partially based on the following articles:
A. J. del-Ama, J. C. Moreno, A. Gil-Agudo, and J. L. Pons. **Hybrid FES-Robot cooperative control of ambulatory gait rehabilitation exoskeleton for spinal cord injured users,** in 2012 International Conference on Neurorehabilitation (ICNR2012): Converging Clinical and Engineering Research on Neurorehabilitation, 2012, pp. 155-159.
A. J. del-Ama, J. C. Moreno, A. Gil-Agudo, and J. L. Pons. **Hybrid FES-Robot cooperative control of ambulatory gait rehabilitation exoskeleton for spinal cord injured users,** Journal of NeuroEngineering and Rehabilitation. **Invited contribution.** Submitted on 3-03-2013

FIGURE 6.1: Healthy user performing a walking experiment with Kinesis.

6.2 Experimental protocol

Four healthy subjects participated in the experimental protocol (age 30.5±1.7 y.o., weight 77.0±5.5 kg., height 1.8±0.1 m.). The experimental protocol mainly consisted of walking with Kinesis in straight line. However, as concluded in section 2.4.2, the 10mWT and the 6mWT are extensively used in clinical settings to assess walking ability following paralysis, and have have been evaluated for utility, validity and reliability as research tools [202]. Consequently, the experimental protocol was adapted to the 6mWT and the 10mWT, which comprised walking in a straight line for 6 minutes, annotating the time elapsed to walk the first 10 meters.

A Visual Analog Scale (VAS) was used to assess user fatigue and comfort. A Likert-type questionnaire (Quebec User Evaluation of Satisfaction with assistive Technology, QUEST [274]) was used to measure assess perceived satisfaction during the use of Kinesis. The VAS consists of a 10 centimeters rectangle that is extensively used to assess perceived pain in clinical settings [275]. With this scale, the user rates the pain perception placing a mark inside the rectangle, rating from *no pain at all* at the left edge of the rectangle, to *intolerable pain* at the right edge of the rectangle. Measuring the distance from the left edge to the mark gives a value $\in [0, 10]$ that represents the user perceived pain, or fatigue and comfort in this protocol.

The QUEST questionnaire was specifically designed to measure user satisfaction with a broad range of assistive technology devices in a standardized way [274]. It consist of 12 items related to device characteristics (8 items) and assistive technology services (4 items), which are answered by the user rating in a 5 point scale, rating from 1 (not satisfied at all) to 5 (totally satisfied). The items related to device characteristics were included in the protocol:

1: How much satisfied are you with the system's dimensions (size, width, height)?

2: How much satisfied are you with the system's weight?

3: How much satisfied are you with the system's fitting capability?

4: How much satisfied are you with the system's safety?

5: How much satisfied are you with the system's durability?

6: How much satisfied are you with the system's ease of use?

7: How much satisfied are you with the system's comfort?

8: How much satisfied are you with the system's efficacy to solve your problem?

Prior to start the experiment, the subjects signed an informed consent. Three electrodes (Alexgaard, Pals-platinum) were placed over the motor points of *Vastus Lateralis*, *Rectus Femoris* and *Vastus Medialis* knee extension muscles, and two electrodes over the motor points of *Semitendinosus* and *Biceps Femoris* knee flexion muscles [276]. Then, a muscular warming period with electrical stimulation was carried out during 5 minutes. Stimulation parameters were: pulse width 200 μs, frequency 8 Hz, train 14 seconds, duty cycle 43% and the amplitude set to the contraction thresold. As described in section 5.2, after the warming period, the maximum tolerable stimulation intensty (user pain threshold), was obtained through iterative increments on the stimulation amplitude while pulse width was fixed to 450 μs and train frequency to 70 Hz.

After a relaxing period of 10 minutes, the walking test begun. Given that the main objective was to test Kinesis cooperative approach, subjects were instructed to simulate the functional ability of the target population: *walk passively avoiding voluntary movements of both knee and ankle, bending to the side to lift the heel, and drag the hip.* This would give a better understanding of Kinesis performance partially emulating target population. The walking trial consisted of walking with Kinesis during 6 minutes in straight line assisted by a walker. The skin under the electrodes was inspected after the walking trial, as well as exoskeleton and cabling conditions.

6.2.1 Data analysis

Mean and standard deviation were computed for the time needed to walk 10 meters, distance covered in 6 minutes, and VAS scores. Mode and inter-quartile range were computed for QUEST scores. Kinesis performance was assessed in terms of actual knee angle, TTI, NILC, and modulation of the knee force field parameter K_k. Energy delivered by the knee actuator was estimated by the electrical power consumed by the motor, neglecting mechanical efficiency. It was assumed that mechanical losses are low and of constant value. Data from both legs of all subjects were gathered, and a correlation analysis was performed between estimated energy and TTI (Spearman's Rho correlation test, p-value$<$0.05).

6.3 Results

All subjects completed the 6 minutes walking test. Operation of Kinesis was well tolerated and was perceived as comfortable. No dangerous situations were reported. After the experiment, electrodes were removed and the skin revealed some erythema that disappeared within 10 minutes. Furthermore, no adverse effects were reported during the experiments. In one experiment, data from one leg were lost due to connection malfunction.

To illustrate the system's operation during hybrid walking, results from one subject's leg are shown in figure 6.2 and 6.3 (subject 3). Time evolution of the main controlled variables with Kinesis during the first steps of an experiment for left leg of participant number 3 is shown in 6.2: knee trajectory, interaction torque, TTI during swing phase, and ILC stimulation output.

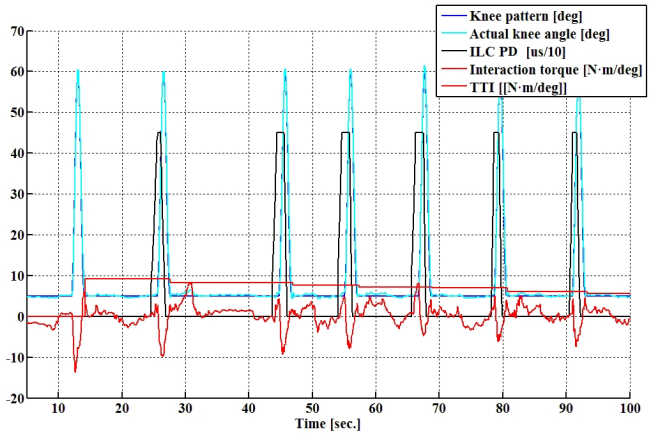

FIGURE 6.2: Representative data in time domain from left leg of participant 3 during the first 100 seconds of the experiment. Knee reference angle (blue), actual knee angle (light blue), user-exoskeleton interaction torque (red curve), TTI (red step-like curve) and ILC output (black). A decrease on interaction torque during swing phase, due to increasing muscle contribution to the movement during this phase, can be noticed.

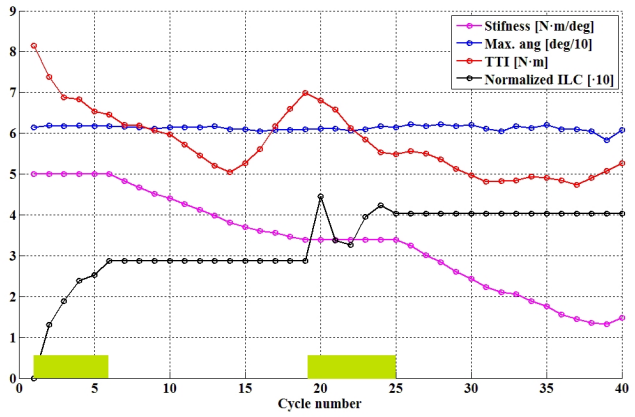

FIGURE 6.3: Representative results in cycle domain. Data from the same subject, leg and trial than showed in figure 6.2 for the entire experiment. Note that x-axis is cycle number. TTI (red), maximum knee flexion angle (blue), exoskeleton stiffness (pink), NILC (black) for each step are shown. Green boxes shows *learning* state active. No box means *monitoring* state active.

During stance phase, it can be observed that a knee position near 5 degrees was successfully maintained, with a small compliant deviation. Maximum range of knee deviation for all experiments ranged between 2 to 8 degrees for all the experiments. Figure 6.4 shows the normalized quadriceps stimulation output during stance for both legs of all participants. Normalization was performed relative to maximum stimulation during stance phase, similarly to the procedure for calculating the NILC. It can be observed that stimulation during stance was in average small, below 30%. Figure 6.5 shows the actual normalized knee angle of an experiment for left leg of subject 3. Note that the reduction in the displayed stiffness of Kinesis (figure 6.6 left, participant 3, left leg) does not impact on the actual knee trajectory, while toe clearance is guaranteed by achieving 60 degrees of knee flexion.

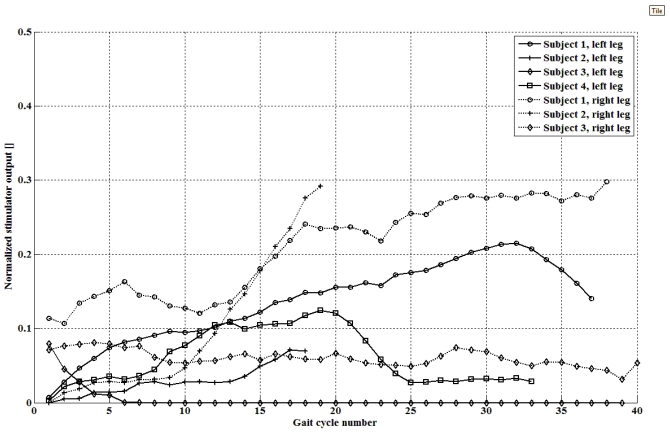

FIGURE 6.4: Normalized quadriceps stimulation PD during stance. Data from both legs of all four subjects.

Transitions amongst stance and swing were smooth during the experiments and no jerky movements were noticed (figure 6.5). Swing knee trajectory of first steps was sucessfully controlled (figure 6.2, blue and light blue curves) while the ILC was iterating (figure 6.3, cycles 1 to 6). Interaction torque during swing shows a progressive reduction in the peak flexor torque when comparing subsequent steps (figure 6.2, red curve). This reduction and modulation can be related to the stimulation effect during swing (figure 6.2, black curve). This reduction can be better noticed when looking at the TTI during swing in figure 6.2, red step-like curve, or in figure 6.3, where the main controlled variables of the same experiment are represented in cycle domain, for the entire experiment. NILC was calculated as described in section 5.2.2.2.

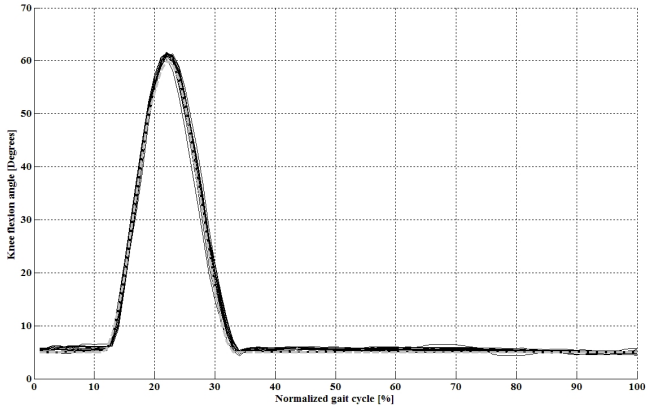

FIGURE 6.5: Actual normalized knee kinematics from the same subject, leg and trial than showed in figure 6.2 for the entire experiment. Knee reference angle is superimposed (dashed, gray curve). As noticed, actual kinematics remains closer to the reference.

Figure 6.3 presents the progress of the *learning state*, from the start until cycle number 6. During this state, ILC stimulation is gradually increased (NILC, black curve), TTI decreases, and the maximum flexion angle is maintained above 60 degrees. From cycle 4 to 6, a stabilization in ILC stimulation can be observed. In cycle 6 the relative change in NILC is lower than 5%, therefore convergence is assumed and the system enters in *monitoring state*. Within this state stiffness for

the swing phase is progressively decreased, while actual knee trajectory and maximum flexion angle are maintained. Therefore the corrective actions of the robotic exoskeleton over the knee are also decreasing. A further TTI decrease is observed (figure 6.3, cycles 7 to 14). Although stimulation is held constant, this can be understood as an effect due to potentiation of the stimulated muscle[2]. Besides, users could voluntary activate muscles during movement. After cycle 15 a gradual increase on TTI is observed. This is due to a decrease in muscle performance, indicating muscle fatigue appearance. After overcoming the fatigue threshold in cycle 19, the stimulation parameters are changed. This change in stimulation parameters and muscle dynamics requires a new iteration period, therefore Kinesis enters in *learning* state. In cycle 26 a further ILC convergence is estimated, and Kinesis enters in *monitoring state*. Number of steps for convergence was 11,0±3,3 in average for both legs, and fatigue was detected 19.4±1,5 steps after the beginning of the walking trial.

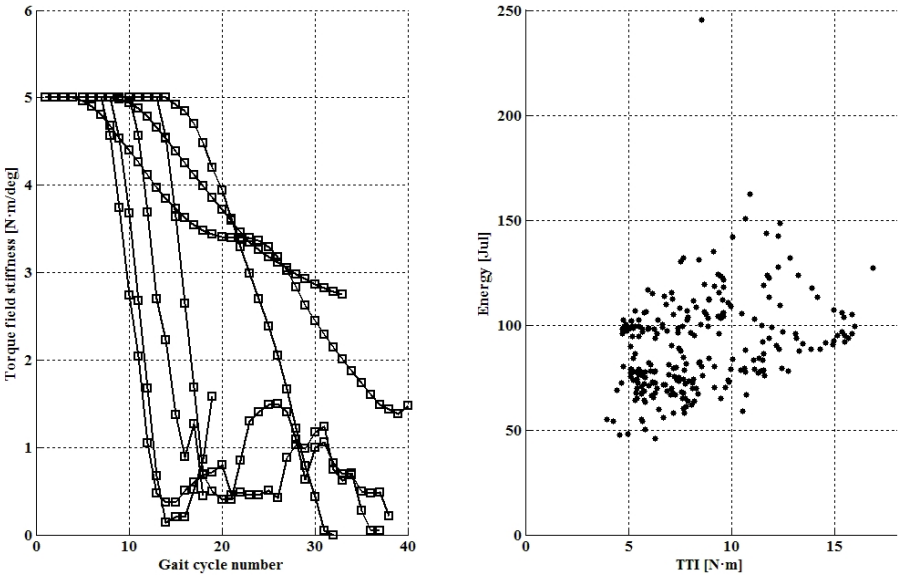

FIGURE 6.6: Compliance adaptation. Left: K_k progress for both legs of all subjects. Right: energy delivered by Kinesis actuator during swing phase versus TTI (R=0.34, p<0.001 Spearman's Rho correlation test). Data from both legs of all four subjects.

Figure 6.6 shows how the control of knee torque field stiffness operates for both legs of all participants. Note that in some cases, the cooperative controller was able to reduce K_k up to 0 $N \cdot m/deg$, indicating that the robotic exoskeleton does not provide assistance to drive the knee during swing, only the stimulated muscles. A correlation analysis between the energy delivered by the exoskeleton during swing phase and the TTI, shows that a reduction in TTI reflects a significative reduction in the energy delivered by the exoskeleton (figure 6.6), thus indicating that the power delivered by the muscles correlates with a decrease on the power consumed by the actuator.

Figure 6.7 and table 6.1 shows group results of functional walking test and questionnaire scores: QUEST and VAS score for pain and fatigue. Average data for subject group were 4.1±1.4 seconds for the 10mWT, and 15.4±5.0 meters for the 6mWT. QUEST items were scored in the

[2]The potentiation effect is described in section 4.2.3

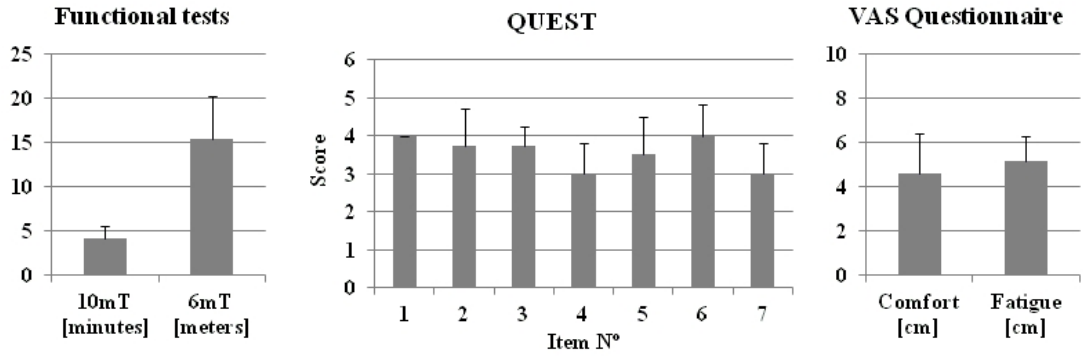

FIGURE 6.7: Group average results for the evaluation experiment with healthy users. Left: 10 meters and 6 minutes walking tests. Center: QUEST score. Right: pain and comfort VAS score.

middle of the scale (type Likert from 0 to 5), except for items 4 and 7. Comfort (4.6±1.8 cm) and fatigue (5.2±1.1 cm) perceived by the users was also set at the middle of the VAS scale.

TABLE 6.1: Results from walking experiments with healthy users. Comfort and fatigue measured by VAS scale, time to cover 10 meters and distance covered in 6 minutes are mean±SD. QUEST scores are median±inter-quartile range.

Variable	Value
Comfort [cm]	4.6±1.8
Fatigue [cm]	5.2±1.1
10mWT [min]	4.1±1.4
6mWT [m]	15.4±5.0
QUEST Item 1	4.0±0.0
QUEST Item 2	3.5±1.3
QUEST Item 3	4.0±0.3
QUEST Item 4	3.0±0.5
QUEST Item 5	4.0±0.5
QUEST Item 6	4.0±0.5
QUEST Item 7	3.0±0.5
QUEST Item 8	Not answered

6.4 Discussion

Firstly, results have shown that the proposed control approach is able to balance NP and robotic contributions with a therapeutic approach to induce locomotor activity. This has been confirmed by means of the correlation analysis of energetic contribution by the robot and performance of artificially activated muscles. However, the efficiency of this control design has not been undoubtedly stated yet, and is further investigated with respect to the therapeutic application in chapter 7. Secondly, our analysis has shown that the muscle performance in hybrid NP-robotic control of walking in a group of healthy subjects can be monitored and quantified in terms of human-robot interaction. The MFE is able to manage stimulation performance for learning and

management of muscular stimulation to counteract the muscle fatigue. A considerable period of training (typically several weeks or even months) with electrical stimulation is needed prior to the use of either NP [128, 130, 277] or hybrid exoskeletons [67, 166, 172] for walking activities, mainly due to changes in muscular characteristics after paralysis. Monitoring muscle performance holds the potential to shorten the stimulation training period significantly, combining part of the training period with the hybrid walking therapy. This will be further investigated in chapter 7 where testing with SCI patients is performed. However, the proposed approach assumes a uniform effect of fatigue for the involved stimulated muscles around the knee joint. Monitoring the activation of each stimulated muscle independently would represent a more precise estimation of fatigue. The methodology proposed aims to manage muscle fatigue due to FES within this unique hybrid actuation context, specifically designed for this application. Therefore this method represents a particular technique that appears to be effective in sustaining average generated joint torques in hybrid actuation context.

Closed loop control of NP is implemented in few hybrid ambulatory exoskeletons [183], and some have a sort of semi-closed loop control [170, 174, 278]. To the best of our knowledge, results on proper closed-loop control of NP have not been reported before. Through quantification of TTI during swing, Kinesis gives an objective measure about stimulation effectiveness of flexor muscles, a highly demanding stimulation. Extensor muscles are only stimulated when knee flexes during stance. Although blocking the knee through the exoskeleton eliminates the need of stimulating the extensor muscle, Kinesis PID stimulation control allows for a more physiological control of the knee during stance. Results showed that stimulation was reduced 80% compared with an on/off stimulation sustained for the entire stance phase. Although semi-active hybrid exoskeletons achieve greater reduction in quadriceps stimulation (e.g. 89% reduction in [170]), our stimulation approach provides a more physiological stimulation, related to joint bending during stance. However, the inability of measuring voluntary muscle activation limits the interpretation of these data. Although the participants were instructed to avoid activation of the leg muscles, verification of this condition was subjective and can be investigated in further experiments. Therefore we rely on the assumption that the obtained stimulation parameters are partially influenced by the natural activation of the quadriceps muscles during stance.

ILC control of NP have been recently proposed for position control of ankle [270] and hybrid control of knee [263] combined with the Lokomat. In both cases, ILC controls the entire gait phase, as it is timely-defined by the fixed step cadence of Lokomat. ILC control is limited in Kinesis to the swing phase, with smooth and continuous transitions between gait phases. In [263], the control task is similar to Kinesis, where the interaction torque is minimized by the stimulation. Results in both cases are similar, although in [263] ILC converges in approximately 15 cycles whilst in Kinesis ranges from 5 to 10 gait cycles in average. This can be attributed to our conservative convergence criterion, established to avoid muscle fatigue with further ILC iterations that would not be monitored by the system. Additional iterations would only give little improvements in muscle force production but they would contribute to generating muscle fatigue.

As shown, muscle fatigue monitoring allows to also monitor stimulation performance while learning, by continuously monitoring muscle performance. Results showed that a reduction in average of 30-40% of the first TTI within the first ILC iteration, which is directly related to stimulation

performance. In addition, estimation of muscle fatigue and continuous monitoring of TTI allows for a robust management of muscle performance, implementing novel fatigue management strategies in hybrid neuroprosthesis.

Kinesis is, to the author's best knowledge, the first ambulatory hybrid rehabilitation exoskeleton with stiffness control of knee trajectory. The cooperative control approach takes advantage of stiffness control in *monitoring state*, increasing the compliance of the robotic exoskeleton, balancing its assistance with the muscular force production, in a *reactive* version of the AAN concept. Experimental results have shown that Kinesis have reduced its stiffness during the swing phase to a minimum of approximately 0 N·m/deg. The correlation between the energy consumed by the actuator and the TTI shows that the cooperative controller effectively balances the robotic and neuroprosthetic power sources. During stance, Kinesis allows for a certain degree of knee motion, similar to [279]. However, specific analysis of stance phase was not undertaken, therefore we cannot extend the results from [279] to the approach presented here.

Imposing both a kinematic and a time defined pattern on the patient is one of the limitations of Kinesis exoskeleton control. Further developments would include a more adaptable kinematic pattern to increase the cooperation between Kinesis and the residual abilities of the user. Surface electrical stimulation, although closed-loop modulated, is still not achieving a physiological activation pattern. Muscle activation in healthy conditions have several characteristics that are not synthesized with this approach, as muscle co-contractions and synergic activations, that contrast with the mechanistic approach implemented here. Further developments for rehabilitation purposes would include more bio-inspired stimulation controllers [280].

Optimal balance between neuroprosthetic and robotic actuation has been proposed in several works, but only results from simulation have been published [281–284]. These control approaches relies on accurate models of the systems controlled, which is still a subject of major research. Despite the theoretical effort done in those proposals, control and interaction with biological structures is still a challenging task, and more research on the areas of muscle modeling, physical human-robot interaction and hybrid control is needed, in order to design control strategies that optimally balance the neuroprosthetic, robotic and user contribution to movement. In our approach, the correlation between the energy delivered by the robotic exoskeleton and TTI verifies that Kinesis cooperative control balances neuroprosthetic and robotic contributions. However this balance, although effective, cannot be demonstrated as optimal.

The study with healthy subjects presented in this section aimed to verify the control approach and also testing the behavior of Kinesis hardware. In addition, it was also aimed to test the protocol to be used with SCI patients, in order to prepare it for clinical experimentation. Estimated walking velocity obtained in this experiment from the 10mWT (0.44±0.14 m/sec.) is in line with previously published data of walking with passive orthosis (0.34 m/sec. for a reciprocating gait orthosis and 0.24 m/sec. for the Wearable Orthosis [61]; 0.14 m/sec. for a isocentric reciprocating gait orthosis [285]), and hybrid orthosis (0.14 to 0.45 m/sec. for a hybrid reciprocating gait orthosis [156]). These data are still far from normative data regarding walking ability of people with SCI: 1.37 m/sec for the 10mWT [286]. Nevertheless, operation of Kinesis needs to trigger the step whenever the user is stable and ready to take it. This leads to a semi-automatic walking pattern that significatively reduces walking velocity, but provides safe operation to the patient.

Questionnaires scores were included here in order to have information of healthy users perception. A general limitation arises with testing with healthy users, as they obviously functionally behave

different from impaired subjects. Testing with healthy subjects must be done prior to patient testing in order to ensure system stability and integrity, and refine control methods. In the experiments presented here the healthy users were instructed to functionally behave similarly to impaired users, but it cannot be ensured to what extent this was actually achieved.

6.5 Conclusion

The cooperative control strategy for the hybrid NP-robot system, designed to deliver hybrid walking therapy with fatigue management have demonstrated ability to balance the stimulation and robotic actuation. The correlation between the energy consumed by the actuator and the TTI shows that the cooperative controller effectively balances the exoskeleton and NP power sources. Closed-loop control of NP allows to manage changes in muscle performance and gait phase. This design overcomes several disadvantages related to NP control of movement: muscle fatigue is estimated through muscle performance and managed by closed-loop control of NP, and trajectory control through a compliant actuation of the exoskeleton. Experiments with patients have to confirm these results.

6.5.1 Answer to research questions

This chapter provides the following answer to research question Q9 stated in section 1.6.2 as follows:

Q9: **How to design the hybrid controller to balance NP and exoskeleton actuation?** The proposed dual FSM design (t-FSM and c-FSM) allowed to switch between open- and closed- control of stimulation to balance the NP and robotic contribution to the movement and furthermore, monitoring muscle performance regarding muscle fatigue.

Chapter 7

Clinical evaluation[1]

This chapter presents the clinical evaluation of the hybrid-cooperative approach for walking therapy within a group of SCI patients. This evaluation analyzes several aspects: control performance, patient-robot adaptation during hybrid walking, and the impact on the walking function of the patients. Results show that the hybrid-cooperative approach successfully adapted to the diverse functional conditions. The patients tolerated the walking therapy. The impact on patient's walking function was positive. These results motivate further research on hybrid walking therapy for SCI rehabilitation. Besides, several areas for improvement of the hybrid walking control approach are identified.

7.1 Introduction

The objective of this chapter is to evaluate the performance of Kinesis and the hybrid-cooperative walking therapy within the target population. As discussed earlier in chapter 2, there is no consensus on end-user assessment methods and measures for evaluation of hybrid exoskeletons. Only two studies [80,81] presented a extensive assessment of the immediate effects of walking with the device, featuring a evaluation protocol aligned with the recommendations given in chapter 2. These recommendations were followed for designing a walking experiment for validation of the hybrid-cooperative control approach, already tested with healthy users in chapter 6. The protocol for evaluation with patients presented in this chapter share the walking experiment. A comprehensive protocol was designed around the walking experiment, including additional variables for evaluation of the immediate effects of hybrid walking and the impact on the walking function of the patient.

The clinical evaluation follows two objectives: 1) to assess walking performance due to the use of Kinesis, focusing on control aspects and Kinesis-patient mutual adaptations. 2) to assess the impact on the patient's own walking function, whether it is modified or not after using the device for a period of time.

[1]This chapter is partially based on the following articles:
J.L. Pons, A. J. del-Ama, A. Gil-Agudo and J.C. Moreno. **Combined Application of Neurorobotics and Neuroprosthetics in Rehabilitation of Spinal Cord Injury,** in International Neuromodulation Society 11th World Congress. Rehabilitation, Spinal Cord Injury and Functional Electrical Stimulation Session. Berlin, Germany 8-13 June 2013

7.1.1 Experimental protocol

The study designed protocol was comprised by two weeks. During the first week (*intervention week*) hybrid walking training was provided. During the second week (*no intervention week*) no intervention was administered. The objective of this design was to assess patient walking function before and after the intervention with Kinesis (and associated experiments) for comparison of effects with routine rehabilitation. For that purpose, assessment of walking function was made before and after each week. Figure 7.1 shows the study protocol.

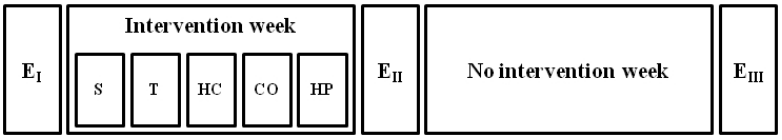

FIGURE 7.1: Study protocol for Kinesis evaluation within target population. E stands for walking function evaluation session, S stands for stimulation test session, T stands for training session, HC, CO and HP stands for walking experiments as described in the text.

The walking function assessment, denoted as $\mathbf{E_I}$, $\mathbf{E_{II}}$ and $\mathbf{E_{III}}$ in figure 7.1, took place in separated days. The protocol was equal for all evaluation sessions, and was comprised by a MMT [5] score of the sagital plane, spasticity assessment by the Asworth and PENN scales[2], and a 6mWT walking test, where the time to cover the first 10 meters was registered (10mWT). The walking tests were performed by the patient using its regular devices for walking. Thus, results from these tests ought to reflect patient walking ability. All evaluations were made by a physiotherapist.

During the *no intervention week*, the patients followed his/her customary rehabilitation schedule. The *intervention week* was comprised by five sessions, with different testing goals. The first session consisted of a stimulation test similar to the fatigue test described in section 4.2 (**S** in figure 7.1). The objectives were to quantify the muscular response to the stimulation and also to get the patient used to the stimulation. Within this session, both flexor and extensor knee muscle groups of both legs were stimulated for 15 minutes. At the following session (**T** in figure 7.1), the patient first met Kinesis and learning exercises were carried out. The objective of this session was to train the patient to use Kinesis and getting acquainted with the walking technique: bend to the side to lift the heel prior to initiate a step and then pressing the button. Kinesis was adjusted to the patient anthropometry within this session. The total walking time in this session did not exceed from 10 minutes.

The remaining three sessions (**HC**, **CO**, and **HP** in figure 7.1) consisted of walking trials (figure 7.2), where the controller configuration differed among sessions. As discussed in chapter 5, Kinesis hybrid-cooperative controller modulates both stimulation and robotic assistance during walking. But, in order to provide a better understanding of adapting capabilities of Kinesis while providing walking therapy to the patient, stimulation and robotic assistance were tested separately incorporating two additional walking experiments, where either the robotic assistance or the stimulation are fixed. All three walking experiments shared the experimental protocol. The experiments codes corresponded to the following:

[2] Asworth scale measures the severity of the spasticity in a range from 0 to 4. PENN scale measures the frequency of spasmodic event in a range from 0 (no spasms) to 4 (more than 10 spasms in one hour)

FIGURE 7.2: Patient performing a walking experiment.

HC: Hybrid-cooperative controller configuration. This is the main controller configuration (presented in chapter 5), where both stimulation and robotic assistance are modulated during walking. This configuration was validated with healthy users in chapter 6.

CO: Cooperative-only controller configuration. For this configuration, the stimulation ILC controller is disabled, thus Kinesis can only bring adaptable robotic assistance to the patient during the swing phase through modulation of actuator stiffness. Stimulation of extensor muscles was not disabled to provide support during the stance phase.

HP: Hybrid-stiff controller configuration. For this configuration, actuator stiffness is held constant; stimulation controller is enabled and the c-FSM learning-monitoring is kept in normal operation.

Each configuration was tested in separated sessions to avoid fatigue-related effects. The configurations were tested in the same order for all patients: HC-CO-HP. The experimental procedure for walking trials was presented in section 6.2. Measuring of blood pressure (BP) and heart rate (HR) immediately prior and after the walking test were included for monitoring the physiological impact. Besides, three additional items to the QUEST questionnaire. These items were taken from the validation studies published for the Rewalk exoskeleton [80,81]. The questions included were related to user perceived spasticity as follows:

A: The device diminished spasticity in my legs.

B: I did not have breathing difficulties while using the device.

C: After completing the experiment I felt safe during the use.

7.2 Results

This section is structured in three main parts. The first part presents the *case studies* for each patient, comprised by the experimental results for each tested configuration (sections 7.2.1 to 7.2.3). These sections describe the performance of Kinesis during the experiments, focusing on the adaptations between the patient and the system, similarly to the healthy group analysis

(section 6.3). The second part is comprised by section 7.2.4, where the group-averaged immediate effects of walking for each tested configuration is presented. Finally, section 7.2.5 addresses the impact of Kinesis on walking function of SCI subjects.

Seven patients were recruited for participating in the experiments. There were four dropouts due to diverse reasons. One patient developed neurophatic pain after the stimulation testing session, not related with the intervention. Two patients were discharged prior to initiation of the intervention week, and the forth patient abandoned adducing time shortage. The remaining three patients that completed the study protocol are named here as 1, 2 and 3.

7.2.1 Case study 1.

Patient 1 is a male of 35 y.o., 65 kg. and 1.8 m. height. He had an acute disseminated encephalomyelitis with sixth nerve palsy, resulting in a SCI L5 AIS D. As consequence, he had lower extremities paralysis resulting in mild walking impairment, which functional characteristics met the inclusion criteria stated in section 3.1. A secondary consequence of the lesion was impaired balance during left leg stance.

Results from the stimulation test performed are shown in table 7.1. It is noticeable the low performance obtained from the stimulation of the extensor muscles despite the stimulation parameters were maximal, near the pain threshold.

TABLE 7.1: Stimulation test results for patient 1: maximum force-time integral achieved (absolute and normalized by patient's leg weight). Stimulation PD was set to 450 μs, train frequency to 70 Hz, pulse train duration 14 sec. and duty cycle 43%.

Movement direction	Left leg	Right leg
Extension	15 N (39%)	10 N (26%)
PA	68 mA	68 mA
Flexion	20 N (51%)	20 N (51%)
PA	50 mA	50 mA

7.2.1.1 Hybrid-cooperative control of walking (HC).

The time-evolution of knee patterned and actual kinematics, interaction forces and the ILC stimulation output for the flexor muscles for both legs during walking with the HC are depicted in Figure 7.3. The stimulation output for extensor muscles was not included for representation purposes, although it is further analyzed along with figure 7.5.

Knee kinematics of both legs were successfully controlled, and there were no dangerous situations reported during the experiment. Stimulation of left leg flexor muscles during swing (figures 7.3(a) and 7.3(b), black curves) was significantly lower than for the right leg (figures 7.3(c) and 7.3(d)), were the stimulation was almost saturated for the whole phase. Besides, it is noticeable the hyper-extension pattern of the right leg during stance phases, which increases prior to swing initiation (figures 7.3(c) and 7.3(d), light blue curves). The hyper-extension posture during

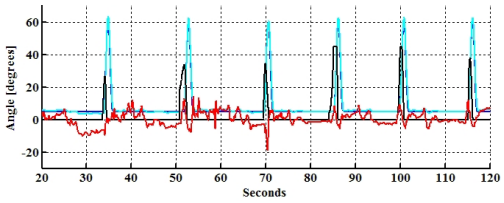

(a) First steps of left leg.

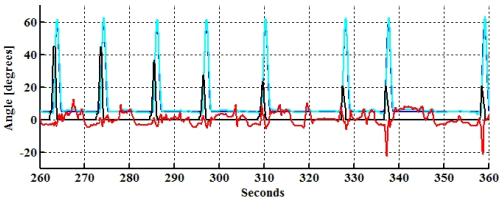

(b) Last steps of left leg.

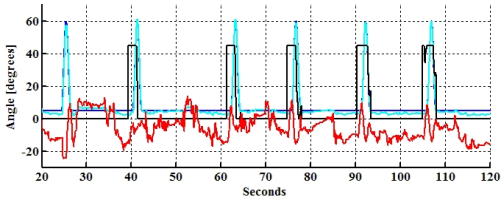

(c) First steps of right leg.

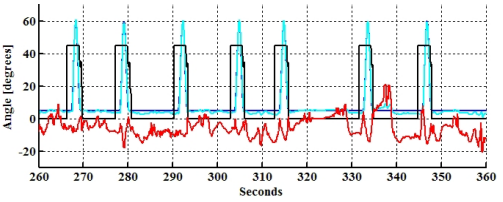

(d) Last steps of right leg.

FIGURE 7.3: Pattern (blue curve, *deg.*) and actual (light blue curve, *deg.*) knee kinematics, interaction (red curve, $N \cdot m/deg$) and stimulation (black curve, μs, ILC only showed) for HC.

stance were reflected in the interaction forces (same figures, red curve, extension is negative). Extensor interaction forces were also observed during swing phase of the right leg.

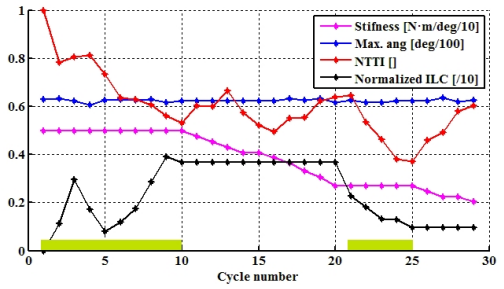

(a) Left leg.

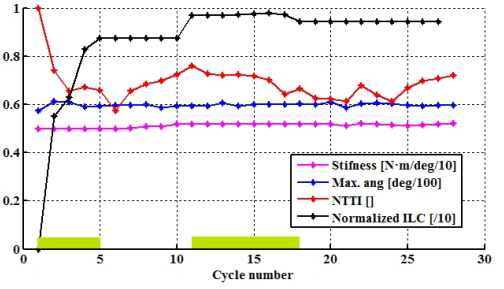

(b) Right leg.

FIGURE 7.4: HC experiment results in cycle domain. Controller stiffness (magenta curve, $N \cdot m/deg$), NTTI (red curve), maximum angle achieved during flexion (blue curve, *deg*) normalized torque-time integral (red curve), and NILC (black curve) of both legs for the entire walking experiment. Green boxes shows *learning* state active. No box means *monitoring* state active. Controller stiffness, maximum angle and normalized stimulation curves are scaled for representation purposes.

Figure 7.4 shows the cycle-related variables for the HC experiment. Comparing figures 7.4(a) and 7.4(b), the differences in the functional status of both legs can be noticed, which impacts on the stimulation intensity and the stiffness of the exoskeleton. The stimulation intensity (NILC[3], black curve) for the left leg was lower than for the right (maximum reached: 40% for the left, 97% for the right), and the first learning period took more steps. Interestingly, after the first muscle fatigue detection of the left leg (cycle 20), the second learning period led to a lower stimulation intensity, while the NTTI further decreased during the second monitoring period (cycles 25 to 29). This decrease could not be attributed to stimulation effect, because the pulse duration was low to produce muscle contraction (10% of NILC. See also figure 7.3(b)). This finding can be

[3]See section 5.2.2.2 for a description of how this magnitude is calculated.

attributed to voluntary muscle activation. A further increase on NTTI is observed for the last 5 cycles of the experiment, due in this case to an increase on muscle fatigue.

There was a marked reduction in the interaction force for both legs, up to a 40% of the initial TTI. The stimulation was considerably high for the rigth leg, above the 80% of the maximum stimulation achievable, for almost the entire experiment (figure 7.4(b), black curve, cycles 4 to 27). A decay on muscle performance was detected at cycle 10, probably due to the fatigue produced by the high stimulation intensity reached in the first iteration period (figure 7.4(b), cycles 1 to 5). The second iteration took a longer period (cycles 11 to 18), achieving a similar reduction in TTI than for the first period (figure 7.4(b), red curve, cycle 21). As in the case of the left leg, an increase on TTI is observed for the last 5 cycles of the experiment.

The evolution of the stiffness during the swing phases (figures 7.4(a) and 7.4(b), magenta curves) also reflects the differences between both legs. The stiffness for the left leg was progressively reduced during the monitoring periods, while the stiffness for the right leg could not be reduced, although the stimulation was high and a reduction in NTTI was achieved.

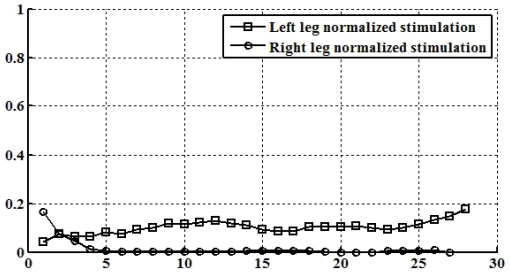

FIGURE 7.5: Normalized quadriceps stimulation during stance for HC experiment. Data from both legs.

Figure 7.5 shows the averaged normalized quadriceps stimulation intensity for the stance phases of the experiment for both legs. It can be clearly noticed that the stimulation of the right leg muscles was almost unnecessary, and a progressively increased is observed for the left leg. Again, the impaired balance perception of the subject during left leg stance had impact here, although the stimulation intensity achieved was likely to produce functional contractions.

7.2.1.2 No stimulation, cooperative control of walking (CO).

Similarly to the HC experiment, results for this experiment shows the same hyper-extension posture of the right leg along with the extensor interaction forces (figures 7.6(c) and 7.6(d)).

Regarding the cycle domain variables, the absence of stimulation in this experiment was reflected on changes on the NTTI values for the right leg. The NTTI oscillates around a constant value of 1.1, due to the trend to extend the leg of the patient, while the stiffness is slightly reduced (figure 7.7(b), red curve). Regarding the left leg, an interesting finding is noticed (figure 7.7(a)). The stiffness was decreased up to 0 $N \cdot m/deg$. This indicates that the exoskeleton assistance was reduced in order to follow the trajectory voluntary exerted by the patient, without impede the movement. This led to insufficient swing knee flexion in some cycles (19, 24, 25, blue curve), which could impede foot clearance.

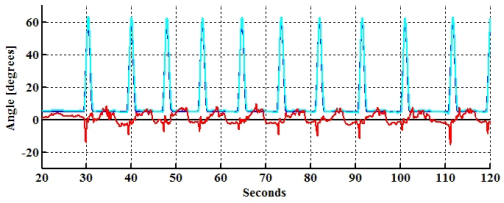

(a) First steps of left leg.

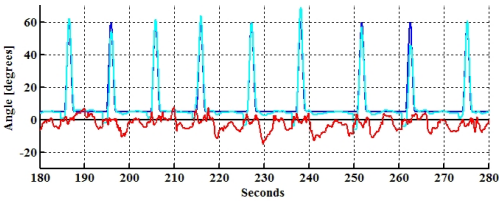

(b) Last steps of left leg.

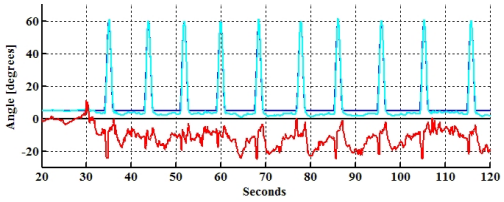

(c) First steps of right leg.

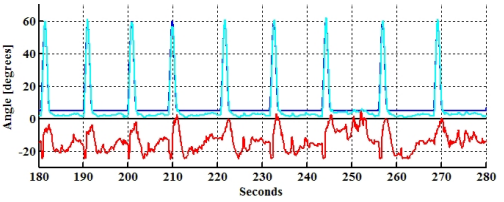

(d) Last steps of right leg.

FIGURE 7.6: Pattern (blue curve, *deg.*) and actual (light blue curve, *deg.*) knee kinematics, interaction (red curve, $N \cdot m/deg$) and stimulation (black curve, μs, ILC only showed) for CO.

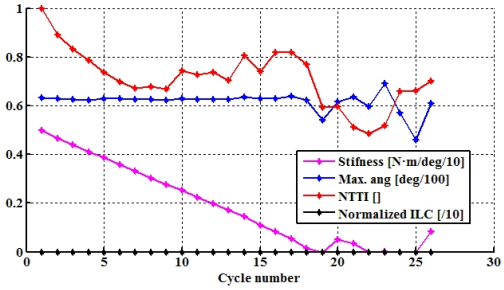

(a) Left leg.

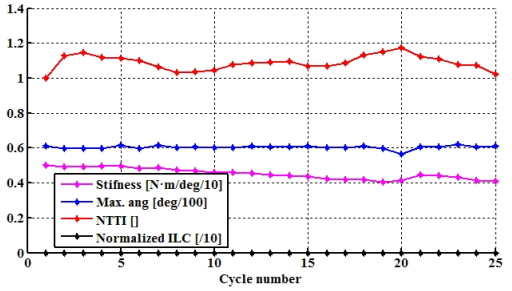

(b) Right leg.

FIGURE 7.7: CO experiment results in cycle domain. Controller stiffness (magenta curve, $N \cdot m/deg$), NTTI (red curve), maximum angle achieved during flexion (blue curve, *deg*) normalized torque-time integral (red curve), and NILC (black curve) of both legs for the entire walking experiment. Green boxes shows *learning* state active. No box means *monitoring* state active. Controller stiffness, maximum angle and normalized stimulation curves are scaled for representation purposes.

Similarly to the HC, the quadriceps stimulation for the stance phase for CO experiment was not significative (figure 7.8).

7.2.1.3 Hybrid-stiff control of walking (HP).

Similarly to the HC and CO, knee kinematics were successfully controlled during the entire experiment and the required stimulation for the right knee flexor muscles was higher than for the left leg muscles (figure 7.9). The hyper-extension posture of the right leg was also observed in this experiment (figures 7.9(c) and 7.9(d)).

In this experiment, similar results to the HC regarding the cycle-domain variables (figure 7.10) were obtained. The stimulation for the left leg was considerably low, unnefective for muscle

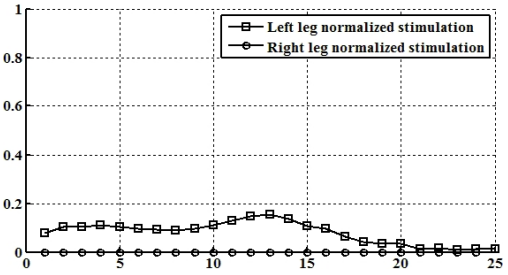

FIGURE 7.8: Normalized quadriceps stimulation during stance for CO experiment. Data from both legs.

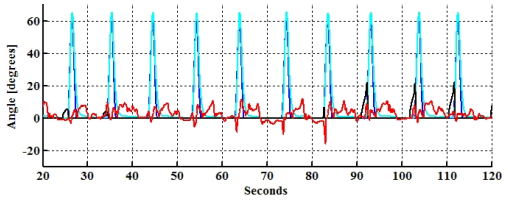

(a) First steps of left leg.

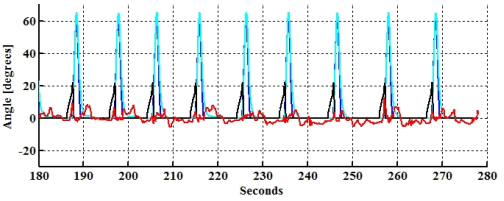

(b) Last steps of left leg.

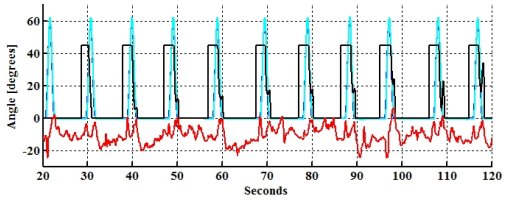

(c) First steps of right leg.

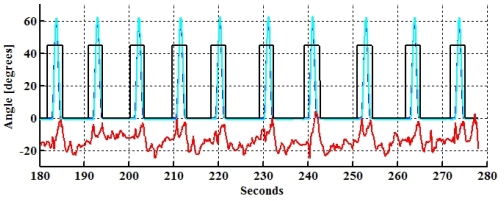

(d) Last steps of right leg.

FIGURE 7.9: Pattern (blue curve, *deg.*) and actual (light blue curve, *deg.*) knee kinematics, interaction (red curve, $N \cdot m/deg$) and stimulation (black curve, μs, ILC only showed) for HP.

activation. The first iteration period took the first 4 cycles, and the NTTI did not decrease. During the first monitoring period (cycles 5 to 7) the NTTI increased. Nevertheless, after the second iterating period the NILC increased slightly, but still inefficiently to provide muscle activation, and the NTTI decreased for the remaining experiment.

Regarding the right leg, similarly to the HC experiment, the stimulation increased rapidly (figure 7.10(b), black curve). A decrease on NTTI was observed for the first 8 cycles and a increase for the remaining 6 cycles of the learning period. After convergence, the NTTI remained stable.

Similarly to the HC and CO experiments, the average stimulation for the stance phases of both legs was unsignificant, higher for the left leg, and zero for the right, due to the trend to extend the leg exhibited by the patient during this HP experiment (figure 7.11).

7.2.1.4 Discussion

The specific impairment of the legs of the patient have conditioned the system performance, or in other words, the system adapted to the specific functional characteristics, which were different for each leg. The impaired balance perception during left leg stance led the patient to keep the right foot close to the ground during swing. This was reflected in the interaction forces during swing,

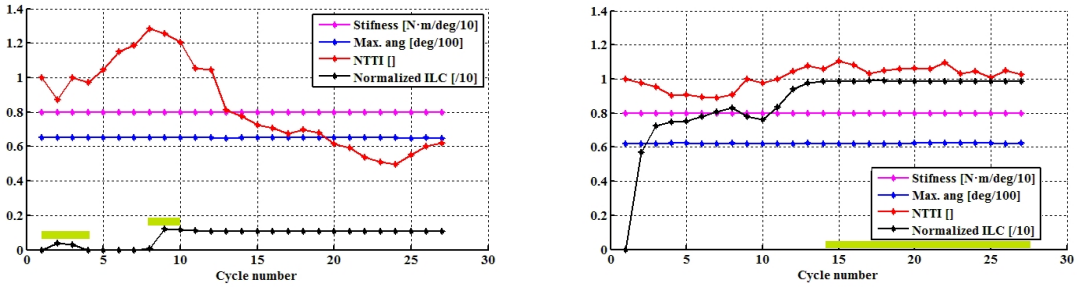

(a) Left leg.

(b) Right leg.

FIGURE 7.10: HP experiment results in cycle domain. Controller stiffness (magenta curve, $N \cdot m/deg$), NTTI (red curve), maximum angle achieved during flexion (blue curve, deg) normalized torque-time integral (red curve), and NILC (black curve) of both legs for the entire walking experiment. Green boxes shows *learning* state active. No box means *monitoring* state active. Controller stiffness, maximum angle and normalized stimulation curves are scaled for representation purposes.

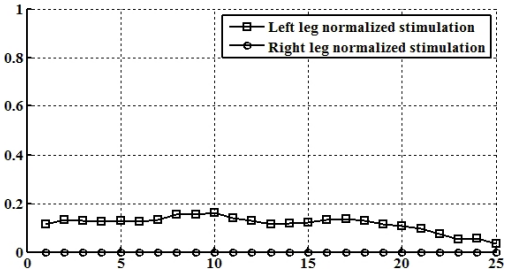

FIGURE 7.11: Normalized quadriceps stimulation during stance for HP experiment. Data from both legs.

which were markedly extensor. The actions provided by Kinesis to the right leg were providing intense stimulation and/or maintaining the stiffness during the swing phase, exerting adequate kinematics and muscle activation over the leg. The efficacy of these actions were reflected in the reduction of the NTTI for the HC and HP, but the in the later was less efficient. A rationale for this can be found on the fact that the day the experiment took place, the patient reported increased unbalance sensation and felt less confident overall. This would increase the effort of the patient in order to keep the right foot close to the floor.

In contrast with the right leg, the patient could voluntary move the left leg during walking. The actions provided by Kinesis to this leg were delivering a low amplitude stimulation pattern, unlikely to produce muscle contraction, and/or reducing the stiffness during the swing phase (The stiffness reached 0 $N \cdot m/deg$ in the CO, which allowed to follow the patient leg movement with a minimal interaction with the exoskeleton). Nevertheless, there is no possibility to verify this hypothesis due to the fact that voluntary and stimulated muscle activation are coupled. The stimulation provided to the left leg call into question the fatigue detections for HC and HP. A false fatigue detection could occur when voluntary contribution diminish, which increase the interaction forces. Note that fatigue is estimated as a consequence of decreased muscle performance reflected in the interaction forces. Therefore, when voluntary muscle activation is predominant, the MFE monitors the voluntary contribution of the patient.

7.2.2 Case study 2.

Patient 2 is a male of 43 y.o., 75 kg. and 1.77 m. height. He had a traumatic lesion, with explosion of L3 and L4 vertebraes and multiple fractures in foots and hip. He was diagnosed as SCI L4 AIS grade D. As consequence of the accident, the patient had a passive limitation on the articular range of both knees, which caused to adapt the kinematic pattern of the left leg to meet these limits (table 7.2). The joint angle for the stance phase of the left leg was set at the maximum knee extension angle, and the kinematic pattern for the swing phase was consequently adapted.

TABLE 7.2: Articular range of knee joint for patient 2.

	Left leg	Right leg
Range of movement	20-100 deg.	5-150 deg.

The differences between both legs on the joint angle for the stance phase influenced the results for all configurations, as is shown in next sections. These differences induced the patient to stance and walk with a leaned posture, due to the differences between the flexion angles of the legs. The results from the stimulation test are showed in table 7.3. The only noticeable finding was a reduced performance of the left leg's flexor muscles.

TABLE 7.3: Stimulation test results for patient 2: maximum force-time integral achieved (absolute and normalized by patient's leg weight). Stimulation PD was set to 450 μs, train frequency to 70 Hz, pulse train duration 14 sec. and duty cycle 43%.

Movement direction	Left leg	Right leg
Extension	60 N (134%)	70 N (156%)
PA	40 mA	48 mA
Flexion	10 N (22%)	25 N (56%)
PA	60 mA	58 mA

7.2.2.1 Hybrid-cooperative control of walking (HC).

Figures 7.12(a) and 7.12(b) show the kinematic pattern designed to meet patient's left knee angular limitation (blue curves). Looking at the right leg, high interaction forces towards flexion during stance were appreciated (figures 7.12(c) and 7.12(d) red curve, leg over exoskeleton). These flexor forces reflected on the kinematics, where the right knee is flexed during stance. In contrast, the interaction forces of the left leg during stance were significative lower, and the actual knee angle during stance remained close to the reference. Transition from stance to swing phase of the right leg resulted also on a transition of the interaction forces from flexor direction for stance, to markedly extensor direction for swing. Stimulation of flexor muscles for both legs exhibited in general a saturated pattern for the swing phase (black curves).

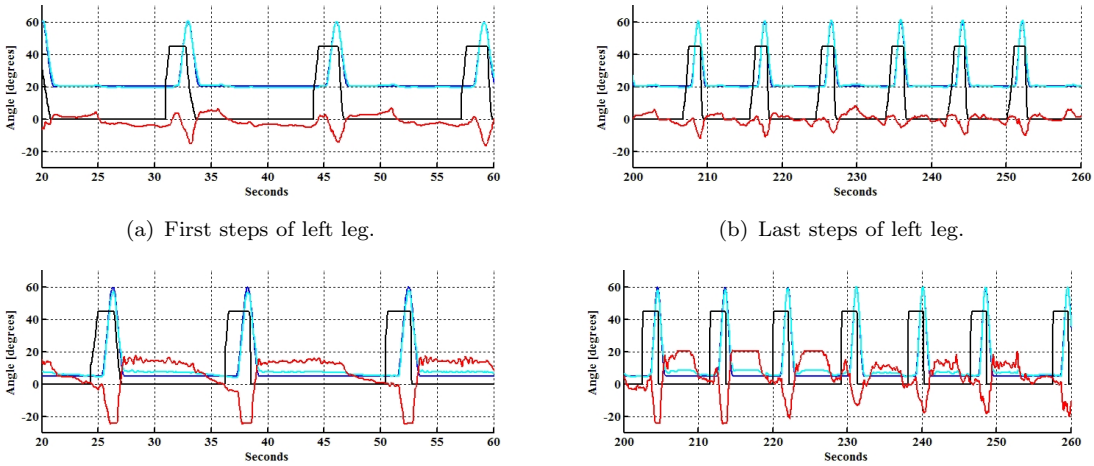

(a) First steps of left leg.

(b) Last steps of left leg.

(c) First steps of right leg.

(d) Last steps of right leg.

FIGURE 7.12: Pattern (blue curve, *deg.*) and actual (light blue curve, *deg.*) knee kinematics, interaction (red curve, $N \cdot m/deg$) and stimulation (black curve, μs, ILC only showed) for HC.

Maximum flexion angle of the right leg for the first learning period was slightly lower than 60 degrees (figure[4] 7.12(c), blue and light blue curves). This was further compensated during the first monitoring period by an increase in the stiffness (figure 7.13(b)). It was also noticeable the difference in step cadence between the beginning and the end of the walking experiment, which indicates that the patient increased expertise and confidence on the use of Kinesis after a number of cycles (figures 7.12(a) versus 7.12(b) and 7.12(c) versus 7.12(d)).

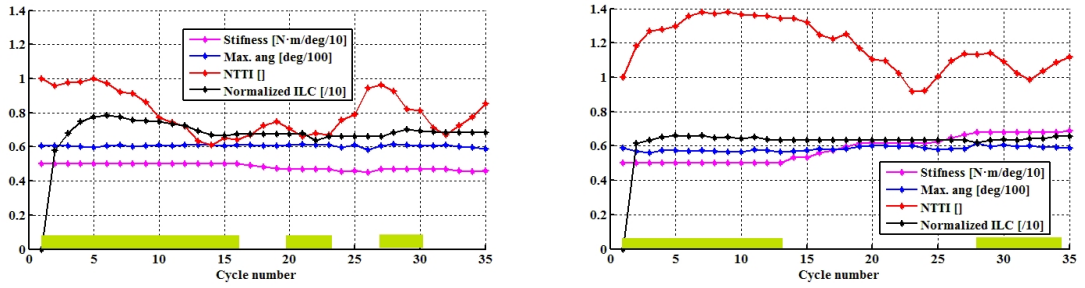

(a) Left leg.

(b) Right leg.

FIGURE 7.13: HC experiment results in cycle domain. Controller stiffness (magenta curve, $N \cdot m/deg$), NTTI (red curve), maximum angle achieved during flexion (blue curve, *deg*) normalized torque-time integral (red curve), and NILC (black curve) of both legs for the entire walking experiment. Green boxes shows *learning* state active. No box means *monitoring* state active. Controller stiffness, maximum angle and normalized stimulation curves are scaled for representation purposes.

The stimulation pattern of both legs in the cycle-domain is summarized in figures figures 7.13(a) and 7.13(b). NILC for both legs achieved the 70% of the maximum achievable stimulation intensity for the swing phase. After the first learning period of the right leg, a decrease on NTTI

[4]This is difficult to observe in the figures. During the first learning period, the maximum flexion angle was 58 degrees in average.

is observed along with an increase on the stiffness. In cycle 27 fatigue was detected and a new learning period took place (figure 7.13(b)).

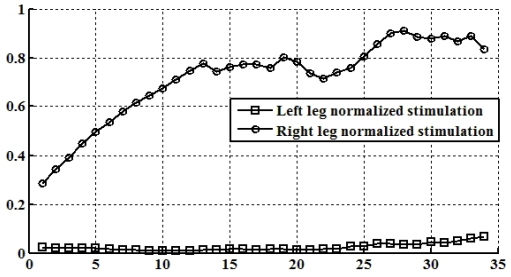

FIGURE 7.14: Normalized quadriceps stimulation during stance for HC experiment. Data from both legs.

Regarding the left leg, a more moderated increase on stimulation intensity (figure 7.13, black curve) for the first learning period was observed, reaching similar stimulation intensity than for the right leg, corresponding with a decrease on NTTI. After the learning period, the stiffness was slightly reduced.

Figure 7.14 shows the averaged quadriceps stimulation intensity for the stance phases, for both legs. It is noticeable the high stimulation intensity applied to the right leg, in response to the flexion posture exhibited by the patient during stance phases. The quariceps stimulation intensity increased across cycles.

7.2.2.2 No stimulation, cooperative control of walking (CO).

Knee kinematics, interaction forces and flexor stimulation during the HP experiment showed in figure 7.15 are similar to results from the HC experiment in the time domain (figure 7.12), and no new findings were noticed.

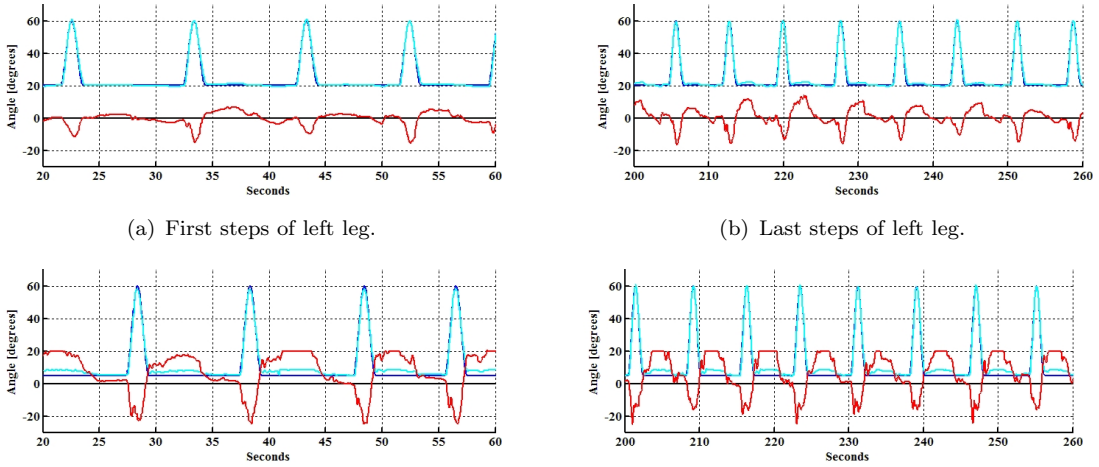

(a) First steps of left leg.

(b) Last steps of left leg.

(c) First steps of right leg.

(d) Last steps of right leg.

FIGURE 7.15: Pattern (blue curve, *deg.*) and actual (light blue curve, *deg.*) knee kinematics, interaction (red curve, $N \cdot m/deg$) and stimulation (black curve, μs, ILC only showed) for CO.

Regarding the cycle-domain variables for the left leg (figure 7.16(a)), a decrease on NTTI for the first 17 cycles was observed (red curve), along with a decrease on the stiffness (magenta curve). A progressive increase on NTTI and a stabilization of the stiffness was observed from the 17th cycle to the end of the experiment.

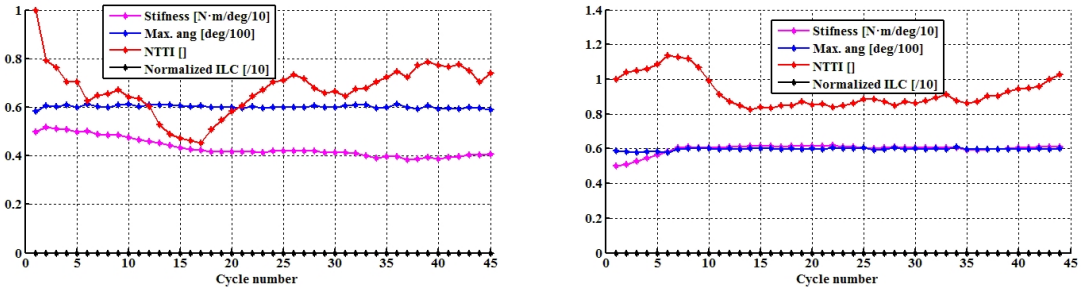

(a) Left leg.

(b) Right leg.

FIGURE 7.16: CO experiment results in cycle domain. Controller stiffness (magenta curve, $N \cdot m/deg$), NTTI (red curve), maximum angle achieved during flexion (blue curve, deg) normalized torque-time integral (red curve), and NILC (black curve) of both legs for the entire walking experiment. Green boxes shows *learning* state active. No box means *monitoring* state active. Controller stiffness, maximum angle and normalized stimulation curves are scaled for representation purposes.

Cycle-domain results for the right leg (figure 7.16(b)) show an increase on NTTI for the first 6 cycles. As occurred in the HC experiment, the subject reacted to the mobilization of the leg by increasing the trend to extend the leg during swing. This was counterbalanced by the CO controller by increasing the stiffness to achieve 60 degrees of knee flexion during swing. After this balance between the patient and Kinesis, a stationary situation can be observed, where the NTTI increases slowly, probably due to patient fatigue, while the stiffness remained constant.

Quadriceps stimulation intensity for this configuration exhibited the same pattern as for HC experiments (figure 7.17). Nevertheless in this experiment, the stimulation was more intense overall, as the trend to flex the left leg of the patient was more intense for this case.

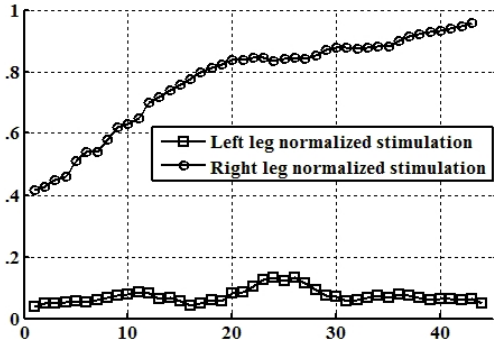

FIGURE 7.17: Normalized quadriceps stimulation during stance for CO experiment. Data from both legs.

7.2.2.3 Hybrid-stiff control of walking (HP).

Knee kinematics, interaction forces and flexor stimulation resulting during HP experiment are shown in figure 7.18. These are similar to results from HC and CO experiments (figures 7.12 and 7.15). Nevertheless, the actual maximum flexion angle for the right knee for this experiment was closer to 60 degrees from the beginning for this experiment, although the patient trend to extend the leg during swing was also observed in this experiment.

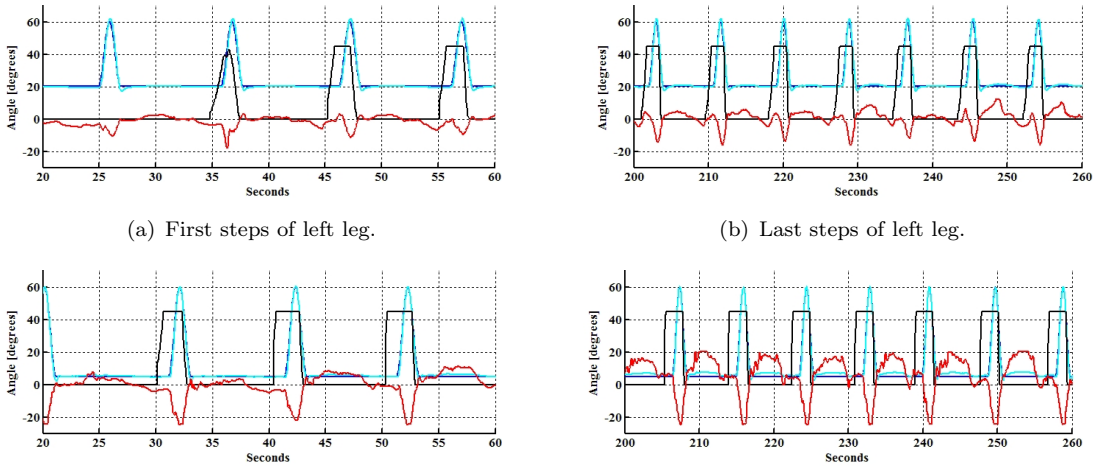

(a) First steps of left leg.

(b) Last steps of left leg.

(c) First steps of right leg.

(d) Last steps of right leg.

FIGURE 7.18: Pattern (blue curve, *deg.*) and actual (light blue curve, *deg.*) knee kinematics, interaction (red curve, $N \cdot m/deg$) and stimulation (black curve, μs, ILC only showed) for HP.

Examining the cycle-domain results in figure 7.19(b)), the NTTI for right leg did not increase for the first steps, contrary to the results with the HC experiment (figure 7.13(b)). As result, the stimulation intensity increased slower during the first learning period (from cycle 1 to 10). The maximum angle for the swing phase was lower than 60 degrees, although closer than for HC experiment (figure 7.19(b), blue curve). In this configuration the stiffness is not increased, as was the case for the HC and CO. Regarding the left leg (figure 7.19(a)), the cycle-domain results were similar to the HC (figure 7.13), except the NTTI, which did not decrease as much.

The results for the averaged quadriceps stimulation intensity for the stance phases of the HP experiment (figure 7.20) were similar to HC and CO experiments. The analysis made for the former experiments are also applicable to these results, although in this experiment, quadriceps stimulation was less intense overall.

7.2.2.4 Discussion

The specific functional deficit of patient 2 resulted in a reduced knee range of motion for the left leg, which caused the patient to exert compensatory actions that were counteracted by Kinesis. During stance, the patient flexed the right knee in an attempt to level with the flexion angle of the impaired left knee. Kinesis counteracted this by increasing the stimulation, while the displayed stiffness was enough to provide compliant but adequate support during stance. Nonetheless, prior to swing initiation, the patient consistently changed the flexor trend towards extensor,

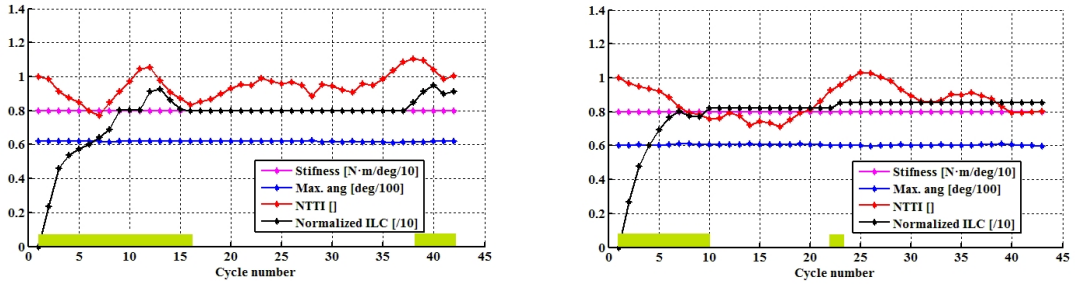

(a) Left leg.

(b) Right leg.

FIGURE 7.19: HP experiment results in cycle domain. Controller stiffness (magenta curve, $N \cdot m/deg$), NTTI (red curve), maximum angle achieved during flexion (blue curve, deg) normalized torque-time integral (red curve), and NILC (black curve) of both legs for the entire walking experiment. Green boxes shows *learning* state active. No box means *monitoring* state active. Controller stiffness, maximum angle and normalized stimulation curves are scaled for representation purposes.

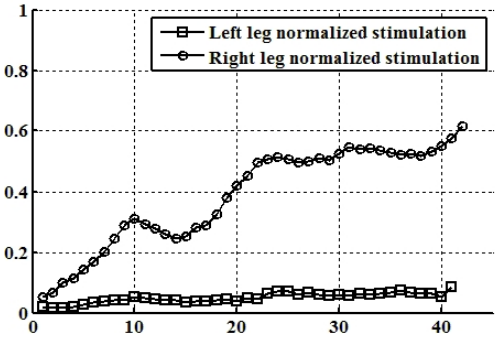

FIGURE 7.20: Normalized quadriceps stimulation during stance for HP experiment. Data from both legs.

in attempt to reduce the foot clearance, similarly to patient 1 walking strategy. Likewise, the actions provided by Kinesis were to increase the stimulation PD and/or the stiffness of the exoskeleton. The increase on the NTTI after the first cycles for HC and CO can be interpreted as a patient's response to Kinesis actions (both stimulation and robotic) to drive the leg through the kinematic pattern: increasing the effort to extend the leg during swing. Nevertheless, Kinesis successfully compensated these actions imposing the correct kinematic pattern. This effect was not observed in HP, probably due to a successful adaptation of the patient to Kinesis.

7.2.3 Case study 3.

Patient 3 is a male of 40 y.o., 70 kg. and 1.8 m. height. He suffered an accident resulting in a vertebral traumatism, with fracture of the L1 vertebrae and posterior displacement of L1 over D12 and fractures of left L2 and right L1, L2 and L3 apofisis. He was operated for artrodesis between T11 and L3. The diagnose was a SCI at L1 level, AIS A, with partial motor preservation at L3 level, and partial sensitive preservation at L4 level. This lesion represents the most impaired functional condition that meet the inclusion criteria. In contrast to patients 1 and 2, this patient had no volitional control over the knee flexor muscles, and some degree of voluntary activation

of the extensor muscles, although it did not enable the patient to extend the knee. Hip flexion ability was partially preserved for the right side, whereas the left was poorly preserved.

During the stimulation test, it was observed that the stimulation was ineffective for generating force with left flexor muscles, and almost ineffective for the right leg flexion muscles (table 7.4). The patient was required to walk between parallel bars, instead of using a walker, given the patient's functional status.

TABLE 7.4: Stimulation test results for patient 3: maximum force-time integral achieved (absolute and normalized by patient's leg weight). Stimulation PD was set to 450 μs, train frequency to 70 Hz, pulse train duration 14 sec. and duty cycle 43%.

Movement direction	Left leg	Right leg
Extension	16 N (38%)	40 N (95%)
PA	78 mA	52 mA
Flexion	0 N (0%)	8 N (19%)
PA	82 mA	62 mA

7.2.3.1 Hybrid-cooperative control of walking (HC).

Knee kinematics, interaction forces and flexor muscles stimulation for HC experiment are shown in figure 7.21. The long stance intervals correspond to the time intervals when the patient reached the extreme of the walkway created with the bars. Hence the parallel bars were displaced while the patient remained standing, to create a new walkway and continue the walking experiment.

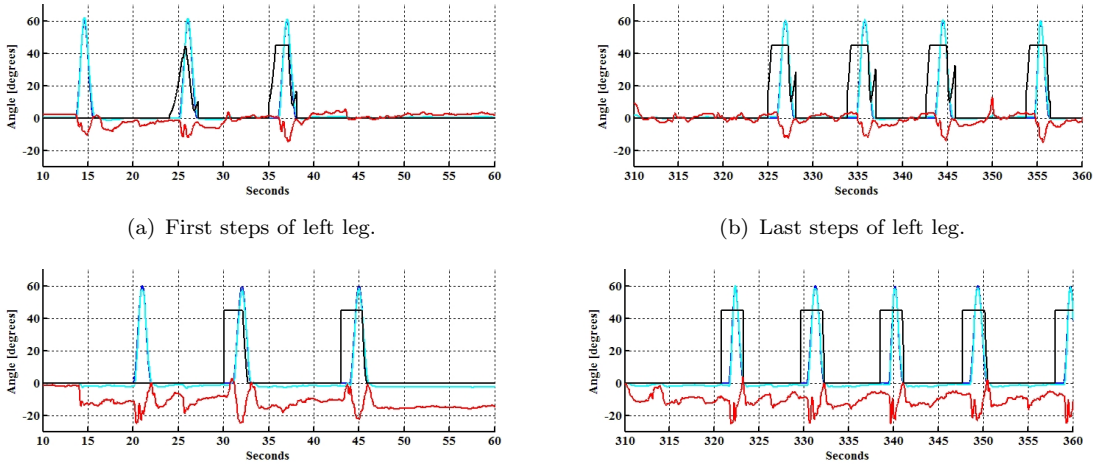

(a) First steps of left leg.

(b) Last steps of left leg.

(c) First steps of right leg.

(d) Last steps of right leg.

FIGURE 7.21: Pattern (blue curve, *deg.*) and actual (light blue curve, *deg.*) knee kinematics, interaction (red curve, $N \cdot m/deg$) and stimulation (black curve, μs, ILC only showed) for HC.

Interaction forces for the left leg were of low magnitude during stance, whereas for the right leg were extensor during the whole gait cycle (figure 7.21). Stimulation of flexor muscles exhibited a saturated pattern from the first cycles the swing phase (black curve).

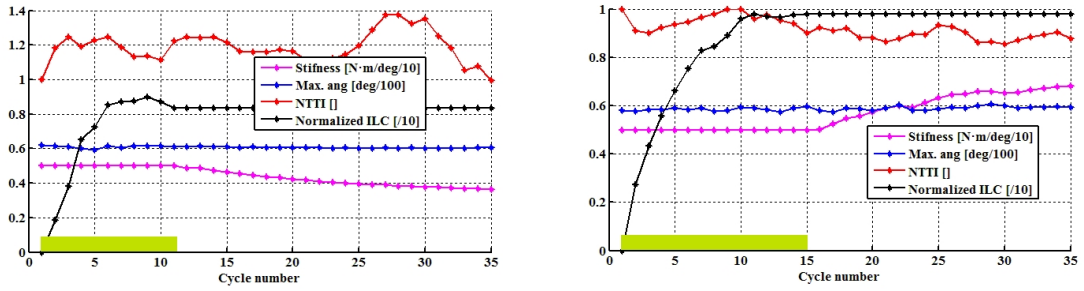

(a) Left leg.

(b) Right leg.

FIGURE 7.22: HC experiment results in cycle domain. Controller stiffness (magenta curve, $N \cdot m/deg$), NTTI (red curve), maximum angle achieved during flexion (blue curve, deg) normalized torque-time integral (red curve), and NILC (black curve) of both legs for the entire walking experiment. Green boxes shows *learning* state active. No box means *monitoring* state active. Controller stiffness, maximum angle and normalized stimulation curves are scaled for representation purposes.

This was also observed in the cycle domain, where the NILC for the right leg after the first learning period reached close to the 100% of the maximum achievable stimulation (figure 7.22(b)). The NTTI shows a slow decrease (red curve) after cycle 10. Interestingly, during the monitoring period the stiffness increased (magenta curve).

Regarding left leg (figure 7.22(a)), after the learning period the stimulation intensity was lower than for the right leg (85% of the maximum achievable intensity, black curve), and the NTTI appears to vary randomly around the 1.2 in average (red curve). The stiffness decreased at a slow pace during the monitoring period.

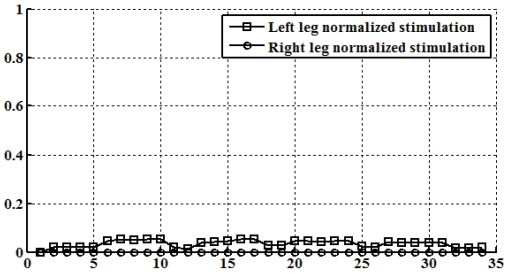

FIGURE 7.23: Normalized quadriceps stimulation during stance for HC experiment. Data from both legs.

Average quadriceps stimulation during the stance phase was ineffective (figure 7.23) for both legs. Particularly the stimulation for the right leg was zero due to the extensor interaction forces during stance.

7.2.3.2 No stimulation, cooperative control of walking (CO).

Results from this experiment are shown in (figure 7.27). These results are similar to the HC experiment, except for the absence of stimulation for the knee flexor muscles.

The cycle domain results presented in figure 7.25 are similar to the results obtained for HC experiment. In this configuration, the stiffness for the left leg (figure 7.25(a), magenta curve)

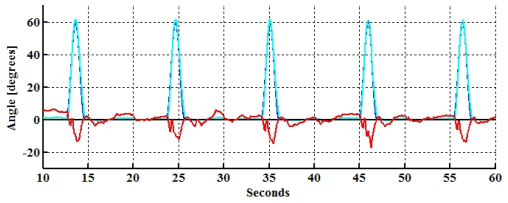

(a) First steps of left leg.

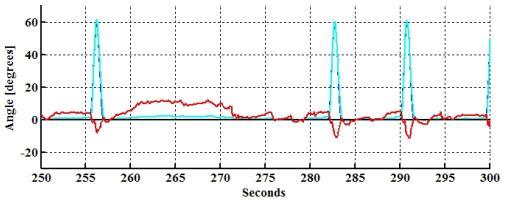

(b) Last steps of left leg.

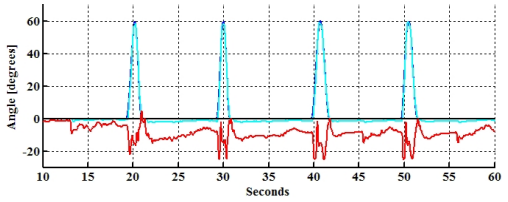

(c) First steps of right leg.

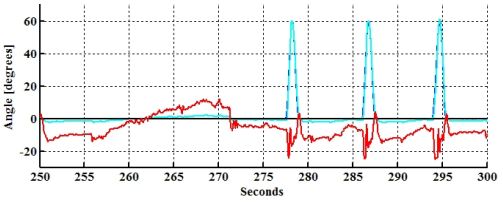

(d) Last steps of right leg.

FIGURE 7.24: Pattern (blue curve, *deg.*) and actual (light blue curve, *deg.*) knee kinematics, interaction (red curve, $N \cdot m/deg$) and stimulation (black curve, μs, ILC only showed) for CO.

decreased, thus indicating that the leg could be successfully driven with less contribution from the exoskeleton. However, the NTTI values did not decreased, indicating that the patient did not contributed voluntary to the movement (red curve). Regarding the right leg (figure 7.25(b)), as noticed in the HC experiment, the extensor interaction forces during swing were counterbalanced by the CO by increasing the stiffness (magenta curve), in order to achieve 60 degrees of knee flexion (blue curve). The NTTI increased for the first 6 cycles, and decreased for the remaining experiment.

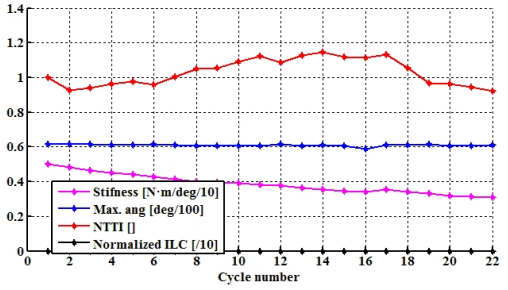

(a) Left leg.

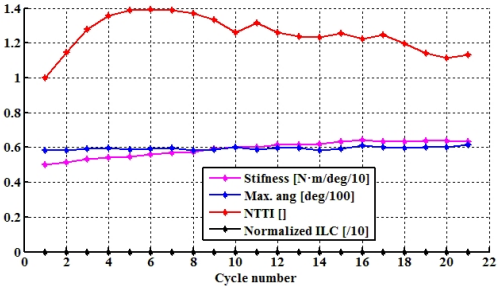

(b) Right leg.

FIGURE 7.25: CO experiment results in cycle domain. Controller stiffness (magenta curve, $N \cdot m/deg$), NTTI (red curve), maximum angle achieved during flexion (blue curve, *deg*) normalized torque-time integral (red curve), and NILC (black curve) of both legs for the entire walking experiment. Green boxes shows *learning* state active. No box means *monitoring* state active. Controller stiffness, maximum angle and normalized stimulation curves are scaled for representation purposes.

Regarding quadriceps normalized stimulation (figure 7.29), the results are similar to the obtained for HC experiment, although a linear increase on the left leg normalized stimulation can be observed.

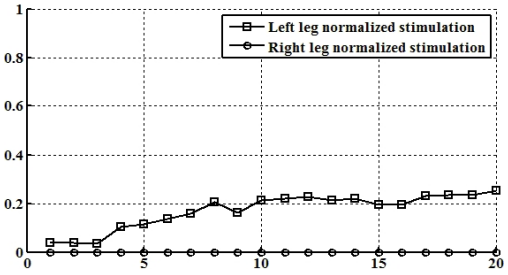

FIGURE 7.26: Normalized quadriceps stimulation during stance for CO experiment. Data from both legs.

7.2.3.3 Hybrid-stiff control of walking (HP).

The results from this configuration experiment showed in (figure 7.27) are similar to HC and CO experiments.

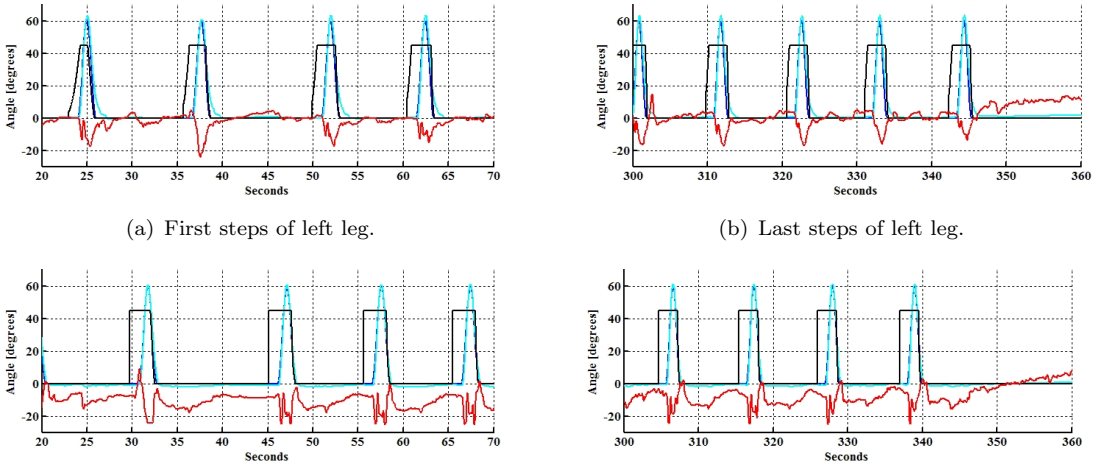

(a) First steps of left leg.

(b) Last steps of left leg.

(c) First steps of right leg.

(d) Last steps of right leg.

FIGURE 7.27: Pattern (blue curve, *deg.*) and actual (light blue curve, *deg.*) knee kinematics, interaction (red curve, $N \cdot m/deg$) and stimulation (black curve, μs, ILC only showed) for HP.

Results from left leg are similar to the HC experiment (figure 7.28(a)). Although the stimulation was also intense (80% of the maximum achievable stimulation intensity), the NTTI increased for the first half of the experiment. Similarly to the HC experiment, this behavior could not be attributed to any muscular action, neither vountary or artificially induced by the stimulation.

Regarding the right leg (figure 7.28(b)), the stimulation reached a 90% of the maximum achievable stimulation. There was an initial plateau for the NTTI (red curve, cycles 1 to 6), and a progressive decrease was observed until the end of the experiment.

The normalized quadriceps stimulation for this experiment is shown in (figure 7.29). The results are similar to the obtained for HC and CO experiments.

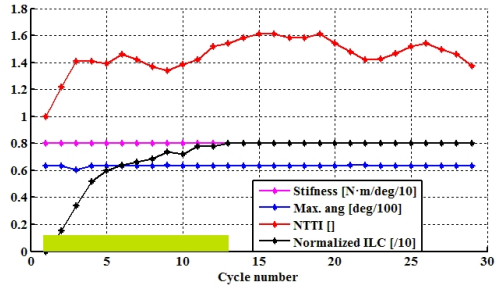

(a) Left leg.

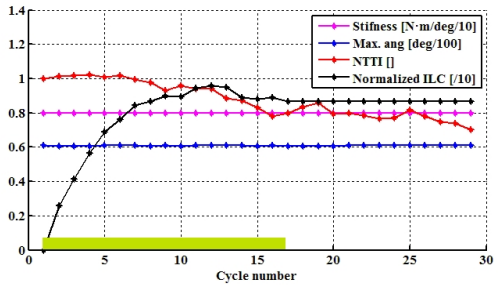

(b) Right leg.

FIGURE 7.28: HP experiment results in cycle domain. Controller stiffness (magenta curve, $N \cdot m/deg$), NTTI (red curve), maximum angle achieved during flexion (blue curve, deg) normalized torque-time integral (red curve), and NILC (black curve) of both legs for the entire walking experiment. Green boxes shows *learning* state active. No box means *monitoring* state active. Controller stiffness, maximum angle and normalized stimulation curves are scaled for representation purposes.

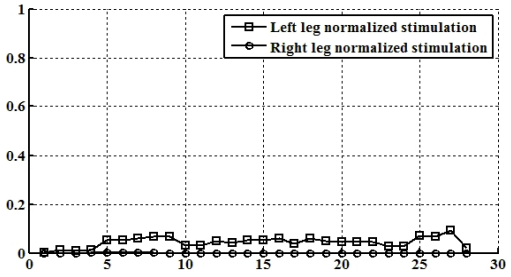

FIGURE 7.29: Normalized quadriceps stimulation during stance. Data from both legs.

7.2.3.4 Discussion

The muscular condition of patient 3 was the most impaired among the patients presented in this dissertation. Among patient's legs, the left one had worse status than the right one, as verified at the stimulation test (table 7.4), specially for the flexor muscles, where the stimulation had no effect at all. On the other hand, this patient was taught to walk and stand in a hyper-extension pattern, a commonly paraplegic walking technique, to ensure safe passive stance. This extension pattern was stronger for the right leg, due to the better muscular status, which also influenced Kinesis control actions.

As shown in all three experiments, the hybrid exoskeleton successfully compensated these functional deficits to achieve walking. The right leg extension pattern had to be compensated by increasing the stimulation (HC and HP) and also increasing the exoskeleton stiffness (HC and CO). In the case of the left leg, the stimulation did not have effect, and thus the leg had to be passively driven. As a consequence, the interaction forces resulted only from weight and inertia. System's response there was to decrease the stiffness of the robotic exoskeleton for HC and CO due to the low inertia of the leg.

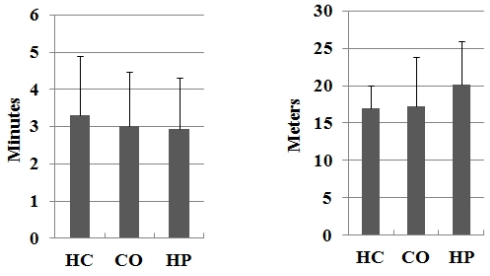

(a) Time to cover first 10 meters (10mWT).

(b) Distance covered in 6 minutes (6mWT).

FIGURE 7.30: Results for 10mWT and 6mWT tests for HC, CO and HP. Data are mean±SD.

7.2.4 Immediate effects of hybrid walking

Figure 7.30 shows the group-average results for the 10mWT and the 6mWT for each tested configuration. It is noticeable an improvement on both test along experiments (table 7.5). Note that the experiments are shown following temporal order. A learning effect of successive testing could influence these results. Compared with the healthy subject test for HC configuration (table 7.5), patients needed less time to cover 10 meters (healthy group: 4.1±1.4 min.; patient group: 3.3±1.6 min.), and walked more distance in 6 minutes (healthy group: 15.4±5.0 m.; patient group: 17.0±20.2 m.). The superior performance exhibited by the patients could be influenced by the more skillful using the walker, and the preliminary training session.

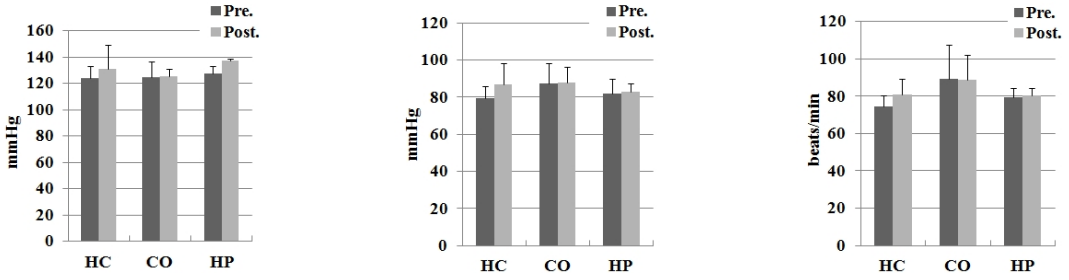

(a) Systolic BP previous and after testing for each configuration.

(b) Diastolic BP previous and after testing for each configuration.

(c) HR previous and after testing for each configuration.

FIGURE 7.31: Physiological effort previous and after testing for each configuration. Data are mean±SD.

Regarding the physiological effort (figure 7.31, table 7.5), the configurations with stimulation, HC and HP, showed an increase in the systolic and diastolic BP after the experiment. The HR after only increased for HC experiment. An excessive time elapsed in recording the HR after the HP experiment for one of the patients could allowed for recovering the HR, affecting the results.

Subjective perception of fatigue and pain were rated under the 50% of the scale for all configurations tested (figure 7.32(a), table 7.5). Greater relative increments for fatigue and pain were found for HC and HP (table 7.5). Interestingly, patients consistently rated lower previous fatigue along experiments (figure 7.32(a). HC=10.0±1.0 mm, CO=8.0±13.0 mm, HP=1.0±1.7 mm). The configurations with stimulation were rated as the less comfortable (figure 7.32(c), table 7.5).

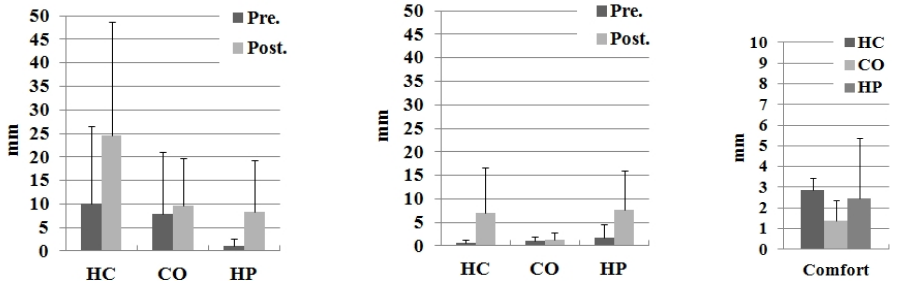

(a) Previous and posterior VAS score for fatigue.

(b) Previous and posterior VAS score for pain.

(c) VAS score for comfort.

FIGURE 7.32: VAS scores for pain, fatigue and comfort for each configuration tested. Data are mean±SD.

Figure 7.33 and table 7.5, shows the group-averaged response to the QUEST questionnaire[5] and the additional items introduced[6], for each tested configuration, and the average for all configurations. Item A was not answered by any patient, as they did not perceived spasticity during the use. Overall, the items received high scores. The lowest scores were assigned to *weight* and *comfort* (3 over 5), whereas *safety*, *durability* and *efficacy* were top rated, as well as *breath difficulty* and *control sensation*. These results indicate that the users positively perceived utility of the system in providing walking therapy.

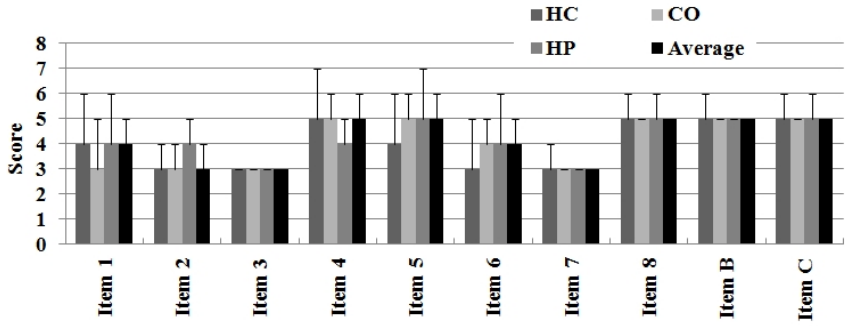

FIGURE 7.33: Scores for QUEST questionnaire and the additional items. Data are median±range.

7.2.5 Impact of hybrid walking on patient's gait function

This section presents the results from the walking test and the assessment of lower limb muscle strength and spasticity. As was described in section 7.1.1, these tests are aimed to assess gait functionality, and were carried out prior, after, and one week after (I, II and III in the figures) the intervention week (figure 7.1). The results are presented in terms of relative changes on variables. It is recalled here that the walking tests were performed with diverse level of support (patient 1 and 2 no external aids, patient 3 used a walker).

Figure 7.34 and table 7.6 show the relative changes on the time needed to reach 10 meters, and the distance covered in 6 minutes. The patients improved after week *I-II*, as they needed

[5]The description of each item is showed in section 6.2
[6]The description of each item is showed in section 7.1.1

TABLE 7.5: Experimental results for HC, CO and HP experiments: 10mWT and 6mWT tests and subjective scales. Data provided for fatigue, pain, BP and HR are pre-post relative increment. Data are mean±SD and median±range for QUEST items.

	Healthy group	HC	CO	HP
10mWT [min.]	4.1±1.4	3.3±1.6	3.0±1.5	2.9±1.4
6mWT [m]	15.4±5.0	17.0±20.2	17.3±6.6	20.2±5.8
Systolic BP [mmHg]	Not evaluated	6.7±20.8	0.7±24.2	9.7±18.1
Diastolic BP [mmHg]	Not evaluated	7.3±15.0	0.3±19.5	1.0±7.3
Hear rate [beat/min.]	Not evaluated	6.0±14.6	-0.3±10.4	0.7±3.7
Pain [cm]	Not evaluated	6.3±17.3	0.33±1.7	6.0±13.0
Comfort [cm]	4.6±1.8	2.9±2.1	1.4±1.9	2.5±1.9
Fatigue [cm]	5.2±1.1	14.7±50.5	1.67±6.4	7.3±18.2
QUEST Item 1	4.0±0.0	4.0±2.0	3.0±2.0	4.0±2.0
QUEST Item 2	3.5±1.3	3.0±1.0	3.0±1.0	4.0±1.0
QUEST Item 3	4.0±0.3	3.0±0.0	3.0±0.0	3.0±0.0
QUEST Item 4	3.0±0.5	5.0±2.0	5.0±2.0	4.0±1.0
QUEST Item 5	4.0±0.5	4.0±2.0	5.0±1.0	5.0±2.0
QUEST Item 6	4.0±0.5	3.0±2.0	4.0±1.0	4.0±2.0
QUEST Item 7	3.0±0.5	3.0±1.0	3.0±0.0	3.0±0.0
QUEST Item 8	Not answered	5.0±1.0	5.0±0.0	5.0±0.0
Item A	Not answered	Not answered	Not answered	Not answered
Item B	Not evaluated	5.0±1.0	5.0±0.0	5.0±0.0
Item C	Not evaluated	5.0±1.0	5.0±0.0	5.0±1.0

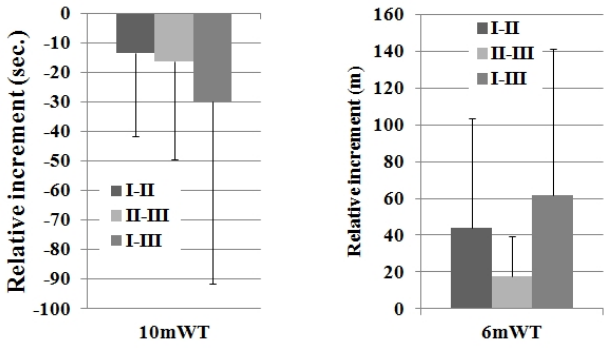

(a) Time needed to walk 10 meters (10mWT).

(b) Distance covered in 6 minutes (6mWT).

FIGURE 7.34: Results for 10mWT and 6mWT walking tests. Data are mean±SD.

less time to complete 10 meters (figure 7.34(a)), and covered more distance in 6 minutes (figure 7.34(b)). One week after completing the protocol, the patients further improved on these tests (*II-III*), but this increment was smaller than for the week *I-II*. The improvement of the week *I-II* was observed added to the improvement of week *II-III* in the final evaluation (*I-III*).

TABLE 7.6: Results for 10mWT and 6mWT tests. Data are mean±SD.

	I-II	II-III	I-III
10mWT [sec.]	-13.6±28.2	-16.2±33.5	-29.8±61.7
6mWT [m]	44.2±59.3	17.8±21.4	62.0±79.6

Figure 7.35 and table 7.7 shows the MMT scores for hip, knee and ankle joints in the sagittal plane. The highest increments on hip MMT score were found for the *I-II* week, which lasted for the *I-III* week (figure 7.35(a), table 7.7). The exoskeleton dose not have hip joint, thus there was no action over the hips. The increase on hip MMT can be attributed to the effort needed to move the extra weight of the exoskeleton. As shown in the figure, a greater impact on flexor muscles than on extensor is observed. It is hypothesized that the effort to extend the hip was lower as result of the passive hip extension produced as consequence of contralateral leg flexion combined with trunk forward lean.

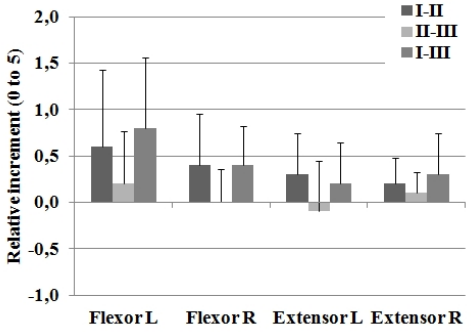

(a) Sagital MMT score for hip joints.

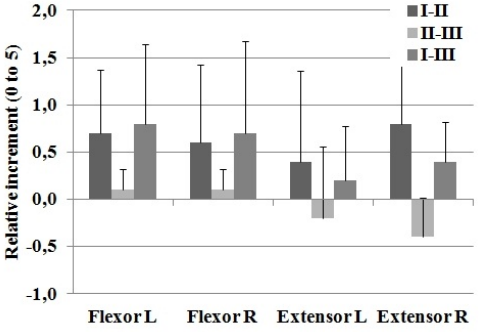

(b) Sagital MMT score for knee joints.

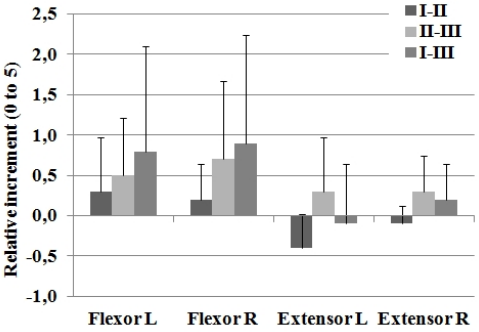

(c) Sagital MMT score for ankle joints.

FIGURE 7.35: Sagital MMT score for the lower limb joints. Scale ranges from 0 to 5. Data are mean±SD.

Regarding the knee MMT score (figure 7.35(b), table 7.7), high increments were observed for both flexor and extensor muscle groups. As in the case of the hip joint, an increment in the

MMT score was observed for week *I-II* for both extensor and flexor muscle groups. In the case of the extensor muscles, the increment was higher than observed in week *II-III*, whereas for the flexor muscle group, a relative decrement on MMT score was observed for this week. The higher increments obtained for week *I-II* are related to the use of Kinesis, specifically the stimulation. Contrary to the hip joint, the knee joint was driven by Kinesis during walking in a hybrid approach. It should be noted that if the knee were passively driven by the exoskeleton, no increments on knee muscular MMT would be obtained. Interestingly, the patients experienced a decrement on the flexor MMT score during week *II-III*. This decrement may be attributed to discontinuing on the use of Kinesis, because flexor muscles were less demanded during usual rehabilitation exercises. As consequence, the increment on the extensor MMT score was not sustained at week *II-III*.

TABLE 7.7: Incremental change in the sagital MMT score for the lower limbs. Scale ranges from 0 to 5. Data are mean±SD.

	I-II	II-III	I-III
Left hip flexor	0.60±0.82	0.20±0.57	0.80±0.76
Right hip flexor	0.40±0.55	0.00±0.35	0.40±0.42
Left hip extensor	0.30±0.45	-0.10±0.55	0.20±0.45
Right hip extensor	0.20±0.30	0.10±0.22	0.30±0.45
Left knee flexor	0.40±0.96	-0.20±0.76	0.20±0.57
Right knee flexor	0.80±0.84	-0.40±0.42	0.40±0.42
Left knee extensor	0.70±0.67	-0.10±0.22	0.80±0.84
Right knee extensor	0.60±0.82	0.10±0.22	0.70±0.97
Left ankle flexor	-0.40±0.42	0.30±0.67	-0.10±0.74
Right ankle flexor	-0.10±0.22	0.30±0.45	0.20±0.45
Left ankle extensor	0.30±0.67	0.50±0.71	0.80±1.30
Right ankle extensor	0.20±0.45	0.70±0.97	0.90±1.34
Left leg score	1.20±1.15	1.10±1.88	2.30±2.56
Right leg score	1.10±1.24	1.10±1.52	2.20±2.61

Finally, regarding the ankle joint (figure 7.35(c) and table 7.7), flexor muscles score increased after *I-II* and *II-III* weeks, and the increment remained one week after (week *I-III*). Interestingly, the increments were higher for the no-intervention week (*II-III* versus *I-II*). A decrement on the MBS of the ankle extensor muscles was observed after the *I-II* intervention week, and an increment after the *II-III* non-intervention week (figure 7.35(c) and table 7.7). An hypothesis for this finding is that the spring-driven ankle actuator of the exoskeleton, which supported the foot during the swing phase, could have reduced the ankle extensor muscle ability. This phenomena have been described previously in experiments with healthy subjects walking with a pneumatic KAFO-type exoskeleton [287]. Nevertheless, other variables not related to the study may have influence on these results.

A further interesting finding was the increase on the knee extension range of movement of patient 2 (table 7.8).

Figure 7.36 shows the relative changes in the ASWORTH and PENN spasticity indexes. As shown in the figure, relative decrements on the indexes were obtained after week *II* (Asworth: -0.2±0.4; PENN: -0.4±0.5) while no changes were observed after week *III*.

TABLE 7.8: Articular knee joint range of movement for patient 2 after week *I-II*.

Movement direction	Left leg	Right leg
Extension	10 deg.	5 deg.
Flexion	110 deg.	120 deg.

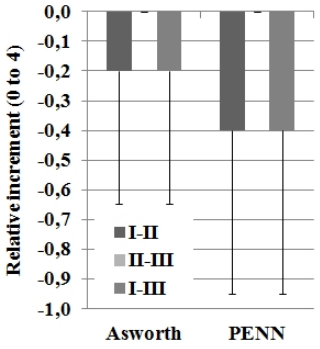

FIGURE 7.36: Results for spasticity ASWORTH and PENN scales. Score can range from 0 to 4. Data are median±range.

7.3 Discussion

The hybrid walking therapy delivered with Kinesis was tolerated by the patients; no adverse effects were produced and the physical demand was tolerable. The patients were able to complete 6 minutes of walking with the system after one day of practice. The improvement in the 6mWT, the 10mWT, lower limb MMT and spasticity indexes demonstrate that walking function of the patients improved after participating in the validation study. The controller of Kinesis adapted to patient residual function during walking, modulating stimulation and robotic assistance.

Comparing the three configurations tested, it was observed that the presence of the stimulation increased physical demand as measured by BP and HR (HC and HP versus CO). Surprisingly, one study that compared the physical demand between hybrid walking and robotic-only walking showed that robotic-only walking demanded higher effort to the patient than hybrid walking [67]. However, this study only reported a case study, and no further discussion of this finding was provided. Interestingly, the physical demand of hybrid walking observed with Kinesis was similar to the one reported for passive walking with the Rewalk [80, 81]. This can be attributed to the differences on patient characteristics. In [80,81], patients were complete thoracic SCI. Compared with the patients participating in the protocol presented in this chapter, the greater effort to be perform with the upper limbs for walking with crutches, and the more impaired cardiovascular autonomic response as consequence of the lesion, could explain the equivalence on the physical demand.

Regarding perceived pain, fatigue and comfort, the stimulation led to higher scores (HC and HP), although the scores were lower than 50 mm (half of the scale), indicating patient's tolerance to the hybrid walking therapy. The literature pertaining hybrid exoskeletons reviewed in chapter 2 showed that these important aspects were not explicitly evaluated. However, different authors

claimed that "the patients did not reported pain" [172], or "improved feeling of safety" by the patients [67]. Comparing with the perception of robotic-assisted walking [80, 81], the results presented here are similar for pain, whereas fatigue rated lower. Again, the more physically impaired patients participating in [80, 81] can explain these differences. On the other hand, subjective opinion regarding Kinesis use was similar to the results reported for Rewalk, although direct comparison can only be made for items 3, 4, 6, 7, B and C [80]. The lowest scores were obtained for items related to weight, comfort and adjustability, a drawback shared with current lower limb wearable robots. Further developments shall optimize the ergonomics of the exoskeleton.

One of the main achievements of these experiments was the fact that the patients were able to use the system after one day of practice. Nonetheless, although subsequent learning effects were noticed among experiments. This is significantly lower than the 25 days (average) needed by the patients to achieve autonomous use of Rewalk for similar period of time (5 to 10 min.) [80, 81]. However, there are several differences between Kinesis and Rewalk systems and protocols that hamper direct comparison. First, Rewalk training sessions aimed the patients to learn several skills apart from walking: sitting up and down, and walking up and down stairs. Second, Rewalk walking is semi-automatic, where the patient triggers walking initiation and stop tilting the trunk. With this sort of automatic walking, the patient needed to learn how to be passively driven by Rewalk, maintaining balance with the help of walking crutches. In the case of Kinesis, the patient triggers each step whenever he/she is stable and ready to take it, and moreover, the walker provided a more stable support than crutches during movement. These key differences are reflected comparing the results for 10mWT and 6mWT walking test between both devices: Kinesis led to double time to walk 10 meters, and half distance covered in 6 minutes than Rewalk. In spite of this apparent lack of performance, Kinesis sequentially triggered walking allowed the patients to use the system early at first training session, which brings the hybrid therapy early to the patient, avoiding long training periods as reported for using NP for walking [161]. Nevertheless, improved capabilities for semi-automatic control of walking are needed in order to allow the patients to interface more naturally with the system's controller, and thus increase the capabilities of the system for functionally compensate walking function. This semi-automatic walking control approach was recently proposed for use within the Vanderbilt hybrid exoskeleton, although there are not published data yet regarding its performance for control of hybrid walking [190, 288].

The AAN capabilities of Kinesis are beyond the control approaches for hybrid walking found in the literature pertaining hybrid exoskeletons. Regarding control of the NP, the proposed dual controller allowed to adapt the stimulation patterns to the functional ability of the patients while monitoring muscle performance. A recently proposed hybrid controller features an approach similar to the ILC controller proposed in this dissertation, but was only tested during lifting task with one SCI patient [191]. The dual stimulation controller of Kinesis allowed to stimulate both flexor and extensor knee muscles regarding gait phase and the specific functional deficit of the patient. This originated customized stimulation patterns for each leg of the patients. The patterns varied from no stimulation (patient 1, HP, left leg) to maximum stimulation (patient 3, HC and HP). Stimulation of knee extensor muscles also adapted to the specific functional need during stance phases of gait, although stimulation intensities were low to produce muscular contraction except for patient 2, where quadriceps muscles were highly stimulated regarding the right leg flexor trend during stance. These results reveal the importance of closed-loop control of

stimulation as a means to stimulate the muscles from a functional standpoint. However, closed-loop control of stimulation does not adequately manages the relationship between stimulation intensity and force production. As described above, for several experiments the stimulation was unlikely to produce any muscular contraction for normalized stimulation intensity typically under 20%. Moreover, the opposite case was also noticed in several experiments, where a saturated output of the NP controller did not produced muscle contraction (patient 3, flexor muscles of left leg). Both effects were derived from controller design, which did not take into account the non-linear relationship between muscle stimulation and force production. Incorporating this characteristic in the controller design would provide an criteria for more efficient modulation of the stimulation amplitude regarding minimum and maximum muscle activation.

Regarding the exoskeleton control, only the Vanderbilt [189] and the HAS [67] exoskeletons were equipped with compliant joint control. To the author's knowledge no studies have been reported on modulation of exoskeleton assistance during walking for SCI users. The study presented in this chapter reveals the interplay between the AAN capabilities of Kinesis and the voluntary actions of the patient, through the comparative analysis of the three configurations tested. All three configurations managed successfully the specific walking impairment for each leg of the patient, although key differences were noticed among them. With the CO, the stiffness was modulated after the first step as a consequence of patient's leg impairment (patient 1, left leg, patient 2, right leg, patient 3, both legs). These modulations were not produced until the first learning period with HC, neither with HP. Further developments will have to address the modulation of the robotic assistance simultaneously with stimulation modulation, for example based on impedance control schemes for exoskeleton control. From direct comparison within HC and HP, no major differences were observed, neither in the cycle-domain variables nor in the immediate walking impact. This similarity is consequence of the configuration equivalence for the first HC learning period and the HP; during learning, Kinesis drives the patient's leg inside a stiff force field, similarly to HP. On the other hand, the main reason for developing a compliant control of the robotic exoskeleton, was to allow the patient to deviate from the kinematic trajectory and thus reduce exoskeleton assistance. From comparison of HP with HC and CO, increased interaction forces were expected with the HP, that is, greater NTTI. That was not the case for the left leg of patient 1, which was fully functional during walking, comparing HP versus HC and CO. However, it was the case for the left leg of patient 2, in a more impaired condition. Therefore no conclusions can be made about the effect of the compliant controller of the robotic exoskeleton on the leg-exoskeleton physical interaction, and further specific studies are needed.

Muscle fatigue estimation has been addressed by off-line methods, such as the isometric recruitment curve [172]. This method is performed offline, thus the walking therapy have to be interrupted for obtaining the fatigue estimation. The online MFE integrated within Kinesis allowed not only to estimate muscle performance during walking, but assessing system behavior and adaptations between the patient and the system. Furthermore, monitoring the leg-exoskeleton physical interaction is feedback for modulating the configuration of the hybrid controller. The application of the muscle fatigue management strategy proposed in chapter 4 delays muscle fatigue. However, the results obtained from the experiments presented in this chapter indicates that the voluntary leg movements influence the physical interaction, hence the accuracy of fatigue estimation. There were two mechanism that had impact on the physical interaction: 1) the varying force voluntary exerted by the patient, which could not be ensured to be constant throughout the experiment. In this case, patient slacking would led to false detection of muscle fatigue. 2) the normalization of the FTI values, where the FTI value from the first step is taken

to normalize the following FTI. In this case, the first step could not belong to the further stationary steps sequence, and thus mislead the normalization of the FTI. This could be the case for the right leg of patient 1 in the CO experiment (figure 7.7(b)), and/or the right leg of patient 2 for the HC experiment (figure 7.13(b)). Therefore, more robust methods to uncouple patient contribution to the movement from stimulated muscle performance and robot contribution to the movement are needed to better manage muscle fatigue, maximize patient voluntary contribution, and thus modulate robotic and stimulation assistance.

A further contribution of this chapter to the field of hybrid exoskeletons is the assessment of the impact of the hybrid walking therapy on patient walking abilities. The assessment of Kinesis as a tool for treatment of walking function was therefore revealed. Greater improvements in gait function, sagital MMT score, and spasticity, for the intervention week *I-II* were concluded with the observation week *II-III*. However, there are several limitations for interpretation and discussion with literature. Firstly, the patient sample size was small with heterogeneous lesions, which obviously limits generalization of these results. Secondly, there were mixed effects from each of the three configurations tested and the stimulation test, which also limits linking the improvements to any of the experiments made. Lastly, the extra rehabilitation time that represented all the experiments underwent by the patients was not controlled between weeks, and further limits data interpretation. Other limitations include the non-randomized testing order of configurations, which led to learning effects as discussed above, and the non-blinded evaluation of patient's muscular balance score. Nevertheless, these findings encourages further research about the effects of hybrid walking therapy on motor-incomplete SCI patients.

7.4 Conclusion

The hybrid walking therapy delivered with Kinesis was tolerated by the patients; no adverse effects were produced and the physical demand was tolerable. The patients were able to complete 6 minutes of walking with the system after one day of practice. Mutual adaptations occurred between Kinesis and the patient which were assessed through physical leg-robot interaction. The cooperative control approach adapts both stimulation and robotic assistance to specific functional deficits and voluntary actions during walking. The improvement in the 6mWT, the 10mWT, lower limb MMT and spasticity indexes demonstrate that walking function of the patients improved after participating in the validation study. Results shows that hybrid walking therapy holds potential for rehabilitate walking in motor incomplete SCI patients, guaranteeing further research on this topic. Besides, from these results further work is envisioned regarding several aspects of hybrid walking control: stimulation control based on muscle activation estimate, improved semi-automatic control of walking, and improved muscle fatigue monitoring.

7.4.1 Answer to research questions

This chapter provides provides answer to the remaining research question stated in section 1.6.2 as follows:

Q10: **What is the impact of hybrid walking therapy on SCI patients?** Hybrid walking therapy is tolerated by patients, while the hybrid-cooperative control approach adapt

system's actions to patient walking ability. Furthermore, hybrid walking therapy has shown a positive impact on patient's walking function. These results supports further research focused on patient impact of hybrid walking therapy.

Chapter 8

Summary, conclusions, and future work

In paraplegic individuals with upper motor neuron lesions the descending path for signals from central nervous system to the muscles are lost or diminished. Motor NP based on electrical stimulation can be applied to induce restoration of motor function in paraplegic patients. Furthermore, electrical stimulation of such motor NP can be more efficiently managed and delivered if combined with powered exoskeletons that compensate the limited force in the stimulated muscles and bring additional support to the human body. Such hybrid overground gait therapy is likely to be more efficient to retrain the spinal cord in incomplete injuries than conventional, robotic or NP approaches. However, the control of bilateral joints is difficult due to the complexity, non-linearitly and time-variance of the system involved. Also, the effects of muscle fatigue and spasticity in the stimulated muscles complicate the control task. Furthermore, a compliant joint actuation is required to allow for a cooperative control approach that is compatible with the AAN rehabilitation paradigm.

These were direct motivations for this research. The overall aim was to generate the necessary knowledge to design a novel hybrid walking therapy with fatigue management for incomplete spinal cord injured subjects. Specifically, the goal was to establish the required methods and (hardware and software) systems that are required to proof the concept with a pilot clinical evaluation.

The analysis of the state-of-the-art in hybrid exoskeletons provided information regarding design requirements and specific challenges that are addressed in this dissertation (chapter 2, Q1). From this analysis, the criteria for assessing the impact of the hybrid walking therapy on SCI patients was established (chapter 2, Q2).

The group of patients with incomplete SCI that can benefit from hybrid walking therapy was identified from a clinical perspective (chapter 3, Q3). The functional characteristics of the target population were added to the technical requirements for designing a lower limb robotic exoskeleton (Kinesis). A key feature of Kinesis is the ability of monitoring leg-robot physical interaction for: 1) to assess muscle performance (chapter 3, Q5), and 2) to provide compliant control of walking (chapter 3, Q7).

An experimental study determined the feasibility of detecting significant changes in muscle performance, by measuring the average joint torque produced by stimulated muscles. Quantitative criteria was obtained for detection of muscle fatigue in knee extensor and flexor muscle groups (chapter 4, Q4). Furthermore, the technique to monitor and detect muscle fatigue during dynamic gait by means of wearable force sensing solutions was established (chapter 3, Q5). A second experimental study was conducted to provide a specific strategy for muscle fatigue management compatible with the hybrid control of walking (chapter 4, Q6).

A tailored closed-loop NP control strategy was developed regarding the biomechanical role of the knee joint during walking and the presence in parallel of the robotic exoskeleton. The resulting NP controller is comprised by two architectures operating in parallel: a PID for extensor muscle control, and a ILC for flexor muscle control (chapter 5, Q8). Experiments with healthy subjects were conducted in order to characterize the controllers and obtaining general configuration rules. This reduced the set-up time during the walking experiments.

A novel design was developed for implementing hybrid-cooperative control of walking. The hybrid controller is comprised by two sequential FSM (c-FSM), one for each leg, coordinated by a FSM that controls walking events and states (t-FSM). Each c-FSM operates within the cycle domain. This design allowed for: 1) adapts stimulation patterns to the user, 2) modulate exoskeleton assistance, and 3) uncouple closed-loop control of the NP and monitoring muscle performance. An experimental study conducted with four healthy subjects validated the hybrid control approach and its adaptability features (chapter 6, Q9).

A pilot clinical evaluation with SCI patients was conducted in order to assess the impact of the hybrid walking therapy. Results demonstrate that: 1) the hybrid controller adapts to patient residual function during walking, 2) the therapy is tolerated by patients, and 3) the walking function of the involved patients improved after participating in the study (chapter 7, Q10).

8.1 Conclusions of the dissertation

The main conclusions attained from this dissertation are the following:

1. The AAN approach implemented within hybrid-cooperative controller modulates the neuroprosthetic and robotic contributions to the movement, adapting to the abilities of the patient.
2. The neuroprosthetic dual closed-loop controller adapts the stimulation patterns to the patient and regarding the functional task.
3. Monitoring leg-robot physical interaction while providing hybrid walking therapy allows to assess the mutual adaptations between the robotic system and the patient.
4. Muscle fatigue due to stimulation can be estimated from monitoring changes in leg-robot physical interaction.
5. The hybrid walking therapy provided with Kinesis improved walking function of the patients that participated in the experiments.

8.2 Contributions of the dissertation

This dissertation has contributed to the scientific knowledge with the following:

- The first review on hybrid exoskeletal technology has been provided by this dissertation, focusing on technological and clinical aspects of hybrid walking therapy.
- The ambulatory walking exoskeleton developed in this dissertation is the first that implements stiffness control of walking for SCI patients.
- A muscle fatigue estimation criteria for knee extensor and flexor muscle groups.
- A muscle fatigue management strategy, based on muscle fatigue estimation.
- A Hybrid-cooperative control strategy that actively manages muscle fatigue, through closed-loop control of stimulation.
- The first implementation of the AAN concept for balancing stimulation and robotic assistance regarding user contribution.
- Relevant findings about the potential of hybrid walking therapy for providing a new rehabilitation intervention that will constitute the background of further clinically oriented research.

8.2.1 Publications

8.2.1.1 Journal articles

- **A. J. del-Ama**, A. D. Koutsou, E. Bravo-Esteban, J. Gómez-Soriano, S. Piazza, A. Gil-Agudo, J. L. Pons and J. C. Moreno. "A comparison of customized strategies to manage muscle fatigue in isometric artificially elicited muscle contractions for incomplete SCI subjects." *Journal of Automatic Control* (Submitted 30/08/2013).
- **A. J. del-Ama**, A. Gil-Agudo, J. L. Pons and J. C. Moreno. "Hybrid FES-Robot Cooperative Control of Ambulatory Gait Rehabilitation Exoskeleton for Spinal Cord Injured Users." *Journal of NeuroEngineering and Rehabilitation* (Submitted 01/03/2013).
- **A. J. del-Ama**, J. C. Moreno, A. Gil-Agudo, A. de-los-Reyes and J. L. Pons. "Online Assessment of Human-Robot Interaction for Hybrid Control of Walking." *Sensors*, vol. 12, no. 1, pp. 215-225, 2012.
- **A. J. del-Ama**, A. D. Koutsou, J. C. Moreno, A. de-los-Reyes, A. Gil-Agudo and J. L. Pons. "Review of Hybrid Exoskeletons to Restore Gait Following Spinal Cord Injury." *Journal of Rehabilitation Research and Development*, vol. 49, no. 4, pp. 497-514, 2012.
- J. C. Moreno, **A. J. del-Ama**, A. de-los-Reyes, A. Gil-Agudo, R. Ceres and J. L. Pons. "Neurorobotic and Hybrid Management of Lower Limb Motor Disorders: a Review." *Medical and Biological Engineering and Computing*, vol. 49, no. 10, pp. 1119-30, 2011.

8.2.1.2 Conference proceedings

- J. L. Pons, **A. J. del-Ama**, A. Gil-Agudo, and J. C. Moreno. "Combined Application of Neurorobotics and Neuroprosthetics in Rehabilitation of Spinal Cord Injury", in *11th World Congress of the International Neuromodulation Society*, 2013.
- **A. J. del-Ama**, E. Bravo-Esteban, A. D. Koutsou, J. Gómez-Soriano, S. Piazza, A. Gil-Agudo, J. L. Pons and J. C. Moreno. "Customized Strategies to Manage Muscle Fatigue in SCI Patients During Isometric FES-Driven Muscle Contractions", in *18th Annual Conference of the International Functional Electrical Stimulation Society (IFESS2013)*, 2013.
- **A. J. del-Ama**, J. C. Moreno, A. Gil-Agudo and J. L. Pons. "Hybrid FES-Robot Cooperative Control of Ambulatory Gait Rehabilitation Exoskeleton for Spinal Cord Injury Subjects," *in 2012 International Conference on Neurorehabilitation (ICNR2012): Converging Clinical and Engineering Research on Neurorehabilitation*, 2012, pp. 155-159. **Contribution selected for publication in a Special Issue of the Journal of NeuroEngineering and Rehabilitation.**
- **A. J. del-Ama**, E. Bravo-Esteban, J. C. Moreno, J. Gómez-Soriano, A. D. Koutsou, A. Gil-Agudo, J. L. Pons and J. C. Moreno. "Knee Muscle Fatigue Estimation During Isometric Artificially Elicited Contractions in Incomplete Spinal Cord Injury Subjects," in *2012 International Conference on Neurorehabilitation (ICNR2012): Converging Clinical and Engineering Research on Neurorehabilitation*, 2012, pp. 329-333. **Finalist contribution in student paper competition.**
- M. Canela, **A. J. del-Ama**, and J. L. Pons. "Design of a Pediatric Exoskeleton for the Rehabilitation of the Physical Disabilities Caused by Cerebral Palsy," in *2012 International Conference on Neurorehabilitation (ICNR2012): Converging Clinical and Engineering Research on Neurorehabilitation*, 2012, pp. 255-258.
- S. Piazza, D. Torricelli, F. Brunetti, **A. J. del-Ama**, A. Gil-Agudo and J. L. Pons. "A Novel FES Control Paradigm Based on Muscle Synergies for Postural Rehabilitation Therapy with Hybrid Exoskeletons", in *34th Annual International Conference of the Engineering in Medicine and Biology Society (EMBC2012).*
- S. Piazza, D. Torricelli, F. Brunetti, **A. J. del-Ama**, A. Gil-Agudo and J. L. Pons. "Un Modelo de Controlador FES Basado en Sinergias Musculares para la Rehabilitación del Equilibrio con Exoesqueletos Híbridos," in *XXXIII Jornadas de Automática*, 2012.
- **A. J. del-Ama**, M. Bortole, A. Garza-Cervantes, J. C. Moreno, A. Gil-Agudo and J. L. Pons. "Actuadores Multimodales para la Compesnación de la Marcha de Personas con Patología Neurológica," in *XXXIII Jornadas de Automática*, 2012.
- **A. J. del-Ama**. "Hybrid FES-Robot Cooperative Control of Ambulatory Gait Rehabilitation Exoskeleton for Spinal Cord Injury Users," in *Workshop on Innovative technologies for Rehabilitation Exoskeletons, IEEE International Conference on Biomedical Robotics and Biomechatronics (BIOROB)*, 2012.
- **A. J. del-Ama**, A. D. Koutsou, J. C. Moreno, A. de-los-Reyes, A. Gil-Agudo and J. L. Pons. "Diseo Preliminar de un Exoesqueleto Híbrido para la Compensación de la Marcha en Lesionados Medulares," in *XXXII Jornadas de Automática*, 2011.

- **A. J. del-Ama**, J. C. Moreno, A. Frizera-Neto, A. Gil-Agudo and J. L. Pons. "Propuesta de Control en Trayectoria de un Actuador de Rodilla para la Compensación Funcional de la Marcha en Lesionados Medulares," in *VI Congreso Iberoamericano de Tecnologías de Apoyo a la Discapacidad (IBERDISCAP)*, 2011.
- **A. J. del-Ama**, J. C. Moreno, A. Gil-Agudo and R. Palazón. "A Design to Compensate Gait," in *12th International Conference on New Actuators (ACTUATOR)*, 2010.
- **A. J. del-Ama**, A. D. Koutsou, J. C. Moreno, A. de-los-Reyes, A. Gil-Agudo and J. L. Pons. "Diseo Preliminar de un Exoesqueleto Híbrido para la Compensación de la Marcha en Lesionados Medulares," in *XXXI Jornadas de Automática*, 2010.

8.2.1.3 Book chapters

- **A. J. del-Ama**, J. C. Moreno and A. Gil-Agudo. "Neurorobotic and Hybrid Approaches for Gait Rehabilitation in Spinal Cord Injury," in *Spinal Cord Injuries: Causes, Risk Factors and Management*, 1st ed., A. A. Martin and J. E. Jones, Eds. Hauppauge, NY: Nova Science Publishers, 2012, pp. 289-308.

8.2.1.4 Other dissemination activities

- **A. J. del-Ama**. "Exoesqueleto Híbrido RehaBot: Resultado de las primeras experiencias con pacientes." Presented at the open clinical session at the National Hospital for Spinal Cord Injury, 28 February 2013.
- **A. J. del-Ama**. "Exoesqueletos Biomecatrnicos." Presented at I Symposium on Technologies applied to Accessibility, at the Autonomous University of Madrid, 3 May 2010.
- TVE1 channel reportage: "Comando Actualidad. Milagro médico: Exoesqueleto". Broadcasted live on 31 January 2013

8.3 Future work

The work presented in this dissertation sets out several research areas for further research, which are the following:

Robot design and control:

- Improved methods of control and sensors that enable a natural interaction between the patient and the robot.
- Smaller and optimized actuators, to provide lighter and more compliant exoskeletons.
- Increased usability and autonomy, to provide systems that provide therapy while functionally compensating walking.

Neuromuscular stimulation:

- Study of applicability of new multi-channel stimulation to hybrid walking control.
- New methods for estimate muscle activation due to stimulation.
- Development of model-based controllers that allow to uncouple voluntary and artificial muscle activation
- Multidimensional controllers that optimally manage the three main stimulation parameters: PD, PA and frequency.

Hybrid control of movement:

- Expanding hybrid-cooperative control approach to all three joints.
- Research on new hybrid control strategies, based on optimal criteria.

Clinical impact of hybrid control of walking:

- Comparative assessment of the effects of hybrid walking therapy on patient walking function with respect to traditional rehabilitation interventions.
- Study of the long-term effects of hybrid walking therapy.
- Application of the hybrid-cooperative walking approach to other pathologies, such as stroke or cerebral palsy.

Several of those works are already ongoing activities within several research projects. Within the *HYPER* project, a second version of Kinesis exoskeleton have been developed, optimizing several features (figure 8.1). HYPER has actuation at hip, knee and ankle joints, allowing to provide therapy to patients with more severe impairments. These actuators were designed following the same procedure that one presented in chapter 3, but taking into consideration biomechanical data from SCI walking instead of healthy walking, which resulted in optimized actuators. Further improvements were made for the control electronics and sensor system, which comprised interaction force sensors for thigh, leg and foot segments, as well as a multi-modal sensor suit, that includes EMG and EEG to explore different levels of neural activity to characterize the required support and the user involvement, and thus modify the intervention at the periphery with hybrid robotic-NP systems. Within this research framework, the hybrid-cooperative control strategy presented in this dissertation has been adopted for HYPER, extending the concepts to hip and ankle joints, which needed new developments due to the specific role of these joints and its related musculature during walking.

FIGURE 8.1: HYPER lower limb exoskeleton.

A clinical study has already started within the framework of HYPER hybrid walking scenario, where the study design targets the comparison between traditional and hybrid approaches for walking rehabilitation, matching the dose-effect and increasing the treatment periods. From this clinical study a better quantification of the outcomes from the hybrid walking therapy will be obtained. Founding for this clinical study have been requested in the AES 2013 call.

A further project is *BioMot* (Smart Wearable Robots with Bioinspired Sensory-Motor Skills), an FP7 European research project which aims to improve existing wearable robotic exoskeletons, exploiting dynamic sensory-motor interactions and developing cognitive capabilities that can lead to symbiotic gait behavior in the interaction of a human with a wearable robot. Within BioMot, research on new light and compliant actuators and control methods will be carried out, providing novel capabilities to perform walking in unstructured environments. This will provide not only extended capabilities to the therapy, but a way to extend the therapy beyond clinical environment to daily living activities. The findings related to human-robot physical interaction generated in this dissertation will be further investigated within BioMot project. The information obtained will provide new perspectives for designing ambulatory robotic exoskeletons beyond the capabilities of current systems. The research conducted in this framework will bring transparent robotic devices, in which the boundary between functional compensation and rehabilitation of walking is interleaved.

Bibliography

[1] A. G. Brown, *Organization in the spinal cord: the anatomy and physiology of identified neurones*. Springer-Verlag Berlin, 1981.

[2] J. F. Ditunno, W. Young, W. H. Donovan, and G. Creasey, "The international standards booklet for neurological and functional classification of spinal cord injury. American Spinal Injury Association.," *Paraplegia*, vol. 32, pp. 70–80, Feb. 1994.

[3] W. Staas, C. Formal, M. Freedman, G. Fried, and M. Schmidt Read, *Spinal cord injury and spinal cord injury medicine*. Philadelphia, NJ: Lippincott-Raven Publishers, 1998.

[4] F. M. Maynard Jr, M. B. Bracken, G. Creasey, J. F. Ditunno Jr, W. H. Donovan, T. B. Ducker, S. L. Garber, R. J. Marino, S. L. Stover, C. H. Tator, and Others, "International standards for neurological and functional classification of spinal cord injury. American Spinal Injury Association.," *Spinal Cord*, vol. 35, no. 5, p. 266, 1997.

[5] H. S. Office, ed., *Aids to the investigation of peripheral nerve injuries*. Medical Research Council (Great Britain). Nerve injuries Comitee, london ed., 1943.

[6] M. McColl, J. Walker, P. Stirling, and P. Corey, "Expectations of life and health among spinal cord injured adults," *Spinal Cord*, vol. 35, pp. 818–828, 1997.

[7] S. Karamehmeto&gbreve, I. K. Ünal, H. Yílmaz, M. E. Togay, M. Dö&scedil, and Others, "Traumatic spinal cord injuries in Istanbul, Turkey. An epidemiological study," *Spinal Cord*, vol. 33, no. 8, pp. 469–471, 1995.

[8] H. Shingu, M. Ohama, T. Ikata, S. Katoh, and T. Akatsu, "A nationwide epidemiological survey of spinal cord injuries in Japan from January 1990 to December 1992," *Spinal Cord*, vol. 33, no. 4, pp. 183–188, 1995.

[9] F. W. A. Van Asbeck, M. W. M. Post, and R. F. Pangalila, "An epidemiological description of spinal cord injuries in The Netherlands in 1994," *Spinal Cord*, vol. 38, no. 7, pp. 420–424, 2000.

[10] J. Mazaira, F. Labanda, J. Romero, M. E. Garcia, C. Gambarruta, A. Sanchez, M. A. Alcaraz, O. Arroyo, A. Esclarín, T. Arzoz, and Others, "Epidemiología de la lesión medular y otros aspectos," *Rehabilitación*, vol. 32, no. 6, pp. 365–372, 1998.

[11] J. Garcia-Reneses, R. Herruzo-Cabrera, and M. Martinez-Moreno, "Epidemiological study of spinal cord injury in Spain 1984-1985," *Spinal Cord*, vol. 29, no. 3, pp. 180–190, 1991.

[12] A. García-Altés, K. Pérez, A. Novoa, J. Suelves, M. Bernabeu, J. Vidal, V. Arrufat, E. Santamaría-Rubio, J. Ferrando, M. Cogollos, C. Cantera, and J. Luque, "Spinal Cord Injury and Traumatic Brain Injury: A Cost-of-Illness Study," *Neuroepidemiology*, vol. 39, no. 2, pp. 103–8, 2012.

[13] American Board of Physical Medicine and Rehabilitation, "Definition of Physical Medicine and Rehabilitation."

[14] L. I. Guttmann, "Organisation of spinal units. History of the National Spinal Injuries Centre, Stoke Mandeville Hospital, Aylesbury.," *Paraplegia*, vol. 5, no. 3, pp. 115–126, 1967.

[15] E. Bors, "The Spinal Cord Injury Center of the Veterans Administration Hospital, Long Beach, California, USA," *Spinal Cord*, vol. 5, no. 3, pp. 126–30, 1967.

[16] G. Bedbrook, "Discerning matters of future importance in paraplegia," *Spinal Cord*, vol. 17, no. 1, pp. 36–45, 1979.

[17] R. Richardson and P. Meyer, "Prevalence and incidence of pressure sores in acute spinal cord injuries," *Spinal Cord*, vol. 19, no. 4, pp. 235–247, 1981.

[18] C. Le and M. Price, "Survival from spinal cord injury," *Journal of Chronic Diseases*, vol. 35, no. 6, pp. 487–492, 1982.

[19] W. Geisler, A. Jousse, M. Wynne-Jones, and D. Breithaupt, "Survival in traumatic spinal cord injury," *Spinal Cord*, vol. 21, no. 6, pp. 364–373, 1983.

[20] W. Donovan, R. Carter, and G. Bedbrook, "Incidence of medical complications in spinal cord injury: patients in specialised, compared with non-specialised centres," *Spinal Cord*, vol. 22, no. 5, pp. 282–290, 1984.

[21] C. Tator, E. Duncan, and V. Edmonds, "Neurological recovery, mortality and length of stay after acute spinal cord injury associated with changes in management," *Spinal Cord*, vol. 33, no. 5, pp. 254–262, 1995.

[22] S. Kirshblum, C. Ho, J. House, E. Druin, C. Nead, and S. Drastal, *Rehabilitation of Spinal Cord Injury*. Philadelphia, NJ: Lippincott Williams & Wilkins, 2002.

[23] G. Whiteneck and J. Gassaway, "New approach to study the contents and outcomes of spinal cord injury rehabilitation: the SCIRehab Project," *The Journal of Spinal Cord Medicine*, vol. 32, no. 3, pp. 251–259, 2009.

[24] J. Eng, R. Teasell, and W. Miller, "Spinal cord injury rehabilitation evidence: method of the SCIRE systematic review," *Topics in Spinal Cord Injury Rehabilitation*, vol. 13, no. 1, pp. 1–9, 2007.

[25] D. L. Wolfe, J. T. C. Hsieh, and S. Mehta, "Rehabilitation Practices and Associated Outcomes Following Spinal Cord Injury," in *Spinal Cord Injury Rehabilitation Evidence.* (J. Eng, l. R. Teasel, W. Miller, D. Wolfe, A. Townson, J. Hsieh, S. Connolly, S. Mehta, and B. Sakakibara, eds.), version 3. ed., 2010.

[26] A. Esclarín, *Lesion medular. Un enfoque multidisciplinario.* Editorial Médica Panamericana, 2010.

[27] National Institute on Disability and Rehabilitation Research, "Notice of final long-range plan for fiscal years 2005-2009," tech. rep., 2006.

[28] P. Kennedy and L. Hamilton, "The needs assessment checklist: a clinical approach to measuring outcome," *Spinal Cord*, vol. 37, pp. 136–139, 1999.

[29] J. Duff, M. Evans, and P. Kennedy, "Goal planning: a retrospective audit of rehabilitation process and outcome," *Clinical Rehabilitation*, vol. 18, pp. 275–286, 2004.

[30] D. Tate, C. Kalpakjian, and M. Forchheimer, "Quality of life issues in individuals with spinal cord injury," *Archives of Physical Medicine and Rehabilitation*, vol. 83, no. 2, pp. 18–25, 2002.

[31] K. D. Anderson, "Targeting recovery: priorities of the spinal cord-injured population," *Journal of Neurotrauma*, vol. 21, pp. 1371–1383, Oct. 2004.

[32] P. L. Ditunno, M. Patrick, M. Stineman, and J. F. Ditunno, "Who wants to walk? Preferences for recovery after SCI: a longitudinal and cross-sectional study.," *Spinal Cord*, vol. 46, pp. 500–506, July 2008.

[33] C. Donnelly, J. J. Eng, J. Hall, L. Alford, R. Giachino, and K. Norton, "Client-centered assessment and the indentification of meaningful treatment goals for individuals with a spinal cord injury.," *Spinal Cord*, vol. 42, pp. 302–307, 2004.

[34] I. Estores, "The consumer's perspective and the professional literature: What do persons with spinal cord injury want?," *Journal of Rehabilitation Research and Development*, vol. 40, no. 4 Suppl 1, p. 93:98, 2003.

[35] K. L. Kilgore, M. Scherer, R. Bobblitt, J. Dettloff, D. Dinbrowsky, N. Godbold, and et al., "Neuroprosthesis consumers' forum: consumer priorities for research directions," *Journal of Rehabilitation Research and Development*, vol. 38, no. 6, pp. 655–60, 2001.

[36] M. MacKay-Lyons, "Central pattern generation of locomotion: a review of the evidence.," *Physical Therapy*, vol. 82, pp. 69–83, Jan. 2002.

[37] V. Dietz, "Body weight supported gait training: from laboratory to clinical setting.," *Brain Research Bulletin*, vol. 76, pp. 459–463, July 2008.

[38] V. Dietz, "Spinal cord pattern generators for locomotion.," *Clinical Neurophysiology*, vol. 114, pp. 1379–1389, Aug. 2003.

[39] M. Schubert, A. Curt, and G. Colombo, "Voluntary control of human gait: conditioning of magnetically evoked motor responses in a precision stepping task," *Experimental Brain Research*, vol. 126, no. 4, pp. 583–8, 1999.

[40] H. J. A. van Hedel and V. Dietz, "Rehabilitation of locomotion after spinal cord injury.," *Restorative Neurology and Neuroscience*, vol. 28, pp. 123–34, Jan. 2010.

[41] A. Curt, H. J. a. Van Hedel, D. Klaus, and V. Dietz, "Recovery from a spinal cord injury: significance of compensation, neural plasticity, and repair.," *Journal of Neurotrauma*, vol. 25, pp. 677–85, June 2008.

[42] M. Knikou, "Neural control of locomotion and training-induced plasticity after spinal and cerebral lesions," *Clinical Neurophysiology*, vol. 121, pp. 1655–1668, Apr. 2010.

[43] M. Knikou, "Plasticity of corticospinal neural control after locomotor training in human spinal cord injury.," *Neural Plasticity*, vol. 2012, p. 254948, Jan. 2012.

[44] H. Harbeau, J. Fung, A. Leroux, and M. Ladouceur, "A review of the adaptability and recovery of locomotion after spinal cord injury," *Progress in Brain Research*, vol. 139, pp. 9–25, 2002.

[45] A. Hicks, K. Martin, D. Ditor, and A. Latimer, "Long-term exercise training in persons with spinal cord injury: effects on strength, arm ergometry performance and psychological well-being," *Spinal Cord*, vol. 41, no. 1, pp. 34–43, 2003.

[46] M. Wirz, H. V. Hedel, and R. Rupp, "Muscle force and gait performance: relationships after spinal cord injury," *Archives of Physical Medicine and Rehabilitation*, vol. 87, no. 9, pp. 1218–22, 2006.

[47] S. Rossignol and A. Frigon, "Recovery of locomotion after spinal cord injury: some facts and mechanisms.," *Annual Review of Neuroscience*, vol. 34, pp. 413–40, Jan. 2011.

[48] R. E. Cowan, B. J. Fregly, M. L. Boninger, L. Chan, M. M. Rodgers, and D. J. Reinkensmeyer, "Recent trends in assistive technology for mobility," *Journal of NeuroEngineering and Rehabilitation*, vol. 9, no. 1, p. 20, 2012.

[49] P. Levin, S. R. Faruqui, and T. Jaeblon, "Ambulatory assistive devices in orthopaedics: uses and modifications.," *The Journal of the American Academy of Orthopaedic Surgeons*, vol. 18, pp. 315–6, June 2010.

[50] M. K. Merrit JL. Yoshida, "Knee-Ankle-Foot orthoses: indications and practical applications of long leg braces.," *Physical Medicine and Rehabilitation*, vol. 14, pp. 395–422, 2000.

[51] R. L. Waters and B. R. Lunsford, "Energy cost of paraplegic locomotion of Paraplegic Locomotion," *The Journal of Bone and Joint Surgery*, vol. 67, pp. 1245–1250, Oct. 1985.

[52] D. A. Yngve, R. Douglas, and J. M. Roberts, "The reciprocating gait orthosis in myelomeningocele.," *Journal of Pediatric Orthopaedics*, vol. 4, pp. 304–310, May 1984.

[53] P. Jaspers, L. Peeraer, W. V. Petegem, and G. V. der Perre, "The use of an advanced reciprocating gait orthosis by paraplegic individuals: a follow-up study.," *Spinal Cord*, vol. 35, pp. 585–589, Sept. 1997.

[54] W. Motloch, "Principles of orthotic management for child and adult paraplegia and clinical experience with the Isocentric RGO," in *7th world congress of the International Society for Prosthetics and Orthotics*, (Chicago; Illinois), p. p28 [Abstract], 1992.

[55] M. Solomonow, R. Baratta, S. Hirokawa, N. Rightor, W. Walker, P. Beaudette, H. Shoji, and R. D'Ambrosia, "The RGO Generation II: muscle stimulation powered orthosis as a practical walking system for thoracic paraplegics.," *Orthopedics*, vol. 12, no. 10, pp. 1309–1315, 1989.

[56] M. Bernardi, I. Canale, V. Castellano, L. D. Filippo, F. Felici, and M. Marchetti, "The efficiency of walking of paraplegic patients using a reciprocating gait orthosis.," *Paraplegia*, vol. 33, pp. 409–415, July 1995.

[57] G. K. Rose, "The principles and practice of hip guidance articulations.," *Prosthetics and Orthotics International*, vol. 3, no. 1, pp. 37–43, 1979.

[58] J. H. Patrick and M. R. McClelland, "Low energy cost reciprocal walking for the adult paraplegic.," *Paraplegia*, vol. 23, no. 2, pp. 113–117, 1985.

[59] C. Kirtley and S. K. McKay, "Principles and practice of paraplegic locomotion: experience with the walkabout walking system," *Australian Orthotics and Prosthetics Magazine*, vol. 7, no. 2, pp. 4–8, 1992.

[60] A. K. L. Leung, A. F. Y. Wong, E. C. W. Wong, and S. W. Hutchins, "The Physiological Cost Index of walking with an isocentric reciprocating gait orthosis among patients with T(12) - L(1) spinal cord injury.," *Prosthetics and Orthotics International*, vol. 33, pp. 61–68, Mar. 2009.

[61] L. A. Harvey, M. B. Smith, G. M. Davis, and S. Engel, "Functional outcomes attained by T9-12 paraplegic patients with the walkabout and the isocentric reciprocal gait orthoses.," *Archives of Physical Medicine and Rehabilitation*, vol. 78, pp. 706–711, July 1997.

[62] S. Lotta, A. Fiocchi, R. Giovannini, R. Silvestrin, L. Tesio, A. Raschi, L. Macchia, V. Chiapatti, M. Zambelli, and C. Tosi, "Restoration of gait with orthoses in thoracic paraplegia: a multicentric investigation.," *Paraplegia*, vol. 32, pp. 608–615, Sept. 1994.

[63] M. Franceschini, S. Lotta, S. Baratta, M. Zampolini, and D. Loria, "Reciprocating gait orthoses: a multicenter study of their use by spinal cord injured patients," *Archives of Physical Medicine and Rehabilitation*, vol. 78, pp. 582–586, June 1997.

[64] S. Fatone, "A review of the literature pertaining to KAFOs and HKAFOs for ambulation," *Journal of Prosthetics and Orthotics*, vol. 18, pp. 137–168, June 2006.

[65] D. S. Z. Vukobratovic M. Hristic, M. Vukobratovic, D. Hristic, Z. Stojilkovic, D. Stojilkovic, Vukobratovic, and M. Hristic, "Development of active anthropomorphic exoskeletons.," *Medical and Biological Engineering and Computing*, vol. 12, no. 1, pp. 66–80, 1974.

[66] M. K. Vukobratovic, "When Were Active Exoskeletons Actually Born?," *International Journal of Humanoid Robotics*, vol. 4, no. 3, p. 459, 2007.

[67] D. Popovic, R. Tomovic, and L. Schwirtlich, "Hybrid assistive system-the motor neuroprosthesis," *IEEE Transactions on Biomedical Engineering*, vol. 36, no. 7, pp. 729–737, 1989.

[68] K. Kong and D. Jeon, "Design and control of an exoskeleton for the elderly and patients," *IEEE/ASME Transactions on Mechatronics*, vol. 11, no. 4, pp. 428–432, 2006.

[69] P. Rabishong, J. P. Bel, J. Hill, E. Peruchon, M. Simeon, J. Screve, M. Pelegrin, A. Benzaken, R. Tomovic, S. Lazarevic, and Others, "The AMOLL project (active modular orthosis for lower limbs)," in *Proc. Int. Symp. External Control Hum. Extremities*, pp. 33–42, 1975.

[70] A. K. Raj, P. D. Neuhaus, A. M. Moucheboeuf, J. H. Noorden, and D. V. Lecoutre, "Mina: A Sensorimotor Robotic Orthosis for Mobility Assistance," *Journal of Robotics*, vol. 2011, pp. 1–8, 2011.

[71] N. Costa, M. Bezdicek, M. Brown, J. O. Gray, D. G. Caldwell, and S. Hutchins, "Joint motion control of a powered lower limb orthosis for rehabilitation," *International Journal of Automation and Computing*, vol. 3, pp. 271–281, July 2006.

[72] J. Grundmann and A. Seireg, "Computer control of multi-task exoskeleton for paraplegics," in *Theory and practice of robots and manipulators: Second International CISM-IFToMM Symposium*, (Warsaw, Poland), p. 233, Elsevier Science & Technology, 1977.

[73] http://www.argomedtec.com/, "ARGO Medical Technologies."

[74] A. Goffer, "Gait-locomotor apparatus.," 2006.

[75] T. Hayashi, "Control method of robot suit HAL working as operator's muscle using biological and dynamical information," in *IEEE/RSJ International Conference on Intelligent Robots and Systems*, pp. 3063–3068, 2005.

[76] H. Kawamoto, "Power assist system HAL-3 for gait disorder person," *Computers helping people with special needs*, pp. 19–29, 2002.

[77] http://eksobionics.com/, "Ekso Bionics."

[78] S. Maeshima, A. Osawa, D. Nishio, Y. Hirano, K. Takeda, H. Kigawa, and Y. Sankai, "Efficacy of a hybrid assistive limb in post-stroke hemiplegic patients: a preliminary report.," *BMC neurology*, vol. 11, p. 116, Jan. 2011.

[79] A. Tsukahara, Y. Hasegawa, and Y. Sankai, "Gait support for complete spinal cord injury patient by synchronized leg-swing with HAL," in *2011 IEEE/RSJ International Conference on Intelligent Robots and Systems (IROS)*, pp. 1737–1742, 2011.

[80] G. Zeilig, H. Weingarden, M. Zwecker, I. Dudkiewicz, A. Bloch, and A. Esquenazi, "Safety and tolerance of the ReWalk exoskeleton suit for ambulation by people with complete spinal cord injury: a pilot study.," *The journal of spinal cord medicine*, vol. 35, pp. 96–101, Mar. 2012.

[81] A. Esquenazi, M. Talaty, A. Packel, and M. Saulino, "The ReWalk Powered Exoskeleton to Restore Ambulatory Function to Individuals with Thoracic-Level Motor-Complete Spinal Cord Injury.," *American Journal of Physical Medicine & Rehabilitation*, vol. 91, pp. 911–21, Dec. 2012.

[82] H. Herr, "Exoskeletons and orthoses: classification, design challenges and future directions," *Journal of NeuroEngineering and Rehabilitation*, vol. 6, p. 21, Jan. 2009.

[83] A. M. Dollar and H. Herr, "Active Orthoses for the Lower-Limbs: Challenges and State of the Art," *IEEE International Conference on Rehabilitation Robotics*, vol. 1, pp. 968–977, June 2007.

[84] S. Mohammed and Y. Amirat, "Towards intelligent lower limb wearable robots: Challenges and perspectives - State of the art," in *IEEE International Conference on Robotics and Biomimetics (ROBIO)*, pp. 312–317, 2008.

[85] I. Díaz, J. J. Gil, and E. Sánchez, "Lower-Limb Robotic Rehabilitation: Literature Review and Challenges," *Journal of Robotics*, vol. 11, pp. 1–11, 2011.

[86] T. Lam, D. . Wolfe, J. J. Eng, and A. Domingo, *Lower Limb Rehabilitation Following Spinal Cord Injury*, vol. Version 3. Vancouver: Spinal Cord Injury Rehabilitation Evidence, version 4. ed., Oct. 2010.

[87] A. Wernig and S. Muller, "Laufband locomotion with body weight support improved walking in persons with severe spinal cord injuries.," *Paraplegia*, vol. 30, no. 4, pp. 229–238, 1992.

[88] V. Dietz, G. Colombo, and L. Jensen, "Locomotor activity in spinal man.," *Lancet*, vol. 334(8932), pp. 1260–1263, 1994.

[89] V. Dietz, G. Colombo, L. Jensen, and L. Baumgartner, "Locomotor capacity of spinal cord in paraplegic patients.," *Annals of Neurology*, vol. 37, no. 5, pp. 555–556, 1995.

[90] E. C. Field-Fote, "Spinal cord control of movement: implications for locomotor rehabilitation following spinal cord injury.," *Physical Therapy*, vol. 80, pp. 477–484, May 2000.

[91] L. Finch, H. Barbeau, and B. Arsenault, "Influence of body weight support on normal human gait: development of a gait retraining strategy.," *Physical Therapy*, vol. 71, no. 11, pp. 855–856, 1991.

[92] S. Hesse, C. Bertelt, A. Schaffrin, M. Malezic, and K. H. Mauritz, "Restoration of gait in nonambulatory hemiparetic patients by treadmill training with partial body-weight support.," *Archives of Physical Medicine and Rehabilitation*, vol. 75, no. 10, pp. 1087–1093, 1994.

[93] V. Lin, D. Cardenas, and N. Cutter, eds., *Spinal Cord Medicine: Principles and Practice*, ch. Rehabilitative Strategies for Ambulation. Demos Medical Publishing, 2003.

[94] W. Grooten, P. Wernstedt, and M. Campo, "Related musculoskeletal disorders in female Swedish physical therapists with more than 15 years of job experience: Prevalence and associations with work exposures," *Physiotherapy Theory and Practice*, vol. 27, no. 3, pp. 213–22, 2011.

[95] M. Campo, S. Weiser, and K. Koenig, "Job strain in physical therapists," *Physical Therapy*, vol. 89, no. 9, pp. 946–56, 2009.

[96] A. Darragh, W. Huddleston, and P. King, "Work-related musculoskeletal injuries and disorders among occupational and physical therapists," *American Journal of Occupational Therapy*, vol. 63, no. 3, pp. 351–62, 2009.

[97] P. King, W. Huddleston, and A. Darragh, "Work-related musculoskeletal disorders and injuries: differences among older and younger occupational and physical therapists," *Journal of Occupational Rehabilitation*, vol. 19, no. 3, pp. 274–83, 2009.

[98] B. Bork, T. Cook, and J. Rosecrance, "Work-related musculoskeletal disorders among physical therapists," *Physical Therapy*, vol. 80, no. 4, pp. 336–51, 1996.

[99] V. Dietz, "Body weight supported gait training: from laboratory to clinical setting.," *Brain Research Bulletin*, vol. 78, pp. 459–463, July 2008.

[100] J. L. Emken, J. E. Bobrow, and D. J. Reinkensmeyer., "Robotic movement training as an optimization problem: designing a controller that assists only as needed.," in *9th International Conference on Rehabilitation Robotics. CORR 2005*, pp. 307–312, 2005.

[101] L. L. Cai, A. J. Fong, C. K. Otoshi, Y. Liang, J. W. Burdick, R. R. Roy, and V. R. Edgerton, "Implications of assist-as-needed robotic step training after a complete spinal cord injury on intrinsic strategies of motor learning.," *Journal of Neuroscience*, vol. 26, pp. 10564–10568, Oct. 2006.

[102] V. R. Edgerton and R. R. Roy, "Robotic Training and Spinal Cord Plasticity," *Brain Research Bulletin*, vol. 78, no. 1, pp. 4–12, 2009.

[103] G. Colombo, M. Jorg, and V. Dietz, "Driven gait orthosis to do locomotor training of paraplegic patients," in *Proceedings of the 22nd Annual International Conference of the IEEE Engineering in Medicine and Biology Society*, vol. 4, (Chicago, Il), pp. 3159–3163, 2000.

[104] G. Colombo, M. Joerg, R. Schreier, and V. Dietz, "Treadmill training of paraplegic patients using a robotic orthosis," *Journal of Rehabilitation Research and Development*, vol. 37, no. 6, pp. 693–700, 2000.

[105] A. Duschau-Wicke, A. Caprez, and R. Riener, "Patient-cooperative control increases active participation of individuals with SCI during robot-aided gait training," *Journal of NeuroEngineering and Rehabilitation*, vol. 7, p. 43, Jan. 2010.

[106] J. F. Veneman, R. Kruidhof, E. E. G. Hekman, R. Ekkelenkamp, E. H. F. Van Asseldonk, and H. van der Kooij, "Design and Evaluation of the LOPES Exoskeleton Robot for Interactive Gait Rehabilitation," *IEEE Trans Neural Syst Rehabil Eng*, vol. 15, no. 3, pp. 379–386, 2007.

[107] C. C. Simons, E. E. van Asseldonk, M. Folkersma, J. van den Hoek, M. Postma, J. J. Buurke, and J. Folkersma, "First clinical results with the new innovative robotic gait trainer LOPES," *Gait & Posture*, vol. 30, p. S7, Nov. 2009.

[108] S. Freivogel, J. Mehrholz, T. Husak.Sotomayor, and S. D., "Gait training with the newly developed LokoHelp?-system is feasible for non-ambulatory patients after stroke, spinal cord and brain injury. A feasibility study," *Brain Injury*, vol. 22, no. 7-8, pp. 625–632, 2008.

[109] S. Freivogel, D. Schmalohr, and J. Mehrholz, "Improved walking ability and reduced therapeutic stress with an elec- tromechanical gait device," *Journal of Rehabilitation Medicine*, vol. 41, no. 9, pp. 734–739, 2009.

[110] A. Pennycott, V. Ureta, D. Wyss, H. Vallery, V. Klamroth-Marganska, and R. Riener, "Towards more effective robotic gait training for stroke rehabilitation: a review," *Journal of NeuroEngineering and Rehabilitation*, vol. 9, Sept. 2012.

[111] E. Swinnen, S. Duerinck, P. Baeyens, Jean-Pierre, R. Meeusen, and E. Kerckhofs, "Effectiveness of robot-assisted gait training in persons with spinal cord injury: A systematic review," *Journal of Rehabilitation Medicine*, vol. 42, pp. 520–526, June 2010.

[112] C. F. J. Nooijen, N. Ter Hoeve, E. C. Field-Fote, and N. T. Hoeve, "Gait quality is improved by locomotor training in individuals with SCI regardless of training approach.," *Journal of NeuroEngineering and Rehabilitation*, vol. 6, p. 36, Jan. 2009.

[113] B. H. Dobkin and P. W. Duncan, "Should body weight-supported treadmill training and robotic-assistive steppers for locomotor training trot back to the starting gate?," *Neurorehabilitation and Neural Repair*, vol. 26, pp. 308–17, May 2012.

[114] E. C. Field-Fote and K. E. Roach, "Influence of a locomotor training approach on walking speed and distance in people with chronic spinal cord injury: a randomized clinical trial," *Physical Therapy*, vol. 91, no. 1, pp. 48–60, 2011.

[115] N. J. Tester, D. R. Howland, K. V. Day, S. P. Suter, A. Cantrell, and A. L. Behrman, "Device use, locomotor training, and the presence of arm swing during treadmill walking post-spinal cord injury," *Spinal Cord*, vol. 49, no. 3, pp. 451–456, 2011.

[116] R. van den Brand, J. Heutschi, Q. Barraud, J. DiGiovanna, K. Bartholdi, M. Huerlimann, L. Friedli, I. Vollenweider, E. M. Moraud, S. Duis, N. Dominici, S. Micera, P. Musienko, and G. Courtine, "Restoring voluntary control of locomotion after paralyzing spinal cord injury," *Science*, vol. 336, pp. 1182–5, June 2012.

[117] S. Thuret, L. D. F. Moon, and F. H. Gage, "Therapeutic interventions after spinal cord injury.," *Nature reviews. Neuroscience*, vol. 7, pp. 628–643, Aug. 2006.

[118] D. J. Reinkensmeyer and M. L. Boninger, "Technologies and combination therapies for enhancing movement training for people with a disability," *Journal of NeuroEngineering and Rehabilitation*, vol. 9, no. 1, p. 17, 2012.

[119] L. L. Baker, C. L. Wederich, D. R. McNeal, C. Newsam, and R. L. Waters, *Neuro Muscular Electrical Stimulation. A practical guide.* Downey, CA: Los Amigos Research & Education Institute, 4 ed., 2000.

[120] W. T. Liberson, H. J. Holmquest, D. Scot, and M. Dwon, "Functional electrotherapy: stimulation of the peroneal nerve synchronized with the swing phase of the gait of hemiplegi patients," *Archives of Physical Medicine and Rehabilitation*, vol. 42, pp. 101–5, 1961.

[121] P. H. Peckham and J. S. Knutson, "Functional Electrical Stimulation for Neuromuscular Applications.," *Annual Review of Biomedical Engineering*, vol. 7, no. 1, pp. 327–360, 2005.

[122] D. Prodanov, E. Marani, and J. Holsheimer, "Functional electric Stimulation for sensory and motor functions: progress and problems," *Biomedical Reviews*, vol. 14, pp. 23–50, 2003.

[123] M. R. Popovic, T. Keller, I. P. I. Papas, V. Dietz, and M. Morari, "Surface-stimulation technology for grasping and walking neuroprostheses," *IEEE Engineering in Medicine and Biology Magazine*, vol. 20, no. 1, pp. 82–93, 2001.

[124] V. K. Mushahwar, P. L. Jacobs, R. a. Normann, R. J. Triolo, and N. Kleitman, "New functional electrical stimulation approaches to standing and walking.," *Journal of Neural Engineering*, vol. 4, pp. S181–97, Sept. 2007.

[125] J. Moe and H. Post, "Functional electrical stimulation for ambulation in hemiplegia," *The Journal-Lancet*, vol. 82, pp. 285–88, 1962.

[126] Www.sigmedics.com, "Parastep."

[127] A. Kantrowitz, *Electronic physiological aids: A report of the Maimonides Hospital.* Brooklyn (NY): Maimonides Hospital, 1960.

[128] A. Kralj, T. Bajd, R. Turk, J. Krajnik, H. Benko, and Others, "Gait restoration in paraplegic patients: a feasibility demonstration using multichannel surface electrode FES.," *Journal of Rehabilitation Research and Development*, vol. 20, pp. 3–20, July 1983.

[129] D. Graupe and K. H. Kohn, "Transcutaneous functional neuromuscular stimulation of certain traumatic complete thoracic paraplegics for independent short-distance ambulation," *Neurological Research*, vol. 19, pp. 323–333, 1997.

[130] E. B. Marsolais and R. Kobetic, "Functional electrical stimulation for walking in paraplegia," *Journal of Bone and Joint Surgery*, vol. 69, pp. 728–733, June 1987.

[131] R. Kobetic, R. J. Triolo, and E. B. Marsolais, "Muscle selection and walking performance of multichannel FES systems for ambulation in paraplegia.," *IEEE Trans Rehabil Eng*, vol. 5, pp. 23–29, Mar. 1997.

[132] D. B. Popović, M. Popovic, and S. Dosen, "Neural Prostheses for Walking Restoration," *Journal of Automatic Control*, vol. 18, no. 2, pp. 63–71, 2008.

[133] L. Yang, D. N. Condie, M. H. Granat, J. P. Paul, and D. I. Rowley, "Effects of joint motion constraints on the gait of normal subjects and their implications on the further development of hybrid FES orthosis for paraplegic persons," *Journal of Biomechanics*, vol. 29, no. 2, pp. 217–226, 1996.

[134] K. Fujita, Y. Handa, N. Hoshimiya, and M. Ichie, "Stimulus Adjustment Protocol for FES-Induced Standing in Paraplegia Using Percutaneous Intramuscular Electrodes," *IEEE Transactions on Rehabilitation Engineering*, vol. 3, no. 4, pp. 360–366, 1995.

[135] J. A. Hoffer, M. Baru, S. Benard, E. Calderon, G. Desmoulin, and P. Dhawan, "Initial results with fully implanted Neurostep FES system for foot drop.," in *10th Annual Conference of the International Functional Electrical Stimulation Society*, pp. 53–55, 2005.

[136] P. N. Taylor, J. H. Burridge, A. L. Dunkerley, D. E. Wood, J. A. Norton, and C. Singleton, "Clinical use of the Odstok dropped foot stimulator: its effect on the speed and the effort of walking.," *Archives of Physical Medicine and Rehabilitation*, vol. 80, no. 12, pp. 1577–1583, 1999.

[137] T. A. Thrasher and M. R. Popovic, "Functional electrical stimulation of walking: function, exercise and rehabilitation.," *Annals de Rèadaptation et de Mèdecine Physique*, vol. 51, pp. 452–460, July 2008.

[138] B. M. Doucet, A. Lam, and L. Griffin, "Neuromuscular electrical stimulation for skeletal muscle function.," *The Yale Journal of Biology and Medicine*, vol. 85, pp. 201–15, June 2012.

[139] E. J. Nightingale, J. Raymond, J. W. Middleton, J. Crosbie, and G. M. Davis, "Benefits of fes gait in a spinal cord injured population.," *Spinal Cord*, vol. 45, pp. 646–657, Oct. 2007.

[140] G. H. Creasey, C. H. Ho, R. J. Triolo, D. R. Gater, A. F. DiMarco, K. M. Bogie, and M. W. Keith, "Clinical applications of electrical stimulation after spinal cord injury.," *Journal of Spinal Cord Medicine*, vol. 27, no. 4, pp. 365–375, 2004.

[141] K. Nosaka, A. Aldayel, M. Jubeau, and T. Chen, "Muscle damage induced by electrical stimulation," *European Journal of Applied Phisiology*, vol. 111, no. 10, pp. 2427–37, 2011.

[142] M. Jubeau, M. Muthalib, and G. Millet, "Comparison in muscle damage between maximal voluntary and electrically evoked isometric contractions of the elbow flexors," *European Journal of Applied Phisiology*, vol. 112, no. 2, pp. 429–38, 2012.

[143] A. Mackey, "Evidence of skeletal muscle damage following electrically stimulated isometric muscle contractions in humans," *Journal of Applied Physiology*, vol. 105, no. 5, pp. 1620–1627, 2008.

[144] R. Crameri and P. Aagaard, "Myofibre damage in human skeletal muscle: effects of electrical stimulation versus voluntary contraction," *The Journal of Physiology*, vol. 538, no. 1, pp. 365–380, 2007.

[145] U. Carraro, K. Rossini, W. Mayr, and H. Kern, "Muscle Fiber Regeneration in Human Permanent Lower Motoneuron Denervation: Relevance to Safety and Effectiveness of FES-Training, Which Induces Muscle Recovery in SCI Subjects," *Artificial Organs*, vol. 29, no. 3, pp. 187–191, 2005.

[146] J. Riess and J. J. Abbas, "Adaptative control of cyclic movements as muscles fatigue using functional electrical stimulation," *IEEE Transactions on Neural Systems and Rehabilitation Engineering*, vol. 9, no. 3, pp. 326–330, 2001.

[147] R. Riener, "Model-based development of neuroprosthesis for paraplegic patients.," *Philosophical Transactions of the Royal Society of London*, vol. 354, pp. 877–94, May 1999.

[148] A. H. Vette, K. Masani, J.-Y. Kim, and M. R. Popovic, "Closed-loop control of functional electrical stimulation-assisted arm-free standing in individuals with spinal cord injury: a feasibility study.," *Neuromodulation*, vol. 12, pp. 22–32, Jan. 2009.

[149] C. L. Lynch and M. R. Popovic, "A Stochastic Model of Knee Angle in Response to Electrical Stimulation of the Quadriceps and Hamstrings Muscles.," *Artificial Organs*, no. 21, 2011.

[150] A. S. Gorgey, C. D. Black, C. P. Elder, and G. a. Dudley, "Effects of electrical stimulation parameters on fatigue in skeletal muscle.," *The Journal of orthopaedic and sports physical therapy*, vol. 39, pp. 684–92, Sept. 2009.

[151] S. A. Binder-Macleod and L. Snyder-Mackler, "Muscle fatigue: clinical implications for fatigue assessment and neuromuscular electrical stimulation," *Physical Therapy*, vol. 73, no. 12, pp. 902–910, 1993.

[152] H. M. Franken, S. Member, P. H. Veltink, M. Fidder, and H. B. K. Boom, "Fatigue of intermittently stimulated paralyzed human quadriceps during imposed cyclical lower leg movements.," in *Proceedings of the Annual International Conference of the IEEE Engineering in Medicine and Biology Society*, vol. 3, pp. 1341–1342, Ieee, Jan. 1992.

[153] P. E. Crago, N. Lan, P. H. Veltink, J. J. Abbas, and C. Kantor, "New control strategies for neuroprosthetic systems.," *Journal of Rehabilitation Research and Development*, vol. 33, pp. 158–72, Apr. 1996.

[154] C. Lynch and M. Popovic, "Closed-loop control for FES: Past work and future directions," in *10th Annual Conference of the International FES Society*, (Montreal, Canada), pp. 2–4, July 2005.

[155] N. M. Malesević, L. Z. Popović, L. Schwirtlich, and D. B. Popović, "Distributed low-frequency functional electrical stimulation delays muscle fatigue compared to conventional stimulation.," *Muscle & Nerve*, vol. 42, pp. 556–62, Oct. 2010.

[156] L. Sykes, E. R. Ross, E. S. Powell, and J. Edwards, "Objective measurement of use of the reciprocating gait orthosis (RGO) and the electrically augmented RGO in adult patients with spinal cord lesions.," *Prosthetics and Orthotics International*, vol. 20, no. 3, pp. 182–190, 1996.

[157] K. A. Ferguson, G. Polando, R. Kobetic, R. J. Triolo, and E. B. Marsolais, "Walking with a hybrid orthosis system," *Spinal Cord*, vol. 37, pp. 800–804, Nov. 1999.

[158] G. Merati, P. Sarchi, M. Ferrarin, A. Pedotti, and A. Veicsteinas, "Paraplegic adaptation to assisted-walking: energy expenditure during wheelchair versus orthosis use.," *Spinal Cord*, vol. 38, no. 1, pp. 37–44, 2000.

[159] A. V. Nene and J. H. Patrick, "Energy cost of paraplegic locomotion using the ParaWalker–electrical stimulation "hybrid" orthosis.," *Archives of Physical Medicine and Rehabiltiation*, vol. 71, pp. 116–120, Feb. 1990.

[160] D. Graupe, H. Cerrel-Bazo, H. Kern, and U. Carraro, "Walking performance, medical outcomes and patient training in FES of innervated muscles for ambulation by thoracic-level complete paraplegics.," *Neurological Research*, vol. 30, pp. 123–130, Mar. 2008.

[161] T. A. Thrasher, H. M. Flett, and M. R. Popovic, "Gait training regimen for incomplete spinal cord injury using functional electrical stimulation.," *Spinal Cord*, vol. 44, pp. 357–361, June 2006.

[162] R. Tomovic, D. Popoviv, and F. Gracanin, "A technology for self-fitting of orthoses.," *VI Advances in External Control of Human Extremities (ECHE)*, pp. 231–238, 1978.

[163] W. K. Durfee and J. M. Hausdorff, "Regulating knee joint position by combining electrical stimulation with a controllable friction brake.," *Annals of Biomedical Engineering*, vol. 18, pp. 575–596, Jan. 1990.

[164] E. B. Marsolais, R. Kobetic, G. Polando, K. Ferguson, S. Tashman, R. Gaudio, S. Nandurkar, and H. R. Lehneis, "The Case Western Reserve University hybrid gait orthosis.," *The Journal of Spinal Cord Medicine*, vol. 23, no. 2, pp. 100–108, 2000.

[165] R. Kobetic, E. B. Marsolais, R. R. J. Triolo, D. D. T. Davy, R. Gaudio, and S. Tashman, "Development of a hybrid gait orthosis: a case report.," *The Journal of Spinal Cord Medicine*, vol. 26, no. 3, pp. 254–258, 2003.

[166] R. Kobetic, C. S. C. To, J. J. R. Schnellenberger, M. L. M. Audu, T. C. T. Bulea, R. Gaudio, G. Pinault, S. Tashman, and R. R. J. Triolo, "Development of hybrid orthosis for standing, walking, and stair climbing after spinal cord injury.," *Journal of Rehabilitation Research and Development*, vol. 46, no. 3, pp. 447–462, 2009.

[167] C. To, R. Kobetic, and R. Triolo, "Hybrid orthosis system with a variable hip coupling mechanism," in *Annual International Conference of the IEEE Engineering in Medicine and Biology Society, 2006. EMBS'06. 28th*, pp. 2928–2931, IEEE, 2008.

[168] C. S. To, R. Kobetic, J. R. Schnellenberger, M. L. Audu, and R. J. Triolo, "Design of a Variable Constraint Hip Mechanism for a Hybrid Neuroprosthesis to Restore Gait After Spinal Cord Injury," *IEEE/ASME Transactions on Mechatronics*, vol. 13, no. 2, pp. 197–205, 2008.

[169] M. L. Audu, C. S. To, R. Kobetic, and R. J. Triolo, "Gait evaluation of a novel hip constraint orthosis with implication for walking in paraplegia.," *IEEE Transactions on Neural Systems and Rehabilitation Engineering*, vol. 18, pp. 610–8, Dec. 2010.

[170] M. Goldfarb and W. K. Durfee, "Design of a controlled-brake orthosis for FES-aided gait.," *IEEE Transactions on Rehabilitation Engineering*, vol. 4, pp. 13–24, Mar. 1996.

[171] W. K. Durfee and M. Goldfarb, "Design of a Controlled-Brake Orthosis for Regulating FES-Aided Gait," in *14th International Conference of the IEEE Engineering in Medicine and Biology Society*, vol. 4, pp. 1337–1338, Ieee, 1992.

[172] M. Goldfarb, K. Korkowski, B. Harrold, and W. Durfee, "Preliminary evaluation of a controlled-brake orthosis for FES-aided gait.," *IEEE Transactions on Neural Systems and Rehabilitation Engineering*, vol. 11, pp. 241–248, Sept. 2003.

[173] S. Gharooni, M. O. Tokhi, B. Heller, M. O. H. Gharooni S. Tokhi, and M.O., "The Use of Elastic Element in a Hybrid Orthosis for Swing Phase Generation in Orthotic Gait," in *5th Annual Conference of the International Functional Electrical Stimulation Society*, pp. 1–4, 2000.

[174] S. Gharooni, B. Heller, and M. O. Tokhi, "A new hybrid spring brake orthosis for controlling hip and knee flexion in the swing phase," *IEEE Transactions on Neural Systems and Rehabilitation Engineering*, vol. 9, pp. 106–107, Mar. 2001.

[175] R. Jailani, M. O. Tokhi, S. C. Gharooni, and Z. Hussain, "PID Control of Knee Extension for FES-Assisted Walking with Spring Brake Orthosis," in *2010 Fourth Asia International Conference on Mathematical/Analytical Modelling and Computer Simulation (AMS)*, pp. 261–266, 2010.

[176] R. J. Farris, H. A. Quintero, T. J. Withrow, and M. Goldfarb, "Design of a joint-coupled orthosis for FES-aided gait," in *2009 International Conference on Rehabilitation Robotics, ICORR 2009*, pp. 246–252, 2009.

[177] R. J. Farris, H. a. Quintero, T. J. Withrow, and M. Goldfarb, "Design and simulation of a joint-coupled orthosis for regulating FES-aided gait," in *2009 IEEE 11th International Conference on Robotics and Automation*, (Kyoto (Japan)), pp. 1916–1922, 2009.

[178] W. K. Durfee and A. Rivard, "Design and simulation of a pneumatic, stored-energy, hybrid orthosis for gait restoration.," *Journal of Biomechanical Engineering*, vol. 127, pp. 1014–1019, Nov. 2005.

[179] A. Kangude, B. Burgstahler, J. Kakastys, and W. Durfee, "Single channel hybrid FES gait system using an energy storing orthosis: preliminary design.," in *31th Annual International Conference of the IEEE Engineering in Medicine and Biology Society*, pp. 6798–6801, Minneapolis (USA), 2009.

[180] A. Kangude, B. Burgstahler, and W. Durfee, "Engineering evaluation of the energy-storing orthosis FES gait system.," in *Annual International Conference of the IEEE Engineering in Medicine and Biology Society*, vol. 1, pp. 5927–30, Jan. 2010.

[181] S. Fukada, G. Obinata, K. Hase, A. Nakayama, Y. Shimada, T. Matsunaga, T. Iwami, K. Miyawaki, and M. Tsunetou, "Development of a Hybrid Power Assist Orthosis with FES," in *11th Annual Conference of the International FES Society.*, (Zao, Japan), pp. 124–126, 2006.

[182] G. Obinata, S. Fukada, T. Matsunaga, T. Iwami, Y. Shimada, K. Miyawaki, K. Hase, and A. Nakayama, "Hybrid control of powered orthosis and functional neuromuscular stimulation for restoring gait.," in *29th Annual Int. Conf. of the IEEE Engineering in Medicine and Biology Society EMBS 2007*, vol. 2007, pp. 4879–4882, 2007.

[183] Y. Stauffer, Y. Allemand, M. Bouri, J. Fournier, R. Clavel, P. Metrailler, R. Brodard, and F. Reynard, "The WalkTrainer–a new generation of walking reeducation device combining orthoses and muscle stimulation.," *IEEE Transactions on Neural Systems and Rehabilitation Engineering*, vol. 17, pp. 38–45, Feb. 2009.

[184] C. Schmitt, P. Métrailler, A. Al-Khodairy, R. Brodard, J. Fournier, M. Bouri, and R. Clavel, "A Study of a Knee Extension Controlled by a Closed Loop Functional Electrical Stimulation.," in *9 Annual Conference of the International Functional Electrical Stimulation Society.*, pp. 3–5, 2004.

[185] B. Ashworth, "Preliminary trial of carisoprodol in multiple sclerosis.," *The Practitioner*, vol. 192, pp. 540–542, 1964.

[186] P. Metrailler, V. Blanchard, I. Perrin, R. Brodard, R. Frischknecht, C. Schmitt, J. Fournier, M. Bouri, and R. Clavel, "Improvement of rehabilitation possibilities with the MotionMaker TM," in *First IEEE/RAS-EMBS International Conference on Biomedical Robotics and Biomechatronics, 2006. BioRob 2006.*, vol. 50, pp. 359–364, 2006.

[187] P. Métrailler, R. Brodard, R. Clavel, and R. Frischknecht, "Closed loop electrical muscle stimulation in spinal cord injured rehabilitation," in *6th Mediterranean Forum of Physical Medicine and Rehabilitation*, (Villamura, Portugal), pp. 18–21, 2006.

[188] M. Bouri, B. Le Gall, and R. Clavel, "A new concept of parallel robot for rehabilitation and fitness: The Lambda," *2009 IEEE International Conference on Robotics and Biomimetics (ROBIO)*, pp. 2503–2508, Dec. 2009.

[189] R. J. Farris, H. a. Quintero, and M. Goldfarb, "Preliminary evaluation of a powered lower limb orthosis to aid walking in paraplegic individuals.," *IEEE Transactions on Neural Systems and Rehabilitation Engineering*, vol. 19, pp. 652–9, Dec. 2011.

[190] H. A. Quintero, R. J. Farris, and M. Goldfarb, "Control and implementation of a powered lower limb orthosis to aid walking in paraplegic individuals.," in *2011 IEEE International Conference on Rehabilitation Robotics*, vol. 2011, pp. 1–6, January 2011.

[191] H. A. Quintero, R. J. Farris, K. Ha, and M. Goldfarb, "Preliminary assessment of the efficacy of supplementing knee extension capability in a lower limb exoskeleton with FES.," in *34th Annual International Conference of the IEEE Engineering in Medicine and Biology Society.*, no. 1, pp. 3360–3, Jan. 2012.

[192] K. H. Ha, H. A. Quintero, R. J. Farris, and M. Goldfarb, "Enhancing stance phase propulsion during level walking by combining fes with a powered exoskeleton for persons with paraplegia.," in *34th Annual International Conference of the IEEE Engineering in Medicine and Biology Society*, pp. 344–7, 2012.

[193] G. Obinata, T. Ogisu, K. Hase, Y. Kim, and E. Genda, "State estimation of walking phase and functional electrical stimulation by wearable device," in *Proc. Annual Int. Conf. of the IEEE Engineering in Medicine and Biology Society EMBC 2009*, pp. 5901–5904, 2009.

[194] C. Schmitt, P. Métrailler, A. Al-Khodairy, R. Brodard, J. Fournier, M. Bouri, and R. Clavel, "The MotionMaker: a Rehabilitation System Combining an Orthosis With Closed Loop Electrical Muscle Stimulation," in *8 Vienna International Workshop on Functional Electrical Stimulation*, pp. 117–20, 2004.

[195] R. Riener, L. Lunenburger, S. Jezernik, M. Anderschitz, G. Colombo, V. Dietz, and L. Lünenburger, "Patient-cooperative strategies for robot-aided treadmill training: first experimental results," *IEEE Transactions on Neural Systems and Rehabilitation Engineering*, vol. 13, pp. 380–394, Sept. 2005.

[196] A. Duschau-Wicke, J. von Zitzewitz, A. Caprez, L. Lunenburger, and R. Riener, "Path control: a method for patient-cooperative robot-aided gait rehabilitation.," *IEEE Transactions on Neural Systems and Rehabilitation Engineering*, vol. 18, pp. 38–48, Feb. 2010.

[197] S. Jezernik, R. Schärer, G. Colombo, and M. Morari, "Adaptive robotic rehabilitation of locomotion: a clinical study in spinally injured individuals.," *Spinal Cord*, vol. 41, pp. 657–66, Dec. 2003.

[198] L. Zimmerli, A. Duschau-Wicke, R. Riener, A. Mayr, and L. Lunenburger, "Virtual reality and gait rehabilitation Augmented feedback for the Lokomat," in *Virtual Rehabilitation International Conference*, pp. 150–153, 2009.

[199] P. Rossier and D. Wade, "Validity and reliability comparison of 4 mobility measures in patients presenting with neurologic impairment," *Archives of Physical Medicine and Rehabilitation*, vol. 82, pp. 9–13, 2001.

[200] R. Butland, J. Pang, E. Gross, A. Woodcock, D. Geddes, H. C. Simpson, J. I. Mann, R. Chakrabarti, J. D. Imeson, Y. Stirling, M. Tozer, L. Woolf, and T. W. Meade, "Two-,

six-, and 12-minute walking tests in respiratory disease.," *British Medical Journal (Clinical research Ed.)*, vol. 284, pp. 1607–8, May 1982.

[201] P. L. Ditunno and J. F. Ditunno Jr, "Walking index for spinal cord injury (WISCI II): scale revision," *Spinal Cord*, vol. 39, pp. 654–656, 2001.

[202] A. B. Jackson, C. T. Carnel, J. F. Ditunno, M. S. Read, M. L. Boninger, M. R. Schmeler, S. R. Williams, and W. H. Donovan, "Outcome measures for gait and ambulation in the spinal cord injury population," *The Journal of Spinal Cord Medicine*, vol. 31, no. 5, pp. 487–499, 2008.

[203] H. J. van Hedel, M. Wirz, and V. Dietz, "Assessing walking ability in subjects with spinal cord injury: validity and reliability of 3 walking tests.," *Archives of Physical Medicine and Rehabilitation*, vol. 86, pp. 190–6, Feb. 2005.

[204] J. Ditunno and G. Scivoletto, "Clinical relevance of gait research applied to clinical trials in spinal cord injury," *Brain Research Bulletin*, vol. 78, pp. 35–42, Jan. 2009.

[205] K. Hayes, J. Hsieh, D. Wolfe, P. Potter, and G. Delaney, "Classifying incomplete spinal cord injury syndromes: Algorithms based on the international standards for neurological and functional classification of spinal cord injury patients," *Archives of Physical Medicine and Rehabilitation*, vol. 81, no. 5, pp. 644–652, 2000.

[206] M. M. Adams and A. L. Hicks, "Spasticity after spinal cord injury," *Spinal cord*, vol. 43, no. 10, pp. 577–586, 2005.

[207] J. Sánchez-Lacuesta, J. Prat Pastor, J. Víctor Hoyos, E. Viosca, C. Soler-García, M. Comin, M. Lafuente, A. Cortés, and P. Vera Luna, *Biomecánica de la marcha humana normal y patológica*. Valencia: IBV Instituto de Biomecánica de Valencia, 1993.

[208] J. Perry, *Gait analysis: normal and pathological function*, vol. 12. Thorofoare: SLACK Incorporated, 1992.

[209] J. H. Campbell, "Linked Hip-Knee-Ankle-Foot Orthoses Designed for Reciprocal Gait," *JPO Journal of Prosthetics and Orthotics*, vol. 18, pp. 204–208, June 2006.

[210] D. A.M. and H. Herr, "Lower Extremity Exoskeletons and Active Orthoses: Challenges and State-of-the-Art," *IEEE Transactions on Robotics*, vol. 24, no. 1, pp. 144–158, 2008.

[211] F. Heinz and W. Dauber, *Pocket atlas of human anatomy*. 4 ed., 2000.

[212] J. Moreno, F. Brunetti, E. Rocon, and J. Pons, "Immediate effects of a controllable knee ankle foot orthosis for functional compensation of gait in patients with proximal leg weakness," *Medical and Biological Engineering and Computing*, vol. 46, no. 1, pp. 43–53, 2008.

[213] A. Cullell, J. Moreno, E. Rocon, A. Forner-Cordero, and J. Pons, "Biologically based design of an actuator system for a knee-ankle-foot orthosis," *Mechanism and Machine Theory*, vol. 44, no. 4, pp. 860–872, 2009.

[214] J. M. B. Bertomeu, J. M. B. Lois, R. B. Guillem, A. P. D. Pozo, J. Lacuesta, C. G. Mollà, P. V. Luna, and J. P. Pastor, "Development of a hinge compatible with the kinematics of the knee joint.," *Prosthetics and Orthotics International*, vol. 31, pp. 371–83, Dec. 2007.

[215] A. Gil-Agudo, E. Pérez-Rizo, A. J. Del-Ama, B. Crespo-Ruiz, S. Pérez-Nombela, and A. Sánchez-Ramos, "Comparative biomechanical gait analysis of patients with central cord syndrome walking with one crutch and two crutches.," *Clinical Biomechanics*, vol. 24, pp. 551–7, Aug. 2009.

[216] L. Ortiz Berrocal, *Resistencia de materiales*. 1997.

[217] D. Winter, *The biomechanics and motor control of human movement*. Hoboken, New Jersey: John Wiley and Sons, 4 ed., 2009.

[218] N. Hogan, "Impedance control: An approach to manipulation Part I: Theory," *Journal of Dynamic Systems, Measurement, and Control*, vol. 107, 1985.

[219] G. Zeng and A. Hemami, "An overview of robot force control," *Robotica*, vol. 15, pp. 473 – 482, 1997.

[220] M. Ueberle and M. Buss, "Control of Kinesthetic Haptic Interfaces," in *IEEE/RSJ International Conference on Intelligent Robots and Systems. Workshop on Touch and Haptics*, 2004.

[221] H. Kooij, J. Veneman, and R. Ekkelenkamp, "Compliant Actuation of Exoskeletons," in *Mobile Robots: towards New Applications* (A. Lazinica, ed.), vol. 281, ch. Compliant, pp. 129–148, I-Tech Education and Publishing, 2006.

[222] J. G. Ziegler and N. Nichols, "Optimum settings for automatic controllers," *Transatcions of ASME*, vol. 64, no. 11, pp. 759–765, 1942.

[223] J. R. Clinkingbeard, J. Gersten, and D. Hoehn, "Energy cost of ambulation in the traumatic paraplegic," *American Journal of Physics and Medicine*, vol. 43, pp. 157–165, 1964.

[224] M. Vanderthommen and J. Duchateau, "Electrical stimulation as a modality to improve performance of the neuromuscular system," *Exercise and Sport Sciences Reviews*, vol. 35, no. 4, pp. 180–185, 2007.

[225] C. S. Bickel, C. M. C. Gregory, and J. J. C. Dean, "Motor unit recruitment during neuromuscular electrical stimulation: a critical appraisal," *European Journal of Applied Phisiology*, vol. 111, pp. 2399–2407, Aug. 2011.

[226] C. Gregory and C. Bickel, "Recruitment patterns in human skeletal muscle during electrical stimulation," *Physical Therapy*, vol. 85, no. 4, pp. 358–354, 2005.

[227] A. Carpentier, "Motor unit behaviour and contractile changes during fatigue in the human first dorsal interosseus," *The Journal of Physiology*, vol. 534, no. 3, pp. 903–912, 2001.

[228] C. Thomas, L. Griffin, S. Godfrey, E. Ribot-Ciscar, and J. E. Butler, "Fatigue of paralyzed and control thenar muscles induced by variable or constant frequency stimulation," *Journal of Neurophysiology*, vol. 89, pp. 2055–2064, 2003.

[229] P. H. Peckham, J. T. Mortimer, and E. B. Marsolais, "Alteration in the force and fatigability of skeletal muscle induced by chronic electrical stimulation," *Clinical Orthopaedics and Related Research*, vol. 90, pp. 326–334, 1976.

[230] A. Lopez-Guajard0, H. Sutherland, J. C. Jarvis, and S. Salmons, "Induction of a fatigue-resistant phenotype in rabbit fast muscle by small daily amounts of stimulation," *Journal of Applied Physiology*, vol. 90, pp. 1909–1918, 2000.

[231] S. Harridge, J. L. Andersen, A. Hartkopp, S. Zhou, F. Biering-Sorensen, C. Sandri, and M. Kjaer, "Training by low-frequency stimulation of tibialis anterior in spinal cord-injured men," *Muscle & Nerve*, vol. 25, pp. 685–694, 2002.

[232] H. Sutherland, J. C. Jarvis, and S. Sal, "Pattern dependence in the stimulation-induced type transformation of rabbit fast skeletal muscle," *Neuromodulation*, vol. 6, pp. 176–189, 2003.

[233] M. Gaviria and F. Ohanna, "Variability of the fatigue response of paralyzed skeletal muscle in relation to the time after spinal cord injury: mechanical and electrophysiological characteristics," *European Journal of Applied Physiology and Occupational Physiology*, vol. 80, no. 2, pp. 145–53, 1999.

[234] N. Maffiuletti, M. Minetto, D. Farina, and R. Bottinelli, "Electrical stimulation for neuromuscular testing and training: state-of-the art and unresolved issues.," *European Journal of Applied Phisiology*, pp. 2391–2397, Aug. 2011.

[235] T. Matsunaga, Y. Shimada, and K. Sato, "Muscle fatigue from intermittent stimulation with low and high frequency electrical pulses," *Archives of Physical Medicine and Rehabiltiation*, vol. 80, pp. 48–53, 1999.

[236] S. Lee, A. Braim, C. Becker, and L. Prosser, "Diminished fatigue at reduced muscle length in human skeletal muscle," *Muscle & Nerve*, vol. 36, no. 6, pp. 789–797, 2007.

[237] Z. Z. Karu, W. K. Durfee, and A. M. Barzilai, "Reducing muscle fatigue in FES applications by stimulating with N-let pulse trains," *IEEE Transactions on Biomedical Engineering*, vol. 42, pp. 809–17, Aug. 1995.

[238] S. A. Binder-Macleod, S. C. K. Lee, D. W. Russ, and L. J. Kucharski, "Effects of activation pattern on human skeletal muscle fatigue," *Muscle & Nerve*, vol. 21, no. 9, pp. 1145–1152, 1998.

[239] S. A. Binder-Macleod and C. B. Barker, "Use of a catch-like property of human skeletal muscle to reduce fatigue," *Muscle & Nerve*, vol. 14, no. 9, pp. 850–587, 1991.

[240] D. Graupe, P. Suliga, C. Prudian, and K. H. Kohn, "Stochastically-modulated stimulation to slow down muscle fatigue at stimulated sites in paraplegics using functional electrical stimulation for leg extension," *Neurological Research*, vol. 22, pp. 703–704, 2000.

[241] T. A. Thrasher, G. M. Graham, and M. R. Popovic, "Effect of random modulation of FES parameters on muscle fatigue," in *9th Annual Conference of the International FES Society*, (Bournemouth, UK), pp. 6–9, 2004.

[242] L. W. Chou, T. M. Kesar, and S. A. Binder-macleod, "Using customized rate-coding and recruitment strategies to maintain forces during repetitive activation of human muscles," *Physical Therapy*, vol. 88, no. 3, pp. 363–375, 2008.

[243] D. Tepavac and L. Schwirtlich, "Detection and prediction of FES-induced fatigue," *Journal of Electromyography and Kinesiology*, vol. 7, no. 1, pp. 39–50, 1997.

[244] N. C. Chesler and W. K. Durfee, "Surface EMG as fatigue indicator during FES-induced isometric muscle contractions," *Journal of Electromyography and Kinesiology*, vol. 7, no. 1, pp. 27–37, 1997.

[245] E. H. Estigoni, C. Fornusek, R. M. Smith, and G. M. Davis, "Evoked EMG and muscle fatigue during isokinetic FES-cycling in individuals with SCI.," *Neuromodulation*, vol. 14, no. 4, pp. 349–55, 2011.

[246] H. M. Franken, P. H. Franken, M. Fidder, and H. B. K. Boom, "Fatigue of intermittently stimulated paralyzed quadriceps during imposed cyclical liwer leg movements," *Journal of Electromyography and Kinesiology*, vol. 3, no. 1, pp. 3–12, 1993.

[247] D. W. Russ, K. Vandenborne, and S. A. Binder-Macleod, "Factors in fatigue during intermittent electrical stimulation of human skeletal muscle," *Journal of Applied Physiology*, vol. 93, pp. 469–478, 2002.

[248] S. A. Binder-Macleod and W. A. McLaughlin, "Effecs of asynchronous stimulation on the human quadriceps femoris muscle," *Archives of Physical Medicine and Rehabilitation*, vol. 78, pp. 294–297, 1997.

[249] B. Bigland-Ritchie, I. Zijdewind, and C. K. Thomas, "Muscle fatigue induced by stimulation with and without doublets," *Muscle & Nerve*, vol. 23, no. 1348-1355, 2000.

[250] L.-W. Chou and S. A. Binder-Macleod, "The effects of stimulation frequency and fatigue on the force-intensity relationship for human skeletal muscle," *Clinical Neurophysiology*, vol. 118, pp. 1387–1396, 2007.

[251] T. Kesar, L. W. Chou, and S. A. Binder-Macleod, "Effects of stimulation frequency versus pulse duration modulation on muscle fatigue," *Journal of Electromyography and Kinesiology*, vol. 18, pp. 662–671, 2008.

[252] S. A. Binder-Macleod, J. C. Dean, and J. Ding, "Electrical stimulation factors in potentiation of human quadriceps femoris," *Muscle & Nerve*, vol. 25, pp. 271–279, 2002.

[253] M. B. Kebaetse, A. E. Turner, and S. A. Binder-Macleod, "Effects of stimulation frequencies and patterns on performance of repetititve, nonisometric tasks," *Journal of Applied Physiology*, vol. 92, pp. 109–116, 2002.

[254] M. B. Kebaetse and S. A. Binder-Macleod, "Strategies that improve human skeletal muscle performance during repetitive, non-isometric contractions.," *Pflügers Archives. European Journal of Physiology*, vol. 448, pp. 525–32, Aug. 2004.

[255] T. Kesar and S. Binder-Macleod, "Effect of frequency and pulse duration on human muscle fatigue during repetitive electrical stimulation.," *Experimental Physiology*, vol. 91, pp. 967–76, Nov. 2006.

[256] H. M. Franken, P. H. Veltink, G. Baardman, R. a. Redmeyer, and H. B. Boom, "Cycle-to-cycle control of swing phase of paraplegic gait induced by surface electrical stimulation.," *Medical and Biological Engineering and Computing*, vol. 33, pp. 440–51, May 1995.

[257] S. Jezernik, R. G. V. Wassink, and T. Keller, "Sliding mode closed-loop control of FES: controlling the shank movement.," *IEEE Transactions on Bio-Medical Engineering*, vol. 51, pp. 263–72, Mar. 2004.

[258] A. Ajoudani and A. Erfanian, "A neuro-sliding-mode control with adaptive modeling of uncertainty for control of movement in paralyzed limbs using functional electrical stimulation.," *IEEE Transactions on Biomedical Engineering*, vol. 56, pp. 1771–80, July 2009.

[259] H. Gollee, D. J. Murray-Smith, and J. C. Jarvis, "A nonlinear approach to modeling of electrically stimulated skeletal muscle.," *IEEE Transactions on Biomedical Engineering*, vol. 48, pp. 406–15, Apr. 2001.

[260] S. Jonić, T. Janković, V. Gajić, and D. Popović, "Three machine learning techniques for automatic determination of rules to control locomotion.," *IEEE Transactions on Biomedical Engineering*, vol. 46, pp. 300–10, Mar. 1999.

[261] H. Kobravi and A. Erfanian, "Decentralized adaptive robust control based on sliding mode and nonlinear compensator for the control of ankle movement using functional electrical stimulation of," *Journal of Neural Engineering*, vol. 6, 2009.

[262] C. Freeman, A. Hughes, J. Burridge, P. Chappell, P. Lewin, and E. Rogers, "Iterative learning control of FES applied to the upper extremity for rehabilitation," *Control Engineering Practice*, vol. 17, pp. 368–381, Mar. 2009.

[263] R. Nguyen, A. M. González, S. Micera, and M. Morari, "Increasing muscular participation in robot-assisted gait training using FES," in *16th Annual international FES Society Conference*, (Sao Paulo, Brasil), 2011.

[264] K. Kurosawa, R. Futami, T. Watanabe, and N. Hoshimiya, "Joint angle control by FES using a feedback error learning controller.," *IEEE Transactions on Neural Systems and Rehabilitation Engineering*, vol. 13, pp. 359–71, Sept. 2005.

[265] B. Ibrahim, M. Huq, and M. Tokhi, "Identification of active properties of knee joint using GA optimization," *World Academy of Science, Engineering and Technology*, vol. 55, pp. 441–446, 2009.

[266] H. Dou, K. Tan, T. Lee, and Z. Zhou, "Iterative learning feedback control of human limbs via functional electrical stimulation," *Control Engineering Practice*, 1999.

[267] C. T. Freeman, D. Tong, K. Meadmore, Z. Cai, E. Rogers, a. M. Hughes, and J. H. Burridge, "Phase-lead iterative learning control algorithms for functional electrical stimulation-based stroke rehabilitation," *Proceedings of the Institution of Mechanical Engineers, Part I: Journal of Systems and Control Engineering*, vol. 225, pp. 850–859, July 2011.

[268] D. Bristow, M. Tharayil, and A. Alleyne, "A survey of iterative learning control," *IEEE Control Systems*, no. June, pp. 96–114, 2006.

[269] H.-S. Ahn, Y. Chen, and K. L. Moore, "Iterative Learning Control: Brief Survey and Categorization," *IEEE Transactions on Systems, Man and Cybernetics, Part C (Applications and Reviews)*, vol. 37, pp. 1099–1121, Nov. 2007.

[270] R. Nguyen, S. Micera, and M. Morari, "Iterative learning control for FES of the ankle," in *16th Annual international FES Society Conference*, (Vienna. Austria.), 2011.

[271] A. Vette, K. Masani, and M. Popovic, "Time Delay from Muscle Activation to Torque Generation during Quiet Stance: Implications for Closed-Loop Control via FES," in *13th Annual Conference of the International Functional Electrical Stimulation Society IFESS2008*, (Freiburg, Germany), p. 124, 2008.

[272] P. C. Sweeney, G. M. Lyons, and P. H. Veltink, "Finite state control of functional electrical stimulation for the rehabilitation of gait," *Medical and Biological Engineering and Computing*, vol. 38, pp. 121–126, Mar. 2000.

[273] D. Popovic, R. Tomovic, and R. Stein, "Finite State Models For Gait With Hybrid Assistive Systems," in *Proceedings of the Annual International Conference of the IEEE Engineering in Medicine and Biology Society, 1991.*, vol. 13, pp. 928–930, IEEE, 1991.

[274] L. Demers, M. Monette, Y. Lapierre, D. L. Arnold, and C. Wolfson, "Reliability, validity, and applicability of the Quebec User Evaluation of Satisfaction with assistive Technology (QUEST 2.0) for adults with multiple sclerosis," *Disability & Rehabilitation: Assistive Technology*, vol. 15, no. 24, pp. 21–30, 2002.

[275] J. DeVine, D. Norvell, E. Ecker, and D. Fourney, "Evaluating the correlation and responsiveness of patient-reported pain with function and quality-of-life outcomes after spine surgery," *Spine*, vol. 36, no. 21, pp. S69–74, 2011.

[276] A. Botter, G. Oprandi, F. Lanfranco, S. Allasia, N. a. Maffiuletti, and M. A. Minetto, "Atlas of the muscle motor points for the lower limb: implications for electrical stimulation procedures and electrode positioning.," *European Journal of Applied Phisiology*, pp. 2461–2471, July 2011.

[277] T. Fuhr, J. Quintern, R. Riener, and G. Schmidt, "Walking with WALK! A cooperative, patient-driven neuroprosthetic system.," *IEEE Engineering in Medicine and Biology Magazine*, vol. 27, no. 1, pp. 38–48, 2008.

[278] M. Huq, R. Massoud, C. Gharooni, and M. Tokhi, "Effectiveness of Control Strategies in Reducing Muscle Fatigue," in *9th Annual Conference of the International FES Society*, (Bournemouth, UK), pp. 8–10, 2004.

[279] T. C. Bulea, R. Kobetic, and R. J. Triolo, "Restoration of stance phase knee flexion during walking after spinal cord injury using a variable impedance orthosis.," in *33th Annual International Conference of the IEEE Engineering in Medicine and Biology Society*, pp. 608–611, Jan. 2011.

[280] S. Piazza, D. Torricelli, F. Brunetti, and J. L. Pons, "A novel FES control paradigm based on muscle synergies for postural rehabilitation therapy with hybrid exoskeletons," in *2012 Annual International Conference of the IEEE Engineering in Medicine and Biology Society (EMBC)*, pp. 1868 – 1871, 2012.

[281] T. Ohashi, G. Obinata, Y. Shimada, and K. Ebata, "Control of hybrid FES system for restoration of paraplegic locomotion," in *Proceedings of the 2nd IEEE International Workshop on Robot and Human Communication, 1993*, pp. 96–101, 1993.

[282] T. Yukawa, M. Khalid, M. Uchiyama, H. Inooka, T. Ohashi, G. Obinata, H. Kagaya, and Y. Shimada, "Modular hybrid functional electrical stimulation system," in *Proceedings of the 1996 IEEE International Conference on Robotics and Automation*, vol. 2, (Minneapolis, Minnesota), pp. 1184–1190, 1996.

[283] H. Vallery and M. Buss, "Towards a hybrid motor neural prosthesis for gait rehabilitation: a project description," *Journal of Automatic Control*, vol. 15, pp. 19–22, 2005.

[284] H. Vallery, T. Stützle, M. Buss, D. Abel, and Others, "Control of a Hybrid Motor Prosthesis for the Knee Joint," in *Proceedings IFAC World Congress, International Federation of Automatic Control*, 2005.

[285] M. W. Whittle, G. M. Cochrane, A. P. Chase, A. V. Copping, R. J. Jefferson, D. J. Staples, P. T. Fenn, and D. C. Thomas, "A comparative trial of two walking systems for paralysed people.," *Paraplegia*, vol. 29(2), pp. 97–102, Feb. 1991.

[286] L. Olmos, O. Freixes, M. Gatti, D. Cozzo, S. Fernandez, C. Vila, P. Agrati, and I. Rubel, "Comparison of gait performance on different environmental settings for patients with chronic spinal cord injury," *Spinal Cord*, vol. 46(5), pp. 331–4, 2008.

[287] P.-C. Kao and D. P. Ferris, "Motor adaptation during dorsiflexion-assisted walking with a powered orthosis.," *Gait & posture*, vol. 29, pp. 230–236, Feb. 2009.

[288] H. A. Quintero, R. J. Farris, K. Ha, and M. Goldfarb, "Preliminary assessment of the efficacy of supplementing knee extension capability in a lower limb exoskeleton with FES.," in *34th Annual International Conference of the IEEE Engineering in Medicine and Biology Society*, no. 1, pp. 3360–3, Jan. 2012.